Urban Maglev Technology Development Program
COLORADO MAGLEV PROJECT
FINAL REPORT
COMPREHENSIVE TECHNICAL MEMORANDUM

U. S. Department of
Transportation

**Federal Transit
Administration**

June 2004

FTA

**Federal Transit
Administration**

OFFICE OF RESEARCH, DEMONSTRATION, AND INNOVATION

CDOT Disclaimer

REPORT DOCUMENTATION PAGE		*Form Approved* *OMB No. 0704-0188*
Public reporting burden for this collection of information is estimated to average 1 hour per response, including the time for reviewing instructions, searching existing data sources, gathering and maintaining the data needed, and completing and reviewing the collection of information. Send comments regarding this burden estimate or any other aspect of this collection of information, including suggestions for reducing this burden, to Washington Headquarters Services, Directorate for Information Operations and Reports, 1215 Jefferson Davis Highway, Suite 1204, Arlington, VA 22202-4302, and to the Office of Management and Budget, Paperwork Reduction Project (0704-0188), Washington, DC 20503.		

1. AGENCY USE ONLY *(Leave blank)*	2. REPORT DATE June 2004	3. REPORT TYPE AND DATES COVERED Part 3 of 3: Comprehensive Technical Memorandum of Final Report
4. TITLE AND SUBTITLE Colorado Maglev Project		5. FUNDING NUMBERS CO-26-7002
6. AUTHOR(S) Maglev Transit Group: Vladimir Anisimow (vlad@adnc.com), Dr. J. R. Wilson, Dr. W. C. Womack Sandia National Laboratories: Ron J. Kaye, Abbas A. Akhil, Orman H. Paananen, John M. Covan. Colorado Intermountain Fixed Guideway Authority:Dr. D. Munoz; PTG Itochu/CHSST: Michio Takahashi, Junro Kato TY Lin International: Mark Ashley		
7. PERFORMING ORGANIZATION NAME(S) AND ADDRESS(ES) Maglev Transit Group, Sandia National Laboratories, Colorado Intermountain Fixed Guideway Authority, Itochu/CHSST, TY Lin, PTG		8. PERFORMING ORGANIZATION REPORT NUMBER
9. SPONSORING/MONITORING AGENCY NAME(S) AND ADDRESS(ES) U.S. Department of Transportation , Federal Transit Administration, Office of Technology, 400 Seventh Street, SW, Washington, DC 20590 Colorado Department of Transportation		10. SPONSORING/MONITORING AGENCY REPORT NUMBER FTA-CO-26-7002-2004
11. SUPPLEMENTARY NOTES FTA COTR Mary Anderson / Current, Venkat Pindiprolu / Thru January 2004		
12a. DISTRIBUTION/AVAILABILITY STATEMENT Available through the National Technical Information Service, 5825 Port Royal Road, Springfield, VA		12b. DISTRIBUTION CODE N/A

13. ABSTRACT *(Maximum 200 words)*

The overall objective of the urban maglev transit technology development program is to develop magnetic levitation technology that is a cost effective, reliable, and environmentally sound transit option for urban mass transportation in the United States. This project will include the design of an urban maglev system and the development and demonstration of advanced hardware subsystems to verify advanced technology aspects of proposed system concepts. The system design may be derived from integrating existing subsystem technologies (to create a new system) or by improving an existing system using advanced technologies. The Colorado Maglev Project represents the prototype system design for a full-scale maglev system in the U. S.

As part of its findings the Colorado Maglev Project has determined that with minor modifications an existing system, CHSST, based on linear induction motors (LIMs), can feasibly be deployed in the Colorado I-70 corridor. The project reports fully evaluate and present the modified CHSST technology's capability to accommodate the terrain and service levels of the I-70 corridor. The full report is presented in three parts. Part I is this Executive Summary. Part II is the Final Report. Part III is provided in CD format only upon request from the FTA and provides additional technical detail and support to the Part I and Part II reports.

14. SUBJECT TERMS Maglev Systems, Route, System Requirements, Performance, Analysis, Magnetic Levitation, Propulsion Trade Study, Control System, Safety/Security, Design, Deployment and Cost	15. NUMBER OF PAGES 238
	16. PRICE CODE N/A

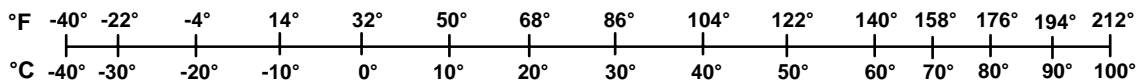| 17. SECURITY CLASSIFICATION OF REPORT Unclassified	18. SECURITY CLASSIFICATION OF THIS PAGE Unclassified	19. SECURITY CLASSIFICATION OF ABSTRACT Unclassified	20. LIMITATION OF ABSTRACT

NSN 7540-01-280-5500

Standard Form 298 (Rev. 2-89)
Prescribed by ANSI Std. 239-18
298-102

METRIC/ENGLISH CONVERSION FACTORS

ENGLISH TO METRIC

LENGTH (APPROXIMATE)

1 inch (in)	=	2.5 centimeters (cm)
1 foot (ft)	=	30 centimeters (cm)
1 yard (yd)	=	0.9 meter (m)
1 mile (mi)	=	1.6 kilometers (km)

AREA (APPROXIMATE)

1 square inch (sq in, in^2)	=	6.5 square centimeters (cm^2)
1 square foot (sq ft, ft^2)	=	0.09 square meter (m^2)
1 square yard (sq yd, yd^2)	=	0.8 square meter (m^2)
1 square mile (sq mi, mi^2)	=	2.6 square kilometers (km^2)
1 acre = 0.4 hectare (he)	=	4,000 square meters (m^2)

MASS - WEIGHT (APPROXIMATE)

1 ounce (oz)	=	28 grams (gm)
1 pound (lb)	=	0.45 kilogram (kg)
1 short ton = 2,000 pounds (lb)	=	0.9 tonne (t)

VOLUME (APPROXIMATE)

1 teaspoon (tsp)	=	5 milliliters (ml)
1 tablespoon (tbsp)	=	15 milliliters (ml)
1 fluid ounce (fl oz)	=	30 milliliters (ml)
1 cup (c)	=	0.24 liter (l)
1 pint (pt)	=	0.47 liter (l)
1 quart (qt)	=	0.96 liter (l)
1 gallon (gal)	=	3.8 liters (l)
1 cubic foot (cu ft, ft^3)	=	0.03 cubic meter (m^3)
1 cubic yard (cu yd, yd^3)	=	0.76 cubic meter (m^3)

TEMPERATURE (EXACT)

[(x-32)(5/9)] °F = y °C

METRIC TO ENGLISH

LENGTH (APPROXIMATE)

1 millimeter (mm)	=	0.04 inch (in)
1 centimeter (cm)	=	0.4 inch (in)
1 meter (m)	=	3.3 feet (ft)
1 meter (m)	=	1.1 yards (yd)
1 kilometer (km)	=	0.6 mile (mi)

AREA (APPROXIMATE)

1 square centimeter (cm^2)	=	0.16 square inch (sq in, in^2)
1 square meter (m^2)	=	1.2 square yards (sq yd, yd^2)
1 square kilometer (km^2)	=	0.4 square mile (sq mi, mi^2)
10,000 square meters (m^2)	=	1 hectare (ha) = 2.5 acres

MASS - WEIGHT (APPROXIMATE)

1 gram (gm)	=	0.036 ounce (oz)
1 kilogram (kg)	=	2.2 pounds (lb)
1 tonne (t)	=	1,000 kilograms (kg)
	=	1.1 short tons

VOLUME (APPROXIMATE)

1 milliliter (ml)	=	0.03 fluid ounce (fl oz)
1 liter (l)	=	2.1 pints (pt)
1 liter (l)	=	1.06 quarts (qt)
1 liter (l)	=	0.26 gallon (gal)
1 cubic meter (m^3)	=	36 cubic feet (cu ft, ft^3)
1 cubic meter (m^3)	=	1.3 cubic yards (cu yd, yd^3)

TEMPERATURE (EXACT)

[(9/5) y + 32] °C = x °F

QUICK INCH - CENTIMETER LENGTH CONVERSION

	0	1	2	3	4	5
Inches						

Centimeters: 0 1 2 3 4 5 6 7 8 9 10 11 12 13
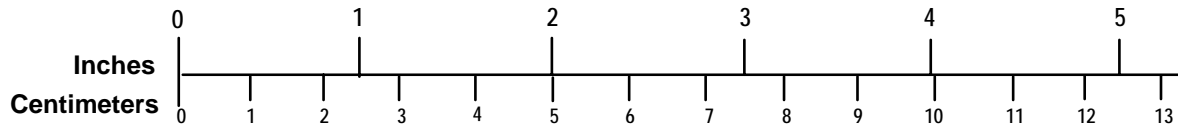
QUICK FAHRENHEIT - CELSIUS TEMPERATURE CONVERSION

°F -40° -22° -4° 14° 32° 50° 68° 86° 104° 122° 140° 158° 176° 194° 212°

°C -40° -30° -20° -10° 0° 10° 20° 30° 40° 50° 60° 70° 80° 90° 100°

For more exact and or other conversion factors, see NIST Miscellaneous Publication 286, Units of Weights and Measures. Price $2.50 SD Catalog No. C13 10286

Updated 6/17/98

Abbreviations, Acronyms, & Definitions

AASHTO	American Association of State Highway and Transportation Officials
ADA	American Disability Act
ANSI	American National Standards Institute
APTA	American Public Transit Association
ASCE	American Society of Civil Engineers
ATC	Automatic Train Control
ATCS	Automatic Train Control System
ATO	Automatic Train Operation
ATP	Automatic Train Protection
ATS	Automatic Train Supervision
CCCS	Command, Control and Communication System
CDOT	Colorado Department of Transportation
CMP	Colorado Maglev Project
dBA	Decibels
EDS	Electro Dynamic System
EMS	Electro Magnetic System
FTA	Federal Transit Administration
HSST	High Speed Shuttle Transport
HVAC	Heating Ventilation and Air Conditioning
ISO	International Standardization Organization
IEEE	Institute of Electrical and Electronic Engineers
JFSA	J.F. Sato and Associates
LIM	Linear Induction Motor
LRT	Light Rail Transit
LSM	Linear Synchronous Motor
MDBF	Mean Distance Between Failure
MTBF	Mean Time Between Failure
MTTR	Mean Time to Restore
NFPA	National Fire Protection Association
O&M	Operations and Maintenance
PEIS	Programmatic Environmental Impact Statement
TSA	Transportation Security Administration
UBC	Uniform Building Code
UTM	Urban Transport Maglev

Urban Maglev Technology Development Program

COLORADO MAGLEV PROJECT
FINAL REPORT
PART 3: COMPREHENSIVE TECHNICAL MEMORANDUM

June 2004

TABLE of CONTENTS

TABLE of FIGURES

1.0 *INTRODUCTION*

The following Comprehensive Technical Memorandum provides a portion of the detailed technical documentation completed by the Colorado Maglev Project (CMP) Team in developing the technical basis for deployment of the Colorado 200 maglev system for use on the Colorado I-70 corridor stretching between Denver International Airport (DIA) and Eagle County Airport, a distance in excess of 250 kilometers (155 miles). Considerable additional documentation was collected and produced, and interested readers should contact the authors they seek additional technical information not included in this Comprehensive Technical Memorandum.

The Comprehensive Technical Memorandum details the work accomplished in relation to the route, the required infrastructure including electrical needs, propulsion motor trade study, greenhouse gas effects, winterization report and a summary of the systems integration efforts.

This Comprehensive Technical Memorandum is in addition to the Executive Summary and the Final Report submitted to FTA and CDOT under separate cover and is provided in an electronic format only.

The Comprehensive Technical Memorandum is divided into the following category chapters:

- SYSTEM REQUIREMENTS
- SYSTEM INTEGRATION
- GREENHOUSE GAS IMPACT
- ELECTRIFICATION
- PROPULSION (TRADE STUDY)
- COMPARISON OF LINEAR SYNCHRONOUS AND INDUCTION MOTORS
- CMP WINTERIZATION REQUIREMENTS

2.0 SYSTEM REQUIREMENTS

2.1. ROUTE

The CMP stretches from DIA, through the Denver urban area, and into the Rocky Mountains to the Eagle County Airport. This corridor is perhaps the most challenging maglev corridor under consideration worldwide. It provides an evaluation of an urban maglev system application in urban, semi-urban and rural environments operating in both winter and summer conditions with difficult mountainous terrain.

The Denver urban area segment of the maglev system will service DIA and portions of the metropolitan area. An assessment has been completed of corridor alignments in the northern, central and southern parts of the Denver metropolitan area. The northern alignment corridor provides the fastest trip with the shortest guideway length from DIA to Golden. The central corridor provides the best service to the highest density portions of Denver, including service to Union Station (Denver Union Terminal, DUT) in downtown. But, due to the high density of development, the central corridor carries a penalty in trip time and cost of construction. The southern corridor alignment provides the best service to the concentration of business parks and to major residential areas in Aurora and Highlands Ranch, but requires longer trip times and higher cost due to greater guideway length.

In the mountain portion of the project, from the C470/I-70 interchange at the western edge of the greater Metropolitan Denver Area to Glenwood Springs (the CDOT I-70 PEIS project corridor), the alignment is more obvious since options are generally limited by construction costs to following the I-70 alignment. Deviations could occur north of the I-70 Twin Tunnels which are east of Idaho Springs and at the Eisenhower-Johnson Memorial Tunnel (EJMT), taking advantage of the grade climbing capability of maglev. At the Twin Tunnels, the need for an additional tunnel would be eliminated by following a grade approaching 12 percent just north of the Twin Tunnels. At the EJMT, a maglev tunnel would be minimized in length by following an alignment north of the existing tunnel bores at a higher elevation and correspondingly steeper grade.

The technical work accomplished through the system requirements task is provided in this chapter:

- a detailed description of the Denver urban area corridor alignments evaluating the benefits of a maglev system operating within each of the three corridors,
- plans and profiles for a first segment from Golden to EJMT,
- general plans and profiles west of Idaho Springs to Eagle County Airport and
- the ridership projections and background data.

Due to the serious year-round I-70 congestion in the mountain corridor during weekends, and due to the cost and right-of-way limitations along much of I-70, transit may be the only viable alternative to extremely costly highway construction beyond an already expensive two-lane (one lane each westbound and eastbound) highway widening. As the I-70 and Blackhawk Programmatic Environmental Impact Statements (PEIS) are completed, additional effort may be required in detailing maglev system requirements west of Idaho Springs and through the Denver metropolitan area.

2.1.1. *Denver Metropolitan Area Corridor Alignments*

The Denver metropolitan area provides both challenges and opportunities for deploying a maglev system. Three broad corridor alignments have been identified and have been assessed from the point of view of a maglev system operating within each corridor; benefits of each corridor have been discussed. The route analysis from Golden west along I-70 has established the physical

parameters and characteristics of the maglev system with the assumption that the system required in the mountainous portion of the overall project will also be able to operate within each Denver urban corridor alignment.

2.1.1.1. Corridor Alignments

The maglev system alignment through the Denver metropolitan area considered three broad corridors:

- Northern circumferential route serving the DIA complex, potential developments north of DIA and industrial and residential property along the I-70/I-76 highway system west to Golden,
- Radial route from DIA through established residential developments west of DIA penetrating the central business district and proceeding west to Golden, and
- Southern circumferential route from DIA serving major employment and residential developments south of DIA along the I-225/I-25 interstate highways, and then west serving major residential development in the southern metropolitan area to Golden.

The northern circumferential corridor is defined as an alignment that will provide direct service from DIA to the proposed Golden Intermodal Transfer Station, providing the fastest and shortest link to mountain travelers. The northern circumferential corridor also would be the least costly due to its shorter length, as compared to the other two corridors.

The central radial route is assumed to be a maglev alignment that provides service from DIA to downtown to Golden with the secondary role of providing additional urban transit service between DIA and Golden for urban commute purposes.

The southern circumferential corridor provides service from DIA to Golden while secondarily providing urban transit service to the business parks along I-225 and I-25, and major residential developments in Aurora and along C-470.

Both the radial and southern circumferential corridors will sacrifice travel time to the mountain corridor to complete the secondary function of urban collector/distributor.

Figure 1 shows the three broad corridor alignments through the Denver Metropolitan Area.
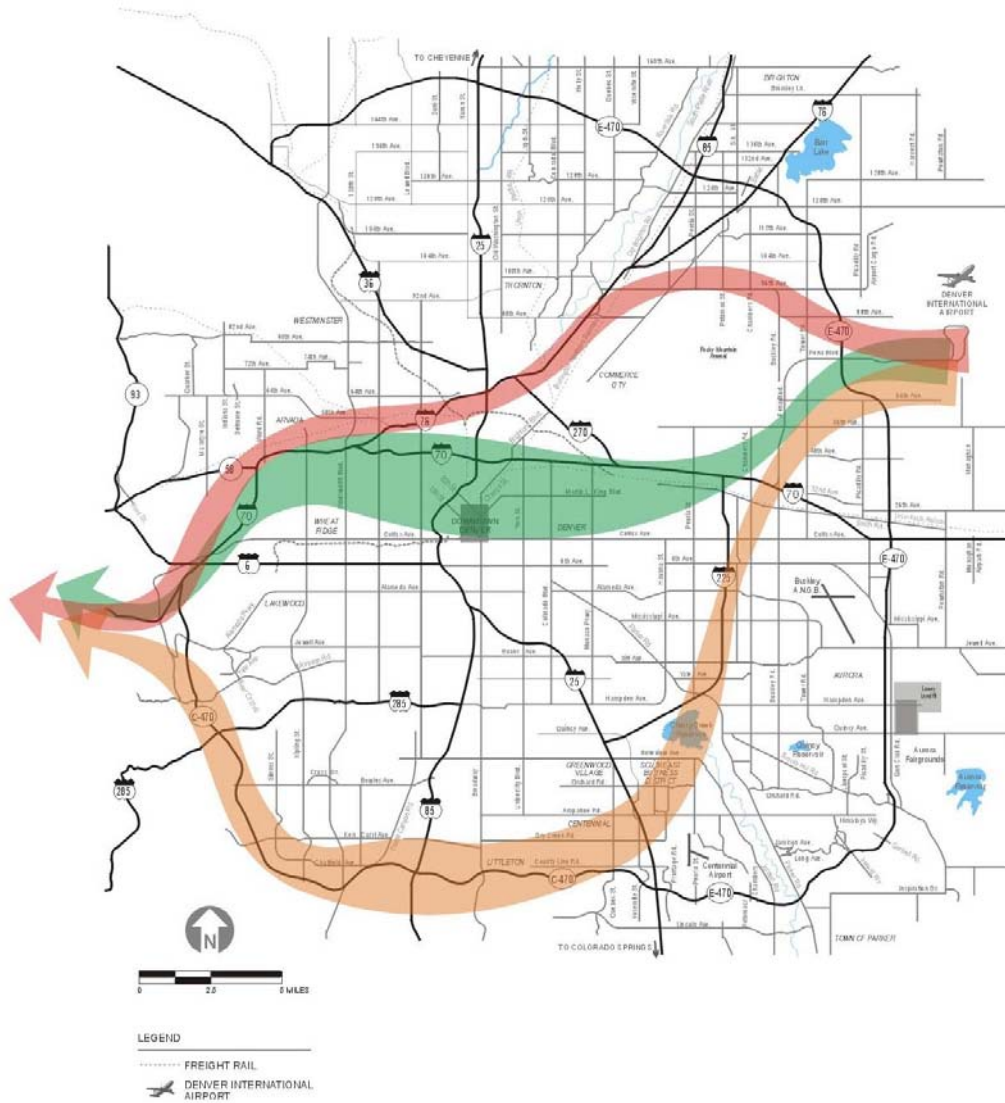
Figure 1: Example Maglev Corridors Through the Denver Metropolitan Area

The following sections detail each of the metropolitan area corridors.

2.1.1.1.1. *Northern Circumferential Corridor*

Beginning at DIA, the Northern corridor alignment could follow the Pena Boulevard corridor west to E-470 or Tower Road, travel north of the Rocky Mountain Arsenal/National Wildlife Refuge to I-76, follow the I-76 corridor to I-70, and then follow the I-70 corridor to the mountains. This alignment would provide the quickest connection between DIA and the mountain corridor portion of the maglev system. As such, it provides a high level of service to trips passing through the metropolitan area. Within the metropolitan area, this alignment passes through industrial and commercial areas, although it intersects several major transportation corridors serving residential areas in the northeast (via I-76 and US 85), north (via I-25), and northwest (via US 36/I-25) portions of the metropolitan region.

Figure 2: Gateway Park at Pena Boulevard and I-70

2.1.1.1.2. *Radial Route – Central Corridor*

The Central corridor provides service to the Denver central business district (CBD) and two major transit transfer centers. The Central corridor alignment could follow Pena Boulevard from DIA and then travel near the Union Pacific (UP) railroad corridor to the CBD. The alignment could be placed within the I-70 corridor until around Brighton Boulevard where it would shift to either the UP railroad corridor from the east or the Burlington Northern-Santa Fe (BNSF) railroad corridor coming from the northeast toward the CBD. From the CBD, the alignment would follow the UP/BNSF railroad corridor to the north and then I-70 to the mountains. While the Central and northern circumferential corridors both provide the most direct alignment to the mountain corridor, the Central corridor would be slower than the northern circumferential due to the penetration of the CBD and the inherently slower travel through the congested and developed Denver core area. In addition to the diversion from the I-70 corridor to serve the DUT station, service to the Stapleton transfer center has been proposed. Since the old Stapleton airport site is being redeveloped into a mixed-use development including substantial tracts of residential development, it is unlikely that an acceptable path from the I-70 corridor from the east to the Stapleton transfer center would be available. Thus, provision of this service would require a "perpendicular" diversion from the east-west I-70 corridor at Quebec. Like the DUT stop, service to the Stapleton transfer center would slow the service to the mountain corridor.

Figure 3: Denver Union Terminal

Figure 4: Stapleton Transfer Center

2.1.1.1.3. *Circumferential Route (Activity Centers) – Southern corridor*

There are at least three distinct alignment options for the Southern corridor. Each of the alignments serves significant commercial centers in the region (the Denver Tech Center, the Meridian and Inverness Business Parks). In addition, the opportunity exists for two of the optional alignments to connect DIA with a major general aviation airport (Centennial Airport). Like the northern corridor, each of the alignments intersects major transportation corridors (I-25, US-85, and US-285). Finally, unlike the Northern or Central corridors, the Southern corridor could serve major population centers in the metropolitan region.

Figure 5: Denver Tech Center　　　　**Figure 6: I-25 at I-225 Looking Northwest**

2.1.2. *Trip Purposes*

There are several purposes that can or will be served by the maglev system as it passes through the metropolitan area, including:

- Provide a path from DIA to the I-70 Mountain Corridor,
- Generate additional revenues for the maglev system,
- Provide additional intra-urban transportation services for the metropolitan area, and
- Operate as a collector/distributor for the mountain portion of the system (i.e., provide an inter-urban system).

The following trip markets are served:

- Pass-through (visitor) trips between DIA and the mountains,
- Visitor trips to the metropolitan area generated by non-residents of the area or I-70 mountain corridor regions,
- Commuter trips between the metropolitan area and the mountains,
- Resident non-work trips between the metropolitan area and the mountains,
- Intra-metropolitan commute trips,
- Intra-metropolitan non-commute trips, and
- Airport access trips.

Due to the constraints imposed upon each corridor, the following conclusions concerning trip purpose are made for each potential corridor:

1. Northern Corridor
    *   provides a path from DIA to the I-70 mountain corridor only serving pass-through trips between DIA and the mountains
    *   provides airport access trips from the Golden Station to DIA

2. Central Radial Corridor/Southern Circumferential Corridor
    *   each corridor provides all trip purposes and serves all trip markets listed in differing degrees

2.1.2.1. Corridor Alignment Considerations

The following corridor alignment considerations were used in assessing the three broad corridor alignments:

*   Route availability and continuity
*   Potential station locations
*   Cost (Capital and Operations and Maintenance)
*   Coordination with existing transit services

These four considerations were viewed to be the key determinants for decision. The route availability and continuity provides the primary cost element for any transit deployment. Transit station locations determines the ridership potential to a new system, while coordination with existing transit services provides the potential for transfer trips, which may provide further ridership enhancements. Cost from both a capital and operations and maintenance aspect will determine whether the system has the possibility to be constructed; this is clearly the most important of the considerations.

2.1.2.1.1. *Route Availability and Continuity*

For any corridor through the metropolitan area, there must be a feasible continuous route available. The benefits of locating the maglev system alignment in a public right-of-way, such as a freeway or existing street, are obvious.

Each of the three broad corridors have available right of way for a maglev system. The northern circumferential corridor and the southern circumferential corridor each have interstate highways that provide opportunity for maglev routing. Both the northern corridor and the central radial corridor could use I-70 from DIA to Golden, although I-70 west from DIA would provide issues due to long viaduct sections west of Colorado Boulevard to I-25 and the geometry of the I-70/I-25 interchange. Another option for the northern circumferential corridor is an even more northerly path following 96th Avenue to I-76, connecting with I-70 westward in the vicinity of the I-25 interchange.

For the central radial corridor, penetrating the downtown area could be problematic due to built up nature of the downtown core. While right-of-way may be found, it is likely to be limited in extent.

The southern circumferential corridor using I-225 and I-25 bisects mature urban neighborhoods. In the C-470 area, the alignment would travel through the highly developed residential suburban area of Highlands Ranch in Douglas County and significant open space in Jefferson County. At the I-225 and I-25 junction, alignment alternatives might be restricted due to the current reconstruction of the interchange. This reconstruction includes the addition of light rail transit in both the I-25 and I-225 corridors and will increase the density of commercial and residential land use around the interchange.

An additional alignment option follows E-470 and C-470 to Golden. This alignment is probably the easiest to follow of the three southern alignment options since it could remain within freeway right-of-way for its entire length. The alignment would travel through newly developing residential

and commercial areas in the eastern, southeastern, and southern portions of the region. Like the first southern alignment option, it might be possible to provide service to Centennial airport. The alignment would also intersect the Southeast and Southwest LRT lines at I-25 and US 85 (if the proposed extension of the Southwest LRT line from Mineral Avenue to C-470 is completed). Connection to these two LRT lines would provide good transit access to the southern part of the region.

Of the three corridors, both the northern and southern circumferential have fewer problems than the radial corridor, which presents major issues both entering and leaving the downtown area. Of the two circumferential routes, both have benefits and drawbacks. Due to the shorter length of the northern circumferential corridor alignment, this routing would provide the path of least resistance to maglev system deployment, assuming that the overriding requirement for maglev service is mountain access through Denver from DIA rather than serving primarily as an urban collection distribution system with secondary mountain access.

2.1.2.1.2. *Station Location*

Station location will be crucial to the service philosophy for the maglev system. The number and location of stations have positive impacts on travel to and from the metropolitan region, since each additional station will potentially increase travel times for all travelers passing through the area. In addition, available land for stations or other considerations might require diversions from a direct path for an alignment, further adding to travel times for pass-through travelers or requiring the addition of switches on the main alignment to provide service for through (express) vehicles and local service vehicles.

For each of the corridors, stations at DIA and Golden will be assumed. The DIA station is assumed to serve air travelers. While substantial parking is provided at DIA (for air travelers), no auto access to the DIA station by local residents of the region will be assumed.

The exact site of the Golden station is not identified, although it will be in the general vicinity of the interchange between US 6 and I-70. Since this station serves as the entrance to the I-70 mountain corridor portion of the maglev system, the station would need to provide adequate parking. The parking could serve metropolitan area residents traveling to the mountains, metropolitan area residents traveling to other metropolitan area destinations or DIA, or mountain area residents traveling to metropolitan area destinations or DIA.

The northernmost corridor would offer an opportunity for two stations in addition to the DIA and Golden stations, a Downtown Denver station at the intersection of I-70/I-25, and a Rolla station at the 96th Avenue/I-76 junction.

The central radial corridor would have three stations:
- The Stapleton transit transfer center,
- DUT, and
- Ward Road.

A DUT station would serve primarily as a transfer station to other transit services provided in the region and as a direct access point to the CBD. Parking at a DUT station should be assumed to be extremely limited or non-existent.

The DUT location may represent another problem. RTD has recently purchased the DUT for conversion into an inter-modal facility. This hub would serve not only all of RTD's fixed guideway and bus services, but would also serve intercity rail (e.g., Amtrak) and bus (e.g., Greyhound) services. At full build-out, DUT would also accommodate commuter rail service from the US 36 Corridor. The addition of a maglev station at DUT might pose a major construction and land use challenge.

The final station location that might be considered for the central radial corridor would be in the vicinity of I-70 and Ward Road. While this location would not intersect major roadways, it could serve as a "relief" park-and-ride location for the Golden station. It could serve some travel by Golden residents that access I-70 via C-58. If the FasTracks system is built by RTD, the Ward Road station would provide a transfer point to the Goldline LRT line. This could provide a transit transfer point for trips made by metropolitan residents to the mountains, or for mountain residents to locations in the metropolitan area.

For the southern corridor, maglev stations should be provided at all intersections of the maglev alignment with major roadways. The following stations might be considered, depending on the selected alignment:

- I-225 and I-70 (for alignment options following I-225),
- I-225 and I-25 (for alignment options following I-225),
- E-470 and I-70 (for the E-470/C-470 alignment option),
- E-470 and I-25 (for the E-470/C-470 alignment option),
- US 285/Hampden and US 85 (for the alignment option following I-225 and US 285/Hampden),
- C-470 and US 85 (for all alignment options following C-470),
- C-470 and US 285 (for all alignment options).

Park-and-ride lots would be called for at five of the stations: E-470 and I-70, E-470 and I-25, C-470 and US 85, C-470 and US 285, and I-225 and I-70. The park-and-ride lots at each of the locations would serve travelers from the metropolitan area to the mountains. A number of the stations could also provide transfer opportunities between the maglev system and the LRT system proposed for the metropolitan area. The stations and LRT interfaces include:

- I-225 and I-25 station with the Southeast LRT,
- E-470 and I-25 station with the Southeast LRT,
- US 285/Hampden and US 85 with the Southwest LRT,
- C-470 and US 85 with the Southwest LRT.

The maglev stations at I-225 and I-25 and at E-470 and I-25 could also serve major metropolitan area destinations: the Denver Tech Center and the Meridian and Inverness Office Parks. In addition, it might be possible to serve Centennial Airport either through shuttle services or possibly by moving the maglev alignment out of the I-25 or E-470 right-of-way.

2.1.2.1.3. *Avoid Duplication of Existing Transit Service*

The Northern corridor as a circumferential route does not specifically duplicate any of the anticipated transit corridors, but rather serves as a connector for three of the northern lines.

The Central corridor option duplicates much of the service provided by the proposed Air Train commuter rail service for operation on Smith Road from the DUT to the airport. The proposed Air Train service includes stations at DUT, 40th/40th, Stapleton, Gateway, and the airport.

In the southern corridor, LRT is currently under construction in the I-25 envelope. Once complete, it will operate from Broadway/I-25 to Lincoln Avenue to Parker Road on I-225. RTD has plans to extend LRT in the I-225 corridor from Parker Road up to I-70. In addition, RTD is considering extending the terminus on the Southwest Corridor from Mineral Avenue to C-470/Santa Fe. Since it is obvious that there is an issue in duplicating transit service on I-225 and portions of I-25, it may be appropriate to drop this alignment as a candidate for maglev.

2.1.2.1.4. *Cost*

Limiting the cost of maglev system deployment may be the one factor that will finally precipitate the successful construction of North America's first maglev system.

In order to minimize the cost of the CMP, the shortest and fastest metropolitan area corridor alignment should only be considered at this time. That corridor is the northern circumferential corridor since there are only two stations and no diversions to Stapleton, downtown, business parks or residential communities. Also the alignment is the shortest of the three, thereby requiring the least guideway cost to deploy.

2.1.2.2. Conclusion

A thorough examination of the issues in each available urban corridor has led to the belief that, for the purposes of this research, the northern corridor should be selected. There are three primary reasons for this choice. First, it provides the most direct path to the mountain corridor, where the technical challenges lie. Second, it permits the addressing of the central issues of the system without entangling the discussion in fruitless efforts to site the system in downtown Denver. Third, this choice will produce the best overall performance profile for the total system, while fulfilling the objective of transporting passengers in the most efficient manner possible to the mountain resort communities. So, the northern corridor, shown in Figure 7, provides an attractive alternative for the urban route.
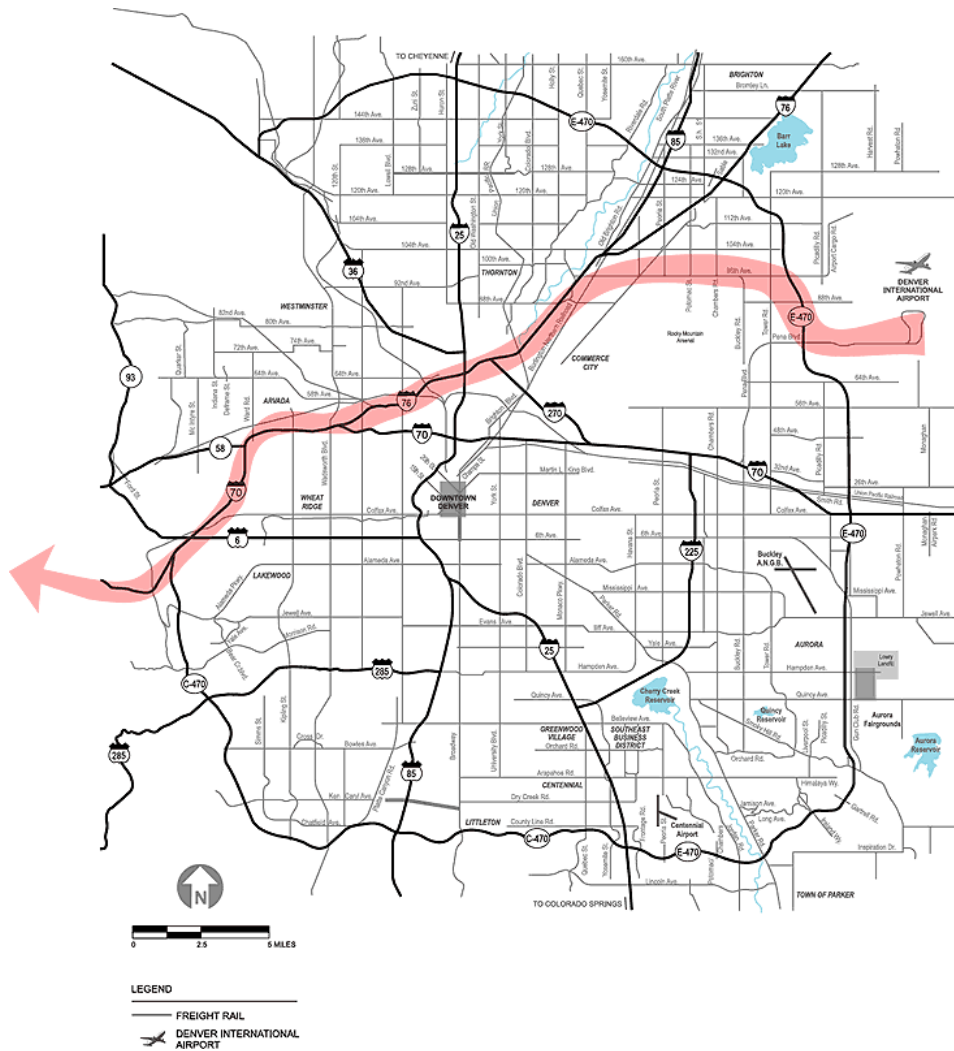
Figure 7: Denver Metropolitan Maglev Corridor

This selection does not assume that other corridors will not be ultimately constructed – it simply assumes this corridor for simulation evaluation.

Next, for purposes of simulations, it is necessary to select approximate station locations. Identification of the approximate locations will permit the calculation and comparison of trip times, and the assessment of various figures of merit for system performance, otherwise impossible without station locations.

In the Denver metropolitan area along the selected northern route, there is considerable undeveloped land. However, the area continues to develop and will undoubtedly develop rapidly at some time in the future. Examining the proximity of potential routes to other transportation facilities immediately makes two locations stand out as potential station sites. The first is the junction of I-76 and 96th Avenue, above the Rocky Mountain Arsenal. This location is largely undeveloped offering ready access to developing Greater East Denver along Tower Road and other arterials. It would also provide a good location for a maintenance facility, as it is close to DIA, but far enough along the route to provide a useful station. Second, the junction of the two major interstate routes, I-25 and I-70, is probably one of the busiest intersections in the Denver area. Locating a station here would contribute to the synergy between existing transportation and

the maglev system, and would create an ideal maglev entry point for West Denver passengers bound for the mountains. The selection of these two stations has additional benefit to the overall system. With only two stops between DIA and the Mountain Corridor, the primary mission of the system is preserved without compromising local access at points other than DIA. The impact of these choices is seen in Figure 8, below.
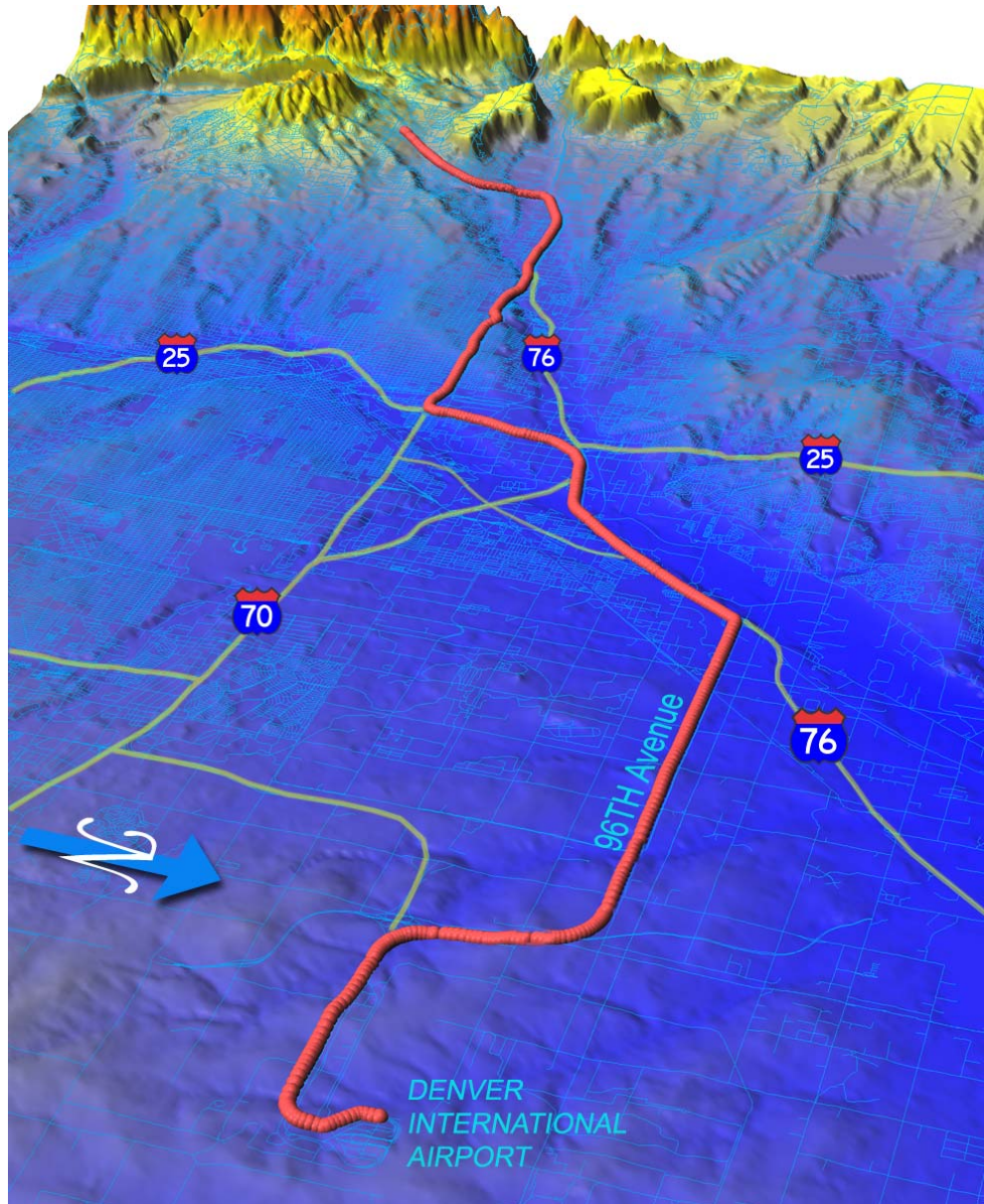
Figure 8: Denver Metropolitan Maglev Route

2.1.3. *I-70 Mountain Corridor Route Alignment Description from East to West*

The entirety of the CMP has been defined into three segments as follows:

- DIA to C470/I-70 at the western edge of the greater metropolitan Denver area.
- C470/I-70 to Idaho Springs
- Idaho Springs to Eagle County Airport (ECA)

The first segment was discussed in the previous section of this chapter.

For purposes of discussion, the I-70 Mountain Corridor transit alignments have been divided into two segments. The first segment is from C470/I-70 to Idaho Springs while the second segment proceeds from Idaho Springs west to the Eagle County Airport west of Vail, Colorado.

The segment from C470/I-70 to Idaho Springs has been the subject of a detailed evaluation defining plans and profiles, including an optional routing avoiding the Twin Tunnels just east of Idaho Springs.

The second segment from Idaho Springs west to Eagle County Airport has been subjected to a less rigorous evaluation, with a simplifying assumption of the maglev alignment operating within the median of I-70. Figure 9 illustrates the entirety of the I-70 mountain corridor transit alignment elevation profile.
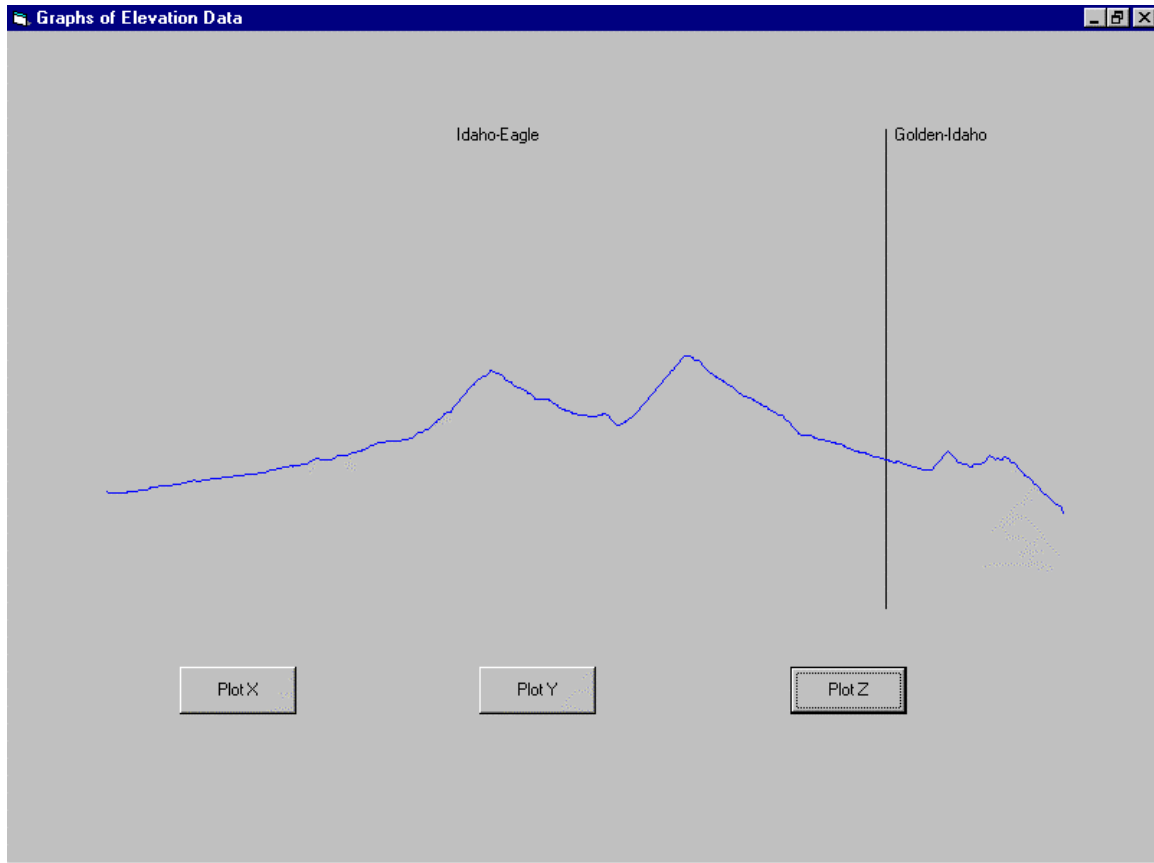
Figure 9: Mountain Corridor Elevation Profile

In addition, optional alignments to avoid the tunnels east of Idaho Springs and the long transit tunnel at EJMT have been evaluated.

Figure 10 below shows the location of the I-70 Mountain Corridor alignment west of the Denver metro area.   The segment numbers on the map correspond to discussion in the following paragraphs. The I-70 Mountain Corridor is best known for numerous accidents, blowing snow, freezing rains, extremely high winds, steep grades and tight curves.
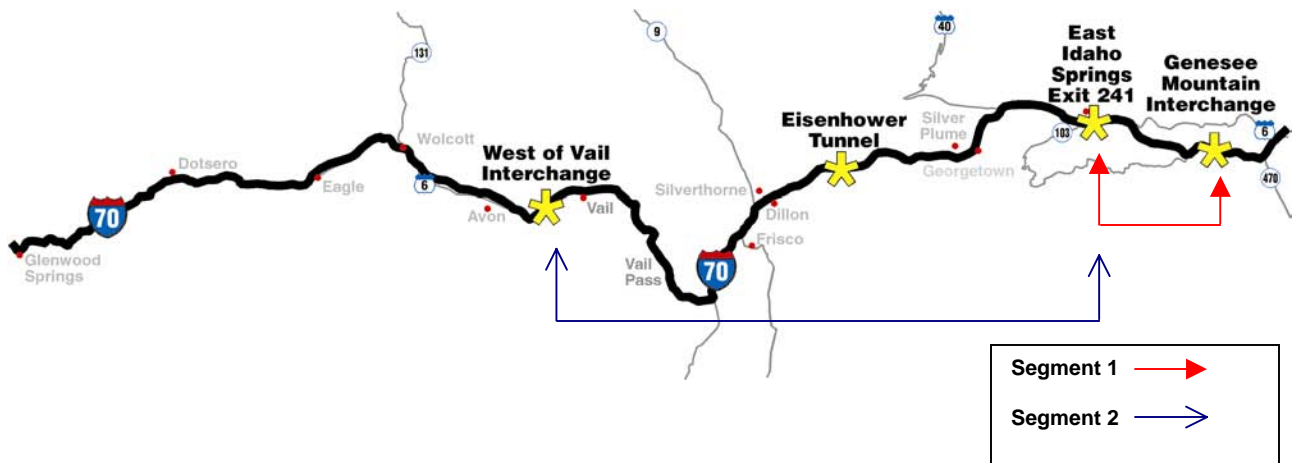
Figure 10: I-70 Mountain Corridor Maglev Route Alignment

2.1.3.1. Segment 1 – C470/I-70 to Idaho Springs

The C470/I-70 to Idaho Springs segment is challenging, with grades up to 12 percent on the off-highway route alternative at the Twin Tunnels and a number of highway sections including the Mt. Vernon Canyon and Floyd Hill sections with grades approaching 7 percent.

2.1.3.1.1. *Plans and Profiles*

Perspectives of the segment are shown on the following pages.
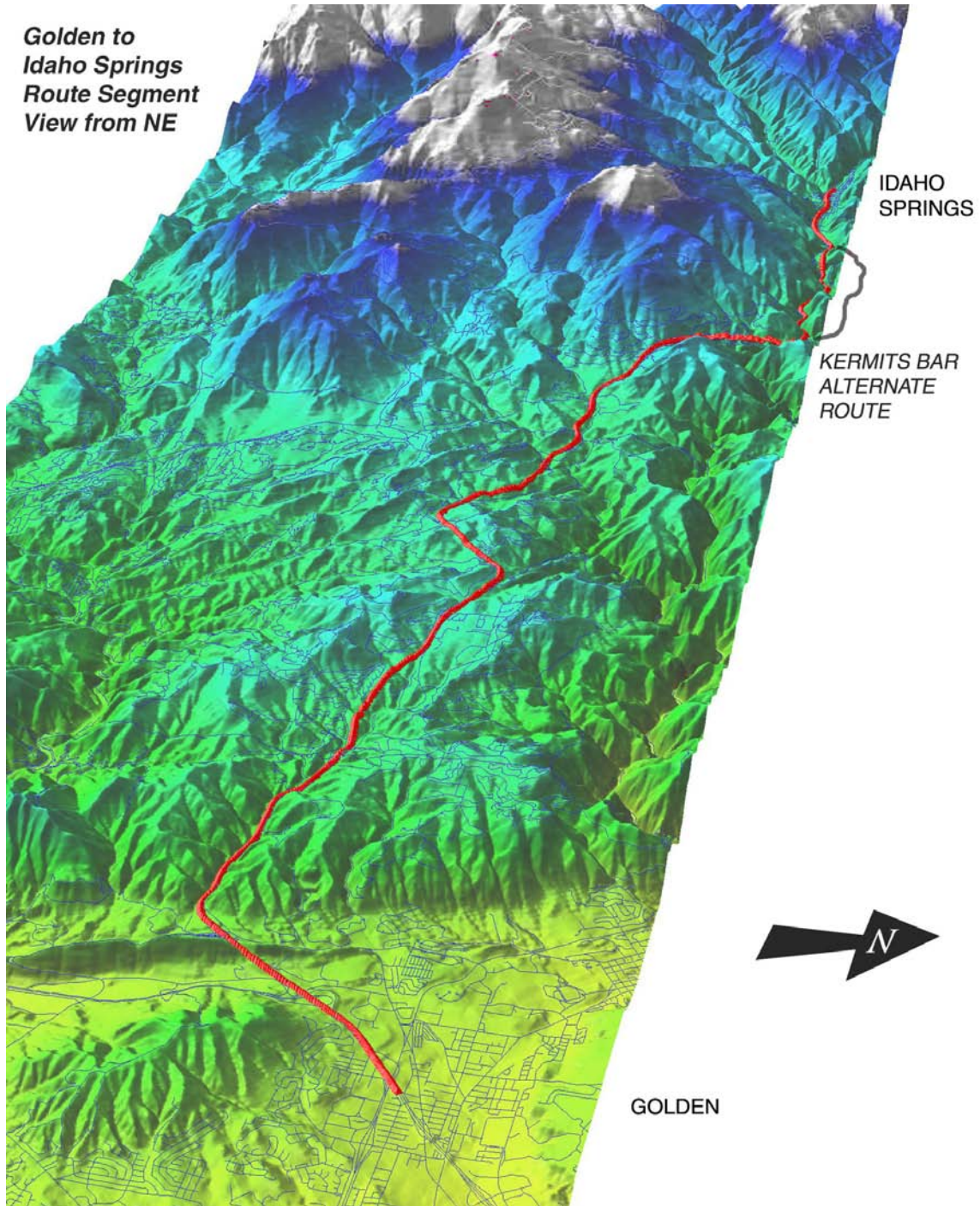
Figure 11: C470/I-70 to Idaho Springs Maglev Route
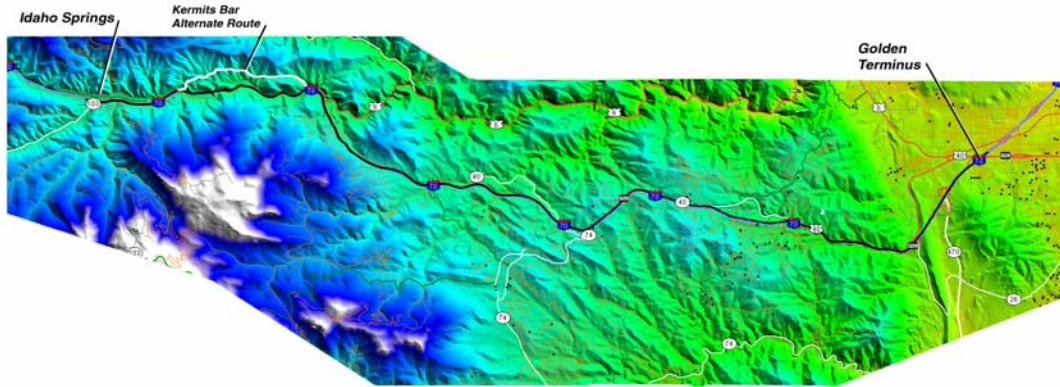
Figure 12: C470/I-70 to Idaho Springs Maglev Route
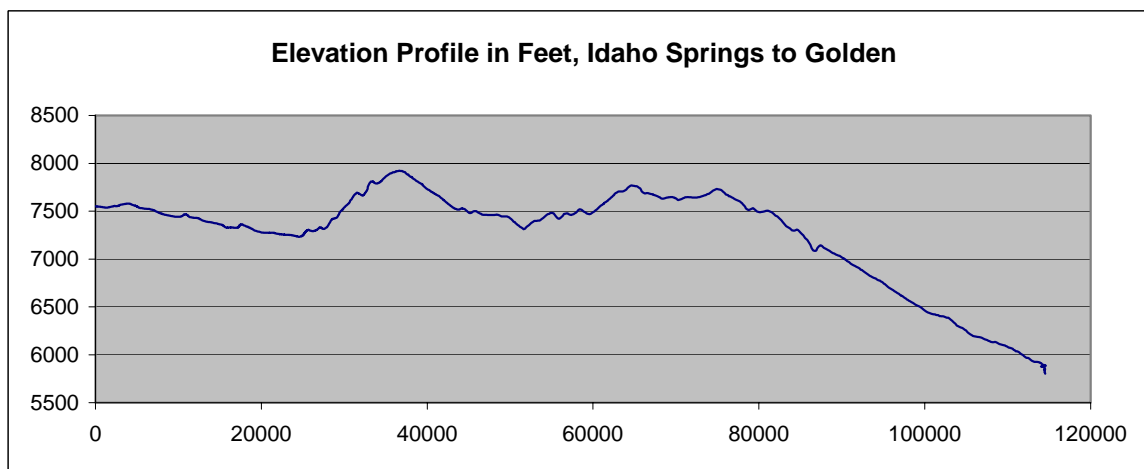
Figure 13: Elevation Profile
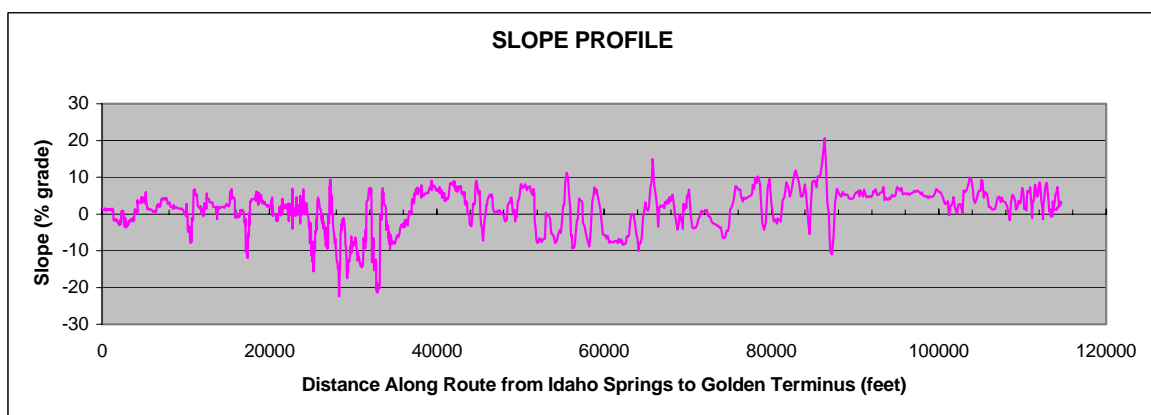
Figure 14: Slope Profile

2.1.3.1.2. *C470/I-70 to Idaho Springs Alignment Description*

Mount Vernon Canyon

Mount Vernon Canyon is a major traffic and alignment challenge nearest Denver with many accidents, weather related delays and brake failures. In summer and winter it is a major generator of traffic delays, accidents, injuries and deaths.

Vertical and Horizontal Alignment Issues

Heading west from the Denver metro area, the proposed maglev alignment follows I-70 from the I-70/C-470 interchange into the foothills of the Rocky Mountains through Mount Vernon Canyon. The alignment immediately encounters both horizontal and vertical alignment challenges. The I-70 alignment begins a steep grade climb at the interchange and continues this grade into the foothills. Just after the interchange, the right-of-way narrows so that the opposing directions of traffic are separated by only concrete ("Jersey") barriers. About 1.6 kilometers (one mile) from the interchange, the alignment passes through a 0.4 km (one-quarter mile) long deep cut through the Hogback, a geologic uplift that runs along the foothills east of Denver. The steep grade continues after passing through the Hogback although the right-of-way widens slightly. Approximately 0.4 km (one-quarter mile) after the cut through the Hogback, a tight, almost 70-degree curve is encountered at the entrance to the canyon.

The I-70 alignment then continues west for about eight additional kilometers (five miles) of winding horizontal alignments and steep grades. The continuing steep grades present difficult climbing conditions–or runaway vehicle hazards in the opposite direction. Six percent grades are common through this area with trucks and cars being slowed considerably due to the grades. In the opposite direction, a runaway truck ramp is provided approximately 1.6 kilometers (one mile) before the tight curve at the entrance to the canyon.

The right-of-way through the canyon varies in width. Some sections, especially near the western end of the canyon that might be better described as a wide valley, are quite wide, grassy areas. However, at the eastern end of the canyon the horizontal alignment is constrained and on a steep slope with the westbound lanes three to six meters (10 to 20 feet) above the eastbound lanes.

Geologic and Environmental

Since this segment of the I-70 alignment passes through an area with very steep side slopes, there is a danger from rockfalls. The danger is the greatest at the eastern end of Mount Vernon Canyon. The deep cut through the Hogback has opened long buried rock to the elements and is particularly vulnerable to rockfalls. The eastern slopes of the Hogback have been identified as potential landslide areas.

Figure 15: I-70 Westbound Toward Floyd Hill Crest

Mount Vernon Canyon to Floyd Hill

Vertical and Horizontal Alignment Issues

At the western end of Mount Vernon Canyon, the I-70 alignment reaches the crest of a hill that provides a scenic view of the mountains defining the Continental Divide. From this point to the top of Floyd Hill there are gentler grades and less severe curves than those encountered in Mount Vernon Canyon. The first half of this segment can be characterized as a long general downgrade (in the westbound direction). From that point,

the second half of the alignment can be characterized as a long general upgrade to the top of Floyd Hill.

Just after the crest of the hill at the west end of Mount Vernon Canyon, the alignment follows a straight four to five percent downgrade for about 1.6 kilometers (one mile). A relatively tight, almost 70-degree curve is encountered at the end of the downgrade. After the curve, the alignment is relatively flat for approximately 1.6 kilometers (one mile), whereupon a 60-degree curve in the opposite direction is encountered. The Evergreen Parkway interchange is located at the beginning of the curve and might cause some localized difficulty with the maglev guideway alignment.

At the end of the second curve, a 1.2 km (three-quarter mile) section of five to six percent downgrade is encountered. The subsequent 4.8 km (three miles) of the alignment is a series of six, 20- to 60-degree curves of moderate radii with varying up- and downgrades of one to three percent. The last 2.4 km (one and one-half miles) of this section of the alignment is a four to five percent upgrade.

This entire section of the I-70 alignment has a fairly wide right-of-way with few constraints. Jersey barriers separate sections of the alignment with moderate to steep slopes at the shoulders of the roadway. Other sections of the alignment are sufficiently wide to allow grassy medians between the opposite directions of the roadway. However, few if any difficulties other than tall columns should be required in the construction of the maglev system guideway.

Geologic and Environmental Considerations
There are no obvious geologic considerations in this section.

Floyd Hill to Idaho Springs
Vertical and Horizontal Alignment Issues
Floyd Hill is a steep, 3.2 km (two-mile) downgrade to Clear Creek. Grades in this section approach six percent and a tight, 70-degree curve exists at the base of hill. Speeds must be slowed significantly from the 70-mile per hour speed limit to safely navigate the curve. The sharp curve is required due to a high, almost vertical rock wall defining the northern bank of Clear Creek at the base of Floyd Hill. The curve is situated over Clear Creek and US 6.

The base of Floyd Hill is the first location where a significant deviation from the I-70 corridor might be considered. Rather than making the sharp left curve to follow I-70 and Clear Creek to Idaho Springs, the

Figure 16: I-70 Westbound at base of Floyd Hill

maglev system alignment might optionally curve to the right to follow the Kermit's Bar alignment. This alignment would require the maglev system to climb a very steep grade (approaching 12 percent) just east of the rock face that greets westbound I-70 travelers at the base of Floyd Hill. The steepness of the grade is beyond that traditional rubber or steel wheel traction technology can traverse. After the initial grade, the optional Kermit's Bar alignment offers the potential for fewer curves and horizontal alignment difficulties than the I-70 alignment and eliminates the need for an additional tunnel bore at the Twin Tunnels.

Back on the I-70 alignment from the base of Floyd Hill, a winding horizontal alignment with a gentle grade rising to the west characterizes this segment of the right-of-way as it follows Clear Creek. Before reaching Idaho Springs, I-70 passes through the twin tunnels, two adjacent, narrow tunnels under a mountainside that separates westbound and eastbound traffic. The maglev system could potentially cross up and over the mountainside or a new tunnel would be required.

Figure 17: I-70 Eastbound at Twin Tunnels

Figure 18: Alternative alignment overlooking I-70 West of Kermit's Bar

Most of this segment of the alignment is in a narrow valley between the mountains and the creek. West of the tunnels, I-70 quickly approaches the City of Idaho Springs, pressed in a narrow strip between I-70 on the south and mountains on the north. In many areas, I-70 comes close to residential and commercial properties.

Geologic and Environmental Considerations
Since this segment of the I-70 alignment passes through an area with very steep side slopes, there is a danger from rockfalls. The danger is the greatest near the twin tunnels.

2.1.3.2. Segment 2 - Idaho Springs to Eagle County Airport

2.1.3.2.1. *Plans and Profiles*
The route for Segment 2, Idaho Springs to Eagle County Airport, is discussed below.

Idaho Springs to U.S. 40 Juncture
Vertical and Horizontal Alignment Issues
West of Idaho Springs, I-70 continues to climb westward with moderate (2-3 percent) vertical grades and frequent tight, horizontal curves following the Clear Creek Valley. At Exit 233, near Douglas Mountain, US 40 splits from I-70 and heads west and north to the Town of Empire and the Winter Park Ski Area. Most of this segment of the alignment is in a narrow valley between the mountains and the creek.

Figure 19: I-70 at US 40 Interchange

Geologic and Environmental Considerations
Since this segment of the I-70 alignment passes through an area with very steep side slopes, there is a danger of rockfalls.

US 40 to Eisenhower Tunnel
Vertical and Horizontal Alignment Issues
West of US 40, I-70 enters a steep, long climb westward with six percent grades. However, the I-70 right-of-way improves as the roadway approaches the Loveland Ski Area on the east side of the Eisenhower Tunnel.   On the east side of the tunnel, US 6 splits from I-70 and heads south over Loveland Pass to the Arapahoe Basin Ski Area. Past the US 6 Juncture, I-70 enters the Eisenhower Tunnel.

At 3,355 m (11,000 feet) above sea level, the Eisenhower Tunnel is the highest auto tunnel in the world. The tunnel is 2.7 km (1.7 miles) long and runs under the Continental Divide. The tunnel is located approximately 97 km (60 miles) west of Downtown Denver. The tunnel provides a 14.7 km (9.1-mile) savings in horizontal distance compared to US 6 over Loveland pass. The tunnel has two bores, the north bore handling westbound traffic and the south bore handling eastbound traffic. Both bores have two through lanes of traffic.

The maglev system would leave the I-70 right of way at the Eisenhower tunnel passing through the mountainside at a higher point thereby reducing the length of the new transit tunnel bore.

Figure 20: I-70 Westbound west of Eisenhower-Johnson Memorial Tunnel

Geologic and Environmental Considerations
West of Silver Plume, debris flow areas and avalanche shoots are visible along the I-70 roadway. Debris, avalanches and rockfalls, when they occur, pose a serious hazard for motorists as well as any new transit system.

Eisenhower Tunnel to Copper Mountain
Vertical and Horizontal Alignment Issues

Having reached the highest elevation on the alignment at the Eisenhower tunnel, I-70 begins a long descent to the west. On the west portal of the Eisenhower tunnel, I-70 right-of-way begins to narrow once more. I-70 follows Straight Creek down steep grades to the west before approaching the towns of Dillon, Silverthorne and Frisco located on Dillon Reservoir along I-70. Stations would potentially be located near Dillon on the east end of Dillon Reservoir and Frisco on the west end of Dillon Reservoir. In this area, US 6 rejoins I-70 on the northeast side of

Figure 21: I-70 Westbound west of Eisenhower-Johnson Memorial Tunnel

the Dillon Reservoir. Past Dillon, the alignment turns southwards and begins a slow ascent. The open valley near the Dillon Reservoir transitions to a narrow, winding mountain valley following Tenmile Creek. As the alignment approaches Wheeler Junction and the Copper Mountain Ski Area it turns sharply west. The Copper Mountain-Wheeler Junction Area is another potential station area. Relatively flat, open land near Wheeler Junction could serve a station and Park-n-Ride.

Figure 22: I-70 at Copper Mountain looking west

Geologic and Environmental Considerations
Rockfall and avalanche areas at the west portal of the tunnel create hazards for motorists. The right-of-way is bordered in many areas by Arapahoe National Forest land.

Vail Pass (Copper Mountain to Vail)
Vertical and Horizontal Alignment Issues
I-70 turns sharply north near Vail Pass. Sharp horizontal curves make a potential maglev system alignment in the I-70 right-of-way challenging. I-70 then turns west at Gore Creek and follows the creek's valley west into the Town of Vail. The Town of Vail is located in a narrow, mountain alley south of I-70 and is a potential station site.

Figure 23: I-70 at East Vail Looking Eastbound Toward Vail Pass

Geologic and Environmental Considerations
Wetlands border I-70 at many places near Vail pass. Rockfall continues to be an issue along this portion of the alignment.

Vail to Eagle County Airport
Vertical and Horizontal Alignment Issues
West of Vail, I-70 heads southwest to a juncture with US 24 and the Denver and Rio Grande Railroad. Here, US 24 runs south to the town of Minturn and Leadville while I-70 and the railroad turn northwest toward the towns of Avon (a potential station site) and Edwards. At this juncture, exit 171, US 6 also splits from I-70 and begins to parallel I-70 on its westward course. The roadway continues to gradually descend to the west.

Past Edwards, the valley becomes more open and dry although many sharp, horizontal curves persist in the alignment

Figure 24: I-70 west of Vail near Eagle County Airport

as I-70 follows the Eagle River. Near Milk Creek, US 6 crosses I-70 and runs parallel to I-70 on the south side of the Eagle River. Near Wolcott, I-70 turns from its northwest course and begins to head southwest toward the town of Eagle. The Eagle County Airport, the final station site, is located 9.7 km (six miles) east of Eagle to the south of I-70, the Eagle River, the Rio Grande Railroad and US 6. To reach the airport from I-70, one must exit I-70 onto US 6 either 9.7 km (six miles) east of the airport at the town of Eagle or approximately six km (four miles) west of the airport at the Town of Gypsum.

Figure 25: Eagle County Airport access roadway

Geologic and Environmental Considerations
Wetlands and limited right-of-way characterize this area and in many places I-70 crosses over swift flowing streams feeding into the Eagle River. Rockfall continues to be an issue along this portion of the alignment.

2.1.4. *Alignment Alternatives*

One of the primary goals of the CMP has been deployability, which relates directly to optimization of cost. Cost optimization has been the basis of a number of decisions for the CMP. The Eisenhower Johnson Memorial Tunnel (EJMT) area is a potentially expensive area if the maglev system would follow the highway through a new EJMT tunnel bore. At this location, as well as in the Twin Tunnels area, the optimization between tunnel length and maximum grade capabilities of the maglev system has been assessed. Although the propulsion motors have been designed for use up to and including 12% grades, grades up to 18% are operationally achievable with additional cooling for the motors as well as using the full performance capability of the inverter.

A key issue for the CMP has been avoiding tunnels, historically proven to be expensive in any construction project. The tunnels just east of Idaho Springs, known as the Twin Tunnels, have had an alternative maglev alignment defined, and the EJMT area has now also been addressed. Maglev technology possesses characteristics, particularly its ability to climb substantial grades and its freedom from dependence on friction for its traction, which permits it to avoid expensive tunnels.

The following discussion relates to avoidance or reduction in length of tunnels for the CMP, specifically at the Twin Tunnels and then at the EJMT.

Much of the information related to the geology at both the Twin Tunnels area and the EJMT was provided by CDOT Region 1.

2.1.4.1. Twin Tunnels Alternative Alignment

I-70 passes through the Twin Tunnels in the region of Idaho Springs. Although not particularly long, avoidance of a tunnel in this area could potentially reduce costs. The geologic conditions at the Twin Tunnels are comprised of biotite gneiss and migmitite. Occasional zones of granitic intrusions may also be encountered. This site is not difficult for tunneling.

For the maglev system, a path around this tunneled area would move to the north of the highway, and would climb slightly, as shown below.
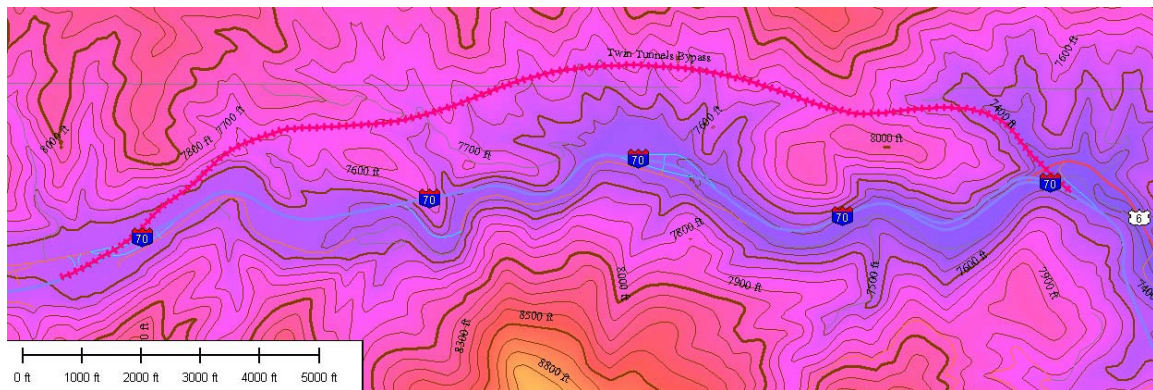
Figure 26: Twin Tunnels Alternative Alignment

The slope required for a guideway in this area would range from 12 to 15%, as can be seen from the plots of the terrain slope along the alternate path. As the elevation plot shows, several cuts would have to be made, and several bridges would have to be built. However, if these actions were taken, the maglev trains could negotiate this alternative route at full speed.
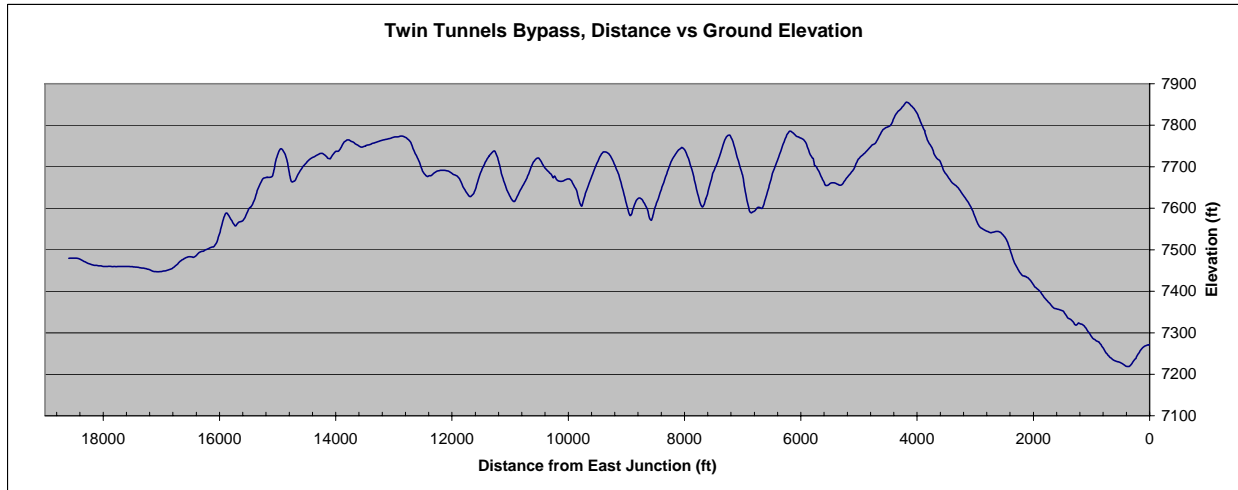
Figure 27: Twin Tunnels Bypass Elevation Profile
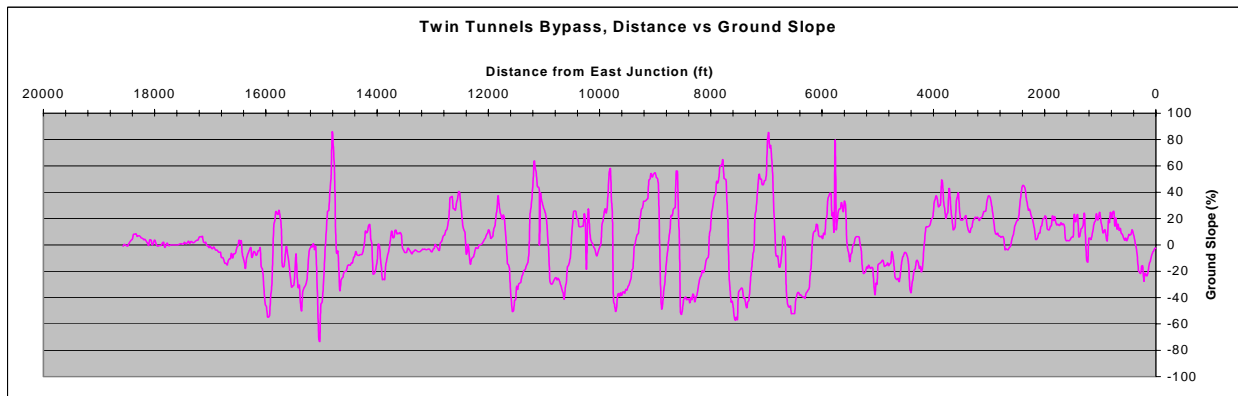
Figure 28: Twin Tunnels Bypass Slope Profile

2.1.4.1.1. *Twin Tunnels Alternative Alignment Cost Tradeoffs*

The cost of the alignment around the Twin Tunnels is $84.5 million, while the cost of a transit tunnel is $10.5 million plus the cost of the guideway along I-70. The 5.67 km (3.52 mile) alternative alignment adds approximately 0.05 km (0.03 miles) to the length of the maglev system (compared to the direct tunneled route) and saves approximately $10.5 million in construction costs due exclusively to tunneling. However, the alternate route in this area will require cuts, fills, and substantial bridging, so these two approaches may, upon further study, be considered roughly equivalent in cost.

2.1.4.2. Eisenhower Johnson Memorial Tunnel Alternative Alignments

The EJMT area is far more complex due to the history and geology of the immediate area.

The Colorado Department of Highways, as the Colorado Department of Transportation was then known, investigated possible tunnel sites through the Continental Divide during 1943-1960. Several routes were considered, namely Berthoud Pass, Vasquez Pass, Devil's Thumb, Jones Pass, Loveland Pass, and the Straight Creek Route. The Straight Creek Route would eventually become the Eisenhower-Johnson Memorial Tunnel.

Topographically, the ground surface above the tunnels consists of steep mountain terrain. The Continental Divide forms a high mountain ridge that trends northeast-southwest across the area. The divide over I-70 is located approximately one-third of the distance from the east portal and two-thirds the distance to the west portal. West of the Divide, the ground is steeply sloping with gradients steeper than 1H:1V. Snow avalanche chutes form in the vicinity of the portal. Glaciation formed the large cirque east of the Divide that is the dominant geomorphic feature of the area overlying the present tunnels. Within the cirque are minor ridges, drainage systems and hummocky terrain consistent with glaciation.

Bedrock at the tunnel site consists of the Silver Plume Granite and the Idaho Springs Formation. The Silver Plume Granite is a medium-to coarse-grained, biotite-rich, igneous rock of Pre-Cambrian age. Biotite schist and gneiss of the older Idaho Springs Formation are metamorphosed sediments which appear as inclusions within the granite. Pegmatite dikes cross-cut the granite and metasedimentary rocks occur throughout the tunnel and range from a few inches to several feet in thickness. Several diorite dikes of probable Tertiary age intrude the older rocks in the west-central portion of the tunnel.

The bedrock within the tunnel region is igneous and metamorphic. The primary rock types within the tunnel are generally granite and meta-sedimentary gneiss and schist. The granite is gneissic, quartzitic and/or pegmatitic with biotite and ranges from slightly to highly weathered, with the feldspar altered to clay. The foliated metamorphic rock is biotitic gneiss with schist. It was estimated that of the metamorphic rock, about half the gneiss and all of the schist was highly decomposed and damp. This rock type represents the most incompetent rock found in the tunnel.

During the course of evaluation of potential sites for the Continental Divide tunnel, a pioneer tunnel bore south of the EJMT was constructed underneath Loveland Pass in 1943. The 2 meter by 2 meter (7 feet by 7 feet) diameter tunnel was driven using drill and blast methods. The tunnel was considered to be in extremely bad ground or rock conditions and likely encountered the Loveland Shear Zone. A larger tunnel diameter was not constructed at that time since it was considered cost prohibitive due to the poor ground conditions.

During construction of the eastern portal location for the proposed EJMT in 1963, a large slope failure, or landslide, was initiated by the removal of the toe of a metastable slope. This slope failure became known as the East Portal Landslide. The initial movement was estimated to encompass 2,000,000 cubic yards of highly fractured bedrock. Subsequent estimates encompassed 3,000,000 cubic yards. Figure 29 illustrates the landslide area in 1965. The photo is looking north.
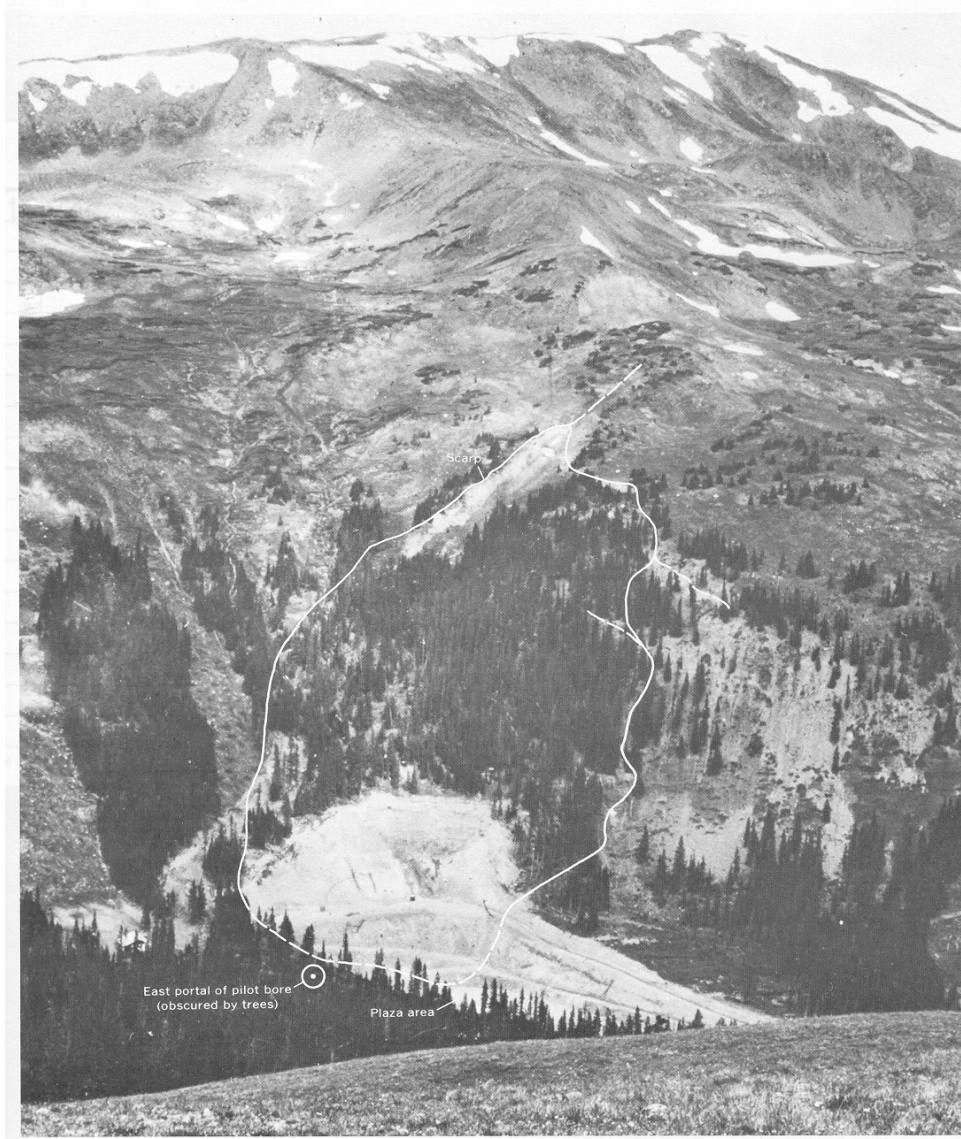
Figure 29: Loveland Basin Landslide, 1965.

The previous discussion is provided to make the point that an alternative to a new transit system tunnel bore near the EJMT would be advisable from both the construction difficulty aspect as well as for reasons of cost. The cost for a transit-only bore is approximately $333,500,000 while for a dual use tunnel the cost is approximately $377,500,000. The location of tunnels represents an issue for CDOT for any highway expansion as well as for highway combined with transit and CDOT should be responsible for any decisions regarding tunneling.

However, for the alternative maglev system alignment, an analysis of prospective alignments to the north of EJMT has been done along with review of alignments to the south of EJMT. The alignments to the south would attempt to use the area of the Loveland Pass pioneer bore that has been deemed poor due to the geology of the area. In addition, an alignment to the south passing under Loveland Pass would lead to a transit alignment through the Keystone Ski Resort paralleling the Snake River rather than following I-70. The alignment through Keystone is beyond

the scope of the FTA project. Comprehensive review of the southern alignment prospects indicates that they are generally inferior to a northern alignment.
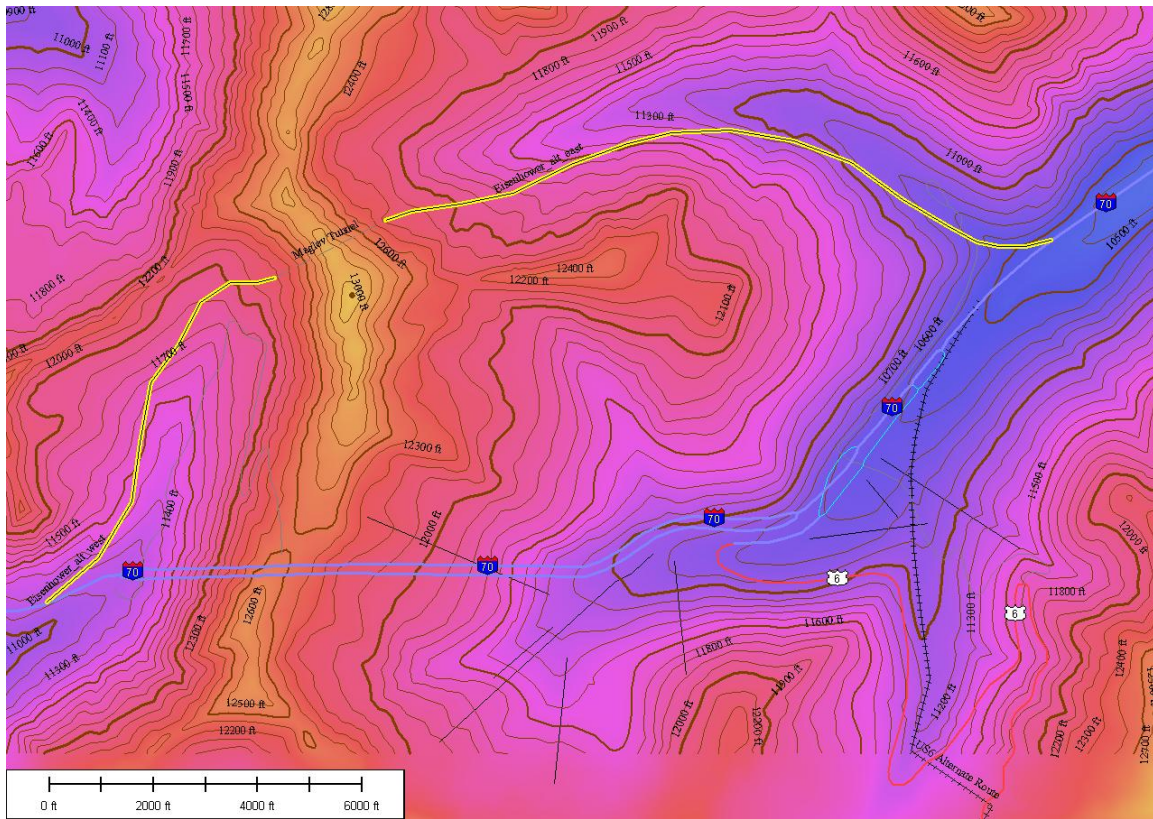
Figure 30: EJMT Alternative Alignment, with Short Tunnel

Herman Gulch, north of EJMT, offers the best opportunity for ascending the Continental Divide. There are a couple of ways to actually cross before heading back down to I-70, as the topological paths clearly show.

The first alternative moves to the top in the region of Hager Mountain, and tunnels quickly under the peak. With a short tunnel, slopes well under 20% for the majority of the crossing are attainable without undue moving of mountains. The tunnel required is 701 meters (2,300 feet) in length. Additionally, all the curves are of reasonably large radius, which would minimize the need to slow down for the crossing.
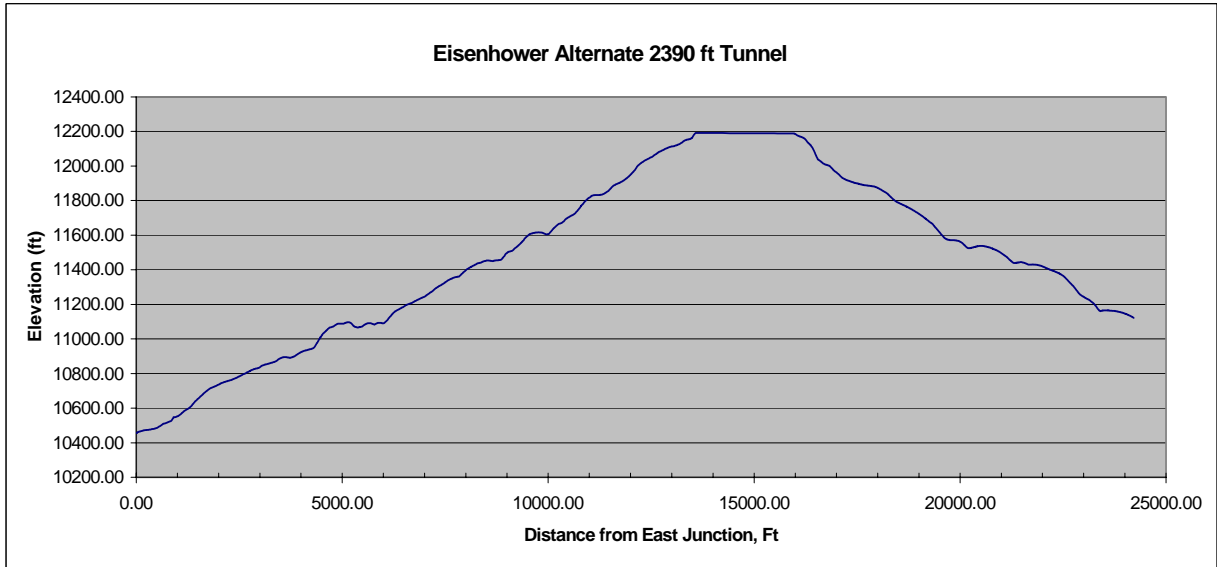
Figure 31: Eisenhower Alternative 2390 foot Tunnel Elevation Profile
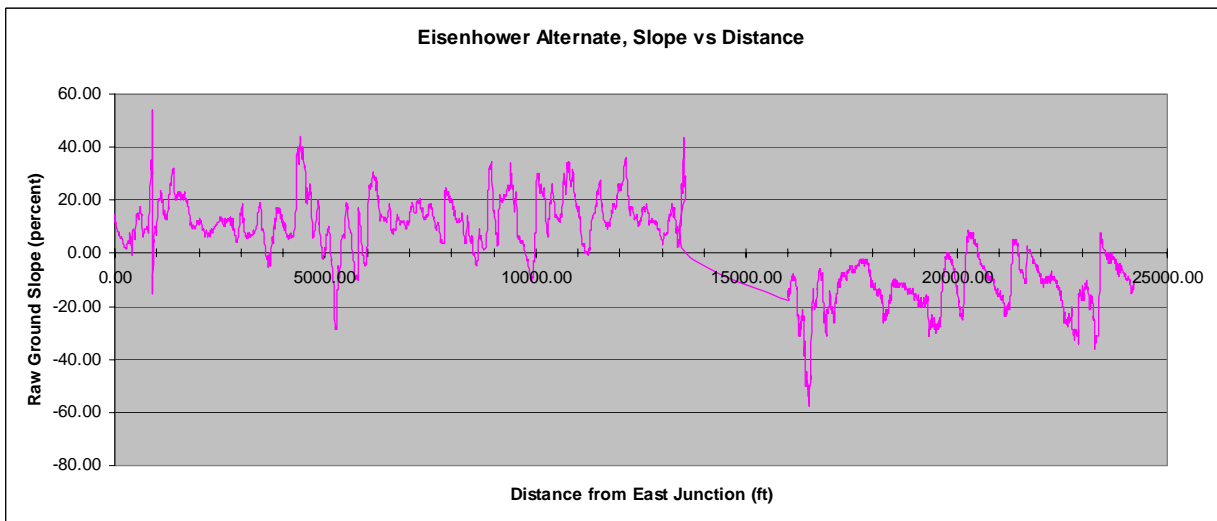
Figure 32: Eisenhower Alternative 2390 foot Tunnel Slope Profile

The second alternative requires no tunnel at all, climbing on up to the full height of the Divide, 3,813 meters (12,500 feet) above sea level, and turning south, beginning its descent through a saddle south of Hager Mountain. From this point, the guideway descends quickly, as shown in the elevation plot.
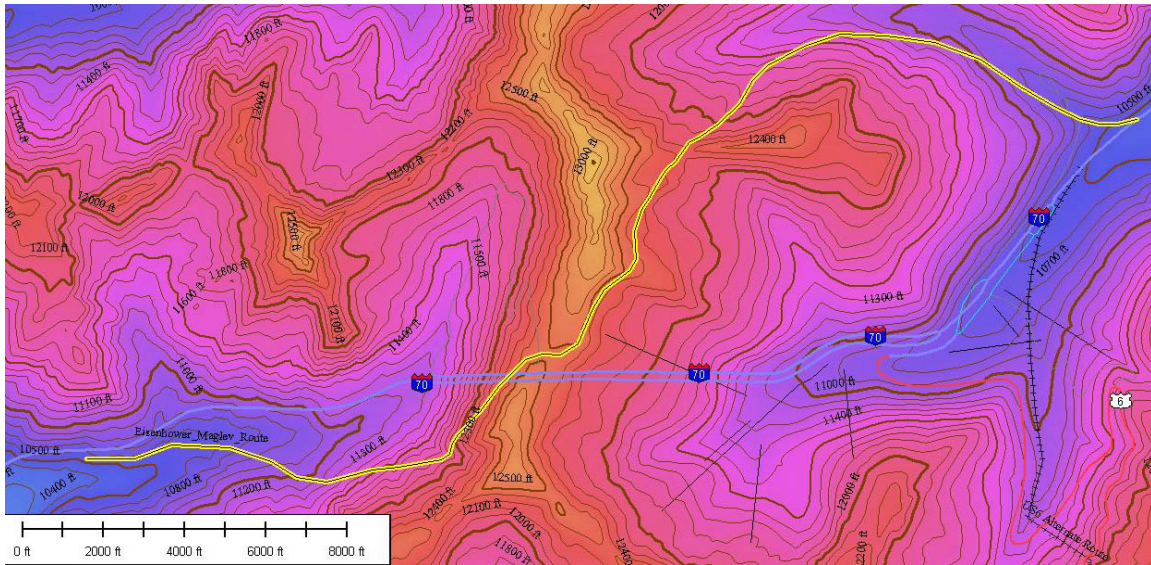
Figure 33: EJMT Alternative Maglev Alignment with No Tunnel

As before, note that although the grades look rugged, the average grade is mostly 20% or less on the eastern segment, and averages little more than 25% on the western segment. On the distance versus elevation plot, if the small ridges and gullies are smoothed, the elevation drops in a fairly linear fashion from 3,813 meters (12,500 feet) to 3, 200 meters (10,500 feet) over a span of 2,745 meters (9,000 feet) horizontal travel, which corresponds to a 22% average grade – very steep, to be certain, but probably close to the abilities of the maglev vehicle (the maximum grade climbing ability for the present motor is 18%).
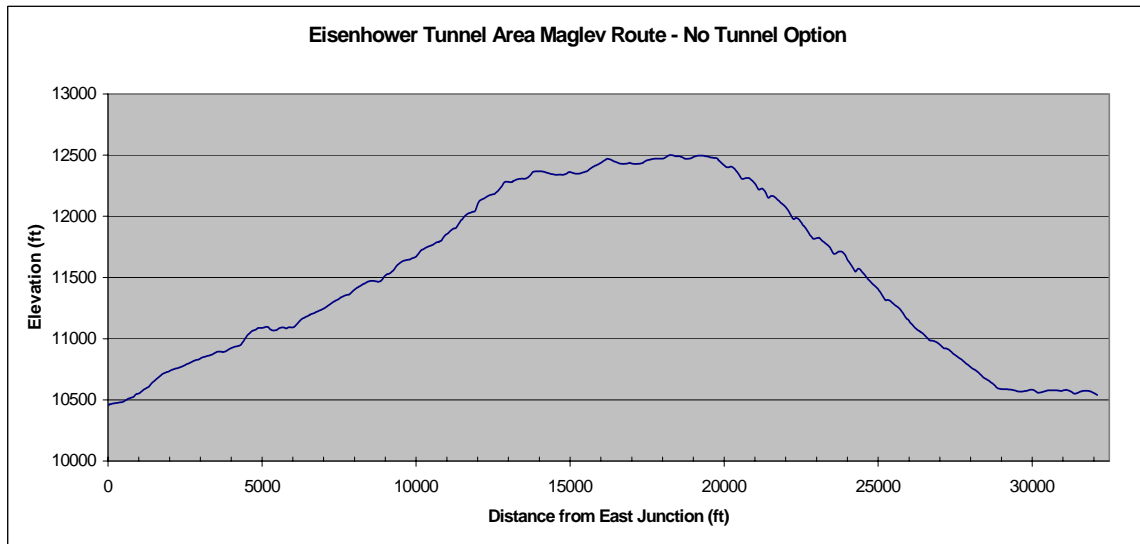
Figure 34: EJMT Alternative (No Tunnel) Elevation Profile

This grade could possibly be improved by taking an even more oblique path down the western side of the mountain, or by a variety of other techniques. There are several approaches to mitigate the slope. For example, it is feasible to employ switchbacks with maglev, due to the bi-directional nature of the trains. If this were to be pursued, the slope could probably be reduced to 10-12%, although the trip time would be lengthened.
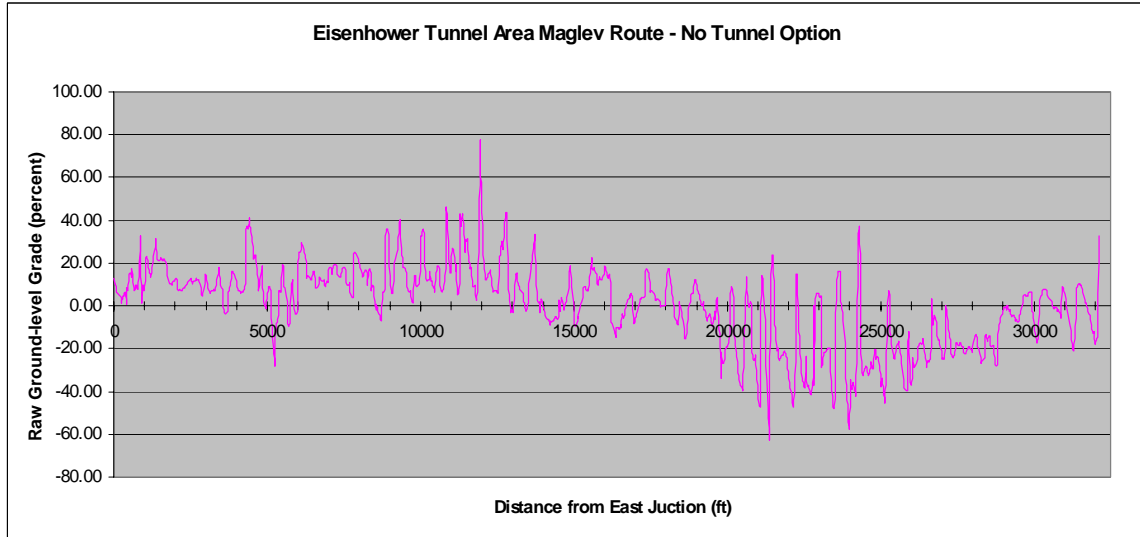
Figure 35: EJMT Alternative (No Tunnel) Slope Profile

There are many strategies to accomplish this transit alignment on the western face of the Divide in a safe manner, and there is no doubt that this would be a spectacular ride, ranking this as a must-see feature of the Rocky Mountains, and of the state.

In any consideration of alternative alignments to the I-70 alignment, consideration must be given to the constructability of the guideway. In areas removed from I-70, access to the construction site would be difficult. In addition, a short construction period due to winter conditions would complicate alternative routing as well as rockfall and avalanche areas. However, with the costs of tunneling these factors will need further scrutiny in order to provide the optimum system cost.

2.1.4.2.1. *EJMT Alternative Alignment Cost Tradeoffs*

The least costly alignment around the EJMT is $165 million while the tunneling cost of a new EJMT transit tunnel is $333.5 million. The alternative alignment is 7,328 m or 7.37 km (24,204 feet or 4.58 miles) in length and bypasses 6329 m or 6.3 km (20750 feet or 3.93miles) in length of I-70 on its alignment through the EJMT. The added length in guideway for this alternative is 1047 m or 1 km (3432 feet or 0.65miles) with 701 m (2300 feet) of this in a tunnel under the Continental Divide. The projected costs for the alternative alignment were derived using the CDOT PEIS estimate for tunneling costs and the FTA Maglev Project costs for guideway.

2.1.4.3. **Alignment Alternative Conclusions**

What these alternates show is that the CMP route will require significant optimization scrutiny before a route can be formally established. A considerable number of further tradeoffs must be considered before any one approach can be said to be superior, although this analysis has shown a significant potential for savings by using the grade climbing capabilities of the maglev system.

The Hagar Mountain Tunnel alternative is the recommended alignment for the CMP Team. This recommendation is based on cost effectiveness since the alternative alignment will save an

estimated $200 million plus in tunnel costs over the longer EJMT tunnel. It is understood that significant design will be required in subsequent phases of this project to assure constructability as well as determining whether permitting would be provided by the National Forest Service over this terrain.

2.1.5. *Summary and Conclusions*

The preceding sections have discussed the basis for the plans and profiles that will be used for the CMP. The maglev system starting at DIA in Denver will utilize a northern corridor alignment generally along the I-70 right-of-way to the Golden Intermodal Transit Station, with no stations other than DIA in the metropolitan area.

From C470/I-70, a detailed plan and profile has been developed for the C470/I-70 to Idaho Springs segment. The alignment is generally within the I-70 right-of-way, with a diversion from approximately the US 6/I-70 interchange to Idaho Springs just north of I-70 eliminating the need for an additional tunnel bore at the Twin Tunnels just east of Idaho Springs.

From Idaho Springs to Eagle County Airport the alignment is assumed to be in the median of I-70; plans and profiles for this alignment have been developed. Alignment alternatives were discussed at both the Twin Tunnels east of Idaho Springs and at the EJMT to allow for cost savings by either eliminating maglev system tunnels or reducing the length of the required tunnels by utilizing the unique grade climbing capabilities of the maglev system. The I-70 alignment plans and profiles have been used in the simulations models in the integration task; the alternative alignments were considered speculative at the present stage of definition, and were not simulated.

Figure 36: CMP Guideway Plan View

Elevation, DIA to Eagle
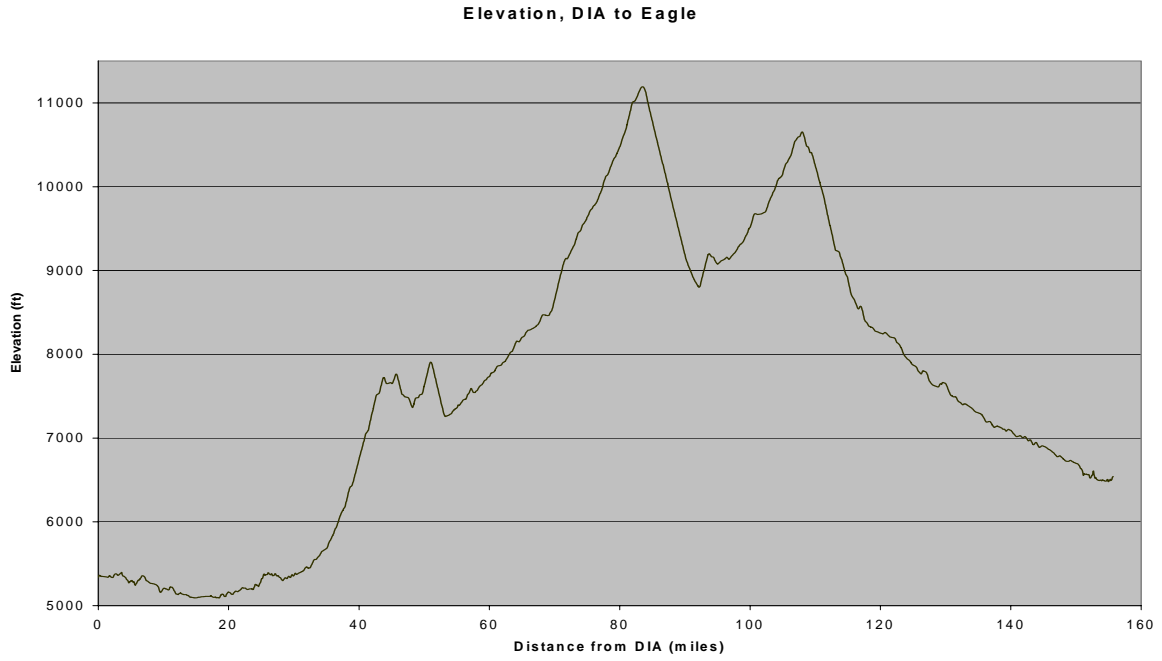
Figure 37: CMP Guideway Elevation Profile

Figure 38: Segments One and Two — Golden to Eagle County Airport

2.2. RIDERSHIP PROJECTIONS

Together with the plans and profiles to be used in simulations models, sizing the system is determined from the patronage demand for the system. A travel model was developed for the I-70 Mountain Corridor as part of the PEIS prepared by CDOT. The PEIS travel model covers the area surrounding the I-70 corridor from DIA to Glenwood Springs. The metropolitan area is included in the I-70 PEIS travel model at a coarse level for the modeling of trips between Denver and the mountain corridor.

CDOT consultants for the I-70 PEIS have completed preliminary ridership forecasts. The patronage forecasts were completed with the following guidelines:

- two day snapshot – winter Saturday & summer Saturday (with a Friday comparison east & west slope)
- 2025 peak hour spreading and annualization of transit ridership in progress
- transit speeds continue to be refined
- net fare definition based on O&M costs in progress (10¢ and 25¢ per mile for comparisons)

The ridership projection to be used in sizing the Colorado maglev system will be 40,000 daily transit passengers.

The ridership tables shown below were produced through the CDOT I-70 PEIS effort. Person-trips were forecasted for each of the alternatives under study for the improvement of I-70, including the maglev alternative, which is shown in the rows labeled "AGS". The CDOT consultants projected ridership numbers for ten locations along the I-70 corridor.

Winter Saturday e/o Genesee — Alternative	2000 Hwy. Vehicle Trips (VT)	2000 Hwy. Person Trips (PT)	WB 2025 Highway VT	EB 2025 Highway VT	2025 Highway VT	2025 Highway PT	% Growth 2000 to 2025 VT	2025 Transit PT	2025 Total PT	% Growth 2000 to 2025 Total PT	Transit as % of Total PT	PT Diff.	Trip Suppression/ Inducement % Diff.	% Diff./yr
Baseline	62,300	125,000	71,000	65,300	136,300	296,700	119%	2,600	299,300	139%	1%			
No Action			52,700	64,100	116,800	254,100	87%	2,600	256,800	105%	1%	(42,500)	-14%	-0.6%
Minimal Action			53,800	64,100	117,900	258,400	89%	11,500	269,900	116%	4%	(29,400)	-10%	-0.4%
Rail Transit			54,400	60,100	114,500	250,700	84%	58,100	308,900	147%	19%	9,600	3%	0.1%
AGS			54,800	60,400	115,200	253,100	85%	66,100	319,200	155%	21%	19,900	7%	0.3%
Dual Mode Bus (DMB)			54,300	62,100	116,400	253,000	87%	65,600	318,600	155%	21%	19,300	6%	0.2%
Diesel Bus			54,400	61,600	116,000	253,900	86%	65,000	319,000	155%	20%	19,700	7%	0.3%
6-Lane Highway Widening			70,600	64,900	135,500	294,800	117%	2,700	297,400	138%	1%	(1,900)	-1%	0.0%
Reversible Lane			70,700	65,400	136,100	296,000	118%	2,600	298,600	139%	1%	(700)	0%	0.0%
Combination 6-Lane Widening & Rail Transit			70,400	62,700	133,100	292,100	114%	58,800	350,900	181%	17%	51,600	17%	0.6%
Combination 6-Lane Widening & AGS			67,100	59,500	126,600	278,300	103%	66,400	344,700	176%	19%	45,400	15%	0.6%
Combination 6-Lane Widening & DMB			69,200	61,400	130,700	284,900	110%	64,700	349,600	180%	19%	50,300	17%	0.6%
Combination 6-Lane Widening & Diesel Bus			69,300	61,500	130,800	286,000	110%	64,500	350,500	180%	18%	51,200	17%	0.6%

Winter Saturday at Floyd Hill (East of Highland Hills) Alternative	2000 Hwy. Vehicle Trips (VT)	2000 Hwy. Person Trips (PT)	WB 2025 Highway VT	EB 2025 Highway VT	2025 Highway VT	% Growth 2000 to 2025 VT	2025 Transit PT	2025 Highway PT	2025 PT	% Growth 2000 to 2025 Total PT	Transit as % of Total PT	Trip Suppression/ Inducement PT Diff.	% Diff.	% Diff./yr
Baseline	49,300	95,000	67,800	61,600	129,400	162%	2,600	280,600	283,200	198%	1%			
No Action			50,100	59,500	109,700	122%	2,600	237,900	240,500	153%	1%	(42,700)	-15%	-0.7%
Minimal Action			51,300	59,700	111,000	125%	10,900	242,500	253,400	167%	4%	(29,800)	-11%	-0.4%
Rail Transit			51,800	55,800	107,600	118%	56,300	234,200	290,500	206%	19%	7,300	3%	0.1%
AGS			52,300	55,100	107,500	118%	64,400	234,800	299,200	215%	22%	16,000	6%	0.2%
Dual Mode Bus (DMB)			52,000	56,700	108,700	120%	63,900	234,700	298,600	214%	21%	15,400	5%	0.2%
Diesel Bus			51,900	56,400	108,400	120%	63,200	235,700	298,900	215%	21%	15,700	6%	0.2%
6-Lane Highway Widening			68,000	61,500	129,500	162%	2,600	280,600	283,200	198%	1%		0%	0.0%
Reversible Lane			68,100	62,000	130,100	164%	2,600	281,800	284,400	199%	1%	1,200	0%	0.0%
Combination 6-Lane Widening & Rail Transit			67,200	59,100	126,300	156%	57,500	275,600	333,100	251%	17%	49,900	18%	0.7%
Combination 6-Lane Widening & AGS			64,400	56,500	120,900	145%	64,900	264,000	328,900	246%	20%	45,700	16%	0.6%
Combination 6-Lane Widening & DMB			66,300	58,100	124,400	152%	63,300	269,300	332,700	250%	19%	49,400	17%	0.6%
Combination 6-Lane Widening & Diesel Bus			66,400	58,200	124,600	153%	62,800	270,600	333,400	251%	19%	50,200	18%	0.7%

Winter Saturday at Twin Tunnels Alternative	2000 Hwy. Vehicle Trips (VT)	2000 Hwy. Person Trips (PT)	WB 2025 Highway VT	EB 2025 Highway VT	2025 Highway VT	2025 Highway PT	% Growth 2000 to 2025 VT	2025 Transit PT	2025 Total PT	% Growth 2000 to 2025 Total PT	Transit as % of Total PT	PT Diff.	Trip Suppression/Inducement % Diff.	% Diff./yr
Baseline	57,000	109,800	47,800	40,300	88,100	186,800	54%	2,500	189,300	72%	1%			
No Action			34,600	35,500	70,100	148,700	23%	2,500	151,100	38%	2%	(38,100)	-20%	-0.9%
Minimal Action			35,600	36,200	71,800	153,600	26%	7,600	161,300	47%	5%	(28,000)	-15%	-0.6%
Rail Transit			35,400	32,900	68,400	143,800	20%	45,500	189,300	72%	24%		0%	0.0%
AGS			35,200	28,800	64,100	135,000	12%	54,200	189,200	72%	29%		0%	0.0%
Dual Mode Bus (DMB)			35,300	29,900	65,200	135,400	14%	53,900	189,300	72%	28%		0%	0.0%
Diesel Bus			35,300	30,300	65,700	136,800	15%	52,500	189,300	72%	28%		0%	0.0%
6-Lane Highway Widening			50,300	41,200	91,500	193,900	60%	2,600	196,400	79%	1%	7,200	4%	0.1%
Reversible Lane			50,800	41,500	92,300	195,200	62%	2,400	197,600	80%	1%	8,300	4%	0.2%
Combination 6-Lane Widening & Rail Transit			47,200	38,600	85,900	180,800	51%	49,500	230,300	110%	21%	41,000	22%	0.8%
Combination 6-Lane Widening & AGS			46,800	38,300	85,000	178,500	49%	56,400	234,800	114%	24%	45,600	24%	0.9%
Combination 6-Lane Widening & DMB			47,400	38,800	86,200	178,500	51%	55,200	233,700	113%	24%	44,400	23%	0.8%
Combination 6-Lane Widening & Diesel Bus			47,600	39,000	86,600	180,400	52%	52,700	233,000	112%	23%	43,800	23%	0.8%

Winter Saturday e/o Empire Jct. Alternative	2000 Hwy. Vehicle Trips (VT)	2000 Hwy. Person Trips (PT)	WB 2025 Highway VT	EB 2025 Highway VT	2025 Highway VT	2025 Highway PT	% Growth 2000 to 2025 VT	% Growth 2000 to 2025 Transit PT	2025 Total PT	% Growth 2000 to 2025 Total PT	Transit as % of Total PT	PT Diff.	Trip Suppression/ Inducement % Diff.	% Diff./yr
Baseline	49,600	95,600	45,600	38,600	84,200	178,000	70%	2,400	180,400	89%	1%			
No Action			33,500	34,600	68,200	144,100	37%	2,400	146,500	53%	2%	(33,900)	-19%	-0.8%
Minimal Action			34,500	35,200	69,700	148,600	40%	7,500	156,100	63%	5%	(24,300)	-13%	-0.6%
Rail Transit			34,100	31,400	65,400	137,000	32%	44,600	181,600	90%	25%	1,200	1%	0.0%
AGS			33,600	27,700	61,400	128,800	24%	52,600	181,400	90%	29%	1,000	1%	0.0%
Dual Mode Bus (DMB)			34,000	29,100	63,100	130,400	27%	52,000	182,400	91%	28%	2,000	1%	0.0%
Diesel Bus			33,600	29,100	62,800	130,100	26%	50,300	180,400	89%	28%		0%	0.0%
6-Lane Highway Widening			47,700	39,400	87,100	184,000	76%	2,500	186,600	95%	1%	6,100	3%	0.1%
Reversible Lane			48,300	39,900	88,200	185,900	78%	2,300	188,300	97%	1%	7,900	4%	0.2%
Combination 6-Lane Widening & Rail Transit			44,900	37,100	82,000	171,900	65%	48,600	220,500	131%	22%	40,000	22%	0.8%
Combination 6-Lane Widening & AGS			44,400	36,700	81,100	169,400	63%	55,000	224,400	135%	25%	44,000	24%	0.9%
Combination 6-Lane Widening & DMB			45,100	37,200	82,300	169,600	66%	53,700	223,200	134%	24%	42,800	24%	0.9%
Combination 6-Lane Widening & Diesel Bus			45,300	37,400	82,700	171,600	67%	51,100	222,600	133%	23%	42,200	23%	0.8%

Winter Saturday at EJMT Alternative	2000 Hwy. Vehicle Trips (VT)	2000 Hwy. Person Trips (PT)	WB 2025 Highway VT	EB 2025 Highway VT	2025 Highway VT	2025 Highway PT	% Growth 2000 to 2025 VT	% Growth 2000 to 2025 Transit PT	2025 PT	Total 2025 Total PT	% Growth 2000 to 2025 Total PT	Transit as % of Total PT	PT Diff.	Trip Suppression/ Inducement % Diff.	% Diff./yr
Baseline	36,200	75,900	31,100	27,100	58,200	120,900	61%	2,200	123,000		62%	2%			
No Action			25,300	27,100	52,400	108,800	45%	2,200	111,000		46%	2%	(12,000)	-10%	-0.4%
Minimal Action			25,900	27,100	53,000	111,000	46%	6,200	117,200		54%	5%	(5,900)	-5%	-0.2%
Rail Transit			24,200	21,100	45,300	92,400	25%	38,500	130,900		72%	29%	7,900	6%	0.2%
AGS			23,000	20,100	43,100	88,300	19%	41,700	130,000		71%	32%	6,900	6%	0.2%
Dual Mode Bus (DMB)			24,700	22,700	47,400	95,000	31%	39,000	134,000		76%	29%	11,000	9%	0.3%
Diesel Bus			24,600	22,400	46,900	94,500	30%	36,000	130,500		72%	28%	7,500	6%	0.2%
6-Lane Highway Widening			31,400	27,400	58,800	121,800	62%	2,200	124,000		63%	2%	1,000	1%	0.0%
Reversible Lane			32,500	28,400	60,900	126,100	68%	2,200	128,200		69%	2%	5,200	4%	0.2%
Combination 6-Lane Widening & Rail Transit			30,000	26,200	56,200	114,900	55%	42,500	157,500		107%	27%	34,400	28%	1.0%
Combination 6-Lane Widening & AGS			29,600	25,800	55,400	112,400	53%	45,900	158,300		108%	29%	35,300	29%	1.0%
Combination 6-Lane Widening & DMB			30,100	26,300	56,500	112,800	56%	43,900	156,600		106%	28%	33,600	27%	1.0%
Combination 6-Lane Widening & Diesel Bus			30,600	26,700	57,200	115,300	58%	40,500	155,800		105%	26%	32,800	27%	0.9%

Winter Saturday between Frisco and Silverthorne — Alternative	2000 Hwy. Vehicle Trips (VT)	2000 Hwy. Person Trips (PT)	WB 2025 Highway VT	EB 2025 Highway VT	2025 Highway VT	2025 Highway PT	% Growth 2000 to 2025 VT	2025 Transit PT	2025 Total PT	% Growth 2000 to 2025 Total PT	Transit as % of Total PT	PT Diff.	Trip Suppression/ Inducement % Diff.	% Diff./yr
Baseline	39,900	83,700	30,800	26,900	57,700	119,300	45%	2,100	121,400	45%	2%			
No Action			25,200	26,900	52,100	107,600	30%	2,100	109,800	31%	2%	(11,700)	-10%	-0.4%
Minimal Action			25,800	26,900	52,700	109,300	32%	6,100	115,400	38%	5%	(6,000)	-5%	-0.2%
Rail Transit			24,000	21,000	45,000	91,300	13%	38,000	129,300	54%	29%	7,900	6%	0.3%
AGS			22,900	20,000	42,900	87,200	7%	41,200	128,400	53%	32%	7,000	6%	0.2%
Dual Mode Bus (DMB)			24,500	22,500	47,000	93,700	18%	38,500	132,200	58%	29%	10,800	9%	0.3%
Diesel Bus			24,400	22,200	46,600	93,300	17%	35,500	128,800	54%	28%	7,400	6%	0.2%
6-Lane Highway Widening			31,100	27,200	58,300	120,300	46%	2,100	122,400	46%	2%	1,000	1%	0.0%
Reversible Lane			32,300	28,100	60,400	124,400	51%	2,100	126,500	51%	2%	5,100	4%	0.2%
Combination 6-Lane Widening & Rail Transit			29,800	26,000	55,700	113,300	40%	41,900	155,300	85%	27%	33,900	28%	1.0%
Combination 6-Lane Widening & AGS			29,300	25,600	54,900	110,800	37%	45,300	156,100	86%	29%	34,700	29%	1.0%
Combination 6-Lane Widening & DMB			29,900	26,100	56,000	111,100	40%	43,300	154,400	84%	28%	33,000	27%	1.0%
Combination 6-Lane Widening & Diesel Bus			30,300	26,400	56,700	113,600	42%	40,000	153,500	83%	26%	32,100	26%	0.9%

Winter Saturday at Vail Pass (w/o Copper Mountain) Alternative	2000 Hwy. Vehicle Trips (VT)	2000 Hwy. Person Trips (PT)	WB 2025 Highway VT	EB 2025 Highway VT	2025 Highway VT	2025 Highway PT	% Growth 2000 to 2025 VT	2025 Transit PT	2025 Total PT	% Growth 2000 to 2025 Total PT	Transit as % of Total PT	Trip Suppression/ Inducement PT Diff.	% Diff.	% Diff./yr
Baseline	17,900	36,400	19,300	16,900	36,200	72,400	102%	200	72,700	100%	0%			
No Action			19,300	16,700	36,000	71,900	100%	200	72,200	98%	0%	(500)	-1%	0.0%
Minimal Action			19,400	16,600	36,000	70,500	101%	2,200	72,700	100%	3%		0%	0.0%
Rail Transit			16,300	13,900	30,300	59,300	69%	13,300	72,700	100%	18%		0%	0.0%
AGS			15,500	13,200	28,700	56,300	60%	16,400	72,700	100%	23%		0%	0.0%
Dual Mode Bus (DMB)			16,300	13,900	30,200	57,800	68%	14,900	72,700	100%	21%		0%	0.0%
Diesel Bus			17,100	14,600	31,700	60,800	76%	11,900	72,600	100%	16%		0%	0.0%
6-Lane Highway Widening			19,700	16,800	36,600	73,100	104%	200	73,300	102%	0%	600	1%	0.0%
Reversible Lane			19,800	16,800	36,600	73,100	104%	200	73,400	102%	0%	700	1%	0.0%
Combination 6-Lane Widening & Rail Transit			18,400	15,700	34,200	67,100	90%	14,600	81,700	125%	18%	9,000	12%	0.5%
Combination 6-Lane Widening & AGS			17,900	15,200	33,100	64,700	85%	17,500	82,200	126%	21%	9,500	13%	0.5%
Combination 6-Lane Widening & DMB			18,200	15,500	33,800	64,400	88%	16,800	81,300	123%	21%	8,600	12%	0.4%
Combination 6-Lane Widening & Diesel Bus			18,800	16,000	34,700	66,700	94%	13,700	80,400	121%	17%	7,700	11%	0.4%

Winter Saturday at Dowd Canyon (e/o Dowd Junction) Alternative	2000 Hwy. Vehicle Trips (VT)	2000 Hwy. Person Trips (PT)	WB 2025 Highway VT	EB 2025 Highway VT	2025 Highway VT	2025 Highway PT	% Growth 2000 to 2025 VT	2025 Transit PT	2025 Total PT	% Growth 2000 to 2025 Total PT	Transit as % of Total PT	PT Diff.	Trip Suppression/ Inducement % Diff.	% Diff./yr
Baseline	30,200	60,600	32,900	28,000	60,900	116,900	102%	3,400	120,200	98%	3%			
No Action			32,900	28,000	60,900	116,900	102%	3,400	120,200	98%	3%		0%	0.0%
Minimal Action			31,800	27,100	58,900	111,300	95%	9,000	120,200	98%	7%		0%	0.0%
Rail Transit			28,400	24,200	52,500	99,700	74%	20,500	120,200	98%	17%		0%	0.0%
AGS			28,100	23,900	52,000	98,700	73%	21,500	120,200	98%	18%		0%	0.0%
Dual Mode Bus (DMB)			29,700	25,300	55,100	102,800	83%	17,400	120,200	98%	14%		0%	0.0%
Diesel Bus			29,700	25,300	55,100	103,000	83%	17,200	120,200	98%	14%		0%	0.0%
6-Lane Highway Widening			33,000	28,100	61,100	117,200	103%	3,400	120,600	99%	3%	400	0%	0.0%
Reversible Lane			33,000	28,100	61,100	117,200	103%	3,400	120,600	99%	3%	400	0%	0.0%
Combination 6-Lane Widening & Rail Transit			31,500	26,900	58,400	110,800	94%	21,700	132,500	119%	16%	12,300	10%	0.4%
Combination 6-Lane Widening & AGS			31,400	26,800	58,200	110,700	93%	22,700	133,300	120%	17%	13,100	11%	0.4%
Combination 6-Lane Widening & DMB			32,600	27,800	60,400	113,000	100%	18,700	131,700	117%	14%	11,500	10%	0.4%
Combination 6-Lane Widening & Diesel Bus			32,900	28,100	61,000	114,100	102%	17,300	131,400	117%	13%	11,200	9%	0.4%

Winter Saturday e/o Eagle Alternative	2000 Hwy. Vehicle Trips (VT)	2000 Hwy. Person Trips (PT)	WB 2025 Highway VT	EB 2025 Highway VT	2025 Highway VT	2025 Highway PT	% Growth 2000 to 2025 VT	2025 Transit PT	2025 Total PT	% Growth Total 2000 to 2025 Total PT	Transit as % of Total PT	PT Diff.	Trip Suppression/Inducement % Diff.	% Diff./yr
Baseline	19,700	36,000	32,800	31,100	63,900	113,800	225%	4,100	117,900	227%	3%			
No Action			32,800	30,700	63,500	113,000	223%	4,100	117,100	225%	3%	(800)	-1%	0.0%
Minimal Action			33,000	30,400	63,400	112,000	222%	5,800	117,800	227%	5%		0%	0.0%
Rail Transit			30,500	28,100	58,600	103,100	198%	14,800	117,900	227%	13%		0%	0.0%
AGS			30,400	28,000	58,400	102,700	197%	15,200	117,800	227%	13%		0%	0.0%
Dual Mode Bus (DMB)			30,600	28,300	58,900	102,300	200%	15,600	117,900	227%	13%		0%	0.0%
Diesel Bus			31,100	28,700	59,900	102,700	205%	15,100	117,900	227%	13%		0%	0.0%
6-Lane Highway Widening			33,300	30,700	64,000	113,900	226%	4,100	118,000	228%	3%	200	0%	0.0%
Reversible Lane			33,300	30,700	64,000	114,100	226%	4,100	118,200	228%	3%	400	0%	0.0%
Combination 6-Lane Widening & Rail Transit			31,900	29,400	61,300	108,600	212%	15,400	124,000	244%	12%	6,100	5%	0.2%
Combination 6-Lane Widening & AGS			31,800	29,300	61,100	108,200	211%	15,700	123,900	244%	13%	6,000	5%	0.2%
Combination 6-Lane Widening & DMB			33,000	30,400	63,400	108,600	223%	16,100	124,700	246%	13%	6,900	6%	0.2%
Combination 6-Lane Widening & Diesel Bus			33,300	30,700	64,000	109,900	226%	15,700	125,600	249%	12%	7,800	7%	0.3%

Winter Saturday w/o No Name / Alternative	2000 Hwy. Vehicle Trips (VT)	2000 Hwy. Person Trips (PT)	WB 2025 Highway VT	EB 2025 Highway VT	2025 Highway VT	2025 Highway PT	% Growth 2000 to 2025 VT	2025 Transit PT	2025 Total PT	% Growth 2000 to 2025 Total PT	Transit as % of Total PT	PT Diff.	Trip Suppression/ Inducement % Diff.	% Diff./yr
Baseline	11,700	21,400	11,200	10,600	21,800	38,300	87%	700	39,000	82%	2%			
No Action			11,300	10,400	21,800	38,300	87%	700	39,000	82%	2%		0%	0.0%
Minimal Action			11,200	10,400	21,600	37,600	86%	1,400	39,000	83%	4%		0%	0.0%
Rail Transit			11,200	10,300	21,500	37,400	85%	1,500	38,900	82%	4%		0%	0.0%
AGS			11,200	10,300	21,500	37,400	84%	1,600	38,900	82%	4%		0%	0.0%
Dual Mode Bus (DMB)			9,700	9,000	18,700	32,200	61%	6,800	39,000	83%	17%		0%	0.0%
Diesel Bus			9,700	9,000	18,700	32,200	61%	6,800	39,000	82%	17%		0%	0.0%
6-Lane Highway Widening			11,300	10,400	21,800	38,300	87%	700	39,000	82%	2%		0%	0.0%
Reversible Lane			11,300	10,400	21,800	38,300	87%	700	39,000	82%	2%		0%	0.0%
Combination 6-Lane Widening & Rail Transit			11,200	10,300	21,500	37,300	84%	1,600	38,900	82%	4%		0%	0.0%
Combination 6-Lane Widening & AGS			11,200	10,300	21,500	37,400	84%	1,600	39,000	82%	4%		0%	0.0%
Combination 6-Lane Widening & DMB			10,500	9,700	20,100	34,600	72%	6,700	41,200	93%	16%	2,300	6%	0.2%
Combination 6-Lane Widening & Diesel Bus			10,500	9,700	20,100	34,600	72%	6,700	41,300	93%	16%	2,300	6%	0.2%

Summer Saturday e/o Genesee Alternative	2000 Hwy. Vehicle Trips (VT)	2000 Hwy. Person Trips (PT)	WB 2025 Highway VT	EB 2025 Highway VT	2025 Highway VT	2025 Highway PT	% Growth 2000 to 2025 VT	2025 Transit PT	2025 Total PT	% Growth 2000 to 2025 Total PT	Transit as % of Total PT	Trip Suppression/Inducement PT Diff.	% Diff.	% Diff./yr
Baseline	85,100	173,200	82,500	74,300	156,800	339,300	84%	4,200	343,500	98%	1%			
No Action			64,800	74,300	139,100	301,000	64%	4,200	305,200	76%	1%	(38,300)	-11%	-0.5%
Minimal Action			65,100	72,100	137,300	298,000	61%	18,800	316,800	83%	6%	(26,700)	-8%	-0.3%
Rail Transit			67,100	67,800	134,900	290,500	59%	78,400	368,900	113%	21%	25,500	7%	0.3%
AGS			67,500	68,200	135,800	291,300	60%	82,600	373,900	116%	22%	30,400	9%	0.3%
Dual Mode Bus (DMB)			66,000	70,100	136,100	293,700	60%	62,100	355,800	105%	17%	12,400	4%	0.1%
Diesel Bus			66,100	70,100	136,100	293,900	60%	58,200	352,100	103%	17%	8,600	3%	0.1%
6-Lane Highway Widening			75,400	72,800	148,200	320,700	74%	4,200	324,800	88%	1%	(18,600)	-5%	-0.2%
Reversible Lane			75,400	72,800	148,200	320,100	74%	4,000	324,100	87%	1%	(19,400)	-6%	-0.2%
Combination 6-Lane Widening & Rail Transit			76,600	69,000	145,600	313,500	71%	76,200	389,700	125%	20%	46,300	13%	0.5%
Combination 6-Lane Widening & AGS			76,800	69,200	145,900	314,100	72%	80,300	394,400	128%	20%	51,000	15%	0.6%
Combination 6-Lane Widening & DMB			76,500	70,500	147,000	317,400	73%	67,200	384,600	122%	17%	41,200	12%	0.5%
Combination 6-Lane Widening & Diesel Bus			76,200	70,400	146,600	316,600	72%	63,200	379,800	119%	17%	36,400	11%	0.4%

Summer Saturday at Floyd Hill (East of Highland Hills)

Alternative	2000 Hwy. Vehicle Trips (VT)	2000 Hwy. Person Trips (PT)	WB 2025 Highway VT	EB 2025 Highway VT	2025 Highway VT	2025 Highway PT	% Growth 2000 to 2025 VT	2025 Transit PT	2025 Total PT	% Growth 2000 to 2025 Total PT	Transit as % of Total PT	PT Diff.	Trip Suppression/Inducement % Diff.	% Diff./yr
Baseline	62,500	128,500	70,000	63,800	133,800	287,500	114%	2,000	289,500	125%	1%			
No Action			56,900	63,700	120,600	259,100	93%	2,000	261,100	103%	1%	(28,400)	-10%	-0.4%
Minimal Action			59,200	62,500	121,600	262,000	95%	15,000	277,000	116%	5%	(12,500)	-4%	-0.2%
Rail Transit			58,000	56,800	114,800	245,000	84%	68,600	313,600	144%	22%	24,100	8%	0.3%
AGS			57,600	56,200	113,800	241,700	82%	73,100	314,800	145%	23%	25,300	9%	0.3%
Dual Mode Bus (DMB)			59,000	59,500	118,500	253,400	90%	54,600	308,000	140%	18%	18,500	6%	0.2%
Diesel Bus			59,000	59,400	118,500	253,600	90%	50,900	304,500	137%	17%	15,000	5%	0.2%
6-Lane Highway Widening			67,000	63,700	130,700	280,800	109%	2,000	282,700	120%	1%	(6,700)	-2%	-0.1%
Reversible Lane			67,000	63,600	130,700	280,200	109%	2,000	282,100	120%	1%	(7,300)	-3%	-0.1%
Combination 6-Lane Widening & Rail Transit			66,400	60,300	126,700	270,500	103%	67,800	338,300	163%	20%	48,800	17%	0.6%
Combination 6-Lane Widening & AGS			66,200	60,100	126,300	269,000	102%	72,400	341,400	166%	21%	51,900	18%	0.7%
Combination 6-Lane Widening & DMB			66,500	61,300	127,900	273,700	105%	59,000	332,700	159%	18%	43,200	15%	0.6%
Combination 6-Lane Widening & Diesel Bus			66,700	61,500	128,200	274,500	105%	54,900	329,300	156%	17%	39,800	14%	0.5%

Summer Saturday at Twin Tunnels / Alternative	2000 Hwy. Vehicle Trips (VT)	2000 Hwy. Person Trips (PT)	WB 2025 Highway VT	EB 2025 Highway VT	2025 Highway VT	2025 Highway PT	% Growth 2000 to 2025 VT	2025 Transit PT	2025 Total PT	% Growth 2000 to 2025 Total PT	Transit as % of Total PT	PT Diff.	Trip Suppression/ Inducement % Diff.	% Diff./yr
Baseline	67,000	137,700	45,400	42,400	87,800	180,500	31%	1,900	182,300	32%	1%			
No Action			39,400	42,100	81,500	167,600	22%	1,900	169,500	23%	1%	(12,900)	-7%	-0.3%
Minimal Action			43,200	42,000	85,200	175,000	27%	7,300	182,300	32%	4%		0%	0.0%
Rail Transit			38,600	35,600	74,200	149,700	11%	48,900	198,600	44%	25%	16,300	9%	0.3%
AGS			37,000	34,100	71,100	141,800	6%	54,000	195,800	42%	28%	13,400	7%	0.3%
Dual Mode Bus (DMB)			41,700	38,500	80,200	162,300	20%	39,600	201,900	47%	20%	19,600	11%	0.4%
Diesel Bus			41,700	38,500	80,200	162,600	20%	36,300	198,800	44%	18%	16,500	9%	0.3%
6-Lane Highway Widening			47,400	43,800	91,200	187,500	36%	1,900	189,400	38%	1%	7,100	4%	0.2%
Reversible Lane			47,400	43,800	91,200	186,900	36%	1,900	188,800	37%	1%	6,500	4%	0.1%
Combination 6-Lane Widening & Rail Transit			44,900	41,500	86,400	174,300	29%	50,900	225,200	64%	23%	42,900	24%	0.8%
Combination 6-Lane Widening & AGS			44,200	40,800	85,000	169,900	27%	56,600	226,500	64%	25%	44,200	24%	0.9%
Combination 6-Lane Widening & DMB			45,200	41,800	87,000	176,400	30%	42,500	218,900	59%	19%	36,600	20%	0.7%
Combination 6-Lane Widening & Diesel Bus			45,800	42,300	88,100	178,700	32%	38,200	216,900	58%	18%	34,600	19%	0.7%

Summer Saturday e/o Empire Jct. Alternative	2000 Hwy. Vehicle Trips (VT)	2000 Hwy. Person Trips (PT)	2025 WB Highway VT	2025 EB Highway VT	2025 Highway VT	2025 Highway PT	% Growth 2000 to 2025 VT	2025 Transit PT	2025 Total PT	% Growth 2000 to 2025 Total PT	Transit as % of Total PT	PT Diff.	Trip Suppression/Inducement % Diff.	% Diff./yr
Baseline	59,700	122,700	42,900	39,600	82,500	169,700	38%	1,900	171,600	40%	1%			
No Action			37,800	39,400	77,200	158,800	29%	1,900	160,600	31%	1%	(11,000)	-6%	-0.3%
Minimal Action			40,900	39,300	80,200	165,000	34%	6,600	171,600	40%	4%		0%	0.0%
Rail Transit			36,400	33,300	69,700	140,600	17%	45,600	186,200	52%	24%	14,600	9%	0.3%
AGS			34,800	31,900	66,700	133,000	12%	50,400	183,300	49%	27%	11,700	7%	0.3%
Dual Mode Bus (DMB)			39,300	35,900	75,200	152,200	26%	37,100	189,200	54%	20%	17,600	10%	0.4%
Diesel Bus			39,300	35,900	75,200	152,500	26%	34,200	186,700	52%	18%	15,100	9%	0.3%
6-Lane Highway Widening			44,900	41,100	86,000	176,900	44%	1,900	178,800	46%	1%	7,200	4%	0.2%
Reversible Lane			44,900	41,100	86,000	176,400	44%	1,900	178,200	45%	1%	6,700	4%	0.2%
Combination 6-Lane Widening & Rail Transit			42,300	38,700	80,900	163,400	36%	47,900	211,200	72%	23%	39,600	23%	0.8%
Combination 6-Lane Widening & AGS			41,700	38,200	79,900	159,500	34%	53,200	212,700	73%	25%	41,100	24%	0.9%
Combination 6-Lane Widening & DMB			42,600	38,900	81,500	165,200	37%	39,900	205,100	67%	19%	33,500	20%	0.7%
Combination 6-Lane Widening & Diesel Bus			43,100	39,400	82,500	167,400	38%	35,800	203,100	66%	18%	31,600	18%	0.7%

Summer Saturday at EJMT

Alternative	2000 Hwy. Vehicle Trips (VT)	2000 Hwy. Person Trips (PT)	WB 2025 Highway VT	EB 2025 Highway VT	2025 Highway VT	2025 Highway PT	% Growth 2000 to 2025 VT	Growth 2025 to Transit PT	2025 Total PT	% Growth 2000 to 2025 Total PT	Transit as % of Total PT	PT Diff.	Trip Suppression/Inducement % Diff.	% Diff./yr
Baseline	44,900	94,200	34,000	29,900	64,000	132,100	42%	1,300	133,500	42%	1%			
No Action			31,500	29,900	61,400	126,800	37%	1,300	128,100	36%	1%	(5,300)	-4%	-0.2%
Minimal Action			32,500	29,900	62,500	129,400	39%	4,000	133,500	42%	3%		0%	0.0%
Rail Transit			28,500	25,300	53,900	108,800	20%	33,800	142,600	51%	24%	9,100	7%	0.3%
AGS			27,100	24,100	51,200	102,200	14%	37,800	140,000	49%	27%	6,500	5%	0.2%
Dual Mode Bus (DMB)			30,700	27,200	57,800	116,800	29%	28,200	145,000	54%	19%	11,500	9%	0.3%
Diesel Bus			30,700	27,200	57,900	117,300	29%	27,000	144,300	53%	19%	10,900	8%	0.3%
6-Lane Highway Widening			35,700	31,700	67,400	139,200	50%	1,300	140,600	49%	1%	7,100	5%	0.2%
Reversible Lane			35,800	31,700	67,500	138,900	50%	1,300	140,200	49%	1%	6,700	5%	0.2%
Combination 6-Lane Widening & Rail Transit			32,900	29,100	62,000	125,300	38%	37,200	162,500	73%	23%	29,100	22%	0.8%
Combination 6-Lane Widening & AGS			32,700	29,000	61,700	123,300	37%	41,100	164,400	75%	25%	31,000	23%	0.8%
Combination 6-Lane Widening & DMB			33,100	29,300	62,400	126,500	39%	30,800	157,300	67%	20%	23,800	18%	0.7%
Combination 6-Lane Widening & Diesel Bus			33,500	29,700	63,200	128,100	41%	27,400	155,400	65%	18%	21,900	16%	0.6%

Summer Saturday between Frisco and Silverthorne / Alternative	2000 Hwy. Vehicle Trips (VT)	2000 Hwy. Person Trips (PT)	WB 2025 Highway VT	EB 2025 Highway VT	2025 Highway VT	% Growth 2000 to 2025 VT	2025 Highway PT	2025 to Transit PT	2025 Total PT	% Growth 2000 to 2025 Total PT	Transit as % of Total PT	PT Diff.	Trip Suppression/Inducement % Diff.	% Diff./yr
Baseline	47,800	100,300	35,900	31,200	67,200	41%	138,800	1,400	140,200	40%	1%			
No Action			32,700	31,300	64,000	34%	132,200	1,400	133,600	33%	1%	(6,600)	-5%	-0.2%
Minimal Action			34,200	31,500	65,700	37%	135,800	4,000	139,800	39%	3%	(400)	0%	0.0%
Rail Transit			29,700	26,100	55,800	17%	112,800	34,100	147,000	47%	23%	6,800	5%	0.2%
AGS			28,100	24,700	52,800	10%	105,500	38,000	143,500	43%	26%	3,300	2%	0.1%
Dual Mode Bus (DMB)			32,400	28,500	60,900	27%	122,800	27,900	150,700	50%	18%	10,500	8%	0.3%
Diesel Bus			32,300	28,400	60,700	27%	123,000	26,900	149,900	50%	18%	9,700	7%	0.3%
6-Lane Highway Widening			38,000	33,400	71,400	49%	147,500	1,400	148,900	49%	1%	8,700	6%	0.2%
Reversible Lane			38,000	33,500	71,500	49%	147,200	1,400	148,600	48%	1%	8,400	6%	0.2%
Combination 6-Lane Widening & Rail Transit			34,600	30,500	65,100	36%	131,600	37,800	169,400	69%	22%	29,200	21%	0.8%
Combination 6-Lane Widening & AGS			34,500	30,400	64,900	36%	129,900	41,500	171,400	71%	24%	31,200	22%	0.8%
Combination 6-Lane Widening & DMB			34,900	30,800	65,700	37%	133,100	30,700	163,800	63%	19%	23,600	17%	0.6%
Combination 6-Lane Widening & Diesel Bus			35,400	31,100	66,500	39%	134,700	27,300	162,000	62%	17%	21,800	16%	0.6%

Summer Saturday at Vail Pass (w/o Copper Mountain) Alternative	2000 Hwy. Vehicle Trips (VT)	2000 Hwy. Person Trips (PT)	WB 2025 Highway VT	EB 2025 Highway VT	2025 Highway VT	2025 Highway PT	% Growth 2000 to 2025 VT	2025 Transit PT	2025 Total PT	% Growth 2000 to 2025 Total PT	Transit as % of Total PT	PT Diff.	Trip Suppression/ Inducement % Diff.	% Diff./yr
Baseline	25,300	53,200	24,300	22,800	47,000	97,500	86%	200	97,700	84%	0%			
No Action			24,300	22,600	46,800	97,100	85%	200	97,300	83%	0%	(400)	0%	0.0%
Minimal Action			24,400	22,500	46,800	95,800	85%	2,000	97,700	84%	2%		0%	0.0%
Rail Transit			22,000	20,300	42,400	86,000	67%	11,800	97,800	84%	12%		0%	0.0%
AGS			21,500	19,800	41,300	83,500	63%	14,200	97,700	84%	15%		0%	0.0%
Dual Mode Bus (DMB)			21,800	20,100	42,000	84,300	66%	13,400	97,700	84%	14%		0%	0.0%
Diesel Bus			22,200	20,500	42,700	86,200	69%	11,500	97,700	84%	12%		0%	0.0%
6-Lane Highway Widening			24,600	22,700	47,300	98,100	87%	200	98,300	85%	0%	600	1%	0.0%
Reversible Lane			24,500	22,700	47,200	97,800	87%	200	98,000	84%	0%	200	0%	0.0%
Combination 6-Lane Widening & Rail Transit			23,700	21,900	45,600	92,600	80%	11,900	104,500	97%	11%	6,800	7%	0.3%
Combination 6-Lane Widening & AGS			23,400	21,600	45,000	90,900	78%	14,800	105,700	99%	14%	8,000	8%	0.3%
Combination 6-Lane Widening & DMB			23,500	21,600	45,100	91,100	78%	13,500	104,500	97%	13%	6,800	7%	0.3%
Combination 6-Lane Widening & Diesel Bus			23,900	22,000	45,900	92,600	81%	11,600	104,200	96%	11%	6,400	7%	0.3%

Summer Saturday at Dowd Canyon (e/o Dowd Junction) Alternative	2000 Hwy. Vehicle Trips (VT)	2000 Hwy. Person Trips (PT)	WB 2025 Highway VT	EB 2025 Highway VT	2025 Highway VT	2025 Highway PT	% Growth 2000 to 2025 VT	2025 Transit PT	2025 Total PT	% Growth 2000 to 2025 Total PT	Transit as % of Total PT	PT Diff.	Trip Suppression/ Inducement % Diff.	% Diff./yr
Baseline	42,200	80,400	31,800	31,700	63,500	117,000	50%	1,400	118,400	47%	1%			
No Action			31,800	31,700	63,500	117,000	50%	1,400	118,400	47%	1%			0.0%
Minimal Action			31,000	31,900	62,900	114,500	49%	3,900	118,400	47%	3%		0%	0.0%
Rail Transit			28,100	29,100	57,100	103,100	35%	15,400	118,500	47%	13%		0%	0.0%
AGS			27,900	29,000	56,900	102,600	35%	15,800	118,400	47%	13%		0%	0.0%
Dual Mode Bus (DMB)			29,300	30,300	59,700	106,500	41%	12,000	118,400	47%	10%		0%	0.0%
Diesel Bus			29,800	30,800	60,600	108,400	44%	10,000	118,500	47%	8%		0%	0.0%
6-Lane Highway Widening			31,400	32,300	63,700	117,500	51%	1,400	118,900	48%	1%	500	0%	0.0%
Reversible Lane			31,500	32,200	63,700	117,400	51%	1,400	118,800	48%	1%	300	0%	0.0%
Combination 6-Lane Widening & Rail Transit			30,400	31,500	61,900	111,700	47%	16,000	127,600	59%	13%	9,200	8%	0.3%
Combination 6-Lane Widening & AGS			30,200	31,400	61,600	112,300	46%	16,800	129,100	61%	13%	10,600	9%	0.3%
Combination 6-Lane Widening & DMB			31,000	32,200	63,200	113,000	50%	13,100	126,200	57%	10%	7,700	7%	0.3%
Combination 6-Lane Widening & Diesel Bus			31,200	32,300	63,500	113,500	50%	11,900	125,400	56%	10%	7,000	6%	0.2%

Summer Saturday e/o Eagle Alternative	2000 Hwy. Vehicle Trips (VT)	2000 Hwy. Person Trips (PT)	WB 2025 Highway VT	EB 2025 Highway VT	2025 Highway VT	2025 Highway PT	% Growth 2000 to 2025 VT	2025 Transit PT	2025 Total PT	% Growth 2000 to 2025 Total PT	Transit as % of Total PT	PT Diff.	Trip Suppression/ Inducement % Diff.	% Diff./yr
Baseline	26,400	54,200		25,000	50,000	97,200	90%	900	98,100	81%	1%			
No Action			25,000	25,000	50,000	97,200	90%	900	98,100	81%	1%		0%	0.0%
Minimal Action			24,800	24,800	49,600	95,900	88%	2,100	98,100	81%	2%		0%	0.0%
Rail Transit			23,500	23,500	47,000	89,700	78%	8,400	98,100	81%	9%		0%	0.0%
AGS			23,500	23,500	47,000	89,500	78%	8,700	98,100	81%	9%		0%	0.0%
Dual Mode Bus (DMB)			23,500	23,500	47,000	89,100	78%	9,000	98,100	81%	9%		0%	0.0%
Diesel Bus			23,600	23,600	47,200	89,300	79%	8,800	98,100	81%	9%		0%	0.0%
6-Lane Highway Widening			25,100	25,100	50,200	97,200	90%	900	98,100	81%	1%		0%	0.0%
Reversible Lane			25,100	25,100	50,100	97,300	90%	900	98,200	81%	1%	100	0%	0.0%
Combination 6-Lane Widening & Rail Transit			23,900	23,900	47,800	91,200	81%	8,500	99,700	84%	9%	1,600	2%	0.1%
Combination 6-Lane Widening & AGS			24,000	24,000	48,000	92,300	82%	8,700	101,100	87%	9%	3,000	3%	0.1%
Combination 6-Lane Widening & DMB			24,200	24,200	48,400	91,500	83%	9,000	100,500	86%	9%	2,400	2%	0.1%
Combination 6-Lane Widening & Diesel Bus			24,300	24,300	48,500	91,500	84%	8,800	100,300	85%	9%	2,200	2%	0.1%

Summer Saturday w/o No Name Alternative	2000 Hwy. Vehicle Trips (VT)	2000 Hwy. Person Trips (PT)	WB 2025 Highway VT	EB 2025 Highway VT	2025 Highway VT	2025 Highway PT	% Growth 2000 to 2025 VT	2025 Transit PT	2025 Total PT	% Growth 2000 to 2025 Total PT	Transit as % of Total PT	PT Diff.	Trip Suppression/ Inducement % Diff.	% Diff./yr
Baseline	22,500	41,200	16,700	16,700	33,300	58,600	48%	400	59,000	43%	1%			
No Action			16,700	16,700	33,300	58,600	48%	400	59,000	43%	1%			
Minimal Action			16,600	16,600	33,200	57,800	48%	1,200	59,000	43%	2%		0%	0.0%
Rail Transit			16,400	16,400	32,900	57,200	46%	1,800	59,000	43%	3%		0%	0.0%
AGS			16,400	16,400	32,900	57,200	46%	1,800	59,000	43%	3%		0%	0.0%
Dual Mode Bus (DMB)			15,600	15,600	31,300	52,400	39%	7,000	59,300	44%	12%	300	1%	0.0%
Diesel Bus			15,700	15,700	31,500	53,000	40%	7,000	59,900	45%	12%	900	2%	0.1%
6-Lane Highway Widening			16,700	16,700	33,500	58,800	49%	400	59,300	44%	1%	200	0%	0.0%
Reversible Lane			16,700	16,700	33,400	58,700	48%	400	59,200	44%	1%	100	0%	0.0%
Combination 6-Lane Widening & Rail Transit			16,500	16,500	32,900	57,300	46%	1,800	59,000	43%	3%		0%	0.0%
Combination 6-Lane Widening & AGS			16,400	16,400	32,900	57,200	46%	1,800	59,000	43%	3%		0%	0.0%
Combination 6-Lane Widening & DMB			16,100	16,100	32,300	54,000	43%	7,000	61,000	48%	11%	2,000	3%	0.1%
Combination 6-Lane Widening & Diesel Bus			16,200	16,200	32,300	54,500	44%	7,000	61,400	49%	11%	2,400	4%	0.2%

3.0 *SYSTEM INTEGRATION*

3.1. INTRODUCTION

The system integration effort of the CMP was intended to verify that all technology elements of the chosen technology, the Chubu HSST (CHSST) maglev system, would work smoothly together in the Colorado environment. Insights from the integration effort have had a major influence on the overall system design for the project.

Two separate parallel efforts comprised the overall integration task. The first effort was analytical, where the technology elements and their interactions were analyzed and the results were used to eliminate incompatibilities that would prevent the elements from operating together successfully. The second effort was predictive: the element characteristics were modeled and incorporated into a simulation, which was then operated to provide further insight about system element interactions. Finally, the results of these two efforts were used to evaluate projected system costs, both capital and operational.

The results conclude that the CHSST 200 vehicle for Colorado (Colorado 200) will successfully operate in the I-70 corridor between DIA and Eagle County Airport, providing a mix of express and commuting transit service which will serve the many recreational destinations on and near the corridor and meet the needs of residents of the mountain counties. The operational system simulation efforts have concluded that the system can operate without conflict under headways of 120 to 150 seconds. Further, route level simulations have concluded that the optimum speed of operation need not exceed 160 kph, while also showing that enhanced propulsion motors are required to handle the grades and curvatures of the alignment.

Extensive integration efforts were undertaken relative to the guideway construction since the guideway costs typically comprise approximately 60 percent of the overall cost of guideway transit systems. This analysis shows that there are a number of opportunities to optimize the costs of the guideway through fabrication methods when utilizing steel trusses. The use of steel trusses is particularly advantageous in Colorado because of the substantial adverse weather conditions. In addition, various options in automating the welding requirements for steel guideways have been discussed as well as options for the final rail alignment procedures. The CMP can use electro-optical techniques with prefabricated, adjustable guideway elements, as compared to the manually intensive techniques that are used by the Japanese in the deployment of the CHSST system in Nagoya, Japan. Finally, it was concluded that the use of large prefabricated, pre-aligned guideway sections is feasible in the Colorado system since transporting these sections to the construction sites appears feasible. The discussion of the guideway fabrication method optimization is found in the Guideway chapter in the Project Part 2: Final Report.

The station element of the integration effort found that as a result of the weather patterns along the I-70 corridor, enclosed stations with platforms protected with elevator-type doors would be needed to provide the passenger environmental control and safety required for this deployment.

Due to the length of the CMP, specific requirements for reliability, availability, and serviceability are imposed by the system. Based on examination of these requirements, the integration effort established an approach to distributed maintenance that would be effective in meeting system availability goals. In this approach, maintenance activities requiring replacement of failed vehicle elements will be supported at selected stations.

One of the more interesting findings of the integration effort addressed the systems controls. Fortunately, the CHSST system is control-neutral. Until this study effort, systems had always been put forward with fixed block controls and manually operated trains. For the CMP the system

design uses a more modern approach, incorporating the control system developed by the Bay Area Rapid Transit District (BART). This control system relies on packet radios and vital wayside computers and circuitry to achieve brickwall headways presently limited to 90 seconds, with the opportunity to safely further reduce this number in the future as technology improves.

The integration research effort determined that it is easier to build generation plants in the corridor than to build the transmission lines necessary to carry the power for the system. This finding opened the way for the consideration of power alternatives. The subsequent finding of the electrification analysis was that use of the guideway route for additional electric transmission facilities would be a valuable supplemental benefit from the construction of the maglev system. In fact, several technologies that could safely support this objective were found and profiled for use. This single result has large potential implications for the financial structure of the overall system, since it has the potential to transform the system into dual roles: transportation and a utility.

Finally, the integration effort has addressed the security issues inherent in any public infrastructure project that deals with many people. Transit systems are vulnerable to acts of terrorism and actions are required to reduce the risks. The integration reports have pointed out various options available to limit death and destruction.

3.2. SIMULATIONS

A considerable number of simulation activities have been conducted to support the integration effort. Kinematic and dynamical simulations have been conducted in both the US and Japan to furnish evidence of compliance with specifications. In particular, CHSST has conducted a large number of simulations on a wide variety of vehicle characteristics, including lateral stability, levitation stability, and ride quality, and have supplemented these simulations with test data, showing, for example, gap variation during various types of vehicle motion. Additionally, Sandia National Laboratories has conducted a wide variety of simulations of the propulsion system, showing that the new motor is quite satisfactory as a source of motive power for the vehicle in the Colorado environment.

Additionally, two system level simulations have been carried out. The first, conducted to verify the guideway geometry, established the maximum safe theoretical speed profile that the guideway could support. Examination of this speed profile, which supported peak speeds of 200 kph although the Colorado 200 vehicle with modification could attain a 250kph +/- speed, led to the conclusion that the higher peak speeds produced very little benefit for service levels while consuming considerably more power than necessary. This provided the basis of the decision to set the maximum system speed at 160 kph. At this maximum speed, the service levels in terms of trip times were still very attractive, as compared to auto traffic over the same route.

Based on projected system ridership demand provided from the I-70 PEIS effort, it was possible to manually assign a schedule of train departures from stations that satisfied the peak demand. These departures, which intermixed several concurrent peak flows on the guideway, required only dispatch intervals greater than 150 seconds. This conservative headway is easily supported by modern control systems, and was achieved with a fleet of 65 trains. To verify these numbers, which have material bearing on the system cost, it was necessary to also conduct a computer-based simulation of the projected passenger and vehicle traffic. This is necessary because manual dispatch of a train creates potential conflict for system resources in the future, and only a computer simulation can verify that these potential resource conflicts can be managed.

A stochastic dynamic simulation was structured using the demand data provided by the PEIS effort. An example of this data is shown in Figure 39.

Projected Winter Peak Boardings (Daily Total 67541)

Legend:
- Eagle Cty Airpt
- Avon
- Vail
- Copper Mtn
- Frisco
- Silverthorne
- Loveland Pass
- Georgetown
- Idaho Springs
- Evergreen
- Golden
- DenDwntwn
- Rolla
- DIA
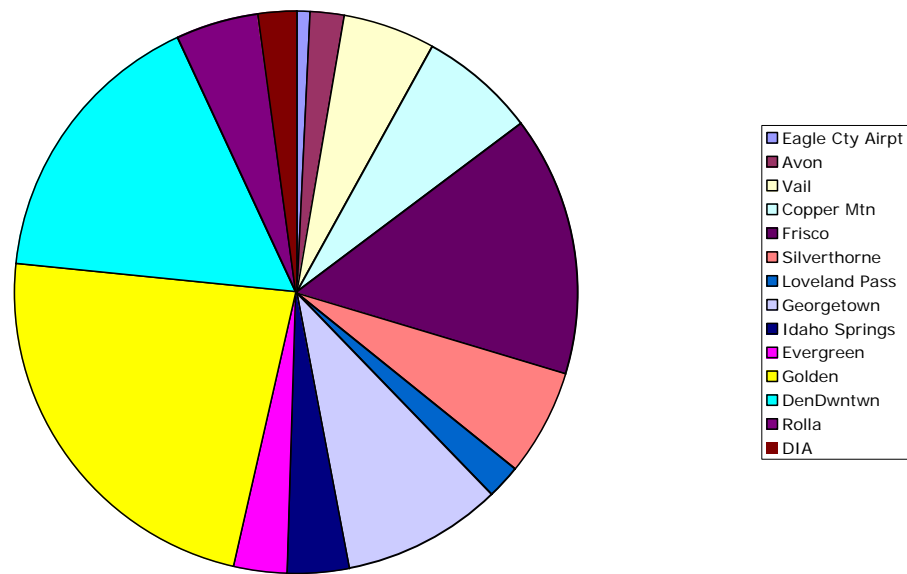
Figure 39: Peak Hour Boardings by Station

To make use of this data, it was necessary to decompose the data into eastbound and westbound flows. A self-consistent optimization method was used to achieve this, with good results. The following figures show the results of this analysis.

Demand by Station
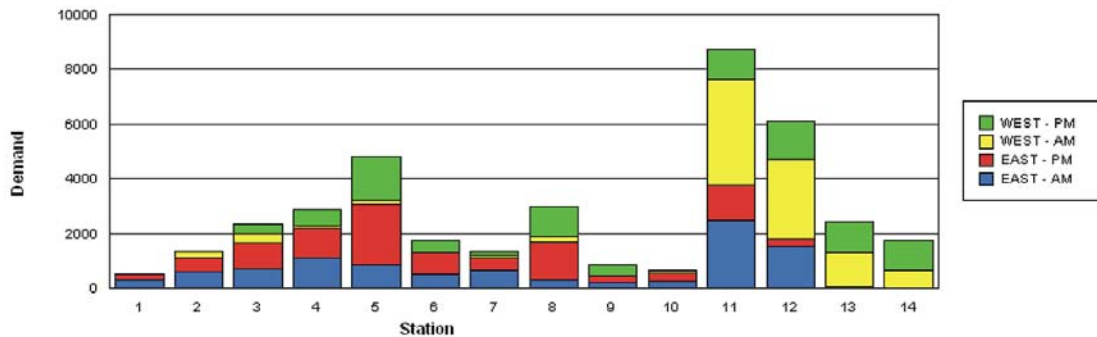
STATION

	1	2	3	4	5	6	7	8	9	10	11	12	13	14	Total
EAST - AM	311	573	700	1,068	862	471	649	271	186	234	2,453	1,512			9,290
EAST - PM	202	505	951	1,124	2,216	798	426	1,432	272	312	1,286	267	30		9,821
WEST - AM		249	311	78	116		115	182			3,894	2,931	1,269	635	9,780
WEST - PM			362	605	1,593	471	137	1,081	367	100	1,077	1,387	1,105	1,087	9,372

Figure 40: Decomposition of Demand to Eastbound and Westbound Flow, by Station

In Figure 40, the stations are numbered sequentially from 1 to 14 in order along the route, beginning with DIA, and ending with Eagle County Airport.

1. *DIA*
2. *Rolla*
3. *Downtown Denver*
4. *Golden*
5. *Evergreen*
6. *Idaho Springs*
7. *Georgetown*
8. *Loveland Pass*
9. *Silverthorne*
10. *Frisco*
11. *Copper Mountain*
12. *Vail*
13. *Avon*
14. *Eagle Airport*.

Verification that this decomposition was successful is shown by summing the eastbound and westbound flows for each station. The result of this process is shown in Figure 41, proving that the decomposition has been successful.

Top number is arrivals, bottom number is departures.

Station

	1	2	3	4	5	6	7	8	9	10	11	12	13	14
EB	 237	148 506	263 835	181 1,467	1,068 2,418	556 1,019	22 858	1,589 2,083	1,586 855	392 715	3,403 1,353	2,744 615	425 6	464
WB	535 	227 130	898 92	1,020 547	1,794 981	1,196 690	605 262	1,558 1,070	983 421	419 446	855 2,256	483 1,444	23 1,552	 769
Total	535 237	375 636	1,161 927	1,201 2,014	2,862 3,399	1,752 1,709	627 1,120	3,147 3,153	2,569 1,276	811 1,161	4,258 3,609	3,227 2,059	448 1,558	464 769

Figure 41: Eastbound and Westbound Passenger Flows

Completion of this procedure provides the data necessary to operate the simulation.

In the simulation, passengers are drawn at random from the pool of those available in the station at any given time, and loaded onto trains. The trains are then moved to their destinations, and the passengers disembarked. Statistics are maintained and resource conflicts are identified. In the end, the results show the necessary train traffic needed to meet the demand during the peak period, and confirmed the operating headway projections, requiring dispatch no more frequently than 150 seconds. Only a few resource conflicts were noted during the simulation runs, indicating that the system was not near full capacity. Additionally, the three or four conflicts that did arise were easily resolved by minor departure delays.

The results for the peak winter operating times are shown in the following figures. As shown, the numbers of trains operating at any interval of the time period are shown according to the station of origination, coded again by serial number, as before. Trains are recycled as they become empty, so that the maximum number of trains needed to carry the load has to be counted by counting individual trains. This count requires approximately 75 trains in service during the peak, in rough agreement with the manual fleet estimates.

No attempt has been made in this simulation to optimize the number of trains. Instead, trains are added as necessary to meet the waiting time restrictions at each station, and each train stops at every station to take on passengers, i.e., this is local service only, with no express trains. It is certain that the optimization of the movement of trains would marginally reduce the number of trains required, achieving both capital and operating cost economies.
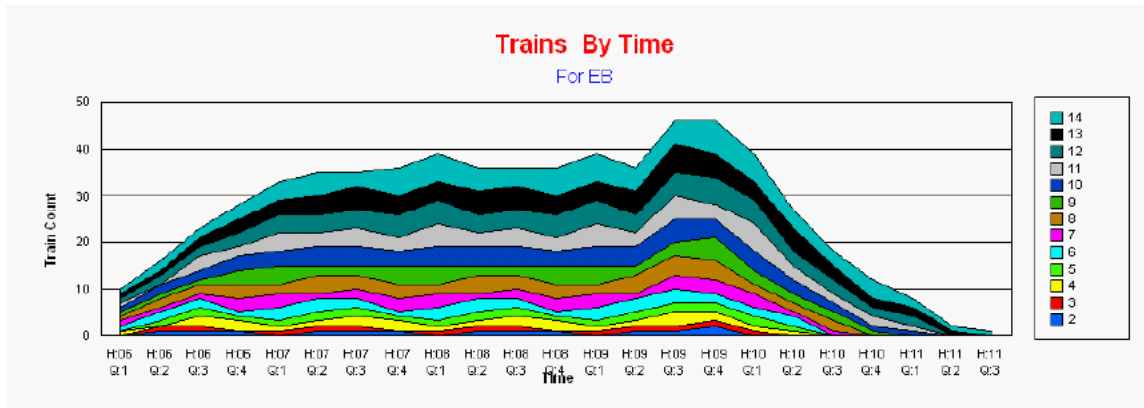
Figure 42: Eastbound Trains on a Winter Saturday Morning
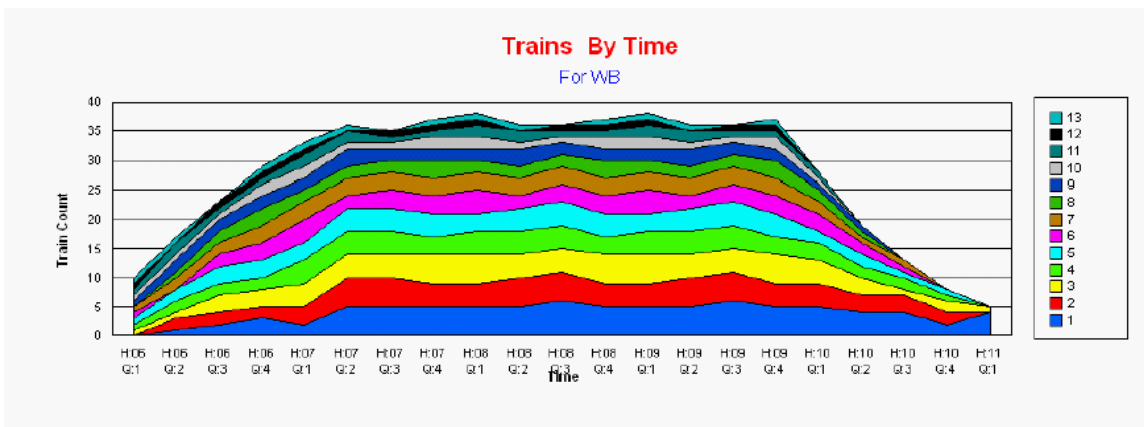
Figure 43: Westbound Trains on a Winter Saturday Morning
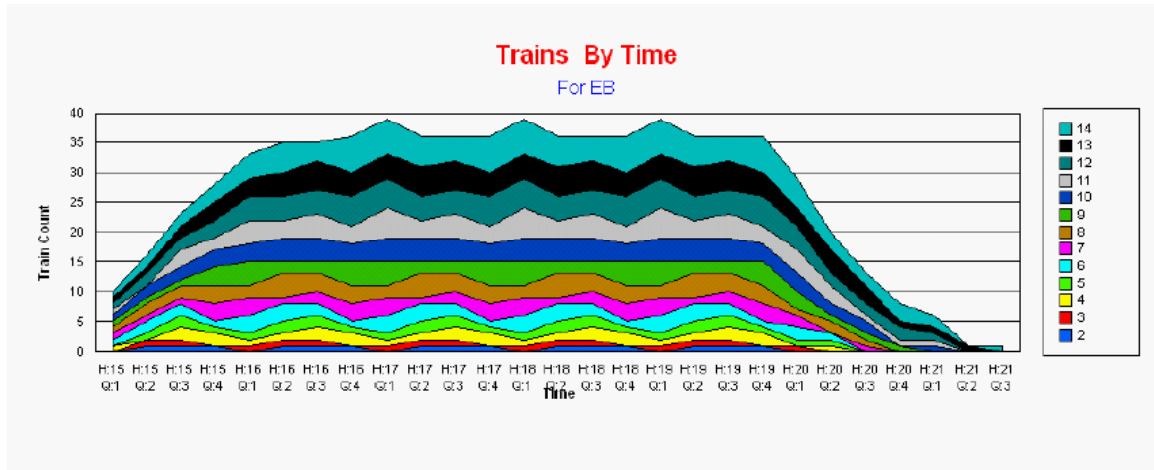
Figure 44: Eastbound Trains on a Winter Saturday Afternoon
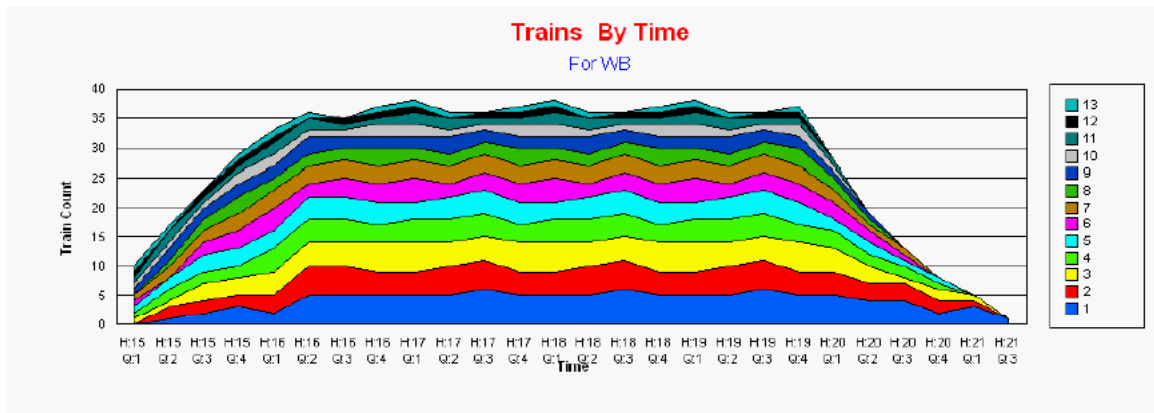
Figure 45: Westbound Trains on a Winter Saturday Afternoon

One of the potential outcomes of further simulation is a cohesive strategy for the management of vehicles that have discharged their passengers, together with requirements for guideway switches and storage and staging facilities for vehicles needed to implement the strategy. These objectives could be pursued in the next stage of system design of the CMP.

3.3. GUIDEWAY

3.3.1. *Route*

Characterization of the guideway route required considerable effort. This was necessary due to the many different forms of available data describing the conformation of the I-70 corridor and the need to produce a guideway that could be constructed at minimum cost. A thorough review of all data sources indicated that an independent GPS dataset would be required to verify the integrity of multiple sources. The GPS data was collected and reconciled with the CDOT PEIS dataset. The guideway was then sited in the median of I-70 and a full guideway dataset was produced for the research effort.

There were two basic reasons for the choice of median siting. First, the research would not become encumbered with discussions of land acquisition, which could be contentious and would potentially cloud an assessment of the system cost. Second, the PEIS effort had identified

environmentally sensitive areas along the corridor and the analysis could benefit directly from this knowledge without having to undertake the same effort in unstudied areas of the corridor.

However, completion of the route dataset did provide an opportunity for evaluation of alternative routing in the tunnel areas of I-70. The evaluation took into account grades, tunneling costs, and climate issues, but did not address land acquisition or environmental sensitivity. This effort led to the establishment of a potential alternative route at Kermit's Bar, just east of the Idaho Springs Twin Tunnels. Further, an elimination of the transit bore at the Eisenhower Tunnel has also been evaluated using the grade climbing capability of the maglev system to cross the Continental Divide, over the area of the Eisenhower Tunnel. For purposes of the system design, identification of these alternates was intended to demonstrate that many tradeoffs must be considered carefully before a final route is selected for any system deployment.

Completion of the route dataset also permitted the computation of maximum kinematic vehicle velocity over the route, consistent with passenger ride comfort constraints. This theoretical maximum speed along the route was in turn used to establish best-case travel times between all station pairs. These times were useful in the simulation activity, which proceeded in parallel with the propulsion trade study.

In future studies of the corridor, this velocity profile would also serve as the starting point for optimization of the route itself, as opportunities for travel time reduction, increased ride comfort, or operational efficiency are further studied.

Further, this guideway dataset and its associated kinematic velocity profile have been used as the point of departure for the Project's propulsion and simulation studies.

3.3.2. *Guideway Design*

Substantial effort was devoted to guideway materials review and analysis. Guideway development in Europe and Asia has produced workable guideway solutions, although guideway cost optimization is still not complete. In particular, lowered cost guideways intended to meet the civil structures lifetime requirements, while preserving acceptable maintenance profiles, still require development.

The primary issue in maglev system guideway structural design is deflection. The weight of the vehicles compared to the guideway structural weight is such that the designer must primarily search for a way to produce a lightweight, stiff structure at minimum cost. This search naturally leads into lightweight steel structures, since steel is roughly three times stiffer than alternative metals. Concrete solutions, although cost effective, have other issues including weight, creep, and operational limitations (potential snow and ice buildup) in harsh environmental conditions.

The results of this analysis have pointed to tubular steel space frame trusses as the guideway system most likely to satisfy all the system requirements in Colorado. Structurally, this design is the most economical in its use of materials, with a ratio of strength to weight higher than that of any alternative structure. The integration effort has focused on a thorough examination of the cost issues associated with this result, since the initial cost of this type of structure may potentially be slightly higher than the costs of concrete or steel box beam structures used to achieve the same result.

The effort has:
1. identified viable suppliers of the materials for construction of these trusses;
2. sought the advice and processes of fabricators who could assemble these materials into trusses for both straight and curved sections;
3. obtained probable costs from both sources;
4. reviewed material handling and assembly techniques through the entire truss manufacturing process;

5. examined structural lifetime and maintenance issues associated with the trusses; and
6. developed recommendations for the lowest cost mechanisms for producing these structural elements.

Because the Colorado system would require more than 16,000 of these trusses, this cost is a central element of system capital cost; accurate definition of this cost is a critical integration task.

3.3.3. *Tolerances*

Careful examination of the necessary tolerances for guideway alignment has led to analysis of techniques for achieving the necessary accuracy in guideway placement. Two factors have influenced this analysis.

First is the experience that, once aligned, the guideway can maintain its alignment over a long period of time. In this regard, it is not like the high-speed train systems, Shinkansen and TGV, which require continuing and extensive track maintenance. So, for example, the Nagoya test track of HSST has required only minor incidental maintenance over a period of nine years.

Second is the experience that the largely manual initial alignment during construction is extremely labor intensive and time consuming. This alignment has been conducted so far with traditional surveying instruments, basically transits and tapes. This approach is challenging in complex curves and needs to be replaced with more modern, electrooptical, techniques. The use of new techniques for this construction task will improve accuracy and reduce costs.

The integration analysis has disclosed real opportunity for reducing the labor cost during the construction process. In the construction processes, the greatest leverage comes from focusing on those structures employing steel members. Two of these have been put forward: one based on a prefabricated steel box truss, and the second on a prefabricated steel space frame truss. Either type offers the prospect of automated construction, and therefore, prealignment of rail attachments to the truss. The truss, with aligned rails, can be transported and installed with only limited final alignment in the field. This contrasts sharply with concrete construction, where a rapidly steam-cured green concrete beam must cure for a considerable amount of additional time, creeping all the while. Only when it has been erected and the precast deck put in place, can the creep be evaluated and the rails installed. The rails and sleepers must be installed and shimmed as a unit, rechecked after a period of time to verify that further creep has not destroyed the alignment, and readjusted if necessary.

3.3.4. *Construction Issues*

The integration effort has also dealt with issues of guideway construction that are separate from the materials issues of guideway elements. Chief among these construction issues are transport of large, prefabricated, pre-aligned guideway components to construction sites, and erection and alignment of guideway structural elements. The reasons for treating these as integration issues is to ensure that cost integrity is preserved through the estimation process, as well as to ensure that important system attributes in the vehicle/guideway interface are not compromised by the construction process. Examination of these issues early in the process can help to assure a consistently usable guideway. As the largest item of capital expenditure in the project, it is important that guideway integrity and functionality not be compromised by unforeseen conditions. This has happened repeatedly in early maglev projects and cannot be tolerated in a project with the scope of the Colorado initiative.

The sizes of girders that must be transported range from 20-30 meters in length. The upper range of these lengths is likely to require special handling in over-the-road transport to insure that such long girders are not a hazard to normal traffic. These lengths are at the upper limits of handling for this type of transport, although they can be handled with appropriate care. The

weights are also significant, ranging from sixteen tons for the tubular steel truss, to thirty tons for the concrete girder.

Earlier in the effort, it was suggested that the guideway itself could be used to transport new guideway sections for installation. That approach, as it turns out, is in use in Japan with good success. The following figures illustrate assembly and movement of guideway sections over the guideway for installation.

Figure 46: Levitation Rail Section Assembly Prior to Installation

Figure 47: Guideway Section Staging for Transport Over the Guideway

Figure 48: Guideway Sections Ready for Transport on the Guideway

3.4. STATIONS

The CMP guideway is roughly 250 kilometers (155 miles) long. Fourteen potential station sites have been identified. These stations will provide the proper functions of typical transit stations including:

- Platforms
- Shelter
- Vertical and Horizontal circulation
- Amenities and Services
    - Climate controlled waiting room
    - Public restrooms
    - Snack service
    - Public telephones
    - Changeable message display
- Safety

All the station designs are planned to be consistent with the character of the buildings in the area of operation or predicated on the local area desires where each station is located.

The station subsystem must meet certain performance requirements. Specifically, it must support the safe movement of passengers through the station at specified flow rates and must also support particular levels of vehicle traffic.

3.4.1. *Locations*

1. ***DIA*** (DIA, mile 0): This station represents one terminus of the entire system, serving DIA.
2. ***Rolla*** (96th Street & I-76, mile 16.6): This station serves the developing north Denver area, potentially connecting with other transit presently under development.
3. ***Downtown Denver*** (I-70 &I-25, mile 25.0): This station is located at a major transportation interchange, and will capture a large portion of riders coming from the northern Front Range cities, including Boulder and Fort Collins.
4. ***Golden*** (I-70/Colfax Avenue & US 40, mile 37.0): This station would serve as the collector for riders coming from South Denver, Pueblo, and Colorado Springs.
5. ***Evergreen*** (Bergen Park/Route 74, mile 47.4): This station would provide access to Evergreen Park recreation area, and also serve numerous small, urbanized areas along Route 74 to the south.
6. ***Idaho Springs*** (mile 59.0): This station would provide access to this historic mining town, and also serve local population in the town and in the surrounding canyons.
7. ***Georgetown*** (mile 70.7): This station would serve three small communities of Empire, Georgetown and Silver Plume.
8. ***Loveland Pass*** (mile 82.4): This station would provide access to the Loveland Ski Area just east of the Continental Divide.
9. ***Silverthorne*** (Dillon, mile 91.9): This station would serve local communities of Silverthorne and Dillon. There are areas of scattered residential development all along Route 9 and US 6. These routes also provide access to Keystone Resort, Arapahoe Basin, and Breckenridge Ski areas.
10. ***Frisco*** (mile 97.9): This station would serve the town of Frisco, and the Breckenridge Ski Area.
11. ***Copper Mountain*** (Wheeler Flats, mile 103.3): This station would provide access to Copper Mountain Ski Resort, and serve residential development along Route 91 as far south as Leadville.
12. ***Vail*** (mile 122.5): This station would serve communities of Bighorn, Vail, and West Vail; Vail Ski Resort; and residential development south along US 24.

13. ***Avon*** (mile 131.9): This station would serve Eagle Valley, Avon (Beaver Creek Ski Area), and Edwards.
14. ***Eagle Airport*** (mile 156.3): This would be the terminal station that would serve Eagle and Wolcott; also Beaver Creek Ski Area to the south, and residential areas along Route 131 to the north.

3.4.2. *Station Types*

The CMP is likely to have four (three passenger and one maintenance) station types, suited to specific station characteristics tied to geographic areas. Each type has unique functions typical of its position in the system. The four types are:

Terminal station - This station type possesses functions unique to high volume origin/destination traffic, providing intermodal interchange without substantial station-specific automotive traffic. The DIA and Eagle stations are likely to be the only stations of this type in the Colorado system. The DIA terminal station benefits from the traffic infrastructure already put in place to support the airport. The Eagle station, although a lower passenger volume station, will have similar characteristics.

Urban/suburban collector station - This station type aggregates traffic from other transportation modes (automobiles, vans and buses) for entry/exit to and from the maglev system. The I-70/I-25 station and the Golden station are examples of this station type.

The rural destination station - This type of station typically receives traffic from the urban/suburban stations, and returns the same traffic over the course of a day (although in the case of mountain-based commuters, the flow is reversed). Most of the mountain corridor stations will be this type. These stations must only support limited amounts of wheeled traffic and must have good support for hotel shuttle and rental car modes.

Maintenance facility - This station type is specialized for the maintenance of the vehicle fleet, and is not intended to accommodate passenger traffic. At least two facilities of this type will be required in the Colorado maglev system. DIA and Eagle stations are likely to be supported by adjacent maintenance facilities.

3.4.3. *Construction*

Station construction must meet well-developed building and safety standards for commercial and transit properties. During the integration effort, station cost information was solicited directly from architects responsible for the design and implementation of stations in various transit properties including San Diego Trolley and Bay Area Rapid Transit. Consensus estimates were produced for station construction in these temperate climates, and were used with modification for environmental factors in the projected costing for the Colorado Project.

3.4.4. *Station Platforms*

Previously, it has been noted that no free passenger access to the guideway will be permitted, for safety reasons. This is mandatory due to the speed and low noise profile of maglev system. The Colorado system is not a commuter-system, wherein every train will stop in, or necessarily slow for a given station. The use of docks and in-station transfer switches means that passing trains, while not necessarily in close proximity to platforms, could injure anyone who strayed into the active main guideway. The only alternative to this is expensive station bypass paths, with large and costly external switches and transition spurs.

The electrical hazard common in commuter rail is not present in the same way with the maglev system. The mounting and shielding of power rails make them very difficult to contact unintentionally, and so electrical hazard is not a primary reason for access restriction.

However, another hazard for anyone attempting to negotiate an open guideway is falling. The open nature of the guideway, and the significant elevation, would make a fall hazardous, if not fatal. Accordingly, free open access to the guideway must be eliminated for passengers.

Instead, guideway access is controlled by elevator-style lobby doors, synchronized to the position of the train. Use of these doors requires precision train positioning, accomplished either by docking, or by platform based stopping control. This design approach has reliability implications, and all access equipment selected for use must have proven reliability characteristics.

3.4.5. *Vehicle Storage and Switching*

Each station must have the capability to store trains not in use, and to switch trains from one direction of travel to the other. In this approach, the main active area of the platform is associated with the dock, a mechanism that moves trains laterally from the main guideway into the station platform. From this docked position at the platform, a train can move backward one train length into the storage position; in this position, it is available to maintenance personnel. A train which is moved directly forward one train length from the docked position is in position to be transferred to the other side of the station, where it can be injected into traffic moving in the opposite direction. Hence, this capability of transferring trains from one guideway direction to the other, while not at full speed, is fully equivalent to switching, although with a number of advantages.

One advantage is that the docking mechanism is less expensive than an equivalent deceleration/acceleration lane, although it would exhibit somewhat less operational effectiveness in short headway situations. However, the headways in the Colorado system are long enough to take advantage of the dock's lower cost, and analysis of the dock's performance shows that it will not impact headway.

A second advantage is the lowered cost of a transfer table switch. Since it is located in the station, it is protected from inclement weather. Further, if properly designed, the transfer mechanism can function as a second docking mechanism, providing redundancy to the primary dock.

3.4.6. *Unique Station Characteristics*

The Colorado system is unique for its length. This length imposes specific requirements for reliability, availability, and serviceability. Based on examination of these requirements, the integration effort established an approach to distributed maintenance that would be effective in meeting system availability goals.

In this approach, selected stations will support maintenance activities requiring replacement of failed vehicle elements. These actions will be restricted to field replaceable units of the vehicle, and will be accommodated in the section of the station reserved for vehicle storage.

3.5. VEHICLE

3.5.1. *Required Capacity*

Based on the predicted demand, a close examination of scheduled service that could accommodate the demand indicated that vehicles with capacity for roughly 200 passengers would suffice. These vehicles, derived from the original prototype HSST-05 vehicle, are only slightly modified from the standard HSST 200 machine, primarily in the propulsion subsystem.

3.5.2. *Performance Characteristics*

Performance characteristics of the vehicle depend heavily on the motor capability. The propulsion trade study, conducted by Sandia National Laboratories, has shown that the proposed

vehicle motor can be optimized to meet the required performance characteristics. The results of this analysis are shown in Section 6.0 of this document, the Propulsion Trade Study.

3.5.3. *Critical Subsystems*

The integration analysis has shown the propulsion subsystem to be the most critical of the vehicle subsystems. The original motor in the HSST 200 vehicle simply did not have enough power, and hence could not provide the necessary thrust to meet the Colorado requirements. Various propulsion alternatives were considered during integration, but all analysis showed that a new LIM would be the best alternative. Fortunately, CHSST had a more powerful LIM under development, and the propulsion trade study has now shown that this motor can be configured to meet the requirements. Next in priority of criticality would be the levitation subsystem, although analysis and testing has shown that this subsystem should perform well within specification. Other subsystems, such as the command, control, and communications subsystems (CCCS) have been proven in operation on other transit properties.

Hence, the question of vehicle adequacy appears to be settled, and the Colorado 200 vehicle represents an entirely new maglev capability: the urban/suburban/rural medium speed, medium capacity train. The vehicle is reminiscent of aircraft technology in both concept and in operation, and should be well accepted by the traveling public. The short time that it would take to deploy this vehicle, since only modification of an existing machine is required, is also a real factor in its favor, along with its technical characteristics.

3.6. CONTROLS

Fortunately, the CHSST system is control-neutral. Until this study effort, CHSST systems had always been put forward with fixed block controls and manually operated trains. CHSST has shown a willingness to embrace more modern controls, and the vehicle control interfaces appear to be compatible with many different control approaches.

It is fortunate that moving block systems are just now coming into operation in several parts of the country. The most promising of these for the CHSST system appears to be the system developed by the Bay Area Rapid Transit District (BART). This system relies on packet radios and vital wayside computers and circuitry to achieve brickwall headways presently limited to 90 seconds, with the opportunity to safely further reduce this number in the future as technology improves. From the simulation results, it appears likely that the CMP can be operated during peak periods at 120 to 150 second headways. Given the demonstrated capability of the BART control system, it seems straightforward to meet or exceed the Colorado operational goals without stressing the controls.

The BART control system is schematically described in Figure 49.
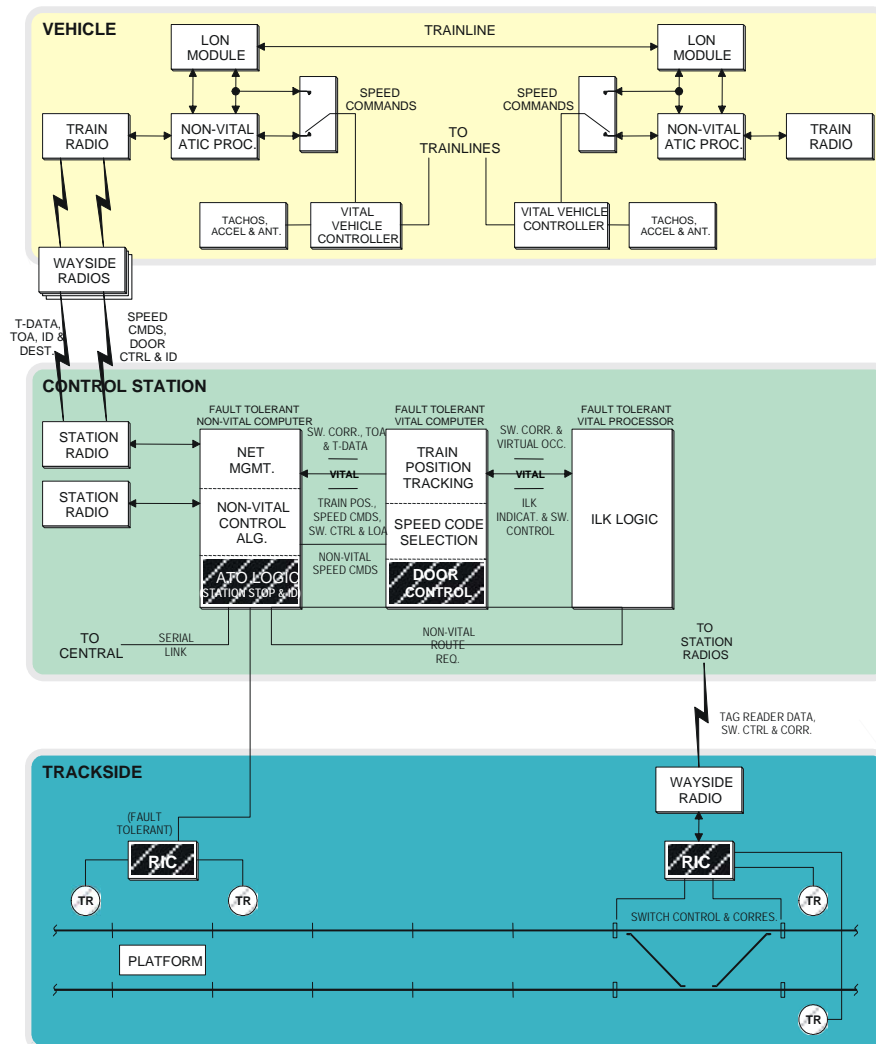
Figure 49: BART Moving Block Train Control

A brief description of this control system follows.

The partition of function places the station control computer(s) at the center of the hierarchy. Based on the service schedule communicated to them by central control, each non-vital station computer manages the vehicles in its region of responsibility. A non-vital processor deals with schedule issues and speed commands to maintain service. A vital processor deals with safe train positions and speeds, and with interlocks (doors, switches, etc.) All these elements are fault tolerant, employing primarily checked redundancy to insure continuous operation. In addition, the vital elements have had special techniques and methods applied to insure that they can only fail in a manner which places the system into a safe state.

Position and velocity information are derived from measurements taken dynamically on and from the cars using radio propagation delay techniques. A series of wayside radios along the track maintain constant communications with train radios, permitting the measurement of signal delays as the information reaches each end of the train. The times of transmission and receipt are known, and since the transmitter positions are also known precisely, the differences in these times can be used to provide precise measures of instantaneous train speed and position. The station computers use this information as their criteria for actions.

This information is also available to control equipment on the train. However, the train controls also make use of independent tachometer and accelerometer data collected directly from the train itself. This information provides a primary verification of information derived from radio propagation. If there is any indication of over-speed or other problem, the on-board control can act independently to place the train in a safe condition, i.e., apply brakes.

While this system is simple in conception, there are many details that require careful thought to resolve correctly. It is a tribute to BART that they have managed to complete the development of this control system and put it into certifiably safe operation. This type of system is economical and offers a high level of performance and safety.

3.7. ELECTRIFICATION

Due to the prospective costs, it was necessary to evaluate the electrification of the system in detail. With the help of CHSST and Sandia National Laboratories, wayside subsystems and rectifiers were specified for costing with the designs reviewed by power engineers. The result of this activity was a workable design for wayside electrification, together with a cost scenario usable in the context of the total system cost. Previous review of the electric utility situation in the corridor had disclosed a shortage (or total lack) of transmission capacity along the route. Discussions with utilities and industrial electrical equipment vendors made it clear that the permitting process to add transmission facilities to the corridor would be a long and arduous process, conceivably lagging behind the construction of the maglev system. As a result, consideration was given to the potential collocation of the transmission facility with the guideway. This approach was enthusiastically accepted by the utility companies providing electricity in the corridor, since these utility companies have been seeking new transmission capacity to serve the growing population and economic activity of the I-70 corridor. All agreed that a successful effort to use the guideway route for additional electric transmission facilities would be a valuable supplemental benefit from the construction of the maglev system. Several indicated interest in financial participation in the system if this proved technically feasible.

This concept was pursued, even though it was clear that it might also face regulatory issues. It was felt that the technologies available might provide a unique way of meeting those issues.

First, it is now possible to routinely consider undergrounding 115 kV transmission facilities. Several of these undergrounding concepts have been proposed in other states, some involving considerable distances. These designs have been based on advances in electrical insulation technology, using a number of different technologies. One relies on new cable technology employing cross-linked polyethylene insulation. There is long experience with this material in Germany, for example, and it seems clear that some use could be made of this technology for solving some undergrounding problems.

However, in the I-70 corridor, full undergrounding of the electrical transmission system is probably impractical, due to a wide variety of factors, such as geologic and environmental conditions, regulatory issues, and costs. Because of these considerations, full undergrounding along the entire guideway route is not a feasible option, although it might prove useful for the solution of some specific engineering problems in limited portions of the alignment.

Second, there may be a way to carry the required transmission capability on or within the guideway structure itself. This type of approach is more speculative because the structural implications are not fully understood. But, there is the well proven technology of the gas insulated transmission line (GIL), developed and proven in Europe and the US over the last 25 years, and this technology is likely adaptable to electrical transport on the guideway structure.

These lines have remarkable safety, structural integrity, electrical capacity and characteristics, and excellent durability. They appear to be fully compatible with other guideway materials, and may even help to mitigate some of the other safety costs associated with necessary guideway functions.

Their operating principles are simple: a coaxial transmission line is constructed with the current carrying conductor configured as the central coaxial element. The central coaxial element is suspended by insulators in an outer metal pipe and then the assembly is filled with a stable insulating gas mixture of 80% nitrogen and 20% sulfur hexafluoride. The resulting assembly is mechanically rugged, thermally stable, and can safely carry huge currents at voltages ranging up to 1200 kilovolts. Because of the coaxial geometry and insulating gas characteristics, the line has low capacitance and, unlike overhead cable transmission systems, has low degradation and sensitivity to environmental conditions over time. These characteristics make it an option for use in the CMP, although the cost may be more than other alternatives. It should be noted here that tabulation of these costs is beyond the scope of the current effort.

A second transmission technology, employing dielectric-insulated cables, is also feasible for the transmission of the needed power along the guideway. Using cross-linked polyethylene insulation, voltages up to 345 kilovolts can safely be carried in underground trenches. There is long experience with this type of insulation, also pioneered in Germany, and it is reliable with long service life when protected from UV radiation. Carried in grounded conduit, this technology may have a cost profile better suited to the overall project.

With either transmission technology a safe way to carry the transmission lines, from auxiliary towers or suspended from auxiliary beams, would have to be found. This is routinely accomplished with bridges and some of those techniques may be applicable to the Colorado Project. However, this approach represents an engineering challenge. Conceptually, there is a way to suspend the needed transmission facility with the emergency egress girder, perhaps even taking advantage of the structural characteristics of both to achieve a stronger guideway. If this can be done, the guideway costs attributable to emergency egress can instead be partially absorbed as system infrastructure costs attributable to the primary electrical transmission system.

Clearly, this represents a direction for future research in guideway design. This preliminary technology identification effort has confirmed that one of these technologies can probably meet the power transmission requirements for the CMP.

The question remains as to whether existing electrical generation has the capacity to support the maglev system operation. Pending resolution of this issue through further study, it is probably sufficient to point out that gas turbine power plants located along the alignment could provide the needed power. Such plants are economical, reliable, and now with newer approaches, even offer acceptable emissions control. With correct design, this approach could provide excess generation and transmission capacity, which could be shared with the utilities for use in serving new growth in electric demand in the corridor; revenues from this source could also help to defray maglev system costs.

Generally speaking, power plants are much easier to permit than transmission lines because they are geographically confined to one place, and the environmental impact is restricted to other considerations. In particular, emissions are a critical factor in modern power plant operation and this would be particularly important at altitude. There are new processes for removal of NO_x and

these processes are well tested. Typically, a well-run turbine generator can now achieve 0.5 ppm NO_x, and effective heat exchangers are also available for waste heat recovery. The co-generation aspect of a local power plant would be welcome in many mountain communities in the corridor, who could also make good use of both the waste heat and the off-peak power generated.

These plants are economical to purchase and to operate. Their reliability is superb and they can run for long periods with only routine maintenance. First class installations can be procured and installed at between $30M and $50M each. However, there are a collection of issues which could prevent serious consideration of this alternative.

The chief problem with this alternative is the location of an adequate fuel supply. These units run from natural gas. Natural gas is not particularly plentiful in the United States, although there are strategies such as coal gasification that might be feasible in Colorado; there are plentiful supplies of coal and oil shale in Colorado. However, there are two large natural gas basins located in the adjacent states of Wyoming and New Mexico, as shown in Figure 50, taken from http://www.energy.ca.gov/naturalgas/western_state_pipelines.html:
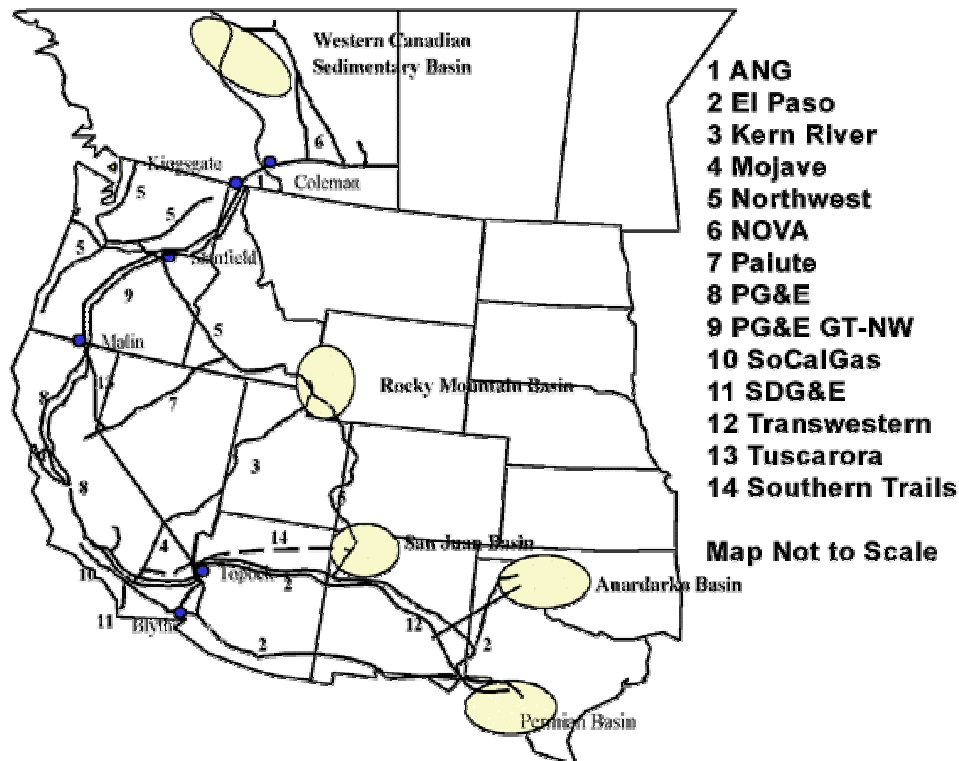
Figure 50: Natural Gas Pipelines in the Western US

The Rocky Mountain Basin and the San Juan Basin are in reasonable proximity to Eagle County Airport. There is a major pipeline connecting these two fields, and there is a compressor station in western Colorado, midway between the two fields. To serve power plants in the I-70 corridor, it would be necessary to construct a connecting pipeline from the compressor station to the Eagle County Airport vicinity, where the first plant would be sited. Then, the pipeline would have to be carried to the next site, say Frisco, using the guideway right-of-way. A third plant could be located in the Idaho Springs/Georgetown area.

For hypothetical purposes, this resolves the power issues for the maglev system, and benefits the mountain communities by increasing the quantity and reliability of their power sources, thereby benefiting the Colorado economy. However, there are several practical considerations, which make this alternative less attractive.

First is the altitude. This has the effect of reducing the efficiency of the power plant, and secondarily of placing more emphasis on emissions control. Power plant engineers who have examined these scenarios have indicated that at 1980 km (6500 feet), the approximate altitude of two of the hypothetical sites, the relative efficiency loss could amount to 10%, which is a tolerable derating. However, at 2600 km (8500 feet) or more, the altitude of several potential sites, the derating climbs rapidly, requiring careful consideration from the standpoint of fuel efficiency, emissions, and cost/benefit.

Second, these plants require a significant amount of water for their operation. This water is used for cooling and is evaporated directly to the atmosphere, and is thereby lost. While wastewater can be used for this purpose, the implications for water may be the most important issue this concept faces. A new technology for secondary generation through waste heat recovery by propane cycle heat transfer may significantly influence the demand for water cooling of conventional generators.

Third, there is considerable cost associated with pipeline construction. It should be pointed out, though, that there also is cost associated with new electric power transmission lines. One way or another, providing energy to operate the maglev system will incur cost. How this is to be accounted for is an open issue, since this increased capacity might be considered as an infrastructure improvement for the entire corridor.

Finally, there is the cost of fuel for plant operation. The price of natural gas is subject to fluctuations and is entering a period of increasing prices, due strictly to supply/demand characteristics. It is not likely that this situation will stabilize in the future, and it may in fact worsen. Strong demand from the eastern US has stimulated the gas fields to produce increasing quantities, and the long term stability of the fuel supply for gas fired plants would have to be studied carefully before it could be recommended as a viable power source for the CMP.

At this point in the research, ways to obtain the electrical power needed by the maglev system have been identified, and are feasible at some level. Regulatory and other issues would have to be studied further, along with additional study of the technical tradeoffs, before a firm recommendation as to power source could be made. Suffice it to say, there are ways to generate and deliver the needed power, although there are challenges to accomplish this in an economically secure manner. This situation mirrors the overall general situation for power consumption in the United States as a whole, wherein secure sources of electrical energy must be provided economically to support future economic growth.

3.8. SAFETY AND SECURITY

As part of the research effort, a comprehensive examination of security issues was conducted. The results of this effort are described in section 9.0 of the CMP Final Report. Since this analysis was completed earlier in the project effort, attacks have occurred in Moscow and Madrid and there have been reports of terrorist planning for the targeting of other urban mass transportation systems, specifically mentioning London and New York subways. One must also believe that Chicago is additionally targeted because of its unique underground structure.

A further safety and security consideration unique to Colorado has come up in later stages of the integration effort as the reliability and maintenance approaches have been studied.

To meet reliability goals for the system, it is essential that a specific maintenance approach be followed. This approach requires that a certain level of maintenance be conducted in the stations, rather than in the maintenance facility. Conducting such activities in stations implies that the stations must be designed to accommodate the activity, meaning that some form of vehicle storage/access for maintenance is available.

This adds to station cost, and would not be pursued in a standard system design. In a standard design, maintenance facilities would be strategically located in the system, and vehicles would be stored either on-line, or on spurs at these facilities. In Colorado, this would be an unwise strategy. The prevalence of high-powered firearms in the state and their use in vandalism events makes open storage of vehicles unwise for this particular system.

The alternative, of course, is distributed storage in the stations. In this concept, each station would have storage positions for as many as six trains, three in each direction, with a transfer table supporting the movement of trains from one track direction to the other. One position (the center position) would be used for normal docking operations, while one would be used for maintenance, and the other for switching through the transfer table mechanism.

Overall, this approach is likely to be less expensive than the conventional approach, due to the relatively low cost of docking mechanisms, which would be used for both normal and transfer operations. This approach, correctly implemented, provides redundancy in docking operations if necessary, although it does present a station design challenge.

3.9. VEHICLE/GUIDEWAY INTERFACE

A thorough analysis of the vehicle/guideway interface has been conducted during the integration effort. All dimensional clearances and tolerances were reviewed, together with constraints for modification of the propulsion system, imposed by the interface. The conclusions of this analysis were that the interface, with suitable modifications for power collection, would be serviceable in the Colorado system.

A simmering issue in the vehicle/guideway interface, first addressed in the propulsion trade study, is the magnetic permeability of the rail itself. This has been little characterized in all past systems, so far as can be discerned, and is a ripe area for further optimization. This fabrication parameter has considerable influence in the interaction between the rail and the motor, and can drastically affect the efficiency of the interaction.

3.10. ANOMALOUS CONDITIONS

Anomalous conditions are any conditions that cause a deviation from normal operating conditions. A considerable number of such events exist, and examples can be grouped in categories:

- Major disruptions
    - Terrorist acts
    - System power loss
    - Fire

- Intermediate disruptions
    - Local power loss
    - Computer problems
    - Vehicle failure

- Minor disruptions
    - Guideway door failure

- Elevator/escalator failure
- Fare equipment malfunction
- Vandalism

At this stage of the definition process, it is only necessary to closely examine events in the first category, although the integration effort has considered all of these in the security context.

The security analysis examined many of these events in detail and produced detailed recommendations for avoiding or managing the most serious. Thorough analysis of some of these events has disclosed prospective weaknesses in maglev system concepts and implementation and has served as a guide for further integration effort.

A specific case in point is vehicle delevitation at speed. While likely to be extremely rare in operation, such events are to be avoided if at all possible. Although it is unlikely that death or injury would result from such an event, uncontrolled maximum speed delevitation could produce damage to both the guideway and vehicle.

What could produce such an unwanted event? After all, CHSST technology incorporates on-board emergency battery holdup for the levitation elements. The difficulty in these cases comes down to braking. Considerable kinetic energy must be removed and dissipated to bring the vehicle to a safe stop from maximum speed, all the while maintaining levitation power.

System-wide or local loss of wayside power (among other causes) can precipitate this event. When this occurs, vehicles at speed must immediately brake at rates that do not violate passenger safety criteria in emergency situations. This implies that all braking systems on the vehicle that can function will come into play to achieve a safe stop. Further, it must be demonstrated that levitation battery backup is sufficient to sustain levitation through this process. The Colorado 200 vehicle will have to be subjected to thorough testing prior to deployment to verify that this occurs safely and reliably at the maximum safe vehicle velocity in the Colorado system, under operating conditions within the system specifications.

4.0 *ELECTRIFICATION*

The electrification analysis identifies the options for meeting the electric power needs of the CMP by comparing its aggregated energy needs with the existing capability of the electric utilities serving the I-70 corridor.   Other power supply options, such as distributed generation, will be evaluated if the incremental cost to the electric utility of meeting the maglev systems energy needs is excessive. Other considerations, such as reliability of service, could also be a factor in supporting alternate power supply options.

The Electrification Analysis is composed of the following sections:

1. Existing and Planned Power Supply Resources
2. Power Requirements and Supply Adequacy
3. Feasibility of Distributed Generation
4. Comparison of Electric Supply Options and Recommendations

The following sections summarize the work performed and the respective findings.

4.1. EXISTING AND PLANNED POWER SUPPLY RESOURCES

This discussion identifies the existing generation, transmission, and distribution resources in Colorado with particular emphasis on resources along the corridor that could potentially supply the maglev system's electricity needs.   For the purposes of this assessment, the "corridor" was arbitrarily defined as a 16 km (10 mile) band north and south of I-70 that straddles the proposed maglev system route. The 16 km (10 mile) distance is the range that a new sub transmission or distribution line could be realistically constructed to meet the maglev project needs. Accordingly, it is necessary to identify all the utilities, generating stations, transmission lines and substations situated within this 16 km (10-mile) north/south band along I-70.

The major outputs include:
- Identifying all electric utility resources, existing and planned, along the maglev route such as transmission and distribution lines, key substations and generating stations that impact the electric supply to the maglev system;
- Ownership, rated capacities and voltage of transmission and sub transmission lines and major substations along the proposed maglev corridor;
- Daily and seasonal loadings on select transmission lines and relevant transmission expansion data from utilities that will potentially supply the maglev system;
- Historical system outage and transmission reliability data from concerned utilities;
- Existing and planned (electric) load growth of major urban areas along the route, their historical outage rates and system expansion forecasts that address the electric load growth.

Results:
The utilities, including municipals and cooperatives serving the maglev corridor, generating plants, transmission lines, and substations have been identified and classified according to their relevant capacities.

Additionally, power pickup points along the proposed route were identified based on the preliminary route selection. The power pickup points will be the interface between the utility and the maglev system. The conversion of the utility power to the maglev system voltage will occur downstream of the power pickup points by rectifier units located along the guideway.   Sixteen such power pickup points were identified for the purpose of this study from the DIA to the Eagle County Airport. These sixteen locations were selected based on where maximum power needs

are expected along the route at a spacing of 11 to 16 km (7 to 10 miles), and at locations where a higher reliability of power supply may be indicated. These pickup points are identified and discussed in more detail in this report, although the data suggests that the largest portion of the maglev system power needs between DIA and Eagle County Airport will be handled by Public Service Company of Colorado or Xcel Energy, with a relatively smaller share by Holy Cross Electric Association.

The information collected has been graphically summarized in Figure 51, showing the existing electric utility resources including power plants, transmission and substations. In addition, Figure 51 also shows the location of the sixteen power pickup points.

4.1.1. *Utilities and Service Areas*

The eight utilities serving the corridor were identified and are listed in Table 4.1-1 Corridor Utility Names. The table also lists the type of utility, Investor Owned (IOU), Municipal or Co-operative District. Public Service of Colorado (PSCO) is the only IOU in this set of eight utilities serving the corridor.

The areas served along the corridor are shared by the utilities identified in Table 4.1-1. In some instances, the utility might serve only a small area that is surrounded by another utility's service area. One approach to determine where such pockets or service boundaries exist is to examine each zip code in the corridor and determine which utilities serve this geographic area. This information is presented in Table 4.1-2, where each zip code includes the names of the utilities operating in this area. The third column in this table indicates the percentage of this geographic area served by each utility, designated by a "% Overlap". If the entire zip code area is served by a single utility, the value in this column is 1 and if the area is shared by two or more entities, the value in this column changes to reflect the percent area served by that utility. Where there is more than one utility serving the same zip code, the aggregate values of all the utilities serving that area equals unity. The data in this table shows that Public Service Company of Colorado serves the largest area along the corridor.

4.1.2. *Power Plants*

The power plants within the defined corridor zone and some within very close proximity to this region were identified along with their ownership and winter capacity ratings in Megawatts. This information is presented in Table 4.1-3 where the list is sorted by increasing plant sizes. The table shows that the largest generation stations along the route are owned by PSCO in the 300 to 700 MW size range, followed by several smaller generation facilities owned by municipals as well as merchant plants.

4.1.3. *Transmission Lines*

Data for all transmission in the voltage class of 115 kV and above was collected for the corridor. These are all existing lines, except for the 500 kV line owned by the Western Power Administration from Denver Terminal to Spence. Ownership, voltage and service area location of each existing substation of interest was identified. Generally, these are single line corridors; however, there are a few parallel circuits as shown in the "Lines" column.

4.1.4. *Substations*

Ownership, voltage and service area location of each existing substation of interest was identified. However, the existing loading at these substations has not been determined. Comparison of the existing substation capacity with the historic peak loading data will determine the capacity that may be available to the maglev system. This is usually a good indicator of the available substation capacity, unless the utility is aware of other developments, which could mortgage it for future use.

4.1.5. *Power Pickup Points*

Sixteen locations were identified along the guideway between DIA and Eagle County Airport. These power pickup points were located where maximum power needs are expected to occur, such as at steep grades, or at locations where the route makes a significant or sharp change in direction. Their spacing varies from 11 to 16 km (7 to 10 miles). A few power pickup points were also located where there may be a greater need for reliability of power supply such as when the route crosses through the EJMT. In this case, a power pickup point is located at both ends of the tunnel providing a dual feed capability for that segment of the route.

The power pickup point locations are preliminary, although they are appropriate for conceptual design purposes. The exact geographic locations will emerge in the final design stages of the project based on how and where the utility chooses to supply the maglev system, most likely with a feeder in the 15 kV class. Conductors from this substation will feed the rectifier units located at frequent intervals along the guideway to convert the AC to the DC voltage of the maglev system.

Coordinate information was used to identify the location of these power pickup points by zip code and the utility serving that zip code as shown in Table 4.1-4. The table shows that United Power Inc. and Intermountain Rural Electric Association serve some of the locations. Both these are rural cooperatives that serve areas around DIA and small pockets West of Denver. However, Public Service of Colorado, or Xcel Energy will in fact handle construction of any substation at these locations for the maglev project due to agreements that exist between these entities. Therefore, twelve of the sixteen locations shown are under Xcel's control, the remaining four are in the Holy Cross Electric Association's service area, which means that Xcel will be the supplier handling almost all the power needs of the maglev system between DIA and Eagle County Airport.

Table 4.1-1 Corridor Utility Names

Company Name	Type	ADDRESS
PSC of Colorado	Investor Owned Utility	1225 17th St., Denver, CO, 80202
Glenwood Springs Electric System	Municipal	806 Cooper Ave., Glenwood Springs, CO, 81601
Grand Valley Rural Power Lines, Inc.	Co-operative District	2727 Grand Ave., Grand Junction, CO, 81501
Holy Cross Electric Association, Inc.	Co-operative District	3799 Hwy. 82, Glenwood Springs, CO, 81601
Intermountain Rural Electric Association	Co-operative District	5496 N. US Hwy. 85, Sedalia, CO, 80135
United Power, Inc.	Co-operative District	18551 E. 160th Ave., Brighton, CO, 80601
Mountain Parks Electric, Inc.	Co-operative District	321 W. Agate Ave., Granby, CO, 80446
Yampa Valley Electric Association, Inc.	Co-operative District	32 10th St., Steamboat Springs, CO, 80477

Table 4.1-2 Zip Codes Along Corridor Shared by Utilities

Zip Code	Company Name	% Overlap	Type
81506	Grand Valley Rural Power Lines, Inc.	0.677926960	ELEC-Non_IOU
81506	PSC of Colorado	0.322073152	ELEC-IOU
81521	Grand Valley Rural Power Lines, Inc.	1.000000000	ELEC-Non_IOU
81524	Grand Valley Rural Power Lines, Inc.	1.000000000	ELEC-Non_IOU
81525	Grand Valley Rural Power Lines, Inc.	0.997108370	ELEC-Non_IOU
81630	Moon Lake Electric Association, Inc.	0.054799559	ELEC-Non_IOU
81630	Grand Valley Rural Power Lines, Inc.	0.597655960	ELEC-Non_IOU
81630	PSC of Colorado	0.347163250	ELEC-IOU
81635	Holy Cross Electric Association, Inc.	0.154393504	ELEC-Non_IOU
81635	PSC of Colorado	0.844467888	ELEC-IOU
81650	Moon Lake Electric Association, Inc.	0.100088849	ELEC-Non_IOU
81650	Holy Cross Electric Association, Inc.	0.133904000	ELEC-Non_IOU
81650	White River Electric Association, Inc.	0.533117965	ELEC-Non_IOU
81650	PSC of Colorado	0.232917848	ELEC-IOU
81652	Holy Cross Electric Association, Inc.	0.733151969	ELEC-Non_IOU
81652	PSC of Colorado	0.266841215	ELEC-IOU
81601	Glenwood Springs Electric System	0.011576465	ELEC-Non_IOU
81601	Holy Cross Electric Association, Inc.	0.879722652	ELEC-Non_IOU
81601	PSC of Colorado	0.108703443	ELEC-IOU
80461	Sangre de Cristo Electric Association, Inc.	0.158506233	ELEC-Non_IOU
80461	PSC of Colorado	0.835579710	ELEC-IOU
80498	Holy Cross Electric Association, Inc.	0.195192354	ELEC-Non_IOU
80498	Yampa Valley Electric Association, Inc.	0.043442279	ELEC-Non_IOU
80498	Mountain Parks Electric, Inc.	0.616974893	ELEC-Non_IOU
80498	PSC of Colorado	0.144416916	ELEC-IOU
81621	Holy Cross Electric Association, Inc.	0.999081284	ELEC-Non_IOU
81631	Holy Cross Electric Association, Inc.	1.000000000	ELEC-Non_IOU
81637	Yampa Valley Electric Association, Inc.	0.068651376	ELEC-Non_IOU
81637	Holy Cross Electric Association, Inc.	0.931348524	ELEC-Non_IOU
81647	Holy Cross Electric Association, Inc.	0.355334753	ELEC-Non_IOU
81647	PSC of Colorado	0.644667602	ELEC-IOU
81657	Holy Cross Electric Association, Inc.	0.812113090	ELEC-Non_IOU
81657	PSC of Colorado	0.186696626	ELEC-IOU
80423	Yampa Valley Electric Association, Inc.	0.617864033	ELEC-Non_IOU
80423	Holy Cross Electric Association, Inc.	0.380741990	ELEC-Non_IOU
80468	Mountain Parks Electric, Inc.	0.992409949	ELEC-Non_IOU
80446	Mountain Parks Electric, Inc.	0.950261672	ELEC-Non_IOU
80446	PSC of Colorado	0.049539587	ELEC-IOU
80421	Intermountain Rural Electric Association	0.881180913	ELEC-Non_IOU
80421	PSC of Colorado	0.118768037	ELEC-IOU
80424	PSC of Colorado	0.995334341	ELEC-IOU
80433	Intermountain Rural Electric Association	0.957532478	ELEC-Non_IOU

Zip Code	Company Name	% Overlap	Type
80433	PSC of Colorado	0.042467734	ELEC-IOU
80435	Holy Cross Electric Association, Inc.	0.036860916	ELEC-Non_IOU
80435	PSC of Colorado	0.961392303	ELEC-IOU
80439	Intermountain Rural Electric Association	0.915297484	ELEC-Non_IOU
80439	PSC of Colorado	0.084702219	ELEC-IOU
80452	Holy Cross Electric Association, Inc.	0.022833052	ELEC-Non_IOU
80452	Intermountain Rural Electric Association	0.142400737	ELEC-Non_IOU
80452	PSC of Colorado	0.833390115	ELEC-IOU
80465	Intermountain Rural Electric Association	0.707921490	ELEC-Non_IOU
80465	PSC of Colorado	0.292078435	ELEC-IOU
80403	Intermountain Rural Electric Association	0.023157112	ELEC-Non_IOU
80403	United Power, Inc.	0.747724907	ELEC-Non_IOU
80403	PSC of Colorado	0.228295588	ELEC-IOU
80422	Intermountain Rural Electric Association	0.923352339	ELEC-Non_IOU
80422	PSC of Colorado	0.076680185	ELEC-IOU
80002	PSC of Colorado	1.000000000	ELEC-IOU
80004	PSC of Colorado	1.000000000	ELEC-IOU
80005	PSC of Colorado	1.000000000	ELEC-IOU
80007	PSC of Colorado	1.000000000	ELEC-IOU
80021	PSC of Colorado	1.000000000	ELEC-IOU
80033	PSC of Colorado	1.000000000	ELEC-IOU
80215	PSC of Colorado	1.000000000	ELEC-IOU
80225	PSC of Colorado	1.000000000	ELEC-IOU
80226	PSC of Colorado	1.000000000	ELEC-IOU
80228	PSC of Colorado	1.000000000	ELEC-IOU
80232	PSC of Colorado	1.000000000	ELEC-IOU
80401	Intermountain Rural Electric Association	0.350284864	ELEC-Non_IOU
80401	PSC of Colorado	0.649095143	ELEC-IOU
80235	PSC of Colorado	1.000000000	ELEC-IOU
80127	Intermountain Rural Electric Association	0.626562021	ELEC-Non_IOU
80127	PSC of Colorado	0.373437825	ELEC-IOU
80128	PSC of Colorado	1.000000000	ELEC-IOU
80227	PSC of Colorado	1.000000000	ELEC-IOU
80020	United Power, Inc.	0.349732850	ELEC-Non_IOU
80020	PSC of Colorado	0.650267808	ELEC-IOU
80027	PSC of Colorado	1.000000000	ELEC-IOU
80234	PSC of Colorado	1.000000000	ELEC-IOU
80221	PSC of Colorado	1.000000000	ELEC-IOU
80003	PSC of Colorado	1.000000000	ELEC-IOU
80030	PSC of Colorado	1.000000000	ELEC-IOU
80031	PSC of Colorado	1.000000000	ELEC-IOU
80260	PSC of Colorado	1.000000000	ELEC-IOU
80205	PSC of Colorado	1.000000000	ELEC-IOU
80202	PSC of Colorado	1.000000000	ELEC-IOU

Zip Code	*Company Name*	*% Overlap*	*Type*
80203	PSC of Colorado	1.000000000	ELEC-IOU
80204	PSC of Colorado	1.000000000	ELEC-IOU
80209	PSC of Colorado	1.000000000	ELEC-IOU
80210	PSC of Colorado	1.000000000	ELEC-IOU
80211	PSC of Colorado	1.000000000	ELEC-IOU
80212	PSC of Colorado	1.000000000	ELEC-IOU
80214	PSC of Colorado	1.000000000	ELEC-IOU
80219	PSC of Colorado	1.000000000	ELEC-IOU
80223	PSC of Colorado	1.000000000	ELEC-IOU
80236	PSC of Colorado	1.000000000	ELEC-IOU
80110	PSC of Colorado	1.000000000	ELEC-IOU
80121	PSC of Colorado	1.000000000	ELEC-IOU
80123	PSC of Colorado	1.000000000	ELEC-IOU
80237	PSC of Colorado	1.000000000	ELEC-IOU
80220	PSC of Colorado	1.000000000	ELEC-IOU
80208	PSC of Colorado	1.000000000	ELEC-IOU
80207	PSC of Colorado	1.000000000	ELEC-IOU
80206	PSC of Colorado	1.000000000	ELEC-IOU
80010	PSC of Colorado	1.000000000	ELEC-IOU
80012	PSC of Colorado	1.000000000	ELEC-IOU
80014	PSC of Colorado	1.000000000	ELEC-IOU
80216	PSC of Colorado	1.000000000	ELEC-IOU
80218	PSC of Colorado	1.000000000	ELEC-IOU
80246	PSC of Colorado	1.000000000	ELEC-IOU
80222	PSC of Colorado	1.000000000	ELEC-IOU
80224	PSC of Colorado	1.000000000	ELEC-IOU
80229	PSC of Colorado	0.993032808	ELEC-IOU
80230	PSC of Colorado	1.000000000	ELEC-IOU
80231	PSC of Colorado	1.000000000	ELEC-IOU
80233	United Power, Inc.	0.223263502	ELEC-Non_IOU
80233	PSC of Colorado	0.776735701	ELEC-IOU
80239	PSC of Colorado	1.000000000	ELEC-IOU
80241	PSC of Colorado	1.000000000	ELEC-IOU
80015	Intermountain Rural Electric Association	0.493871825	ELEC-Non_IOU
80015	PSC of Colorado	0.506130174	ELEC-IOU
80016	Intermountain Rural Electric Association	0.535738280	ELEC-Non_IOU
80016	PSC of Colorado	0.464261828	ELEC-IOU
80111	Intermountain Rural Electric Association	0.039538966	ELEC-Non_IOU
80111	PSC of Colorado	0.960461959	ELEC-IOU
80017	PSC of Colorado	1.000000000	ELEC-IOU
80011	PSC of Colorado	1.000000000	ELEC-IOU
80013	PSC of Colorado	1.000000000	ELEC-IOU
80022	United Power, Inc.	0.408508751	ELEC-Non_IOU
80022	PSC of Colorado	0.591491808	ELEC-IOU

Zip Code	Company Name	% Overlap	Type
80249	PSC of Colorado	0.997563788	ELEC-IOU
80262	PSC of Colorado	1.000000000	ELEC-IOU
80601	United Power, Inc.	0.452468421	ELEC-Non_IOU
80601	PSC of Colorado	0.547530741	ELEC-IOU
80602	United Power, Inc.	0.862431935	ELEC-Non_IOU
80602	PSC of Colorado	0.137568129	ELEC-IOU
80603	United Power, Inc.	1.000000000	ELEC-Non_IOU
80640	United Power, Inc.	0.362998291	ELEC-Non_IOU
80640	PSC of Colorado	0.637004720	ELEC-IOU
80018	PSC of Colorado	1.000000000	ELEC-IOU
80019	PSC of Colorado	1.000000000	ELEC-IOU
80137	Intermountain Rural Electric Association	0.026409507	ELEC-Non_IOU
80137	United Power, Inc.	0.017267194	ELEC-Non_IOU
80137	PSC of Colorado	0.956322025	ELEC-IOU
80102	Intermountain Rural Electric Association	0.804403943	ELEC-Non_IOU
80102	Mountain View Electric Association, Inc.	0.068051411	ELEC-Non_IOU
80102	United Power, Inc.	0.010576074	ELEC-Non_IOU
80102	Morgan County Rural Electric Association	0.027057672	ELEC-Non_IOU
80102	PSC of Colorado	0.089912479	ELEC-IOU
80103	Intermountain Rural Electric Association	0.995377341	ELEC-Non_IOU
80136	Morgan County Rural Electric Association	0.659808432	ELEC-Non_IOU
80136	Intermountain Rural Electric Association	0.340191576	ELEC-Non_IOU
81522	Grand Valley Rural Power Lines, Inc.	0.997959750	ELEC-Non_IOU
81501	Grand Valley Rural Power Lines, Inc.	0.220213582	ELEC-Non_IOU
81501	PSC of Colorado	0.779787735	ELEC-IOU
81503	Grand Valley Rural Power Lines, Inc.	0.568719078	ELEC-Non_IOU
81503	PSC of Colorado	0.431281138	ELEC-IOU
81504	Grand Valley Rural Power Lines, Inc.	0.551393605	ELEC-Non_IOU
81504	PSC of Colorado	0.448606850	ELEC-IOU
81505	Grand Valley Rural Power Lines, Inc.	0.977456360	ELEC-Non_IOU
81505	PSC of Colorado	0.022543419	ELEC-IOU
81520	Grand Valley Rural Power Lines, Inc.	0.441884833	ELEC-Non_IOU
81520	PSC of Colorado	0.558115347	ELEC-IOU
81526	PSC of Colorado	0.999178836	ELEC-IOU
81527	Grand Valley Rural Power Lines, Inc.	0.724203595	ELEC-Non_IOU
81527	PSC of Colorado	0.273150524	ELEC-IOU
81643	Grand Valley Rural Power Lines, Inc.	0.894636992	ELEC-Non_IOU
81643	PSC of Colorado	0.103521893	ELEC-IOU
81623	Delta-Montrose Electric Association	0.020906920	ELEC-Non_IOU
81623	Gunnison County Electric Association, Inc.	0.068976924	ELEC-Non_IOU
81623	Holy Cross Electric Association, Inc.	0.774445689	ELEC-Non_IOU
81623	PSC of Colorado	0.134298527	ELEC-IOU
81624	Grand Valley Rural Power Lines, Inc.	0.685500029	ELEC-Non_IOU
81624	PSC of Colorado	0.309988885	ELEC-IOU

Zip Code	Company Name	% Overlap	Type
80440	Intermountain Rural Electric Association	0.809937713	ELEC-Non_IOU
80440	PSC of Colorado	0.187737267	ELEC-IOU

Table 4.1-3 Generating Stations, Ownership and Winter Capacity Ratings (MW)

Plant Name	Operator Name	Company Name	Capacity (MW)
Foothills Hydro Plant	Denver Water Dept.	Denver, City & County of	0.91
Hillcrest Power Plant	Denver Water Dept.	Denver, City & County of	1.10
Dillon Hydro Plant	Denver Water Dept.	Denver, City & County of	1.81
Peach Queen Powerstation	Hydro-West of Colorado	Hydro-West of Colorado	2.50
Colorado Landfill Gas Gen. Proj.	Energy Developments, Ltd.	Energy Developments, Ltd.	4.80
Metro Wastewater Cogen	Trigen-Colorado Energy Corp.	Trigen-Colorado Energy Corp.	5.00
Metro Wastewater Cogen	Trigen-Colorado Energy Corp.	Denver Metrop. Wastewater Reclam. Dist.	5.00
PDH Cogeneration Project	PDH Energy Partnership, Ltd.	PDH Energy Partnership, Ltd.	6.50
Gross Hydro Plant	Denver, City & County of	Denver, City & County of	7.88
Metro Wastewater Reclam. D	Denver Metro. Wastewater Reclam.	Metropolitan Waste Water Reclamation District	9.80
American Gypsum Cogen.	National Energy Systems Co.	National Energy Systems Co.	9.84
Shoshone (PSCO)	PSC of Colorado	PSC of Colorado	15.00
Golden Plant	Trigen Nations Energy Co.	Trigen-Colorado Energy Corp.	17.70
Golden Plant	Trigen Nations Energy Co.	Nations Energy Corp.	17.70
Fruita	PSC of Colorado	PSC of Colorado	20.00
Total Petroleum	PSC of Colorado	PSC of Colorado	23.00
Glenwood Springs Salt Project	Glenwood Springs Salt Co., L.P.	Glenwood Springs Salt Co., L.P.	34.00
Rifle Generating Station	Tri-State G & T Association, Inc.	Tri-State Generation & Transmissions	85.00
Zuni	PSC of Colorado	PSC of Colorado	107.00
Plains End	PG&E National Energy Group, Inc.	PG&E National Energy Group, Inc.	111.00
DIA Power Project	North American Power Group	North American Power Group	150.00
Arapahoe (Blhige)	Black Hills Generation, Inc.	Black Hills Generation, Inc.	193.00
Cabin Creek (PSCO)	PSC of Colorado	PSC of Colorado	324.00
Blue Spruce Energy Center	SkyGen Services	SkyGen Services	338.00
Cameo	PSC of Colorado	PSC of Colorado	430.70
Arapahoe (PSCO)	PSC of Colorado	PSC of Colorado	472.00
Cherokee (PSCO)	PSC of Colorado	PSC of Colorado	728.50

Table 4.1-4 Power Pickup Coordinates

Power Pickup	Place Name	Coordinates (Degrees, Minutes, Seconds)
Pickup 1	Denver Airport	Lat: 39 52 30 N
		Long: 104 45 00 W
Pickup 2	Denver	Lat: 39 53 30 N
	96th and I-76	Long: 104 54 00 W
Pickup 3	Denver	Lat: 39 44 30 N
	I-70 Bus and I-25	Long: 105 00 40 W
Pickup 3.5	Denver	Lat: 39 43 50 N
	I-70 and I-70 Bus	Long: 105 09 40 W
Pickup 4	Genesee Park	Lat: 39 42 00 N
	Exit 254 I-70	Long: 105 18 45 W
Pickup 5	Exit 244	Lat: 39 44 30 N
	I-70 and 6	Long: 105 26 10 W
Pickup 6	Dumont	Lat: 39 45 50 N
	Exit 236	Long: 105 35 45 W
Pickup 7	Georgetown	Lat: 39 42 30 N
	Exit 228	Long: 105 41 20 W
Pickup 8	Herman Gulch Trail	Lat: 39 41 55 N
	Exit 218	Long: 105 51 00 W
Pickup 9	Loveland	Lat: 39 40 55 N
		Long: 105 53 15 W
Pickup 10	Eisenhower Tunnel Complex	Lat: 39 40 40 N
		Long: 105 53 10 W
Pickup 11	Dillon	Lat: 39 37 45 N
		Long: 106 02 45 W
Pickup 12	Wheeler Junction	Lat: 39 30 30 N
	Exit 195	Long: 106 08 30 W
Pickup 13	Vail Pass	Lat: 39 31 30 N
	Exit 190	Long: 106 13 00 W
Pickup 14	Bighorn Road	Lat: 39 36 30 N
		Long: 106 16 25 W
Pickup 15	Vail	Lat: 39 38 45 N
	Exit 176	Long: 106 22 50 W

Table 4.1-4: Power Pickup Zip Codes and Utility

Pick Up	Approx Place Name	Zip Code	Utility
Pickup 1	Denver Airport	80022	United Power, Inc.
Pickup 2	Denver 96th and I76	80640	United Power, Inc.
Pickup 3	Denver I70 and I25	80204	PSC of Colorado
Pickup 3.5	Denver I70 and I70 Bus	80401	PSC of Colorado
Pickup 4	Genesee Park Exit 254 I70	80401	Intermountain Rural Electric Association
Pickup 5	Exit 244 I70 and 6	80439	Intermountain Rural Electric Association
Pickup 6	Dumont Exit 236	80452	Intermountain Rural Electric Association
Pickup 7	Georgetown Exit 228	80452	Intermountain Rural Electric Association
Pickup 8	Herman Gulch Trail Exit 218	80452	PSC of Colorado
Pickup 9	Loveland	80452	Holy Cross Electric Association, Inc.
Pickup 10	Eisenhower Tunnel Complex	80452	Holy Cross Electric Association, Inc.
Pickup 11	Dillon	80435	PSC of Colorado
Pickup 12	Wheeler Junction Exit 195	80435	PSC of Colorado
Pickup 13	Vail Pass Exit 190	80435	PSC of Colorado
Pickup 14	Bighorn Road	81657	Holy Cross Electric Association, Inc.
Pickup 15	Vail Exit 176	81657	Holy Cross Electric Association, Inc.

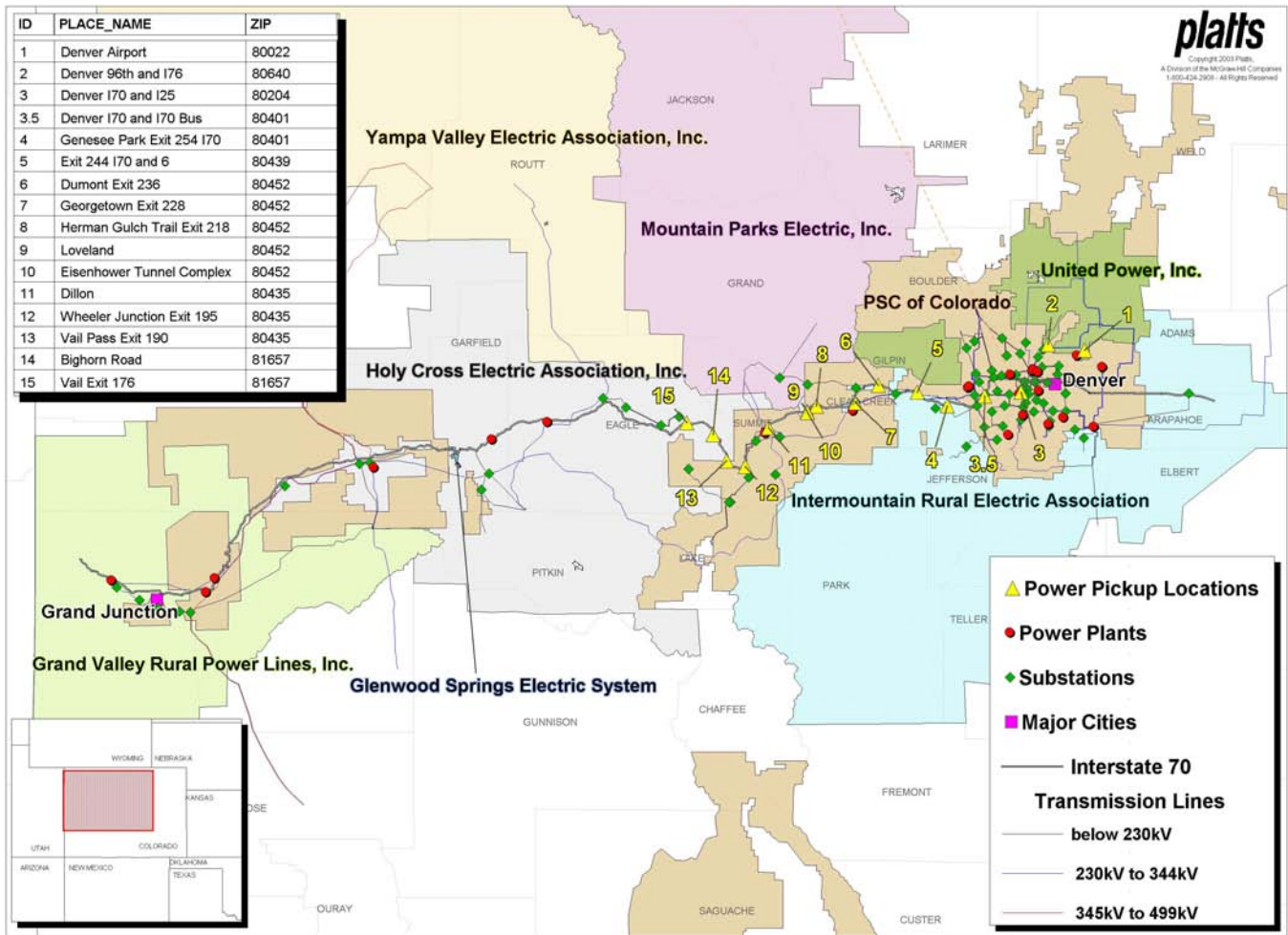| ID	PLACE_NAME	ZIP
1	Denver Airport	80022
2	Denver 96th and I76	80640
3	Denver I70 and I25	80204
3.5	Denver I70 and I70 Bus	80401
4	Genesee Park Exit 254 I70	80401
5	Exit 244 I70 and 6	80439
6	Dumont Exit 236	80452
7	Georgetown Exit 228	80452
8	Herman Gulch Trail Exit 218	80452
9	Loveland	80452
10	Eisenhower Tunnel Complex	80452
11	Dillon	80435
12	Wheeler Junction Exit 195	80435
13	Vail Pass Exit 190	80435
14	Bighorn Road	81657
15	Vail Exit 176	81657

Figure 51: Location of Power Plants, Transmission, Substations and Power Pickup Points Along the Proposed Corridor

4.2. POWER REQUIREMENTS AND SUPPLY ADEQUACY

4.2.1. *Power Requirements*

The maglev system power requirements are proportional to several factors including acceleration, speed, passenger loading, and grade of the track. Of these, acceleration and grade are the predominant factors affecting the power consumption. The terrain west of Denver traverses high mountain passes and generally, the guideway encounters a constantly increasing grade, which exceeds 7% in some locations at the steepest grades, with grades in the 5% - 6% common for significant sections of the guideway.

The power requirements were determined from the MathCAD data from the Propulsion Trade Study, dated August 20, 2003. The key assumptions for the power estimates from this data set are:
- The vehicle specified is the COL-200a, with a 2-car consist for the train
- The average speed of the route is 114 kph (calculation of power assumes a constant speed)

The data is organized in an array of 2,241 data points obtained by dividing the 243.51 km length of the route into discrete segments of approximately 0.1 km each. The thrust and power is

calculated for each discrete segment moving west from a point near the DIA with assumed headwinds of 0, 25, 45 and 90 kph. The MathCAD data set was imported into an Excel spreadsheet to identify the segment where peak power demand occurs and to identify the segments leading into and away from the peak segment, assuming a westerly direction of travel. This provides a clear picture of the location where the peak demand occurs and the grade of the guideway at this location and the adjacent locations.

According to this analysis, the peak demand will be 2,320.12 kW per car, or 4,640.24 kW for each 2-car train. This demand occurs at a 7.48% grade at a distance of 171.85 km (segment 1551) west of DIA on the eastbound track with a 90 kph headwind. Similarly, the peak in the westbound direction will be 2,098.05 kW per car, or 4,0196.10 kW per train and occurs at a 6.59% grade at a distance of 124.45 km (segment 1111) west of DIA under 90 kph headwind conditions. The steeper grades in the route excursions from I-70 are estimated to be on the order of 10% to 12% with grade lengths possibly on the order of a few miles. Such lengths will be sufficient to establish steady speed operation following a transient slowdown from higher speed on a down hill or level section. Given that the motor was designed for maintenance of 160 kph speed on grades up to 7%, at greater grades, the motor will operate at maximum power to achieve the highest speed possible that the grade and wind load will permit, within the limits of the route curvature. At the 12% grade, the peak power demand per car would be 1.7 times the maximum of 2.3 MW per car addressed on the I-70 route at the average speed. This level may well fall within the sizing of the substation when the power available from the local battery system (for storage of regenerated power when braking) is considered. The length of the high-grade sections are very short compared to the entire route length, and offset by the stored, regenerated power from braking, the impact of the additional electrical energy demand is expected to be small.

For purposes of electric supply planning, the maglev corridor is divided into segments of 11 to 16 km lengths as described in the analysis. These are the power pickup points where the 25 kV AC supply grid interfaces with the rectifiers supplying the DC traction power. The power consumption of the maglev system determines the size of the transformers designed for these power pickup points or substations. The current assumptions of peak ridership and headway clearance indicates that there could be no more than two trains in each direction of travel or four trains in both directions between two adjacent substations. Thus the substation load for the train traction power would be no more than four times or (4,640.24 x 4) kW = 18,560.96 kW, or a nominal load of 20 MW at each substation.

The number of active trains on the track for the same ridership assumptions indicates that there are a total of 44 (2-car consist) trains in the corridor. The peak load of each eastbound train of 4,640.24 kW, computed above is used to compute the total traction load for the entire corridor, assuming that all 44 trains are operating on the guideway. This load is (4,640.24 x 44) kW = 204,170.56 kW or 205 MW, nominal.

Similarly, the energy required for the traction power of each train is also computed from the MathCAD/Excel data set for headwinds of 0, 25, 45 and 90 kph. The 0 kph headwind yields the lowest energy consumption due to the absence of drag; the higher headwind conditions yield correspondingly higher consumptions. The energy requirements calculated in the spreadsheet include the reduction from regenerative braking accumulated over the entire route in each direction. The analysis indicates that the eastbound trains require less energy traveling from Eagle to DIA due to the lower elevation of the Denver region by approximately 350 meters. The eastbound train energy consumption benefits both from the decreasing elevations in the easterly direction and the cumulative effects of regenerative braking.

The four headwind assumptions yield both a worst- and best-case estimate of energy consumption bracketed by the 0 and 90 kph envelopes. The worst-case energy estimate is obtained from the 90 kph condition for all westbound trains. Since it is assumed that the peak traffic is 44 trains, then 22 trains would be heading west with 90 kph headwinds, and 22 trains

heading east under a tailwind condition of 90 kph. For the purpose of this analysis, tailwind conditions are assumed to make no contribution, and are treated the same as a 0 kph headwind. Therefore, the westbound trains require (1,225.29 kWh x 22) = 26,962.98 kWh, and the east bound require (682.41 kWh x 22) = 15,013.02 kWh, or a total of 41,976 kWh or approximately 42 MWh.

The more likely average wind conditions on an annual basis for the entire route are assumed to lie between the 25 kph and 45 kph conditions. This results in energy requirements of (884.30 kWh x 22) = 19,454.60 kWh for westbound trains with 25 kph headwind and (844.50 kWh x 22) = 18,579.00 kWh for the eastbound trains with 45 kph headwind. The total energy requirements for this scenario are 38,033.60 kWh or 39 MWh.

The best-case scenario would be 0 kph headwind for both direction of travel which is (795.23 kWh x 22) = 17,495.06 kWh, westbound and (682.41 kWh x 22) = 15,013.02 kWh, eastbound, for a total energy requirement of 32,508.08 kWh or 33 MWh.

Examining the best- and worst-case energy requirements and considering the likely case requirement of 39 MWh, it is estimated that the average consumption is in the 37 MWh to 39 MWh range.

These power and energy requirements are summarized below:

Maximum power required per car	2,320.12 kW (on eastbound leg)
Maximum power required per train	4,640.24 kW (on eastbound leg)
Maximum power needed at each substation	20 MVA (4 trains in each segment)
Total guideway electric load w/44 trains	205 MW
Estimated guideway electric energy w/44 trains	37 – 39 MWh

4.2.2. *Substation Design*

With four trains between adjacent substations, it was determined that each substation could have a peak load of 20 MW. Based on this load, a 25 MVA transformer is selected for each substation, which is approximately 5 MVA larger than the estimated traction load of the trains. The higher rating allows for some margin in the power requirement estimates and accommodates ancillary loads such as station power, communication and control loads. This margin offers operational flexibility and accommodates higher train traffic patterns or off normal operations due to unforeseen conditions as well. Therefore, a standard substation layout, with two 25 MVA transformer banks at each substation is proposed for the maglev system. This substation configuration allows for a high degree of reliability, ease of maintenance and accommodates future growth in the maglev train system.

The conceptual substation layout with two transformer banks is shown in Figure 52. Both Transformer Banks 1 and 2 step down the AC grid voltage from 115 kV to 25 kV, and have a 25 MVA rating, each. Bank 1 is the primary transformer supplying two 25 kV feeders, 1A and 1B, that route the power to the rectifier section that converts the AC to the 3 kV DC required by the maglev system. Transformer Bank 2 is in a standby mode and is used when substation service is required to repair switchgear or other equipment or, if the future train traffic patterns change and more than four trains are operated in each segment. This redundancy provides a higher degree of maintainability and reliability while accommodating future growth and not locking the guideway into an operation mode restricted by transformer capacity. This redundant design is common utility practice and assures a greater degree of flexibility for a nominal increase in the capital cost of the project. Feeder 1A and 1B feed the rectifier section for traction power as shown in Figure 53. The rectifiers convert the 25 kV AC to the 3,000 V DC required for the maglev system.

The substations also have a dual feed from the 115 kV transmission grid shown by the two taps feeding the substation. These two feeds originate from two separate transmission substations – one in the east, perhaps at Dillon, and one in the west, in or near Denver. The maglev system substation breakers are configured to draw power from either source to feed the 25 MVA transformer banks. This configuration extends the reliability deeper into the grid, thus assuring that the substations; hence the guideway has as reliable a power source as is operationally possible.

4.2.3. *Station Power*

Most of the train stations are assumed to be at the higher elevation of the guideway and will require elevators or escalators for passenger use. Additionally, all the stations will have winter heating requirements. Thus, the station load, including lighting will be 50 kW. Additionally, each station is assumed to have a combination pneumatic and electric track switching capability to move the cars between tracks. This load is assumed to be approximately 150 kW. Thus, the total station load is 200 kW, and is supplied by a dedicated 200 kVA/480 V transformer shown in Figure 53.

4.2.4. *Onboard Auxiliary Power*

An allowance is made for on-board auxiliary power of 200 kVA at 13.8 kV to accommodate heating and other loads within the train. A dedicated 200 kVA/13.8 kV transformer is shown for this use in Figure 53.
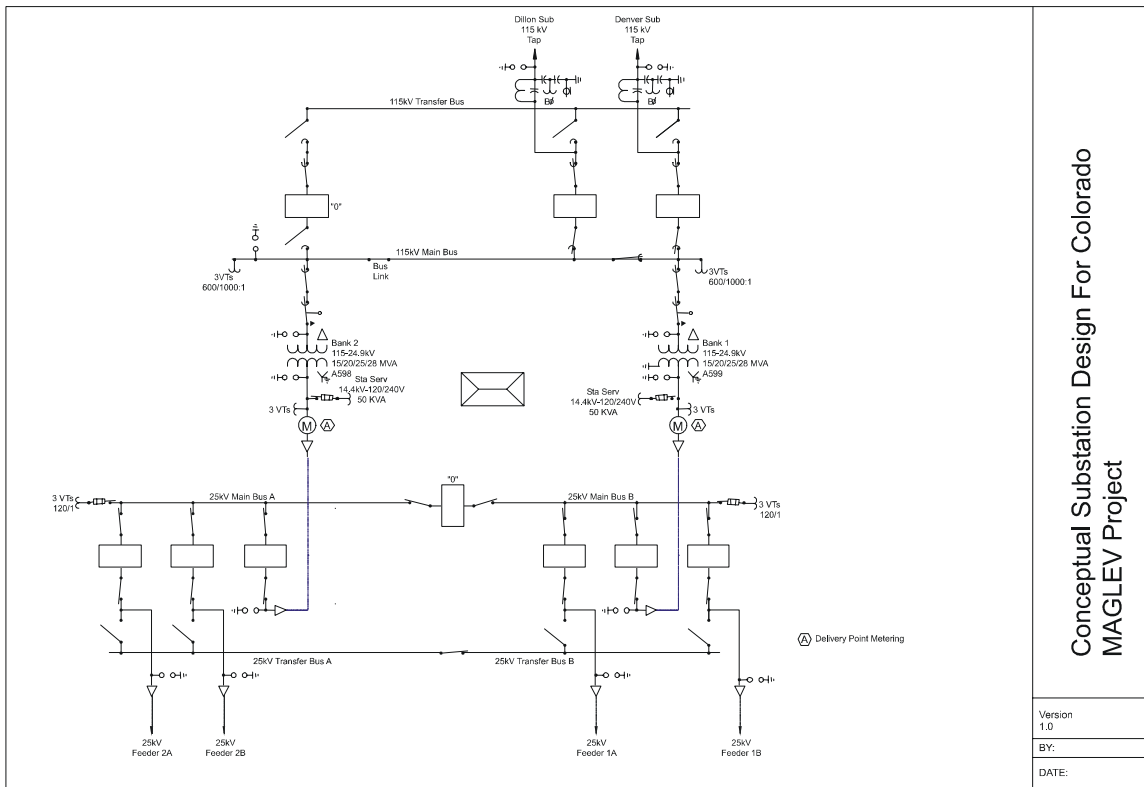

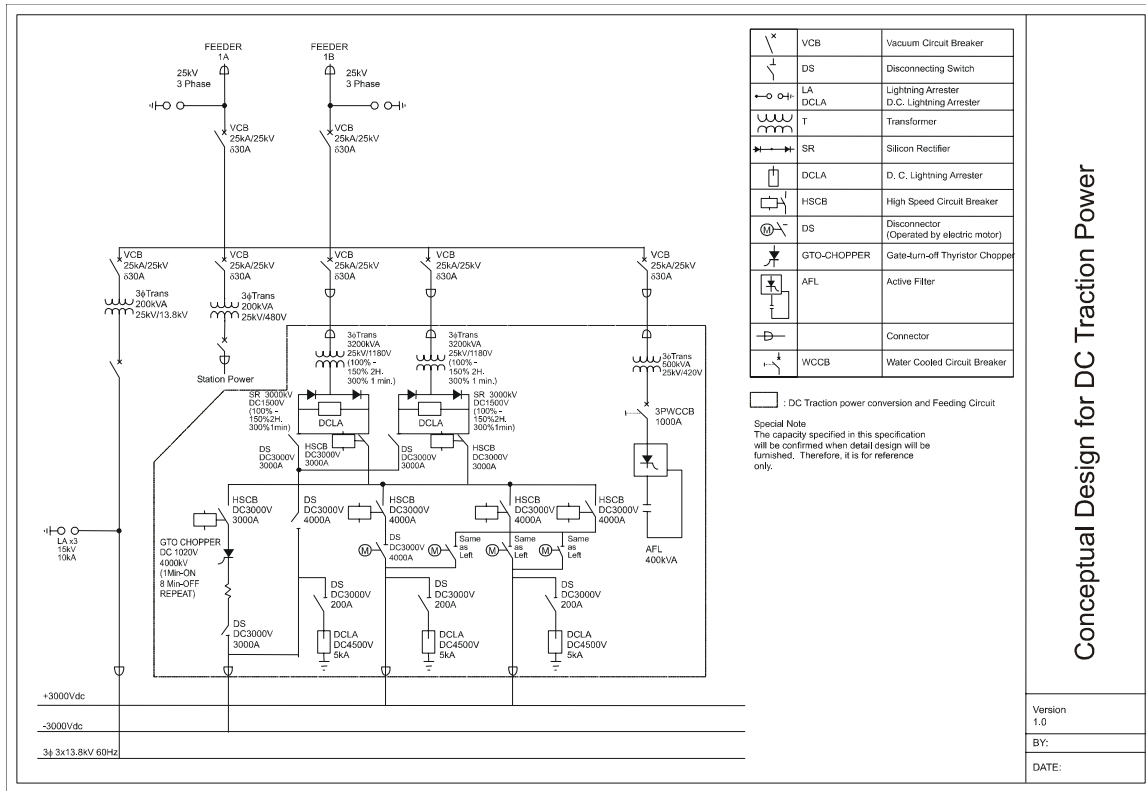**Figure 52: Conceptual Substation Diagram**

Figure 53: Conceptual Diagram of Rectifier Section

4.2.5. *Power Supply Options*

4.2.5.1. Base Case

At the inception of this work, the approach proposed for supplying power to the maglev system was to build power pickup points or substations at 11 to 16 km intervals along the guideway. Each substation would be supplied with a 115 kV or a 25 kV feed where possible. These substations would in turn supply the rectifiers that supplied the guideway with the required 3 kV DC. Upon examining the existing substation capacities near the proposed guideway and consultations with Holy Cross Electric Association, it was clear that the power needs of the maglev system would not be met with the existing substation capacity. Hence each substation would need its dedicated feed from the 115 kV grid directly. Hence the "base option" was to build approximately 25 substations along the guideway, each with a nominal 50 MVA capacity distributed in two 25 MVA transformer banks.

A major drawback to this approach emerged as further work was performed and following discussions with the region's electric utilities regarding the practical implementation of the maglev project's electric infrastructure. The most constraining drawback was the issue of right-of-way and the related permitting to secure the 115 kV feed to each substation. Under this scenario, each substation would require negotiating a separate ROW and permit to provide the 115 kV feed from the transmission corridor. The process of securing the ROW and the permitting process for the new transmission paths, even if each were a few miles long, would introduce a high degree of uncertainty in building each substation. The process would have to be repeated for each of the 25 substations; in other words, each new line to the 25 subs would be treated as an individual project.

4.2.5.2. Alternate Option

The alternate option that emerged as a more feasible approach was to build a 115 kV transmission circuit within the right-of-way of the maglev corridor. The substations would still be 11 to 16 km apart as originally proposed, although they would tap into the 115 kV line, which would be within the guideway's corridor. Using this approach avoids building 25 separate feeds to each of the substations from the 115 kV grid. However, this option restricts the 115 kV line to be buried and designed as an underground transmission line. Safety of operation of the maglev system and the need to minimize public opposition to a new overhead transmission corridor is the forcing function for the underground option.

From a safety perspective, exposed 115 kV conductors suspended from the guideway are not a desirable or practical design option. Further, the catenaries formed by the suspended cable raises issues of ground clearance and clearance from the guideway to operate safely. Thus, an underground option might appear to be the only feasible design choice.

Based on current cable specifications used by Holy Cross Electric, this 115 kV circuit can support over 112 to 120 km of the maglev system's load, before experiencing a 5% voltage drop. This distance is also a convenient midpoint of the approximately 240 km of the proposed guideway length. It is expected that a transmission tap at Denver and another at an intermediate location, such as Dillon should be able to meet all of the maglev systems power needs. The two taps are shown in Figure 51.

A related advantage of building a 115 kV path in the guideway corridor is that it opens up a new transmission path that could be attractive to Xcel and Holy Cross Electric. Both utilities have constraints in building new transmission lines due to public opposition to new corridors. However, a transmission path that is not visible and serves a dual community purpose would be far less likely to draw public opposition and would be inherently more attractive to both the users and the regional suppliers of electricity.

A significant disadvantage of this approach is that the adverse terrain/soil conditions could make it infeasible to bury the cable in the maglev system ROW in some locations. In these instances, the guideway design would have to be altered to accommodate some alternate form of power carrying capability. A second disadvantage is to increase the overall cost of the electric supply infrastructure. It is estimated that a buried 115 kV transmission line would add $2 million per mile to the cost of the electric infrastructure. This would be in addition to the $2 million for each substation. Fortunately, newer technology, in the form of the gas insulated transmission line, provides another feasible alternative for construction of the needed transmission circuit.

4.3. FEASIBILITY OF DISTRIBUTED GENERATION

4.3.1. *Background*

The original work plan for the Electrification task of the CMP specified a study of the Feasibility of Distributed Generation. At the inception of the Electrification effort, the expectation was that the maglev system would be powered by a network of substations individually supplied by 25 kV feeders from existing substations in the corridor vicinity. The information gathered in the Existing and Planned Power Supply Resources, indicated several constraints to this approach, which led to proposing a 230 kV underground transmission corridor parallel to the maglev right of way. This change led to some changes in the scope of this work effort. Specifically, the need to identify natural gas availability and pricing does not necessarily apply to the overall project.

4.3.2. *Typical Substation Design and Cost*

In the earlier discussion it was noted that the 4 trains between adjacent substations generates a peak load of 20 MW at each substation. Based on this estimate, a 25 MVA transformer and associated breakers were selected as the baseline requirement for each substation. (The 25

MVA rating includes a 5 MVA margin for any unexpected design contingencies). Therefore, a standard substation layout, with two 25 MVA transformer banks at each substation is proposed for the maglev system.

The conceptual substation layout with two transformer banks is shown in Figure 52 above. Both Transformer Banks 1 and 2 step down the AC grid voltage from 115 kV to 25 kV, and have a 25 MVA rating, each. Bank 1 is the primary transformer supplying two 25 kV feeders, 1A and 1B, that route the power to the rectifier section that converts the AC to the 3 kV DC required by the maglev system. Transformer Bank 2 is in a standby mode and is used when substation service is required to repair switchgear or other equipment or, if the future train traffic patterns change and more than four trains are operated in each segment. This redundancy provides a higher degree of maintainability and reliability while accommodating future growth and not locking the guideway into an operation mode (train schedule) restricted by transformer capacity. This redundant design is common utility practice and assures a greater degree of flexibility for a nominal increase in the capital cost of the project.

The substations also have a dual feed from the 115 kV transmission grid shown by the two taps feeding the substation. These two feeds originate from two separate transmission substations – one in the west, perhaps at Dillon, and one in the east, in or near Denver. The maglev system substation breakers are configured to draw power from either source to feed the 25 MVA transformer banks. This configuration extends the reliability deeper into the grid, thus assuring that the substations, and further the guideway, have as reliable a power source as is operationally possible.

4.3.3. *Substation Costs*

The conceptual design of the 25 MVA maglev systems substations was used to obtain cost information from utility distribution engineers both in Colorado and New Mexico. The dual information approach was used to bracket the estimated cost of the substations because of wide variations in substation design practice among utilities. Given the same substation design, different utilities specify a wide range of breakers dictated by their protection and interconnection guidelines. Obtaining cost information from the two sources captures this cost variability and provides a higher confidence level in the estimated costs. Tables 4.3-1 and 4.3-2 show the costs obtained from Colorado and New Mexico, respectively.

Table 4.3-1 Colorado Substation Cost Estimate

Standard Profile Substation (115 kV feed)	Single Site Cost		Multiple Site Cost	
Equipment - including:	$ 3,167,165	77%	$ 2,217,015.50	84%
Two 25 MVA transformer bays				
Gas insulated switchgear				
Controls				
Construction	$ 450,000	11%	$ 337,500.00	13%
Engineering	$ 200,000	5%	$ 20,000.00	1%
Construction Mgmt	$ 170,000	4%	$ 17,000.00	1%
Survey and Soil Study	$ 10,000	0.24%		
Architectural Wall Screening	$ 100,000	2%	$ 50,000.00	2%
Sub-Total	**$ 4,097,165**		**$ 2,641,515.50**	

Table 4.3-2 New Mexico Substation Cost Estimate

25 MVA Substation - Double breaker/Double Bus (230 kV Switchgear)	Single Site Cost	Multiple Site Cost
Seven gas insulated breakers	$ 5,250,000	$ 3,675,000
Two 25 MVA transformer bays	$ 1,000,000	$ 700,000
Site specific costs	$ 200,000	$ 100,000
Total	**$ 6,450,000**	**$ 4,475,000**

25 MVA Substation – MAGLEV Layout (230 kV Switchgear)	Single Site Cost	
Three gas insulated breakers	$ 2,250,000	$ 1,575,000
Two 25 MVA transformer bays	$ 1,000,000	$ 700,000
Site specific costs	$ 200,000	$ 100,000
Total	**$ 3,450,000**	**$ 2,375,000**

The two tables highlight the differences in substation design approaches at the two utilities. The Colorado utility builds 25 MVA, 115 kV substations and had a more refined cost estimate including site-specific cost components such as engineering, survey and soils study. The New Mexico utility chose to cost out 230 kV substations, which closely matches the maglev system requirements, with the exception that their primary cost driver is the breaker configuration that requires seven breakers which yields a double breaker/double bus configuration. That cost is shown in the upper part of Table 4.3-2, and a "reconfigured" substation cost utilizing only three breakers (more representative of the standard maglev system substation) is shown in the lower portion.

Both tables show single site and multiple site costs since utilities build only one or two substations at a time. In the maglev project there could be as many as 30 such substations, which clearly indicates the potential for cost savings due to volume purchase of equipment as well as an overall reduction in repetitive site specific costs such as site engineering. The single unit costs of both tables reflect an assumed reduction due to volume procurement of the major components such as transformers and switchgear as well as a reduction of site specific costs.

Normalizing the assumptions of the two substations indicates the single site cost for each maglev system substation to be between $2,375,000 and $2,641,515, through capture of volume discounts.

4.3.4. *Energy Storage Systems*

An energy storage system is needed to provide the levitation and motive power energy needs if there is an outage of electric power from the commercial sources. The maglev system braking time and distance calculations provide the stopping time estimates for a 7% downhill grade with normal and 10% overcurrent to the LIMs as 51 seconds and 38 seconds[1], respectively. Maximum power draw calculations from the Electrification analysis show that each train draws 4,640 kW. Since there could be as many as two trains in each segment, the power requirement is 5,280 kW. Using the longest braking time of 51 seconds gives a gross energy of 131 kWh produced by the train in a regenerative braking mode. An energy storage system is needed to

---

[1] Braking Distance and Time on Grade calculations made for Propulsion Trade Study, November 30, 2003.

absorb the regenerative braking as well as providing the levitation energy to bring the train to a complete stop.

Battery storage systems have been designed and built to support rail systems with the objective of storing the regenerative braking energy and applying it to traction energy as the trains accelerate. The San Diego regional transit system experimented with a 400 kW battery system in the early 1990's. However, this and other systems have full function dc-to-ac inverters, which, in the case of the maglev system could be eliminated with substantial cost benefits. The power conversion system (PCS) in almost all large battery systems constitutes 25% to 30% of installed costs. In the case of the maglev system, the power requirements are greater than the energy requirements that tend to shift the major cost component to the PCS. Eliminating the PCS and keeping the energy storage system entirely DC could reduce the cost of the energy storage systems significantly.

The battery system conceptualized for the maglev system could "float" at the traction voltage of 3,000 Vdc with a storage capacity of approximately 160 kWh, thus eliminating the need for a PCS. The battery would regulate at the track voltage and remain at an average 80% state-of-charge, thus maintaining the capability to absorb the regenerative braking energy during normal operation mode. During the emergency operation mode when there is loss of utility power, the battery would still absorb most of the regenerative braking and also provide levitation power as the train slows to a complete stop.

A battery system with the appropriate charging and control subsystems to meet this requirement would cost approximately $1,100/kWh, with a total cost of $176,000 per system. There are four segments in the maglev system corridor where the grades are in the 7% range, and it is proposed that one such battery system be provided in each of the four segments.

Other storage technologies such as flywheels or superconducting magnetic energy storage could also meet these functional requirements and may have some technical advantage over the conventional lead-acid battery systems. However, there is not as much operating experience with these technologies at this time. It is pertinent to note, though, that the California Energy Commission announced the selection of a flywheel storage system for a regional train application on December 8, 2003. The flywheel system will capture regenerative braking energy and use it to offset commercial energy consumption of the train system. A mature demonstration of the flywheel system could be valuable in assessing its suitability for future maglev system applications.

The technical advantage of the flywheel over a battery system is that it overcomes some of the battery cycle life restrictions and the flywheel acts as a more effective energy buffer in absorbing and discharging the regenerative braking from the train while retaining the rapid charge/discharge response characteristics of the battery. However, at the needed capacities, the battery system is likely to be much more cost effective. There are now battery systems in the 40 MW/20 minute storage capacities in utility frequency regulation applications in Berlin and Puerto Rico and a new one was just installed in Fairbanks, Alaska. The increasing commercial use of these subsystems will reduce their costs further in the near future.

4.4. COMPARISON OF ELECTRIC SUPPLY OPTIONS AND RECOMMENDATIONS

4.4.1. *Background*

The objective of this Electrification section is the development of a "preferred" option for powering the maglev system. Accordingly, this section summarizes the information gathered and the various cost and performance estimates for the electric supply system. It also traces the significant evolution in the conceptual approach that was proposed in the original work plan for this section and the one followed in the implementation.

The concept at the inception of the Electrification effort was to power the maglev system through a network of substations *individually* supplied by 25 kV feeders from existing substations. The information gathered in the Existing and Planned Power Supply Resources section and discussions with area utilities made it clear that providing power to the 25 to 30 maglev system substations from existing utility-owned substations was not a viable option. The constraints included a shortage of spare capacity in the utility-owned substations as well as the difficulty in procuring the right-of-way (ROW) for each feeder to the maglev system substations.

4.4.2. *Development of the Transmission Option*

The latter constraint of acquiring the needed ROW became the most restrictive and led to a re-evaluation of the original proposed electrification approach. Absent the availability of individual feeders to the maglev system substations from existing installations, the only other feasible option was consideration of a new 115 kV transmission line parallel to the maglev corridor. The proximity of such a transmission line would eliminate the ROW for new 25 kV feeders from existing facilities that are generally several miles from the maglev system substations.

Primarily, this approach guarantees a reliable and stiff electric supply system that is dedicated to the maglev system's use and eliminates the other sub-transmission paths that the power supply would include if the substations were tied to existing substations. If these paths were used, their reliability would determine the reliability of supply to that particular substation being served. And reliability statistics for the electric grid show that outages are more frequent in the sub-transmission and distribution systems than in the primary transmission system. Therefore, eliminating a supply path that could include one or more substations upstream of the maglev system substation reduces the probability of an outage.

The other related advantage is that this transmission corridor can be shared by the area utilities. In the current regulatory and economic environment, electric utilities are finding it increasingly difficult to license and build new transmission paths. This region of Colorado is no exception to this national trend and a new, shared access transmission corridor with sufficient capacity to meet the maglev system needs and transmit additional power for use by the utilities in this region could be a valuable resource.

This aspect of the transmission proposal was discussed with the Colorado Public Utilities Commission's (CPUC) Section Chief of Fixed Utilities and Engineering Staff on October 6, 2003. The electric power needs of the maglev system were reviewed during this meeting and the rationale for proposing a new, shared transmission corridor was discussed. The CPUC staff agreed that a shared line would offer distinct benefits by opening up a new transmission pathway in the central region of the State. However, in order to carry sufficient power capacity that could be shared with utilities, the CPUC staff suggested increasing the voltage from 115 kV to 230 kV. This would allow additional capacity of 200 MW to 300 MW beyond the 200 MW baseline need of the maglev system that would be a sufficiently large capacity margin to be of value and interest to the area utilities.

Implementing a new transmission corridor with conventional overhead lines is an impractical proposition, especially near environmentally sensitive communities in the State unless it is made virtually invisible by fully integrating it into the design of the guideway. Passenger safety and operational reliability considerations precluded this option with a bare conductor. However, an insulated transmission system that is structurally integrated into the guideway design such that it meets safety requirements does not have the visual impact of an overhead line. This approach would likely obtain public and regulatory approval.

It should be further noted that CDOT generally has a policy excluding electric transmission facilities from highway right-of-way. A transmission facility design that could potentially be exempted from this policy is the gas insulated transmission line.

4.4.3. *Gas Insulated Transmission*

The solution that emerged as most feasible and technically compatible was the use of a gas-insulated transmission system, specifically, the Gas-Insulated Transmission Line (GIL) made by Siemens, and also by CGIT Westboro (http://www.cgit-westboro.com/). The Siemens GIL is basically a system of three gas-filled pipes, one for each phase of the transmission line. A three-phase transmission system based on the GIL consists of three 500mm – 650mm diameter tubes is shown in Figure 54 below, one for each phase. The outer tube of each phase consists of the phase conductor, again a tube that is surrounded by a high insulation gas mixture.

Figure 54: Cross Section of Siemens GIL

The basic GIL specifications are:

Rated voltage	up to 800 kV
Rated lightning impulse withstand voltage	up to 1550 kV
Rated current	up to 6300 A
Transmission capacity	500-3000 MW
Rated short-time current / duration	63 kA / 3 s
Insulating gas	N_2/SF_6 gas mixture
System length	up to 100 km

Figure 55 illustrates the main components of the GIL system. These consist of a steel (or aluminum) outer enclosure (1) and a concentric inner tube made from a high-strength extruded aluminum alloy (2) that forms the main conducting element for each phase of the three-phase transmission system. The outer tube assembly is filled with an 80/20 mixture of N_2 and SF_6 gas to insulate the inner tube and electrically isolate the outer tube. The inner tube is mechanically supported by pairs of insulators (5) made of epoxy cast-resin and arranged 12m apart at an obtuse angle. These are fixed to the inner tube although they slide on the inside of the outer tube to compensate for thermal expansion of the conductor and enclosure tubes. The tube sections are isolated in approximately 300m sections by a conical epoxy cast-resin insulator (4) such that the pipe sections are compartmentalized and a failure in the outer tube in any section prevents the release of all the insulating gas. Adjacent inner tubes make electrical contact through sliding contacts using silver-plated surfaces and fittings (3a, 3b).
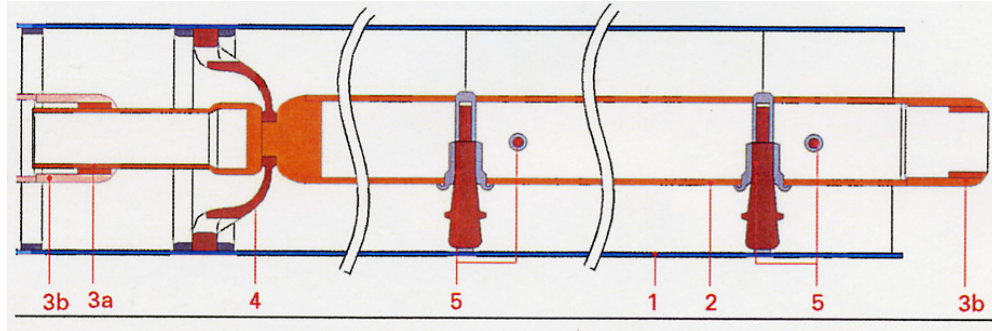
Figure 55: Main Components of Siemens GIL System

The Siemens GIL is a modular system with sections that allows the transmission system to follow any grade or contour. Similarly, fittings allow taps to be made easily in the GIL to connect with any part of the electric grid.

4.4.4. *GIL in Maglev Application*

Proper integration of the steel outer tube into the guideway structure allows the GIL sections to be structurally self-supporting without need for further reinforcement. In the maglev system application, it is proposed that the steel enclosed GIL tubes be mounted in between the east/west guideways in a triangular configuration, as shown in Figure 56. The metal grating above the three GIL tubes serves as a passenger emergency exit path.
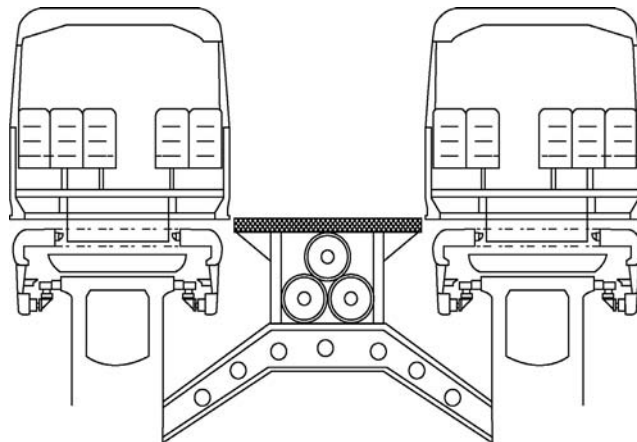

Figure 56: GIL Transmission Shown Between Guideways

As visualized conceptually in Figure 56, the GIL can be one continuous pipe system running in between the guideways. The electrical characteristics of the GIL are such that it lends itself very well to such a continuous run over long distances, without the need for any special vaults or terminations.

Figure 56 is only a conceptual representation and its implementation will require detailed design of the structure supporting the GIL and its attachment to the guideway and related design detail.

GIL costs are likely to be competitive with conventional overhead transmission installations, particularly when it is noted that GIL does not need any active compensation for lengths up to 200+ km. The electrical superiority of this approach cannot be overemphasized, since the need to generate increasing amounts of reactive power has placed a burden on many utilities, and has contributed to recent significant electric power failures in the eastern United States.

5.0 GREENHOUSE GAS IMPACT

5.1. INTRODUCTION

The objective of the Greenhouse Gas Impact analysis is to describe the regional environmental effects of developing a maglev mass transit system along the I-70 corridor west of Denver, Colorado. Environmental effects are measured in the combination of reductions in emissions due to decreased vehicle traffic on I-70, and increases in emissions from additional electric power sources needed to operate the maglev system. For the System Greenhouse Gas and Environmental Impact Analysis, emissions will be defined as CO_2 emissions from cars and light trucks (including pickups, vans, minivans, and SUVs) and CO_2 emissions from electric power sources for the maglev system. Other emissions (hydrocarbons, CO, NOX) are noted but not compared for vehicles and electric power sources.

This analysis first provides estimates of reductions in emissions from reduced I-70 traffic. Analysis of the potential increases in greenhouse gas emissions from added electric power sources is then addressed. Finally the net greenhouse gas impact of the maglev system is calculated.

The estimates developed in this analysis are first-order estimates, based on average values for the parameters used.

5.1.1. *Greenhouse Emissions from Vehicles*

Emissions of CO_2 have been rising in all sectors of the U.S., with transportation the fastest growing sector. In 2000, transportation contributed approximately one third of national CO_2 emissions.[2] Given concerns worldwide about the global heating potential of CO_2 in the atmosphere, an added potential benefit of transit systems is the reduction of greenhouse gas emissions from less automobile traffic.

Development of a maglev system in the I-70 corridor would reduce CO_2 emissions from vehicle traffic as vehicles of individuals selecting the system are driven less miles per day. Emission reductions will depend on several factors, including the proportion of I-70 passengers that divert from vehicles to trains, the resultant reduction in miles driven by train riders, and the mix of vehicles that are diverted from the highway system. The parameters used to estimate reduced CO_2 emissions are listed in the following section.

5.1.1.1. Vehicle Emission Estimation Approach

The methodology used to estimate reductions in CO_2 emissions from reduced vehicle use as passengers shift to the maglev system is shown in Figure 57 below. A baseline estimate has been developed using information obtained from the Colorado Department of Transportation (CDOT), the U.S. Department of Transportation (USDOT), the Federal Highway Administration (FHA), and the U.S. Environmental Protection Agency (USEPA). Once the baseline was established, some baseline parameters were varied to determine the impacts of these changes on annual emission reductions. For example, the proportion of I-70 corridor passenger trips diverted to the maglev system was varied, since the proportion may vary depending on eventual convenience and trip cost on the maglev system.

---

[2] U.S. Department of Transportation, Federal Highway Administration, *Air Quality Fact Book.*
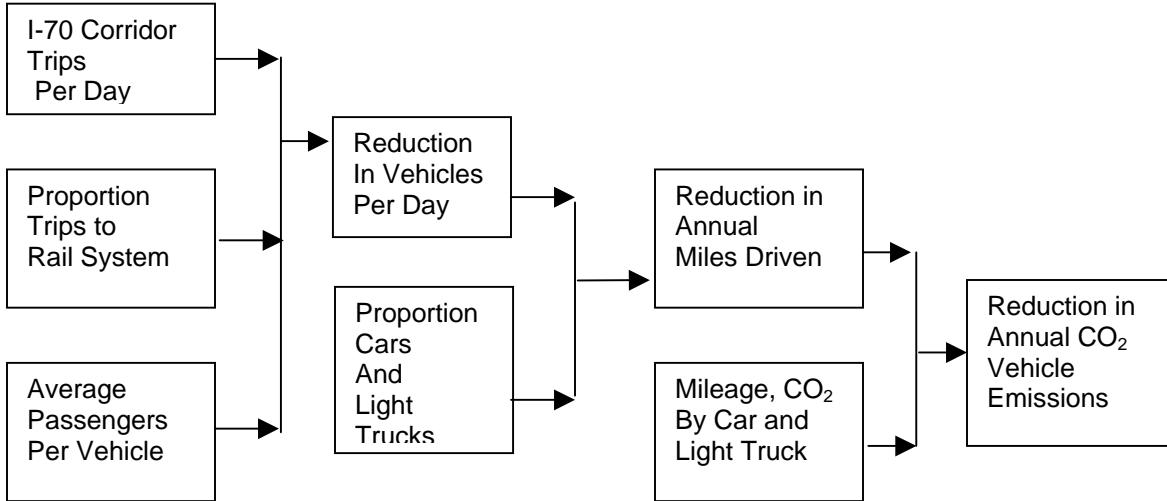
Figure 57: Methodology to Estimate Reductions in Vehicle CO2 Emissions

This approach does not estimate annual mileage reductions for the I-70 corridor directly. Instead, reduction in annual mileage driven is based upon an estimated average reduction in mileage based on national traffic patterns for rail and non-rail passengers.

5.1.1.1.1. *Information for Vehicle Baseline Emissions Estimate*

The baseline parameters for the analysis of reduction in vehicle emissions are listed in the following table.

Table 5.1-1 Parameter Values for Baseline Estimate

Parameter	BASELINE VALUE
Number of transit trips per day	22,000 each direction
Average passengers per vehicle	2.6
Average car mileage per year	13,750
Car CO_2 emissions per mile	0.8 lb.
Average light truck mileage per year	16,100
Light truck CO_2 emissions per mile	1.2 lb.
Reduction in vehicle miles for maglev rail system users	50%
Proportion of cars in vehicle fleet	65%

The baseline parameters were used to develop the initial baseline estimate of annual CO_2 emission reductions due to less vehicle miles traveled. As noted earlier, since the values of the parameters are average values without ranges, the baseline estimate is a first-order estimate. The values listed for number of trips per day, percent highway trips diverted to the maglev system, and average passengers per vehicle are CMP team estimates. Average mileage and CO_2 emissions for cars and light trucks were taken from the U.S. Environmental Protection Agency (EPA). The mileage values were adjusted upward by 10 percent for cars and 15 percent for light trucks to reflect higher annual mileage estimates by the U.S. Department of Transportation Bureau of Transportation Statistics (DOT BTS) for the National Transportation

Analysis Region (NTAR) 157, which includes all of Colorado, portions of southeastern Wyoming and western Nebraska. A map of the NTARs is shown in Figure 58. The reduction in vehicle miles and the proportion of cars in the vehicle fleet were derived from information in the USDOT BTS reports listed in the reference section.
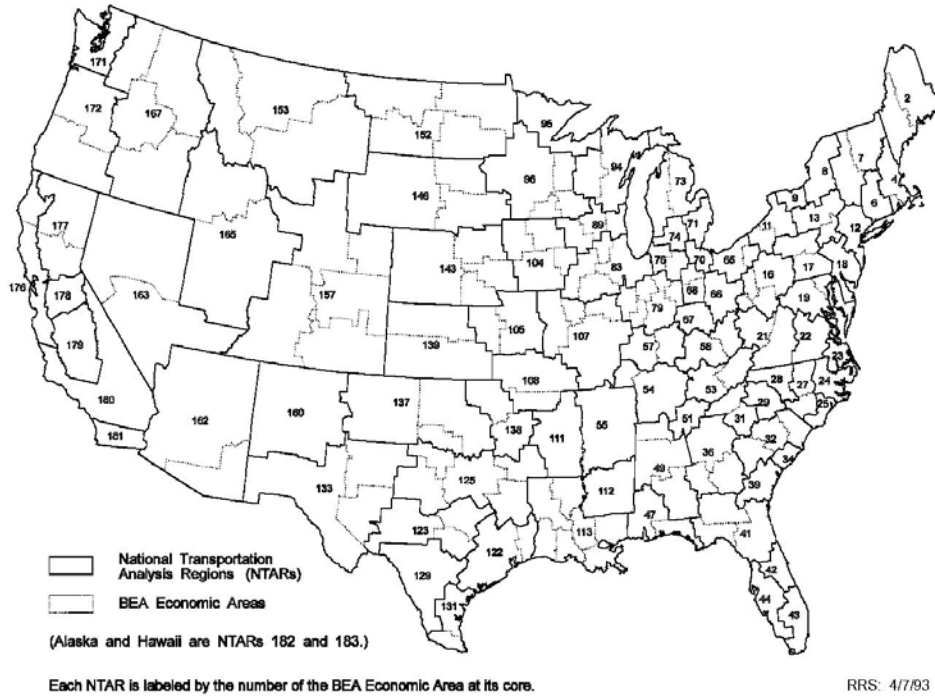
Figure 58: National Transportation Analysis Regions

5.1.2. *Baseline Emissions Estimate*

The baseline estimate for reduction in vehicle CO_2 emissions was developed in three steps:

- Estimate reduction in vehicles per day because of diversion to the maglev system;
- Calculate the decrease in annual miles driven by those using the maglev system;
- Determine the estimated annual reduction in CO_2 emissions because of decreased vehicle miles driven.

5.1.2.1. Reduction in Vehicles

The estimated reduction in vehicles from the highway system as passengers divert to the maglev system is calculated as:

$$V_R = (NR / Day)/(NP / Vehicle)$$

Where:

V_R = Vehicle reductions per day

NR = Number of riders diverted to the maglev system per day
NP/Vehicle = Average number of passengers per vehicle

V_R = 22000/2.9 = 8462 $\approx$ 8500 vehicles/day.

The reduction in vehicles will result in less miles driven, although it will not eliminate all miles for those vehicles. Local trips, trips to other communities not on the maglev line, and vacation trips will still require use of the diverted vehicles.

5.1.2.2. Decrease in Annual Miles Driven

The annual reduction in miles driven is calculated as:

$$MR_i = (P_i)(P_{MR})(V_R)(M_i / Year)$$

Where:

MR_i = reduction in annual miles per year for vehicles replaced with maglev system rides, where *i* denotes either cars (C) or light trucks (LT)
P_i = proportion of vehicles that are cars (C) or light trucks (LT)
P_{MR} = proportion of annual miles per vehicle reduced due to maglev system ridership
V_R = Vehicle reductions per day
$M_i/Year$ = average annual miles driven by either cars (C) or light trucks (LT) in the region

Cars:

MR_C = (.65)(.50)(8500)(13750) = 37,984,375 $\approx$ 38,000,000

Light trucks:

MR_{LT} = (.35)(.50)(8500)(16100) = 23,948,750 $\approx$ 24,000,000

5.1.2.3. Annual Reduction in Vehicle CO2 Emissions

The total reduction in annual greenhouse gas emissions from cars and light trucks is estimated as

$$ER = (MR_C)(C_E / Mile) + (MR_{LT})(C_{LT} / Mile)$$

Where:

ER = annual CO_2 reduction in pounds
MR_C = reduction in annual miles for cars
MR_{LT} = reduction in annual miles for light trucks
$C_E/Mile$ = average car CO_2 emissions per mile in pounds
$C_{LT}/Mile$ = average light truck CO_2 emissions per mile in pounds

ER = (38,000,000)(0.8) + (24,000,000)(1.2) = 59,200,000 lbs, or 26,853 $\approx$ 27,000 metric tons annually. Estimated Colorado CO_2 emissions from all transportation fossil fuel use were about 13.7 million metric tons in 2000.

5.1.2.4. Results of Varying Parameters

The parameters that are most likely to vary from the baseline values when estimating greenhouse gas reductions due to the implementation of a maglev system in the I-70 corridor are the number of passenger trips per day, percent of passenger trips diverted to the system, and percent

reduction in annual vehicle miles driven for train riders.[3] Each of the three parameters was varied by $\pm$ 10 percent to determine changes from the baseline estimate. The results are summarized in Table 5.1-2.

Table 5.1-2 Results from Varying Parameters
(In Metric Tons of CO_2/Year)

Parameter	Range of Emission Reductions	
	High	Low
Passenger trips	29,400	24,000
Percent trips diverted	35,900	17,500
Percent miles reduction	32,200	21,500

These results suggest that, under this estimation approach, the percent of trips diverted to the maglev system and the proportion of reduced miles driven annually by system riders have more impact on the estimated reduced CO_2 emissions than variations in the total passenger trips on the system. Additional information and ranges of values for these parameters would help refine the current estimates.

5.1.3. *Greenhouse Gas Emissions from Power Requirements*

Development of a maglev system along I-70 would require additions to the electric power supply currently available along the corridor. The location and type(s) of power plant to supply the added electric power have not yet been specified. As a result, the approach to estimating increased greenhouse gas emissions is based on an estimate of the energy requirement per train passenger. This approach does not address the power requirements and power plant fuel mix that would be associated with power supplies from the existing power grid compared to a dedicated distributed power system for the maglev system. Additional electric power is assumed to be provided by natural gas based facilities, with an associated increase in CO_2 emissions.

The level of increased CO_2 emissions from added electric power requirements are a function of several factors, including energy requirements for the trains, number of passengers, travel distance, average train speed, and power plant efficiencies.

5.1.3.1. Power Requirements Emission Estimation Approach

The methodology used to estimate increases in CO_2 emissions from added power needs for the maglev system is shown in Figure 59. The estimate has been developed based on information from CDOT, USEPA, and the U.S. Department of Energy (USDOE). Some of the parameters used to develop the CO_2 emissions estimate were varied to determine the sensitivity of the initial estimate to changes in the parameters.

This emissions estimation approach does not calculate the additional number and type of electric power facilities required. Instead, power requirements and associated emissions increases are estimated on the maglev system energy requirements per passenger. This is similar to the approach used to estimate reductions in annual vehicle emissions from reduced vehicle use, where reductions in emissions were based on the number of passengers diverted to the maglev system from I-70 and typical driving patterns, rather than estimated annual mileage reductions. The increased emissions estimate is also a first-order estimate, based on average values for the parameters used.

---

[3] Donald M. Rote, *Guidelines for Estimating Trip Times, Energy Use and emissions for HSGT Technologies, Section 3.*
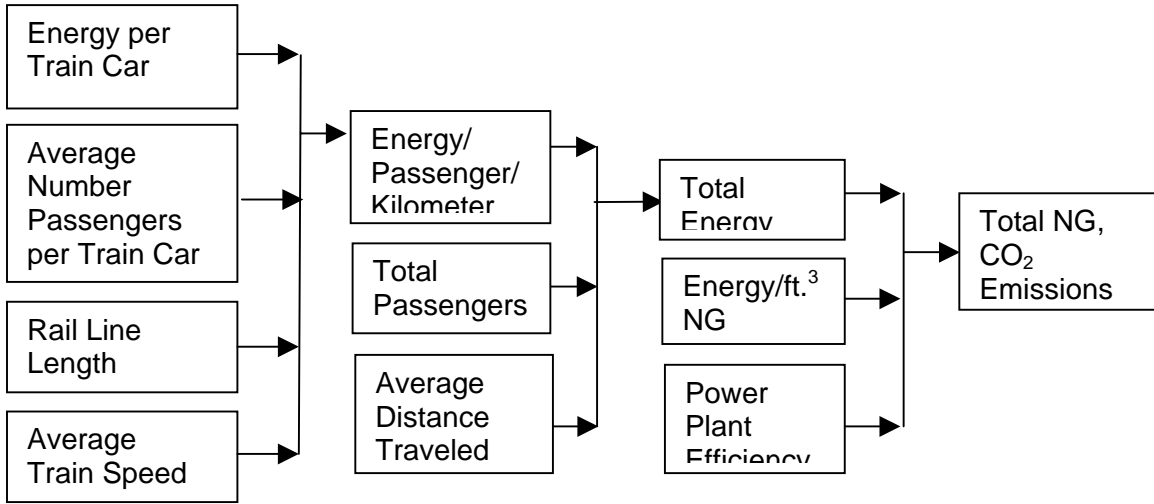
Figure 59: Methodology to Estimate Added CO2 Emissions

5.1.3.2. Information for Power Requirements Emission Estimation Approach

The values of the parameters used to estimate increases in greenhouse gas emissions from additional power for the maglev system are listed in Table 5.1-3.

Table 5.1-3 Parameter Values for Increased Emissions Estimate

PARAMETER	INITIAL VALUE
Energy required per train car	750 kW
Average number of passengers per train car	100
Rail line length	244 Kilometers
Average train speed	138 kilometers/hr
Total passenger trips	22000/day each way
Average distance traveled[1]	150 kilometers
Energy/ft.[3] natural gas	1025 Btu/ft.[3]
Power plant efficiency[2]	30%-50%
CO_2 emissions	3.19×10^{-5} lbs/Btu

[1] Initial value for average distance traveled is based on 50% of passengers traveling the full length of the rail system from DIA, and 50% traveling to/from Golden and DIA, 55 kilometers.
[2] Efficiency ranges are for NG turbines and larger NG combined cycle facilities.

The information for energy per train car and average passenger load was taken from earlier CMP analysis. Maglev system length and average speed are CDOT estimates, total passenger trips, and average-distance-traveled are CDOT team estimates. Natural gas (NG) energy per cubic foot, power plant efficiency, and CO_2 emissions per Btu of natural gas are from DOE EIA publications and conversations with EIA staff in the Electricity Generation and Capacity division of the National Energy Modeling System (NEMS).

The following units conversion were used to express CO_2 emissions in terms of Btu from natural gas required to supply the energy for the maglev system:

1 Kw = 3600 kilojoules (KJ)
1 KJ = 0.948 Btu

5.1.3.3. Increased Emissions Estimate

Estimates of increases in CO_2 emissions from added natural gas powered electric generation were developed in three steps:

- Estimate the energy requirements per passenger per kilometer
- Calculate total daily energy requirements for the maglev system based on total passengers and average travel distance
- Determine the total natural gas required with two different types of facilities (turbines and combined cycle) to produce the daily energy requirements of the maglev system, and develop estimates of associated natural gas CO_2 emissions.

5.1.3.4. Added Energy/Passenger/Kilometer

The estimated required energy per passenger per kilometer is calculated as

$$E_{PK} = \left[\left(K_C / P_C\right)J\right]\left[\left(L_R / S_T\right)/ L_R\right]$$

Where:

E_{PK} = energy in kilojoules per passenger per kilometer

K_C = energy requirements in Kw per car

P_C = average number of passengers per car

J = conversion from Kw to kilojoules (KJ)

L_R = length of maglev rail line

S_T = average train speed

E_{PK} = [(750/100)3600][(244/138)/244] = 195.7 $\approx$ 200KJ/passenger/kilometer

5.1.3.5. Daily Energy Requirements for Maglev Train System

Daily energy requirements for the maglev system are estimated as:

$$E = \left(E_{PK}\right)\left(P\right)\left(D\right)$$

Where:

E = total required rail system energy (in KJ) per day
P = total passenger trips per day
D = average distance in kilometers per trip

E = (200)(44000)(150) = 1.32 x 10^9 KJ = 1.251 x 10^9 Btu/day, or
E_Y = 456.6 x 10^9 Btu/year

5.1.3.6. Natural Gas Requirements and CO2 Emissions

Daily natural gas requirements for electric power to support the maglev system are:

$$NG = E\left(1 / PE_i\right)$$

Where:

NG = daily natural gas requirements
PE_i = power plant energy conversion efficiency for turbine and combined cycle systems

For turbine based power facilities:
NG = (1.251 x 10^9)(1/.30) = 4.17 x 10^9 Btu/day $\approx$ 4 x 10^9 Btu/day or
NG_Y = 1,460 x 10^9 Btu/year
NG_Y = 1.42 x 10^6 ft^3/year

For combined cycle based power facilities:
NG = (1.251 x 10^9)(1/.50) = 2.502 x 10^9 Btu/day $\approx$ 2.5 x 10^9 Btu/day or
NG_Y = 912 x 10^9 Btu/year
NG_Y = .89 x 10^6 ft^3/year

A range of increases in CO_2 emissions is obtained for the two different types of power production facilities:

Turbine: CO_{2T} = (1,460 x 10^9 Btu/year)(3.19 x 10^{-5} lbs/Btu) = 46,570,000 lbs/year.

CO_{2T} = 21,000 metric tons/year

Combined Cycle: CO_{2C} = (912 x 10^9 Btu/year)(3.19 x 10^{-5} lbs/Btu) = 29,090,000 lbs/year.

CO_{2C} = 13,000 metric tons/year

While these first order estimates suggest that CO_2 emissions would be larger if natural gas turbines were used to provide power for the maglev system, such findings are preliminary. For example, no estimates of transmission line losses are considered for the combined cycle facility, which would likely be an addition to the current transmission grid. In addition, neither power option considers the possibility of power regeneration during train braking, which would reduce emissions for both types of facilities.

5.1.4. *Estimates of Net CO2 Changes*

Estimated net greenhouse gas emission changes depend on the values assigned to the parameters when estimating emission decreases due to reduced vehicle traffic on I-70, and when estimating increased greenhouse emissions because of added electric power for the maglev system that would be produced using natural gas. Using the baseline estimate of emission reductions compared with the two types of power facilities considered yields the following results:

Baseline CO_2 reductions vs. turbine facility emissions:

27,000 metric tons – 21,000 metric tons = 6,000 metric tons annual CO_2 reduction

<u>Baseline CO_2 reductions vs. combined cycle facility emissions:</u>

27,000 metric tons – 13,000 metric tons = 14,000 metric tons annual CO_2 reduction

Varying parameters for the estimates of reductions and increases of CO_2 emissions would change these values somewhat. However, the net CO_2 reductions from use of the maglev system are not large when compared to the estimates of approximately 14 million metric tons of annual CO_2 emissions from all transportation-related fossil fuel use in 2000.

5.1.5. *Summary*

The objective of this analysis is to describe the regional environmental effects of developing a maglev transit system along the I-70 corridor west of Denver, Colorado, defined as CO_2 or greenhouse gas emissions. The net greenhouse gas effects are measured in the combination of reductions due to decreased vehicle traffic on I-70, and increases in emissions from additional electric power sources for the maglev system. This analysis documents the initial baseline estimate of reduced greenhouse gas emissions due to less driving by individuals who divert from the highway system to the maglev system, and the increased emissions from additional power sources for the maglev system. Natural gas is assumed to be the fuel of choice for additional electric power facilities. These are first-order estimates, based on average values for the parameters used in the estimation approaches.

Three parameters used in calculating emission reductions - number of passenger trips, percent of passenger trips diverted to the maglev system, and percent reduction in annual miles driven for train riders - were varied to look at the relative impacts on the baseline emission estimate. The results suggest that the percent of trips diverted to the maglev system and the proportion of reduced miles driven for train riders affect emission estimates more than total passenger trips on the system.

Two types of power generating facilities – natural gas fired turbines and combined cycle turbines – were considered when estimating increases in CO_2 emissions to supply added power for the maglev system. The preliminary estimates suggest that use of larger power facilities may result in less CO_2 emissions when meeting the additional power requirements. However, other important factors, such a transmission line losses, have not been evaluated.

Net CO_2 reductions as individuals divert from passenger vehicles on I-70 to the maglev system are modest, ranging from 6,000 metric tons to 14,000 metric tons annually when comparing the baseline CO_2 reductions case with the CO_2 increases for the two different power facilities.

5.1.5.1. References

American Association of State Highway and Transportation Officials 1998. *Transportation and the Economy: National and State Perspectives*

Colorado Department of Public Health and Environment 2000. *2000 Colorado Gas Emissions Update*

Piyushimita, Thakuria, Deepak Virmani, Seongsoon Yun, and Paul Metaxatos 2002. *Estimation of the Demand for Inter-city Travel: Issues with Using the American Travel Survey.*

Rote, Donald M., Zian Wang, and Anant Vyas 1996. *Methodology for Computing Public Benefits of Diverting Passenger Trips from Conventional Modes to HSGT Modes of Travel,* Center for Transportation Research, Argonne National Laboratory, May 1996

Rote, Donald M. 1999. *Guidelines for Estimating Trip Times, energy Use and Emissions for HSGT Technologies,* Center for Transportation Research, Argonne National Laboratory, October 1999.

Texas Transportation Institute 2001. *Annual Mobility Report.*

U.S. Department of Energy, Energy Information Administration 2002. *Emissions of Greenhouse Gases in the United States 2001.*

U.S. Department of Energy, Energy Information Administration 2003. *Assumptions to the Annual Energy Outlook 2003.*

U.S. Department of Transportation, Federal Highway Administration 2002. *Highway Statistics 2001.*

U.S. Department of Transportation, Federal Highway Administration 2002. *Transportation Air Quality - Selected Facts and Figures.*

U.S. Department of Transportation, Bureau of Transportation Statistics 2001. *Transportation in the United States: A Review.*

U.S. Environmental Protection Agency 2001. *Green Book: Nonattainment Areas for Criteria Pollutants.*

U.S. Environmental Protection Agency 2002. *U.S. Emissions Inventory 2002: Inventory of U.S. Greenhouse Gas Emissions and Sinks.*

Table 5.1-4 Annual Emissions and Fuel Consumption for an Average Passenger Car 1

Pollutant	Amount/mile[2]	Miles/year[3]	Calculation	Pollution/year
Hydrocarbons	2.9 grams (g)	12500	2.9g*1lb/454g*12500	80 lbs.
Carbon Monoxide	22 grams	12500	22g*1lb/454g*12500	606 lbs.
Nitrogen Oxides	1.5 grams	12500	1.5g*1lb/454g*12500	41 lbs.
Carbon Dioxide	0.8 lb	12500	0.8lb*12500	10,000 lbs.
Gasoline	.044 gallon[4]	12500	.044 gal*12500	550 gal.

Source: National Vehicle and Fuel Emissions Laboratory, U.S. Environmental Protection Agency
[1] Emission factors and pollution/mile may differ slightly from original sources due to rounding.
[2] Emission factors come from standard EPA emission models, assuming an average properly maintained car in 1999, operating on typical gasoline on a summer day (72-96° F).
[3] Average annual mileage source: EPA Office of Mobile Sources Assessment and Modeling Division.
[4] Fuel consumption is based on average in-use passenger car fuel economy of 22.5 miles per gallon. Source: US DOT/FHA, Highway Statistics 1999.

Table 5.1-5 Annual Emissions and Fuel Consumption for an Average Light Truck (Light trucks include pickups, vans minivans, and SUVs)

Pollutant	Amount/mile[2]	Miles/year[3]	Calculation	Pollution/year
Hydrocarbons	3.7 grams (g)	14000	3.7g*1lb/454g*14000	114 lbs.
Carbon Monoxide	29 grams	14000	29g*1lb/454g*14000	894 lbs.
Nitrogen Oxides	1.9 grams	14000	1.9g*1lb/454g*14000	59 lbs.
Carbon Dioxide	1.2 lb	14000	1.2lb*14000	16,800 lbs.
Gasoline	.056 gallon[4]	14000	.056gal*14000	915 gal.

Source: National Vehicle and Fuel Emissions Laboratory, U.S. Environmental Protection Agency
[1] Emission factors and pollution/mile may differ slightly from original sources due to rounding.
[2] Emission factors come from standard EPA emission models, assuming an average properly maintained light truck in 1999, operating on typical gasoline on a summer day (72-96° F).
[3] Average annual mileage source: EPA Office of Mobile Sources Assessment and Modeling Division.
[4] Fuel consumption is based on average in-use passenger car fuel economy of 22.5 miles per gallon. Source: US DOT/FHA, Highway Statistics 1999.

6.0 *PROPULSION (TRADE STUDY)*

6.1. INTRODUCTION

6.1.1. *Goals and Objectives*

A Propulsion Trade Study was conducted to identify and evaluate prospective linear motor designs that could potentially meet the system performance requirements of the CMP and be applicable to other urban maglev transit corridors. The analysis involves the performance of the linear induction motor (LIM) propulsion system of the Chubu HSST (CHSST) that has been selected as the project baseline technology. Potential near-term improvements to the propulsion system and the relative impact of research and development in critical areas were considered. This report presents the results of field-based simulations of the LIM that meets the requirements of the Colorado route, and the sensitivity of performance to parameters modified from existing CHSST designs. These modifications have been reviewed by CHSST and Toyo Denki Inc., and their implementation appears feasible.

6.1.2. *Scope and Tasks*

- Identify and characterize the CHSST baseline motor and vehicle, and near-term improvement potential;
- Evaluate the HSST-200 series motor;
- Identify the critical developmental elements of the HSST-200;
- Evaluate the forces that the propulsion system imposes on the levitation system;
- Evaluate the prospective motor designs that could potentially meet the system performance requirements of the Colorado Project including parameters identified above and potential deployability;
- Integrate these analyses into vehicle and sub-system requirements and evaluations for the CMP application;
- Identify and analyze potential improvements and optimization of performance parameters for propulsion sub-systems;
- Characterize and compare the advantages/disadvantages of the potential performance of the motor types for maglev system application.

6.1.3. *Resources and Technical Work*

6.1.3.1. Literature Search of Linear Motor Technology

An extensive search of open literature was conducted through the Sandia National Laboratories Library using several electronic databases such as INSPEC, NTIS, SciSearch, and TRIS to locate journal articles and reports related to linear motors for maglev systems from 1980 to 2002. Roughly 800 citations were located which typically have an abstract in English. Most of the papers from international conferences are available in English, but many of the cited reports are in German or Japanese as one would expect. The citations have been cataloged in a searchable database using ProCite software.[4] This search has been very helpful in locating references that are published outside of conference proceedings.

Papers on linear motor technology have also been located through the major maglev conferences such as the International Conferences on Magnetically Levitated Systems and Linear Drives (MAGLEV93, 95, 98, 2000, 2002) and the Linear Drives for Industry Applications (LDIA 95, 98, 2001). These proceedings are very useful as the papers are well referenced and reviewed.

---

[4] ProCite reference manager, version 5, ISI ResearchSoft, Berkeley, Calif. www.procite.com

Several texts on linear induction or synchronous motors have also been located including recent and/or relevant works by Ion Boldea and Syed Nasar, [5,6,7,8], Jacek Gieras [9,10], and Eric Laithwaite [11,12,13]. Each of these covers a section on high or medium speed transportation applications. The analysis and modeling methods for linear motors discussed in these works have been reviewed.

6.1.3.2. Non-Disclosure Agreements

A non-disclosure agreement was executed between Sandia National Laboratories and the Chubu HSST Development Corporation and the Itochu Corporation of Japan that facilitated the exchange of information for the technical evaluation of the HSST propulsion system. Their cooperation, with support from Toyo Denki, provided data, tools, and technical reviews that would not have been available otherwise to execute this study.

6.1.3.3. Technical Consultant

A consulting contract was established with Prof. Eisuke Masada of the Science University of Tokyo. He is a world expert in linear motor propulsion and maglev systems, and his expertise provided invaluable support to the assessments and evaluation of the existing propulsion technology and recommendations for improvement.

6.2. THRUST AND POWER REQUIREMENTS

6.2.1. *Requirements and Assumptions for Analysis*

The requirements for the LIM propulsion system are based on the design of the Colorado 200 vehicle, anticipated environmental conditions, and FTA requirements. [14,15,16] The requirements are shown in Table 6-1.

---

[5] Ion Boldea and Syed Nasar, The Induction Machine Handbook, CRC Press, Boca Raton, Florida, 2002.

[6] Ion Boldea and Syed Nasar, Electric Drives, CRC Press, Boca Raton, Florida, 1999.

[7] Ion Boldea and Syed Nasar, Linear Motion Electromagnetic Devices, Francis and Taylor, New York, 2001.

[8] Ion Boldea and Syed Nasar, Linear Motion Electromagnetic Systems, John Wiley and Sons, New York, 1985.

[9] Jacek Gieras, Linear Induction Drives, Clarendon Press, Oxford, 1994.

[10] Jacek Gieras and Z.J. Piech, eds., Linear Synchronous Motors: Transportation and Automation Systems, CRC Press, Boca Raton, Florida, 1999.

[11] E. R. Laithwaite, Induction Machines for Special Purposes, George Newnes Limited, London, 1966.

[12] E. R. Laithwaite, Propulsion Without Wheels, Hart Publishing Co., New York, 1968.

[13] E. R. Laithwaite, A History of Linear Electric Motors, Macmillan., London, 1987.

[14] FTA Urban Maglev Program, CDOT Team report "Task 3, Transit System Performance Requirements," Final Report 1.1, 17oct02.

[15] FTA Urban Maglev Program, CDOT Team report "Task 10, Vehicle Design, Technical Memo 4.1,Vehicle Interior Configuration" 6Jun03.

[16] FTA Urban Maglev Program, CDOT Team Quarterly Review Meeting, Washington, D.C., 9Jul03.

Table 6-1: Parameters and system requirements for analysis of required thrust and power

- Vehicle mass, loaded: 44 tonne COL-200a,

- Vehicle length, width, and height: 24.3 m, 3.2 m, 3.5 m COL-200a

- Vehicle Drag: Drag force for COL-200a modified to allow for possible reduced drag.

- Number of LIMs per car: 10

- Number of cars per train: 2

- Speed range: 0 to 160 km/hr (kph)

- Average speed: 114 kph

- Climb grade: up to 10%, no-degradation at 7%

- Acceleration rate: 0.16 g's

- Headwind   90 kph

An assessment of the thrust and mechanical output power required for the linear motor was done to establish how closely the existing HSST linear induction motor (LIM) met requirements, and the desired motor's thrust performance curve. This analysis is a point-mass model that considers the drag, grade climbing, and acceleration for a train of several vehicles. The drag force has contributions from aerodynamic loading with headwind, magnetic drag, and power collector friction. The required force is divided by the number of cars in the train to obtain a total force per car as the unit of measure.

Examples of the total drag force and components of that force on the Colorado 200 vehicle without the effect of additional headwind are shown in Figure 60. The influence of a strong head or tail wind is shown in Figure 61. However, these forces are small compared to the required force per car to propel the vehicle up various grades as shown by the drag force (now including grade climbing force) in Figure 62. The required thrust force per car shown in Figure 62 is based on the combined requirement of accelerating the Colorado 200 vehicle from rest at 0.16 g and maintaining the maximum speed of 160 kph on a 7% grade.

The required thrust per LIM is derived by dividing the total thrust required per car by the planned 10 levitation/propulsion modules for the Colorado 200 vehicle. The LIM proposed for this module has been extended 27% longer than the existing HSST-200 LIM design to increase thrust. The thrust requirement and capability of the scaled, existing design are shown in Figure 63. Two maximum thrust levels are shown, one for 0.16 g acceleration (required level), and the other at 0.11 g for reference.
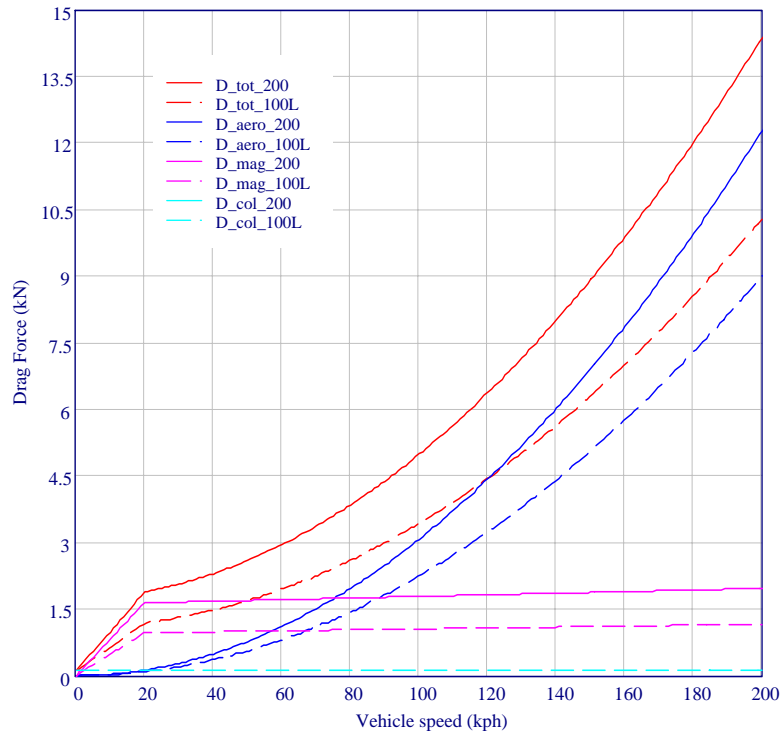
Figure 60: Total drag force for 2-car consist of HSST-100L or Colorado 200 vehicles, and the components of the drag without additional headwind on level grade.
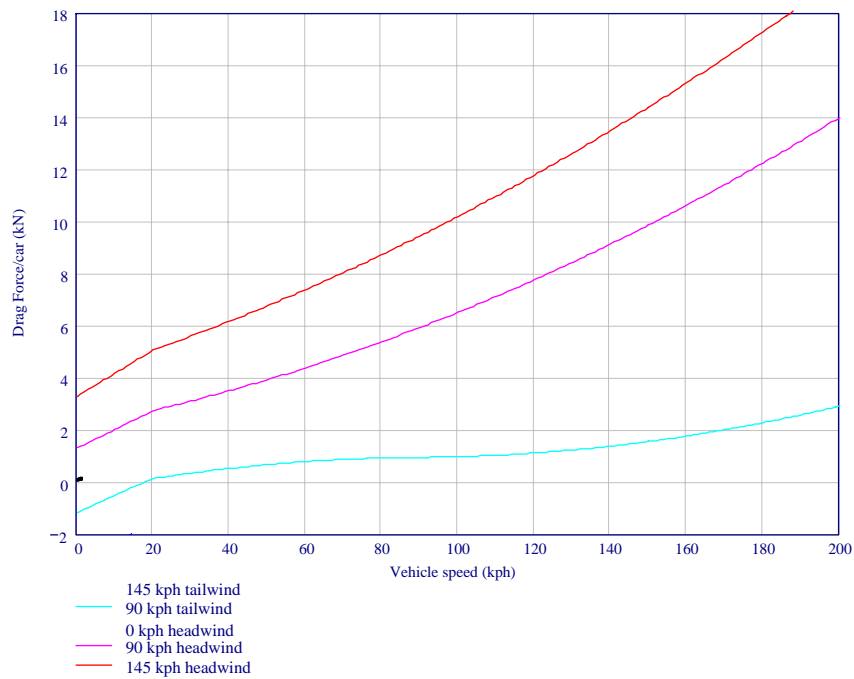

Figure 61: Influence of head or tailwind on the total drag for 2-car consist of Colorado 200 vehicles on level grade.
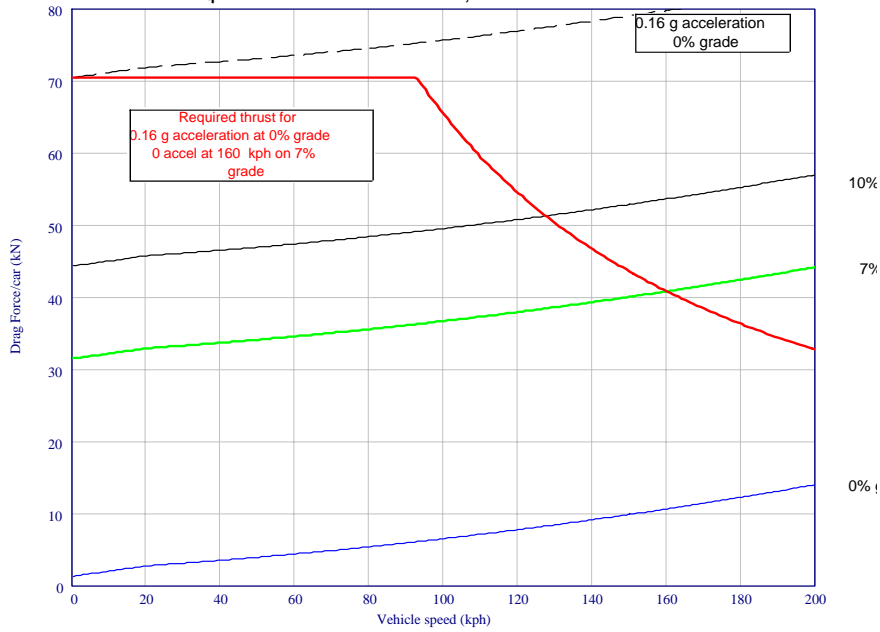
Figure 62: Drag Force (including grade climbing force) per Colorado 200 vehicle based on 2-car consist with a 90 kph headwind.

Red thrust curve is based on achieving 0.16 g acceleration on level grade from rest, and maintaining speed of 160 kph climbing 7% grade.
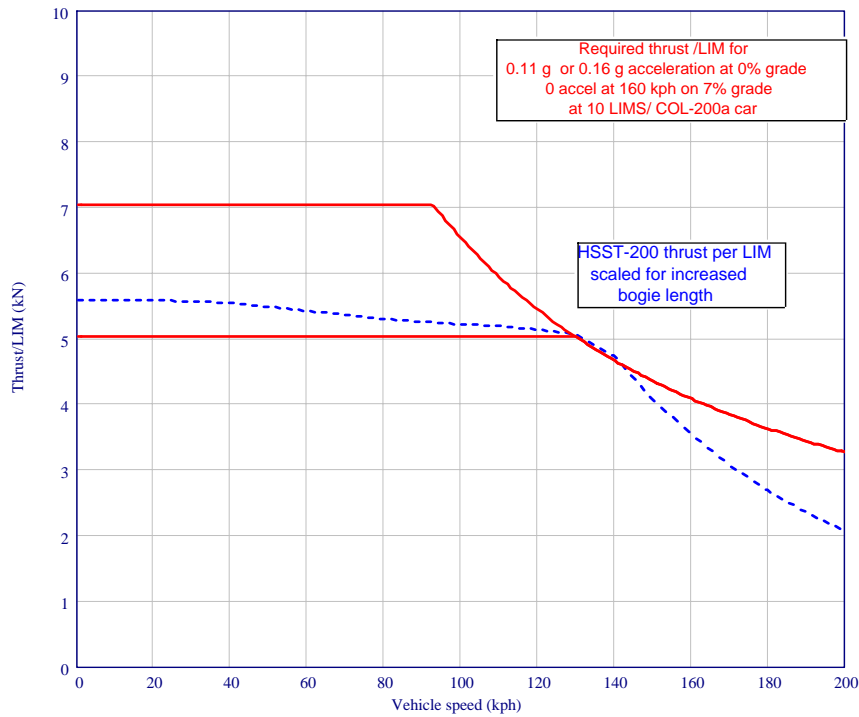

Figure 63: Required thrust per LIM for Colorado 200 vehicle and capability of scaled HSST-200 design based on 2-car consist into a 90 kph headwind.

6.2.2. *Electric Power per Car Along Route*

For the Electrification effort, an estimate was made of the thrust and electric power required per car to propel a 2-car consist of Colorado 200 vehicles at constant speed of 114 kph on I-70 from DIA to Eagle County Airport. The route data is the westbound data set from a GPS survey of I-70. [17] This is not suggested to be the actual proposed route for the I-70 corridor, but was the best data available at the time of the analysis.

The original latitude-longitude-elevation GPS data was slightly modified for the analysis. The first 143 points were deleted as their path is highly irregular. This removes only about 2 km at DIA from the 240 km route. The data was then sampled at 5-point intervals to reduce the number of points from over 11,000 points to 2200 to speed the calculations. The average distance between samples increases from 21 m in the raw data to 109 m, although the coarser sampling is sufficient to represent the route grade and curvature. The latitude-longitude-elevation data was then converted to X(east-west distance), Y(north-south distance), and Z(elevation change) in meters relative to the first point near DIA which is defined as the origin (x,y,z = 0,0,0). The location of this origin is (39.834 deg N latitude, -104.682 deg latitude, 1627 m elevation). To eliminate single-point noise, the sampled original data was filtered with a 5-point moving average taken with a Gaussian weighting distribution over the five points.

For this estimate of power demand an assumption of constant velocity is used. This analysis determined the thrust that is necessary to overcome contactor friction, magnetic and aerodynamic drag, and grade. The speed of 114 kph is the average speed obtained over the route from analysis that includes limitations due to lateral accelerations from route curvature. [18] A 90 kph headwind was also included to obtain an upper bound estimate of power, as this is the maximum operable wind condition for the HSST-100 system.[19] From the required thrust, the mechanical power is derived, and the electrical power is determined from estimated LIM motor and other efficiencies.

Figure 64 shows the westbound grade and elevation change plotted along with the Y coordinate. Note that several of the variables have been scaled to fit the graph, such as Z, or elevation change, has been divided by 20 in the plot. This was done so the abscissa-ordinate scaling was kept at 1:1 and the Y coordinate on the chart could be read also as a map. Locations of several possible power pickup points are also shown along the route path. The shape of the elevation curve appears slightly distorted because all points are plotted with respect to the x-coordinate, not distance along the route.

Figure 65 shows the electric power required per car traveling westbound or eastbound with a 90 kph headwind. Of course, this condition would not occur simultaneously, but the values represent high-power conditions for each direction. Note that the abscissa for this plot is the distance along the route, not the east-west distance. The electric power required per car is based on the required thrust curve (0.16 g) in Figure 66, the estimated efficiency of the LIM, and a 90% forward rectification and transmission efficiency of the DC power to the vehicle. The negative power value represents power from regenerative braking, but a very low, conservative efficiency of 35% is assumed for the power returned to the utility in this example based on lower efficiency of bi-directional inverter/rectifiers and previous user's experience. [20] Present plans are not to return the power to the utility, but use regenerated power for on-board loads or within the station-vehicle power system.

---

[17] David Munoz, "I-70 GPS Survey," Technical memorandum, October 14, 2002.

[18] FTA Urban Maglev Program, CDOT Team report "Task 14, Integration, Technical Memo 4.0," 22Apr03.

[19] FTA Urban Maglev Program, FTA Assessment Team report "Assessment of CHSST Maglev for U.S. Urban Transportation," July 2002, pp. 6-11.

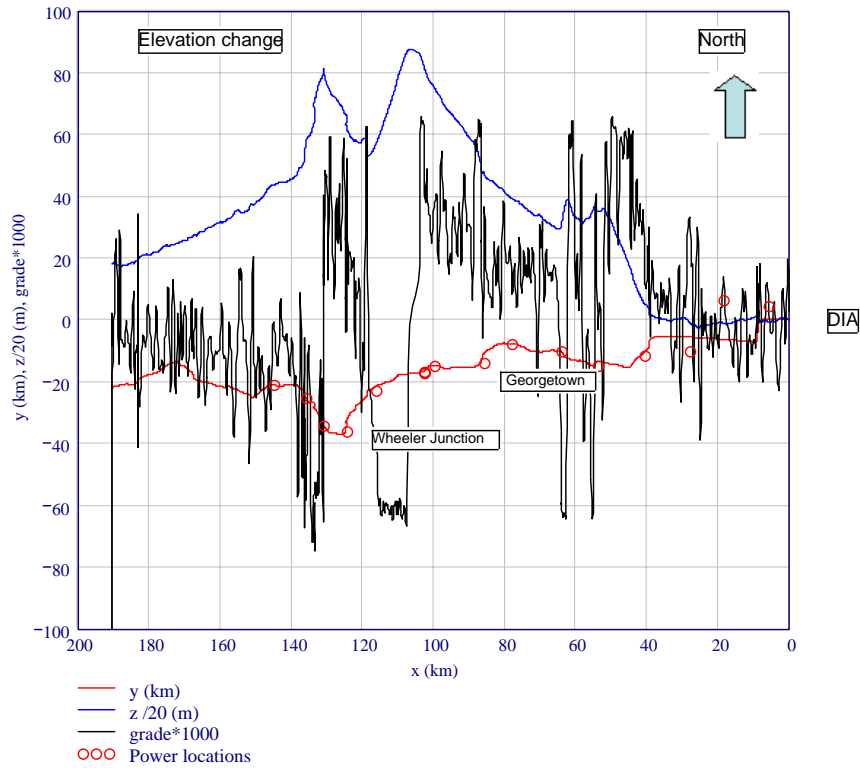[20] Private communication, Prof. E. Masada, Science Univ. of Tokyo, 2003.

Figure 64: Map of I-70 where the origin of coordinates is DIA

Horizontal is east-west distance, and vertical is north-south distance, elevation change divided by 20, or grade times 1000. Power locations are located by circles along route.
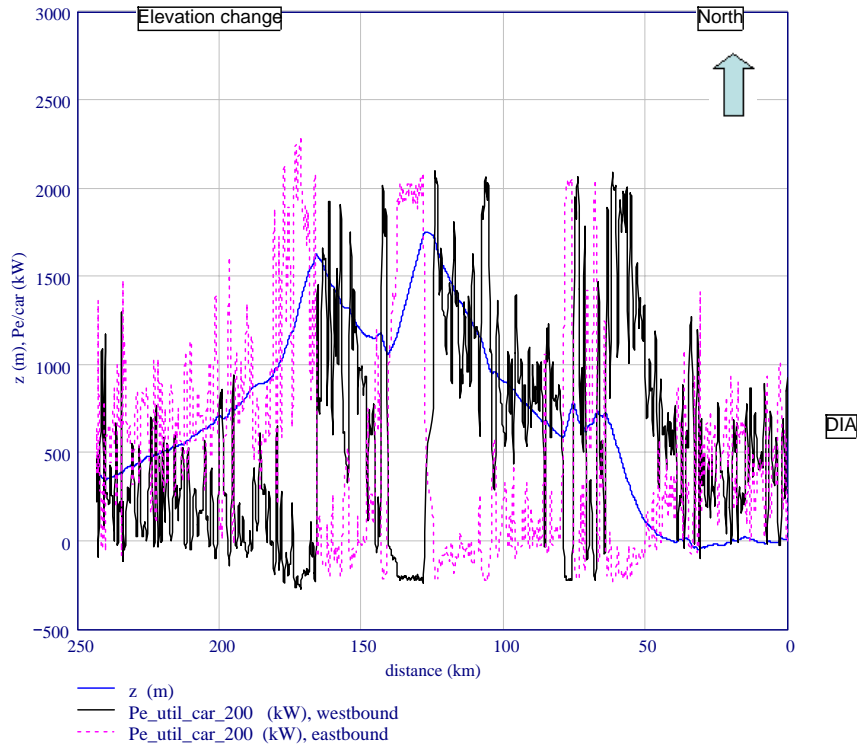
Figure 65: Electric utility power required per COL-200 vehicle for 2-car consist westbound or eastbound at 114 kph along route, with 90 kph headwind.

6.3. OPTIONS FOR IMPROVEMENT OF CHSST LIM TO MEET REQUIREMENTS

A series of independent meetings was held in early June 2003 in Japan with linear motor consultants and commercial suppliers of maglev and LIM-driven urban transit systems to assess the capability of existing systems, and the feasibility of eleven proposed changes for the HSST LIM drive. These proposed changes resulted from several weeks of prior consultation with Prof. Eisuke Masada of the Science University of Tokyo, and Dr. Takafumi Koseki of the University of Tokyo, who has studied under and worked with Prof. Masada. A two-day meeting was held with staff from Chubu HSST Development Corp., Toyo Denki Seizo, and ITOCHU Corp. to negotiate the proposed motor improvements. In addition, a separate meeting was held with staff from Hitachi's Research Lab and Mito Transportation Systems Division to discuss their linear induction motor and wheel-based urban transit technology currently employed in Japanese subway systems.

These options to improve the linear motor performance range from low difficulty (options 1 through 7) to significant difficulty (options 8 through 11) to incorporate:

    1. Increasing the maximum voltage per LIM to permit the motor to operate at constant Voltage/frequency mode to a higher "breakpoint" speed (rated speed), and to permit operation at constant mechanical power at speeds greater than the breakpoint speed.

2. Increase the trolley rail differential voltage to 3000 VDC to permit higher motor voltage, reduce trolley rail current, and potentially reduce the size of the on-board inverter and power conditioning equipment.

3. Change the operating point on the motor's thrust vs. slip frequency characteristic curve toward lower slip frequencies to achieve greater thrust and higher efficiency.

4. Increasing the primary current of the LIM to sufficient values to achieve the required thrust for the 0.16 g acceleration (7 kN/LIM) for a very short duration.

5. Use forced air (or liquid) cooling to prevent overheating of the primary winding to achieve higher thrust at speeds greater than the breakpoint, when higher operating power level is steady-state.

6. Decrease the length of the clearance gap between the LIM and the reaction rail.

7. Utilize solid copper reaction rail in regions of track where higher thrust is needed such as on high-gradient and in station.

8. Utilize two inverters on-board the vehicle and configure the primary windings such that the number of stator poles is small for low-speed operation, but then the phase of the inverters is changed to double the number of stator poles for high-speed operation.

9. Utilize concept of double-fed LIM in regions of track where higher thrust is needed such as on high-gradient and in station. In this case the reaction rail sheet is replaced with a winding on a core similar to the stator, but energized by a separate power supply.

10. Utilize long-stator LIM in guideway where higher thrust is needed IN ADDITION to the existing on-board, short-stator LIM.

11. Incorporate permanent magnets or separately energized coils near the entry end of the LIM to compensate for deleterious end-effects at high speed.

The consensus of the team was that a combination of Options 1-7 for the existing LIM design of the HSST-200 was considered sufficient to yield a LIM design capable of driving a COL-200 vehicle on the Colorado route and meet the requirements of 0.16 g acceleration from station and 160 kph speed on 7% grade. It was recognized that concomitant with the increased thrust, there is increased normal force that has an impact on the levitation system. Each of the options 1 through 7 has been modeled to assess the magnitude of the impact to other systems and the requirements for the inverter.

6.4. CODE DEVELOPMENT TO MODEL LIM PERFORMANCE

A LIM performance model was generated based on Prof. Yamamura's method [21] and techniques further developed by Dr. Takafumi Koseki from the thesis by Dr. Keisuke Fujisaki, both of the Univ. of Tokyo. [22] This model previously demonstrated very good agreement with performance of the HSST-03. Calculations using parameters for a HSST-200 design were done using 1989 parameters, and the results of that early analysis were replicated.

Further calculations were made to compare with HSST-200 calculations that have been completed by CHSST and Toyo Denki with their own codes based on Prof. S. Nonaka's method

---

[21] Sakae Yamamura, Theory of Linear Induction Motors, Second edition, Univ. of Tokyo Press, Tokyo, Japan, 1978.

[22] Keisuke Fujisaki, "A Study on Electromagnetic Suspension Controlled Magnetically Levitated Train," doctoral dissertation, Univ. of Tokyo, December 21, 1985.

and their motor parameters. [23] The difference in the predicted performance between the two models were significant, and misinterpretation of input parameters was originally suspected as the cause. The two analysis methods differ in that the Yamamura method is based on an equivalent current sheet and the Nonaka method is based on spatial harmonics to develop the magnetic field distribution in the LIM gap. Each of these methods utilizes "equivalent factors" that are approximations. After detailed inspection, it was also concluded that the LIM impedance model in the Univ. of Tokyo code was defined over a very narrow LIM geometry range, and further development and testing of this part of the program was needed to address a wide range of LIM parameters. Given that models generated from the benchmarked CHSST and Toyo Denki codes were to be used as the basis for further design, it was decided to utilize the CHSST code for the parameter variation in this study.

Benchmarking of the CHSST code developed by Mr. Yoshiro Higasa of CHSST has been done with HSST-05 and HSST-100 data, but most of this data is at low speed (≤20 kph). [24] The low speed thrust has been shown to be within 7% of HSST-05 data and within 5% for the HSST-100. The measured static thrust and normal force vs. frequency for the HSST-100 is shown in Figure 66, below, along with calculations using the spatial harmonics code (SHRLCM on graph). Toyo Denki utilizes a similar code based on Prof. Nonaka's method that has evolved from codes that were based on work by Prof. Yamamura. [25]   Comparison between the earlier code results and data for a full-scale HSST-200 LIM evaluated on a 2 m diameter test wheel is shown in Figure 67. These results show excellent agreement at speeds up to 200 kph.
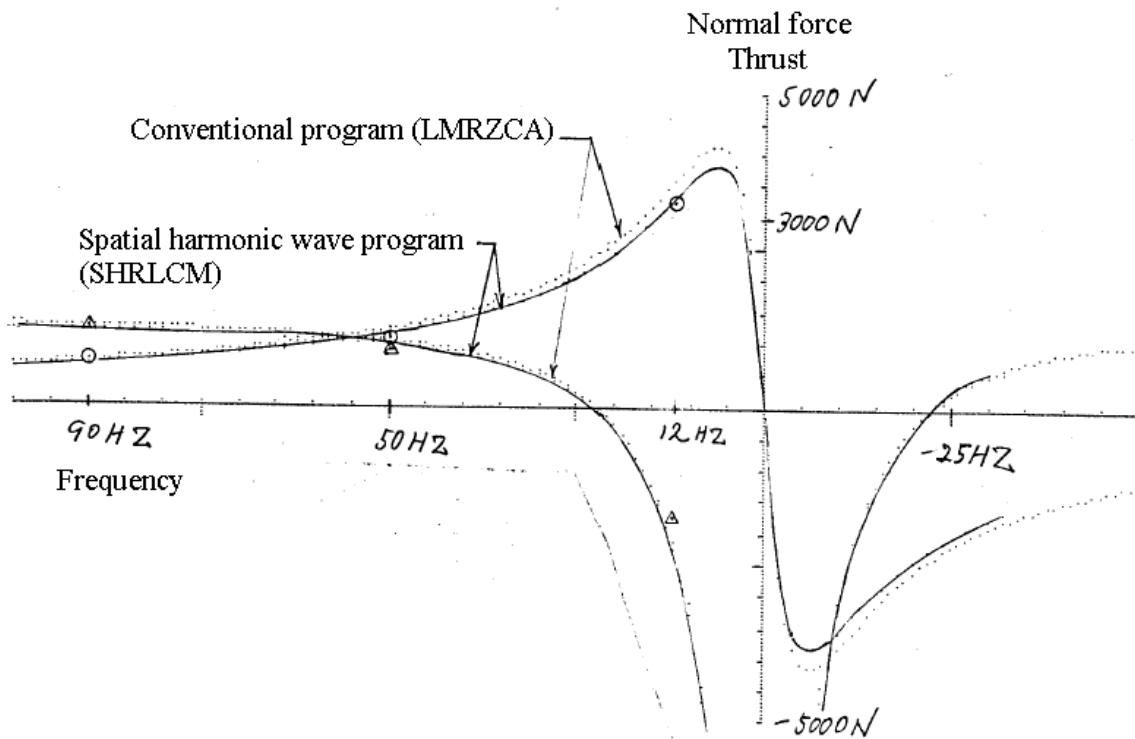

Figure 66: Thrust and normal force for CHSST-100 LIM in static test. Current: 200A. Secondary Temperature: 72 C. [24]

[23]   S. Nonaka and K. Yoshida, "Analysis of Linear Induction Motors Using a Space Harmonics Technique," Chapter 8 in Transport Without Wheels, E. R. Laithwaite ed., Paul Elek Scientific Books, London, 1977. pp. 187-216.

[24]   Y.Higasa, "Comparison of the Method of Calculating LIM Characteristics Based On Spatial Harmonic Theory Against Experimental Data," Chubu HSST Technical Report, 12Nov91.

[25]   Y.Takahashi, "Test Apparatus of Linear Induction Motor for Train," *Dengakuronn D*, vol. 110, 1990-2.
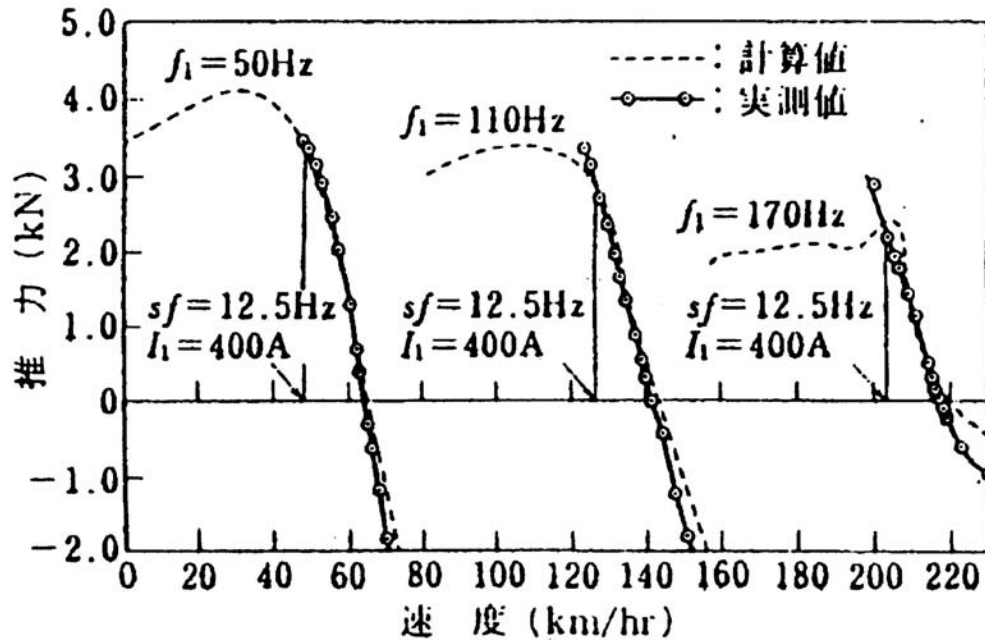
Figure 67: Thrust vs. speed curves for HSST-05 LIM on test wheel at several drive frequencies. Data points are circles and calculation is dotted line. [25]

These benchmark results are highly encouraging to indicate that good agreement can be obtained, but often this agreement can only be generated once an actual LIM has been fabricated and some measurements of primary loss and leakage inductance have been made. These measurements take into account differences that may be due to manufacturing deviations from ideal geometry, and magnetic coupling effects that may be very difficult to model accurately, even with 3D FEA codes. Without such information, agreement between codes and data may be no better than 20%. [26] For this study, the use of CHSST's benchmarked code with parameters based on previous designs having measured primary parameters should yield results with the lowest uncertainty.

Several modifications were made to the CHSST LIM code that is written in Microsoft Visual Basic. The minor improvements were the inclusion of numerous comments to identify variables, collecting all input parameters into one part of the code, and adding subroutines to output results to text files for plotting or use in other simulation programs. More significant was the addition of the capability to calculate performance over a range of slip frequencies while maintaining the parameterization with vehicle speed. Through the detailed review of the analysis method, default parameters, and calculation technique, suggestions have been made to CHSST for future improvements in the model.

6.5. LIM PERFORMANCE CALCULATIONS AND TRADEOFFS

6.5.1. *Performance of HSST-200 Baseline LIM*

The baseline design of the LIM to drive the COL-200 vehicle is the HSST-200 LIM (Toyo Denki model TDK6800) that was designed for the HSST-04 and HSST-05 vehicles. Although these vehicles were operated only at low speed due to short tracks at the 1988 Saitama Expo in 1988

---

[26] Private communication, Prof. Takafumi Koseki, University of Tokyo, and Prof. Eisuke Masada, Science University of Tokyo, Tokyo, Japan, 5jun03.

and the YES'89 Yokohama Expo in 1989 respectively, the motor was designed for operation at speeds up to 200 kph. Specific parameters of the physical geometry, materials, primary electrical winding and secondary of this motor are given in Table 6-2 in the column labeled 'HSST-200 14Jan03c'. [27] This name is also the identifier of the calculation that uses the parameters in that table column. The date of 14Jan03 is applied to this calculation since it was first performed by Mr. Junro Kato of CHSST at about that time with those parameters.

The calculated performance of the baseline HSST-200 LIM using the updated code is shown in Figure 68. Numerous performance parameters are plotted on the same curve so they can be easily compared as a function of speed. Important features to note in these results are that the thrust/LIM is nearly constant up to a "breakpoint" where the motor switches from a constant current mode to a constant voltage mode. Since the motor is operated at a constant slip-frequency, the frequency must be increased with speed so that the synchronous speed of the magnetic traveling wave in the gap is increased consistent with the vehicle speed. Since the motor impedance is proportional to frequency, the voltage across the LIM must also be increased with speed to maintain the current level in the primary winding. This constant current maintains the highest magnetic flux in the gap for thrust, and the motor is said to operate in a constant voltage/frequency mode. However, the voltage can only be increased up to a level that the inverters can support which is dependent upon the series-parallel configuration of the LIMs as a load to the inverters, and the maximum DC voltage of the rail providing power to the vehicle. Once the maximum voltage per LIM is reached (the breakpoint speed), the code holds the voltage constant, but since the frequency and LIM impedance continue to increase, the current now decreases. Thrust is proportional to the square of the current (if the field maintains linearity with current); therefore, there is a significant decrease past this breakpoint.

---

[27] Data from Chubu HSST Corporation, Nagoya, Japan.

Table 6-2: Parameters of HSST-200 LIM used as baseline and two possible configurations of the LIM for COL-200 vehicle. Fields highlighted yellow indicate parameter was changed.

|	HSST-200 14Jan03c	COL-200 11oct03 b	COL-200 19nov03 a
MOTOR PRIMARY PARAMETERS	CHSST	RK-SNL	RK-SNL
Core length in x direction, (meters):	2.30	2.91	2.91
Core transverse width, (meters):	0.22	0.22	0.22
Core height in y direction, (meters):	0.085	0.088	0.088
Number of primary current phases, (integer):	3	3	3
Number of poles:	8	10	10
Pole pitch, (meters):	0.261	0.261	0.261
Total turns per phase,:	120	120	120
Primary winding conductor:	Aluminum	Aluminum	Aluminum
Primary total weight/LIM, calculated (kg)	289	379	379
MOTOR SECONDARY PARAMETERS			
Mechanical clearance gap, primary core to reaction rail, (mm):	15	13	13
Reaction rail material:	Al	Al	Al
Equivalent width of reaction rail, (meters):	0.33	0.33	0.33
Reaction rail thickness, (meters):	0.004	0.004	0.004
Reaction rail temperature for calculation, (deg C):	40	40	40
Thickness of spacer, (meters):	0.001	0.001	0.001
Secondary core material:	steel	steel	steel
Secondary core height in y direction, (meters):	0.010	0.010	0.010
Secondary core electrical conductivity at 20 C, (Siemens):	8.70E+06	8.70E+06	8.70E+06
Relative permeability of secondary iron:	500	100	100
POWER SUPPLY PARAMETERS			
Total LIMs per inverter:	6	20	5
Trolley rails voltage (V DC):	+1500 to gnd	+3000 to gnd	+1500 to gnd or gnd to -1500
Calculation Line current into LIM, (A rms):	280	386	386
Connection type, Wye(Star) or Delta:	Delta	Delta	STAR
Configuration description (series - parallel):	2s-3p	4s-5p	1s-5p
Inverter conversion efficency:	0.91	0.91	0.91
Slip Frequency, (Hz):	12.0	11.5	11.5
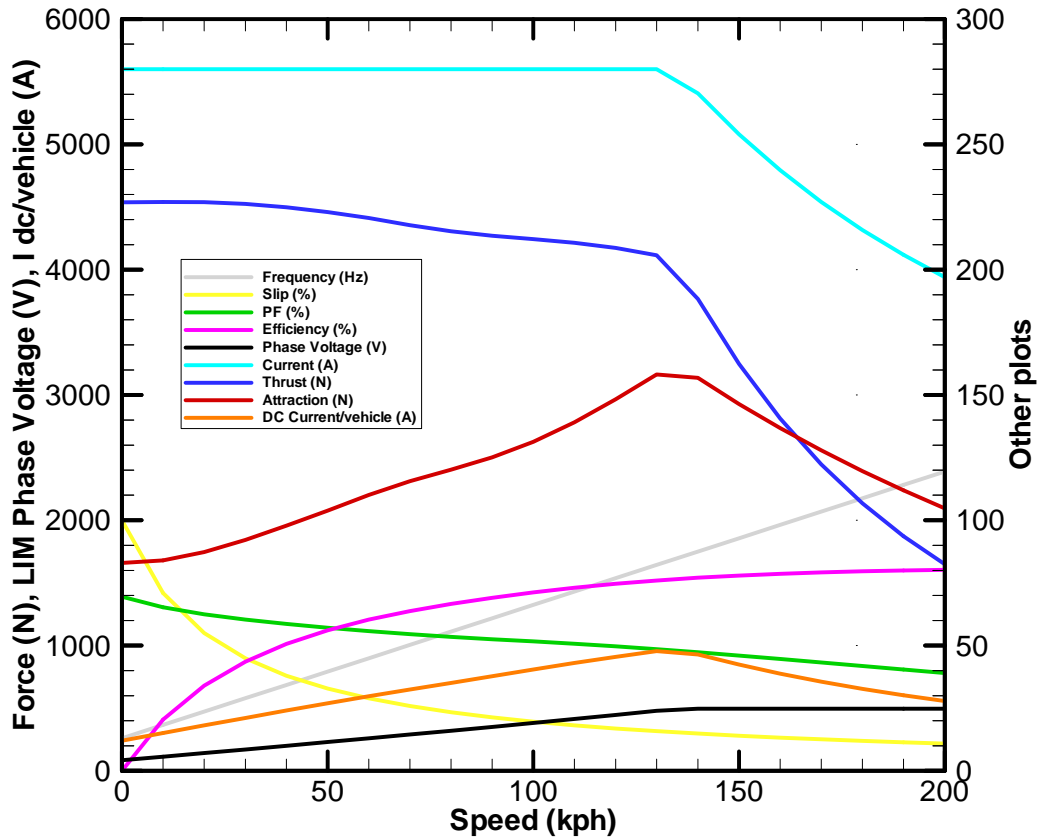
Figure 68: Performance of HSST-200 LIM

with updated spatial harmonics analysis code using parameters labeled HSST-200 14Jan03c in Table 6-2. DC current/vehicle is for all inverters on vehicle feeding 6 LIMs.

Other features to note in Figure 68 are that the current and voltage shown are per LIM and from the input parameters in Table 6-2; the 6 LIMs considered per vehicle are in a 2-series (delta) configuration with 3 groups in parallel. The curve labeled DC current/vehicle is the current to power these 6 LIMs. The voltage on the trolley power rails +1500 VDC to ground for this calculation. This configuration results in the inverter output line-to-line voltage reaching its limit (including derating factors) at about 130 kph. The efficiency shown is the LIM efficiency at the inverter, and the 91% efficiency of the power conditioning equipment must be considered to obtain the efficiency at the trolley rail.

6.5.2. *Modifications to HSST-200 Baseline LIM*

While the thrust of the HSST-200 LIM is significant, even if the length of the motor is increased 26% to fit the length of the bogie in the COL-200 vehicle and the thrust increased proportionally, Figure 68 shows that additional changes are needed to achieve 7 kN at low-speed and 4 kN thrust/LIM at 160 kph. The options 1-7 for modification discussed above were considered in a sequence where calculations were made for a range of values for the changed parameter. Over forty calculations were conducted with parameters that are discussed below as part of the optimization to achieve the desired thrust values. One resulting configuration of parameters is shown in column labeled 'COL-200 11oct03b' in Table 6-2. The cells that are highlighted yellow signify that the parameter value has changed from the HSST-200 case.

1. LIM length is increased to 2.91 m to generate greater thrust per LIM. This increase in length is done by keeping the slots width (direction of motion) and pitch the same as the HSST-200. However, the number of poles was increased from 8 to 10. The 2.91 m length is within the length of the COL-200 vehicle bogie.

2. To keep a high thrust-breakpoint speed, the number of turns per phase was decreased by decreasing the number of turns per preformed primary winding coil from 5 to 4. The wire thickness was then increased 20% to make use of the available space in the slot.

3. There are 10 LIMs per vehicle, and 2 cars per married-pair consist. For the calculation 'COL-200 11oct03b', the 20 LIMs are configured in a 4 series–5 parallel, 3-phase delta configuration that is considered powered by a single inverter for the purposes of the code. It is more likely that multiple, parallel inverters will energize the LIMs of each vehicle. For calculation 'COL-200 19nov03a', the 10 LIMs per vehicle are configured into two groups of 1 series–5 parallel, 3-phase WYE configuration, where each group is energized by its own inverter. This WYE configuration simplifies cabling between LIMs and balances the number of LIMs per inverter. The current into each LIM for either of these configurations is the same.

4. LIM maximum current increased from 280 A to 386 A to generate 7000 N low-speed thrust. Thrust scales as the square of the LIM current if the iron of the primary core can support the increased flux.

5. The difference in voltage between the trolley rails is increased from 1.5 kV to 3 kV DC. The increased voltage provides options to put more LIMs in series and increase the maximum voltage output of the inverters. CHSST staff has noted that 3 kVDC systems are not used in Japan, and there may be a limited number of Japanese manufacturers. [29] However, Hitachi is manufacturing 3 kV rail power conditioning equipment for Russian rail systems and there is an additional manufacturing base in Europe of this equipment that is used in Spain, Italy, and Poland. Three kilovolt systems have been used for rail systems traveling up to 250 kph in Italy from Rome to Florence. [28] The 4 series – 5 parallel, 3-phase delta configuration of calculation 'COL-200 11oct03b' uses trolley voltages at +3 kV DC and ground. In calculation 'COL-200 19nov03a', one set of 1 series – 5 parallel LIMs is energized by an inverter fed from +1.5 kV and ground trolley rails, and the second set of 1 series – 5 parallel LIMs is energized by an inverter fed from the ground and -1.5 kV trolley rails. This latter configuration makes use of the more prevalent 1.5 kV inverters used in conventional rail systems.

6. Clearance gap decreased to increase thrust, but the attractive normal force also increases as shown in Figure 69. Gap value of 13 mm selected based on recommendation by CHSST and Toyo Denki staff for minor change. Note that calculations include additional 1 mm of air gap added to the clearance gap for the adhesive between secondary rail conductor and back iron.

7. Changing the reaction rail from aluminum to copper and varying its thickness and/or the slip frequency has a significant impact on the low-speed thrust and attractive force, but does not yield much improvement in thrust at 160 kph compared to the 4 mm aluminum. This is seen in Figure 70. Replacing the aluminum rail with a copper rail whose 3.2 mm thickness is the same fraction of the classical electrical skin depth reduces the thrust and attractive force. Decreasing either the slip frequency or the thickness to increase the thrust also dramatically increases the attraction force. Given that LIM efficiency changes only by 2 to 3 percent at both the breakpoint speed and at 160 kph compared to the 4

---

[28] Trainspotting Bukkes, www.bueker.net/trainspotting/voltage_comparison, 2003.

mm thick aluminum, changing to a copper rail does not appear warranted due to the cost, unless the clearance gap is further decreased significantly and additional shielding of the attractive normal force is needed.

8. For the calculation 'COL-200 11oct03b' with 4series-5 parallel LIMs, the maximum inverter line-to-line voltage (peak) increased from 1100 V to 2450 V consistent with the increase of the trolley voltage from 1.5 to 3 kV DC to achieve a high thrust-breakpoint speed. With 4 series LIMs, this sets the maximum voltage per LIM at 550 Vrms. As seen in Figure 71, this change has the most direct effect on increasing the thrust at 160 kph to the required 4000 N.

    For the calculation 'COL-200 19nov03a' with 1series-5 parallel LIMs, no increase in line-to-line voltage is needed with the LIMs in a WYE configuration, the maximum voltage per LIM reaches 570 V, achieving the same thrust profile.

9. Wire height was increased 10% from 14 to 15.4 mm to achieve the same Ohmic power dissipation per unit volume as obtained in the HSST-200 14jan03c calculation, 1.05 W/cm3. Height of the primary core slot is increased to accommodate this increase. This does not affect the calculated output given that the primary core cross-section is maintained.
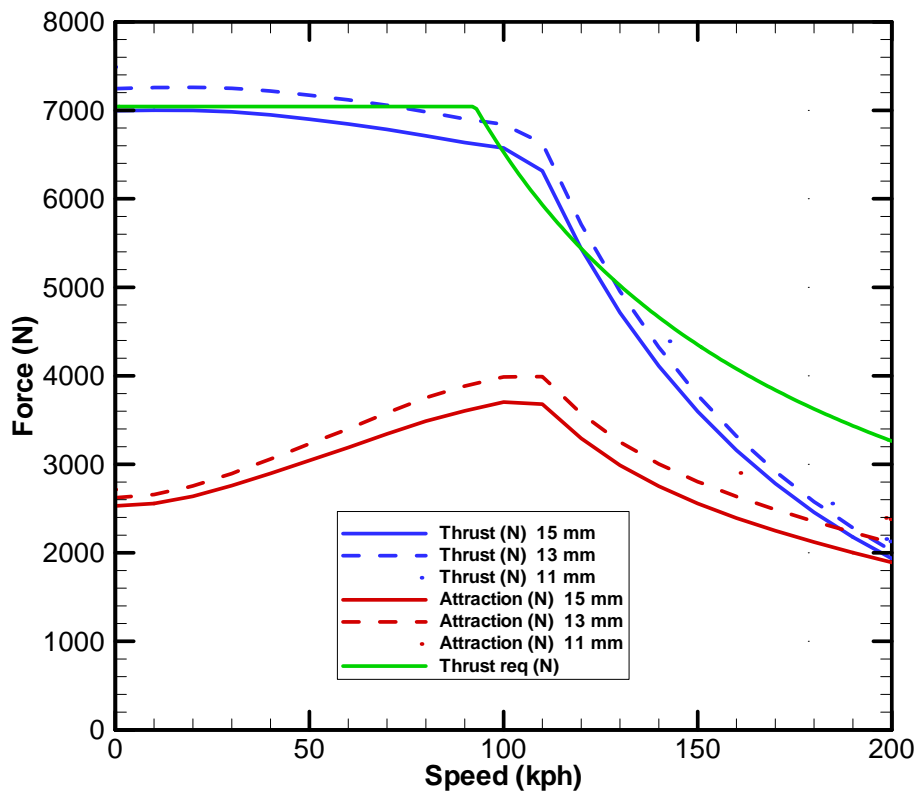

Figure 69: Sensitivity of LIM thrust and attractive normal force to change in clearance gap between LIM and reaction rail.
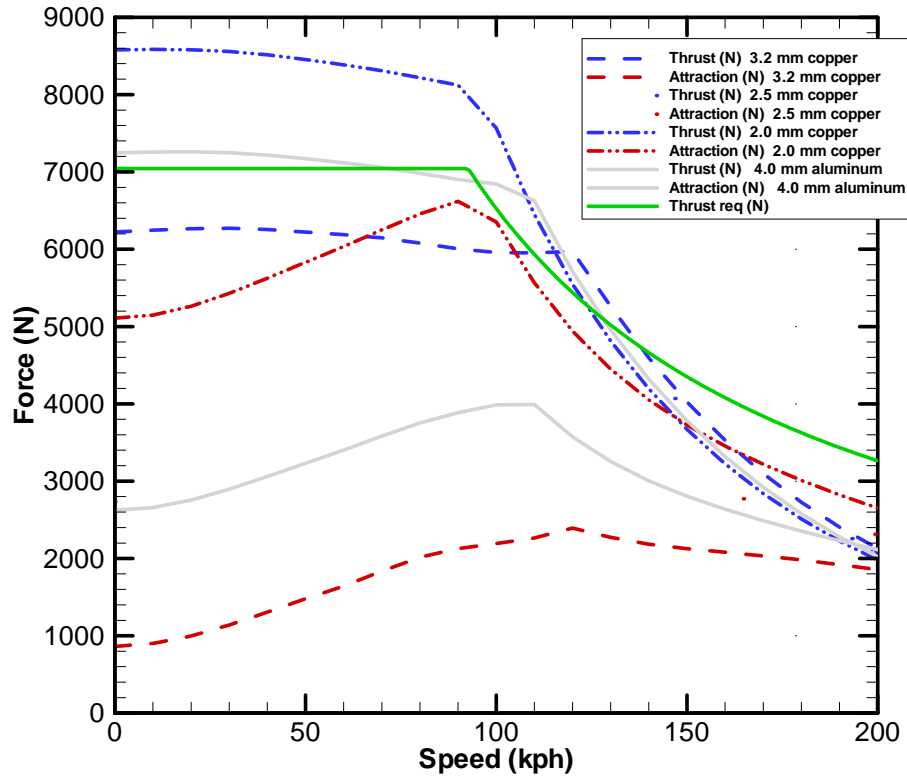
Figure 70: Sensitivity of LIM thrust and attractive force to reaction rail conductor type and thickness.
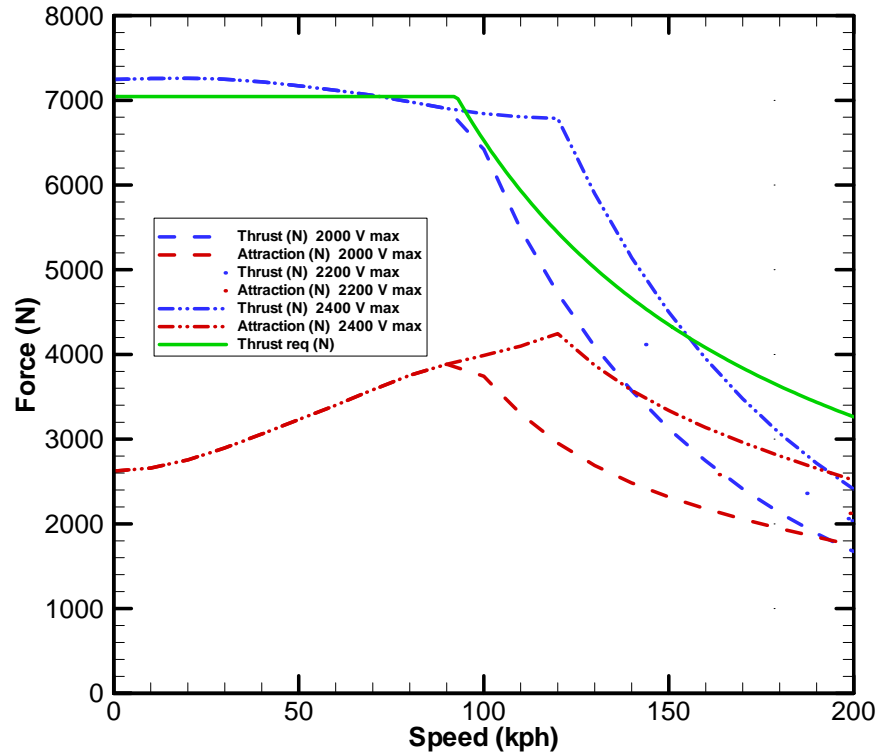
Figure 71: Sensitivity of LIM thrust and attractive normal force to the maximum voltage per LIM adjusted by varying the maximum inverter output line-to-line voltage.

10. The total Ohmic power dissipated per unit length of LIM is only 9% greater than the value estimated from the HSST-200 calculation (7.6 kW/m). It is expected that no additional cooling system is needed to augment the flow of ambient air used in previous CHSST designs. [29] However, design of vehicle chassis with ducting to preferentially force air across the LIM winding ends when moving may be beneficial to remove the additional heat.

11. The calculations shown above utilized a relative permeability of 500 for the secondary back iron, the value that was the default in the code. It is believed that this value is too high for bulk carbon steel and that a value of 100 is more conservative. The sensitivity of the thrust and attraction curves for relative permeabilities of 50, 100, 200 and 500 are shown in Figure 72. The impact of the relative permeability is significant for the low-speed thrust, but much less so at 160 kph. The impact on the attractive force is more dramatic.

12. Neither a permeability vs. magnetization curve nor a B-H curve was available at the time of this analysis for the back iron of the secondary rail used by CHSST. Currently, a search is underway for data of the magnetic properties for the (Japanese Industry Standard) SMA 400AW low-carbon, atmospheric corrosion-resistant steel or its U.S. equivalent. Data on permeability for low-carbon steels that are common to reaction rails is shown in Figure 73. [9] The estimate of a relative permeability of 100 is a conservative value based on the common carbon steel data for the anticipated 6700 A/m field intensity.

13. Calculations were done with UNS copper 110 wire (1.72 μOhm-cm) in the primary winding instead of 2.87 μOhm-cm aluminum. The Ohmic power/volume and total Ohmic power per phase reduced 40%, but the LIM mass increased 38%. Decreasing the wire cross-section to obtain the same 1.06 W/cm3 as achieved with the aluminum wire still yields a heavier winding, thus copper is not considered an option for the primary winding.
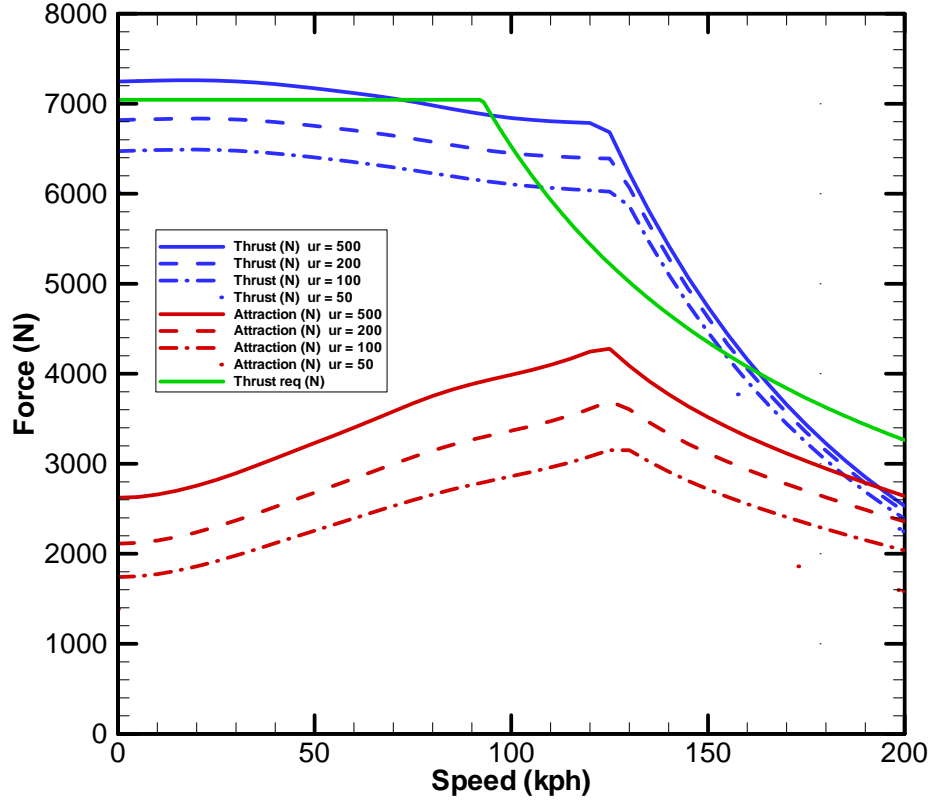

Figure 72: Sensitivity of LIM thrust and attractive normal force to relative permeability of secondary back iron.
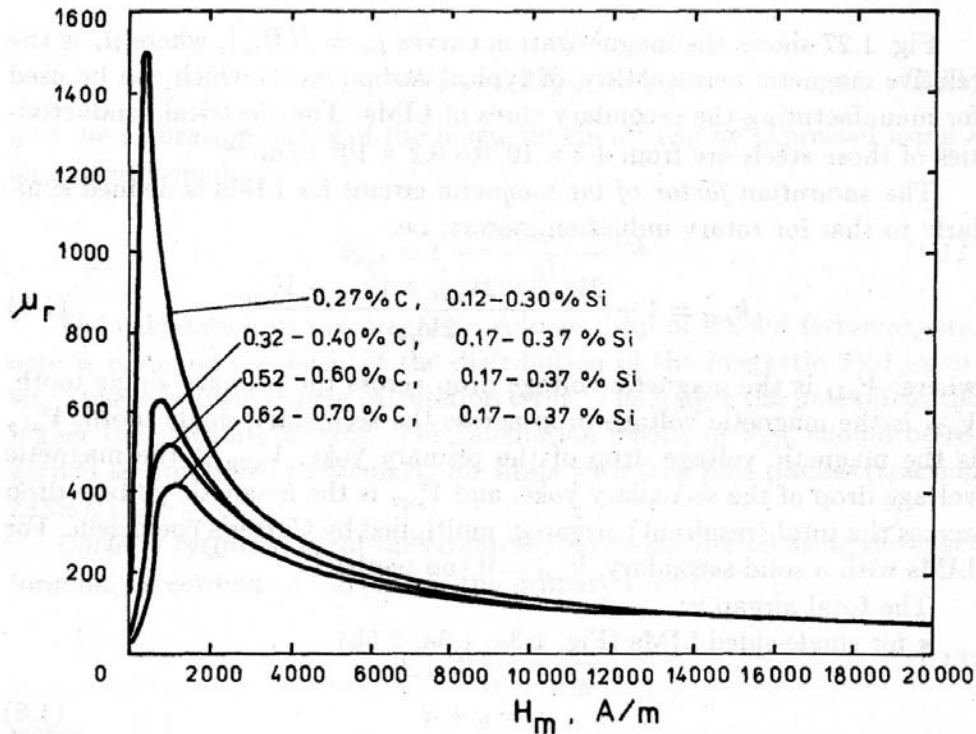
Figure 73: Relative permeability as a function of magnetization for carbon steels commonly used as back iron for LIM secondary reaction rails. [9]

14. With the reduction in relative permeability from previous calculations a change in slip frequency is recommended to increase thrust without requiring an additional increasing in the voltage or current.

15. Figure 76 shows the thrust and attractive force versus slip frequency parameterized with speed for input parameters in "COL-200 11oct03b" in Table 6-2. Decreasing the slip frequency from 13 Hz used in the previous calculations to 11.5 Hz achieves the low-speed thrust of 7000 N, but the thrust at 160 kph is only 3722 N, 9% below the desired value of 4080 N. If the slip frequency were kept at 11.5 Hz for speeds from 0 to 120 kph, then increased up to 15 Hz as the speed was increased between 120 and 160 kph, the desired thrust of 4000 N at 160 kph could be achieved. The frequency would still be increased with speed after the breakpoint, but the change would be consistent with a constant slip (not slip frequency). Such a change in operation is possible with control systems, has been demonstrated with AC drives, and could be utilized for the Colorado system.

These design modifications have been reviewed by staff of CHSST and Toyo Denki, and their response is very encouraging as to the feasibility of incorporating the necessary modification. They have taken the geometry parameters for the COL-200 LIM and generated layout drawings as part of this concept design. These drawings will form the basis for further detailed design of the LIM propulsion system and its integration into the vehicle.

6.5.3. *COL-200 LIM Motoring Performance*

The performance curves for the 4-series-5 parallel LIMs configuration of the COL-200 LIM with parameters as shown for case COL-200 11oct03b in Table 6-2 are shown in Figure 74. Specific

output values are listed in Table 6-3. Note that this calculation is for a fixed slip-frequency of 11.5 Hz, and does not include the improved thrust at 160 kph due to constant slip mode at speeds greater than 125 kph.

The performance curves for the 1-series-5 parallel LIMs configuration of the COL-200 LIM with parameters as shown for case COL-200 19nov03a in Table 6-2 are shown in Figure 75. Specific output values are listed in Table 6-3. Note that the DC current draw is shown per inverter feeding 5 LIMs. As there are two inverters per car connected in series across the +1500 V to -1500 V trolley rails, the current draw per inverter is the same as per car. For the two-car consist, the total current draw is twice the value shown, which is equivalent to the value shown in Figure 74.

The thrust generated with the 1 series – 5 parallel configuration of LIMs is slightly greater at 160 kph than that from the 4 series-5 parallel configuration. Hence the change of the LIM control from constant slip frequency to constant slip at speeds greater than the thrust breakpoint speed would not be absolutely necessary. However, with the change, the performance would still be improved from that shown at constant slip frequency.

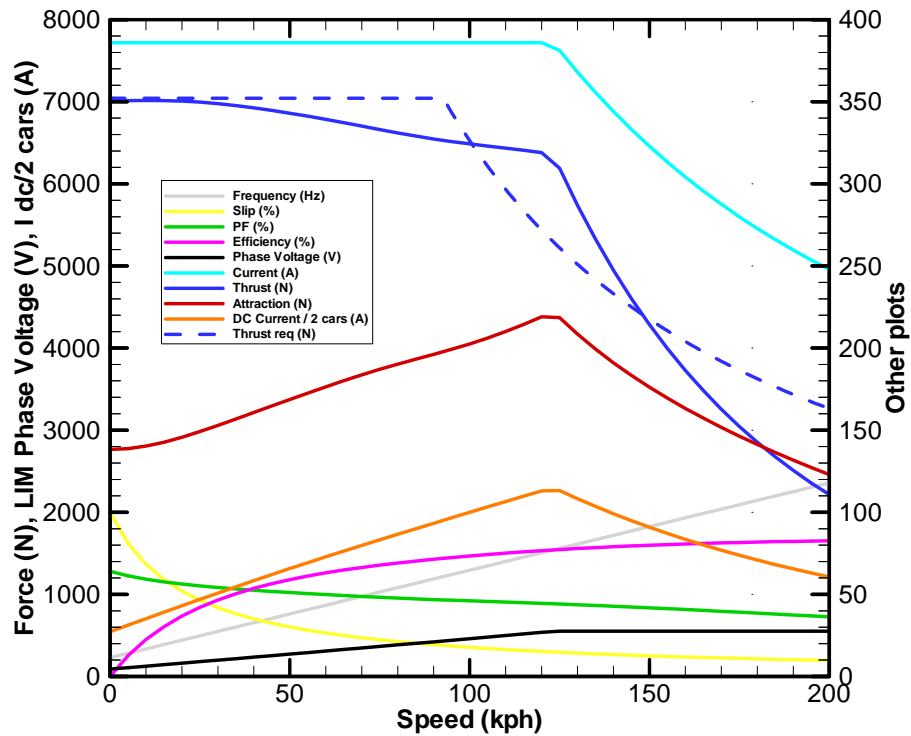**Figure 74: Performance curves for COL-200 LIM with updated spatial harmonics analysis code using parameters labeled 11oct03b in Table 6-2. DC current per 2 vehicles is for all inverters feed the 20 LIMs in a 4 series – 5 parallel configuration.**
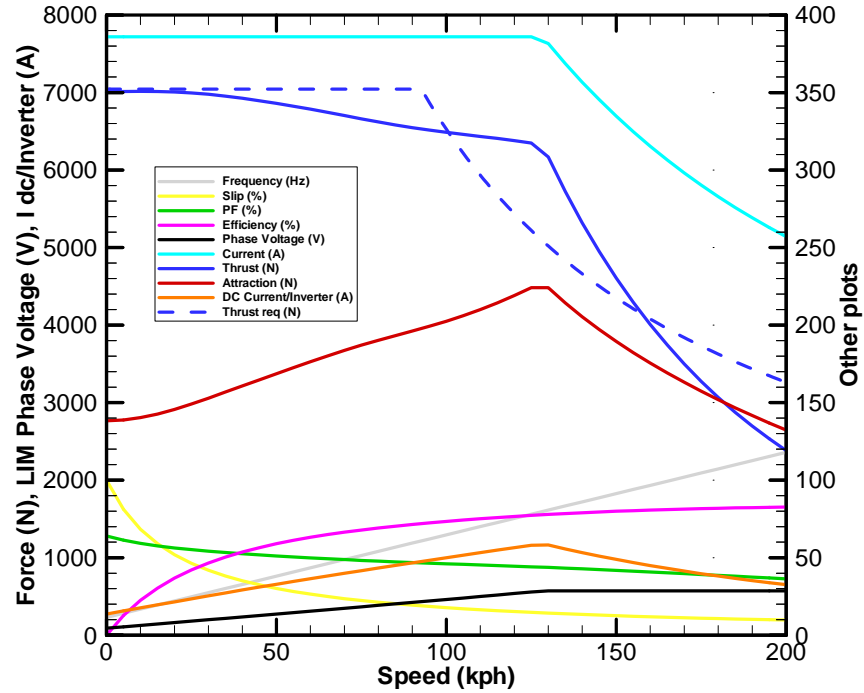
Figure 75: Performance curves for COL-200 LIM with updated spatial harmonics analysis code using parameters labeled 19nov03a in Table 6-2. DC current per inverter is for one inverter feeding the 5 LIMs in a 1 series – 5 parallel configuration. Two inverters are in series per car hence drawing the same trolley current per car.

Figure 76: LIM thrust and attraction force vs slip frequency parameterized by speed for parameters in COL-200 11oct03b in Table 6-2

Vector in thrust curve show recommended change in slip frequency after the breakpoint speed of 120 kph to increase thrust at 160 kph.

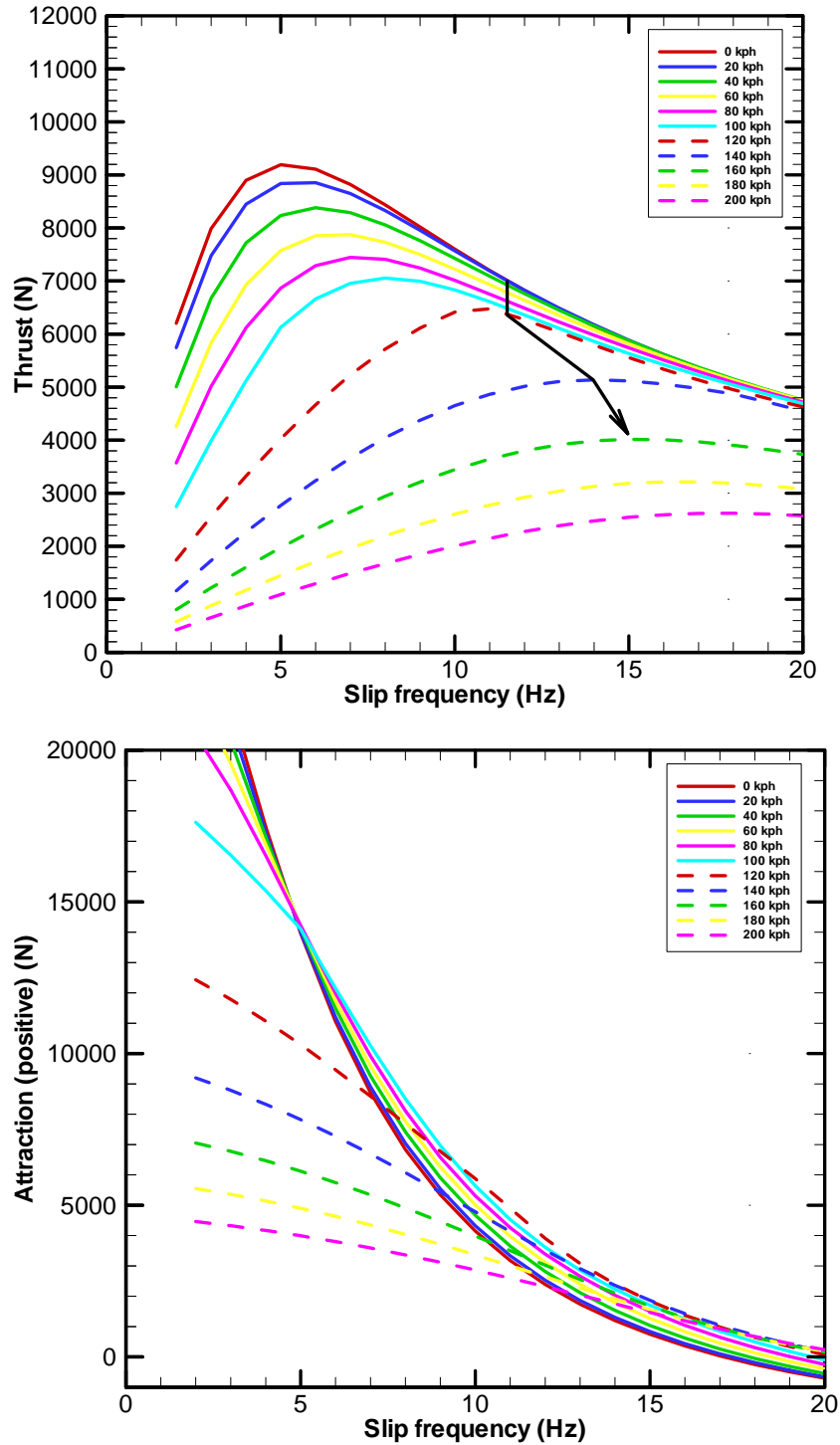**Table 6-3: Summary of output values from calculations for HSST-200 and COL-200 LIMs using input parameters in Table 6-2.**

CALCULATION Results	*HSST-200 14Jan03c*	*COL-200 11oct03 b*	*COL-200 19nov03 a*
Thrust/LIM at zero speed (N)	4538	7008	7008
Attraction/LIM at zero speed (N)	1659	2765	2765
Breakpoint speed (kph)	130	125	130
Thrust/LIM at breakpoint (N)	4115	6191	6191
Attraction/LIM at breakpoint (N)	3163	4169	4483
LIM voltage at breakpoint (V rms)	479	551	571
Efficiency at breakpoint (%)	75	77	77
Thrust/LIM at 160 kph (N)	2812	3726	4007
Attraction/LIM at 160 kph (N)	2736	3265	3510
LIM current at 160 kph (A rms)	239	304	315
Efficiency at 160 kph (%)	78	80	80

The maximum attraction force has increased from 3163 N per LIM for the 33 tonne, 6-LIM HSST-200 vehicle to 4169 N per LIM for the 44 tonne, 10-LIM COL-200 vehicle. Most of this increase is associated with the 26% increase in length of the LIM as expected, and the vehicle will have additional levitation magnets to support the longer, heavier vehicle. The attractive force from the six LIMs of the HSST-200 is 19 kN which represents about 6% of the loaded vehicle mass. The attractive force from the ten LIMs of the COL-200 is 42 - 45 kN which represents about 10% of the loaded vehicle mass. CHSST staff has indicated that while the change is not negligible and attention must be given to the limits of the levitation control system, the problem is not critical. In addition, future advances in levitation control and magnet design will also support mitigation of the impact of the normal force. [29]

The inverters that feed the LIMs have been sized to deliver up to 10% greater current than the 386 A normal operating level. This is done to provide a margin in capability in normal operation and permit emergency braking at high acceleration. Figure 77 shows the thrust curves for the normal and maximum LIM current levels and the drag force/LIM for the 44 tonne vehicle in a 2-car married pair configuration with a 90 kph headwind. A 15% climbing grade appears to be a practical limit under normal operating conditions, while 18% may be possible at maximum current for short durations. If steady operation at the maximum current is considered, additional forced-air (or possibly liquid) cooling of the LIM will be needed.

---

[29] Review of Propulsion Trade Study LIM modifications and calculations, CHSST and Toyo Denki, 21oct2003.
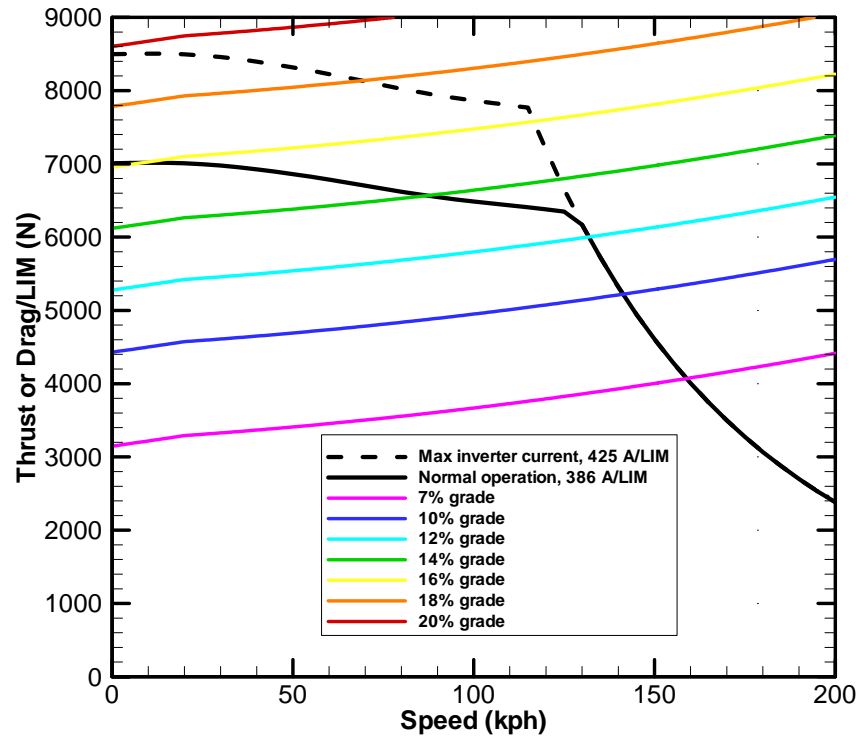
Figure 77: Thrust per LIM at normal operating current of 386 A and maximum inverter output. Drag force/LIM curves for married pair of COL-200 vehicles on various grades into a 90 kph headwind at zero acceleration.

6.5.4. *COL-200 LIM Braking Performance*

In the braking mode, the slip frequency is changed from +11.5 Hz to -11.5 Hz that sets the traveling magnetic wave of the LIM slower than vehicle speed by the amount of the slip frequency times twice the pole pitch. This puts the LIM into a regeneration mode where energy from the vehicle is converted to electrical power that can be delivered back to the trolley line. This is seen as a negative current delivered to the vehicle in Figure 78 that also shows curves for the frequency, LIM voltage and current, power factor and efficiency. The regeneration mode is used from 160 kph down to 22 kph at which point the frequency crosses zero. At lower speeds, the sequencing of the three current phases to the LIM is changed to cause the traveling magnetic wave to reverse direction and travel opposite the vehicle direction, putting the LIM into plugging mode which still delivers braking force, but now the vehicle absorbs power from the trolley line. The braking and normal forces are shown in Figure 79.

The braking force curve shows significant braking capacity up to the maximum operating speed of 160 kph. Considering a 44 tonne vehicle with a 90 kph tailwind, an estimate was made of the stopping distance and time on descending grades under constant magnetic braking force of 67 kN (normal duty) or 80.3 kN (emergency duty) per car. No friction braking is considered in this estimate. The higher force assumes a 10% increase in the LIM current for emergency braking conditions or on high descending grade. The results for an initial speed of 160 kph are shown in Figure 80. A descending grade of -15% is the practical limit for normal current level operation, using the maximum inverter current. At -18% grade, the braking force is only sufficient so speed does not increase, and significant deceleration would take place when the vehicle reached shallower grade.
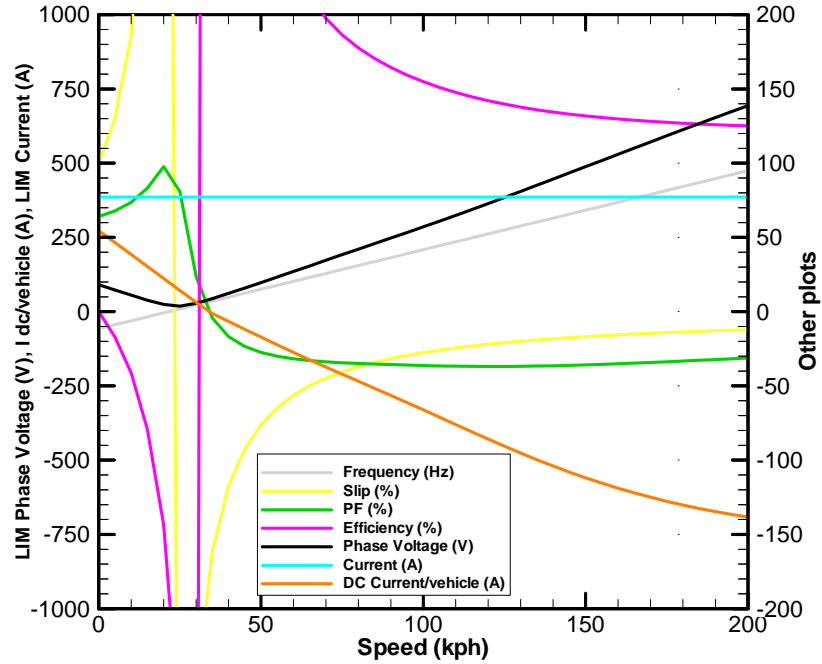
Figure 78: Electrical performance curves for COL-200 LIM in braking mode with 386 A/LIM and slip frequency of -11.5 Hz.

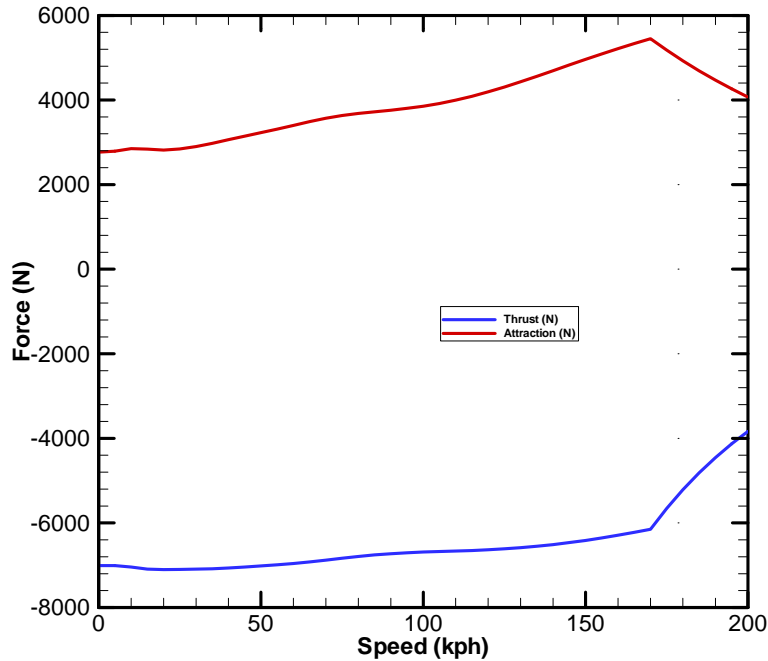Other LIM parameters are same as case 19nov03a in Table 6-2.

Figure 79: Braking and normal force for COL-200 LIM with 386 A/LIM and slip frequency of -11.5 Hz. Other LIM parameters are same as case 19nov03a in Table 6-2.
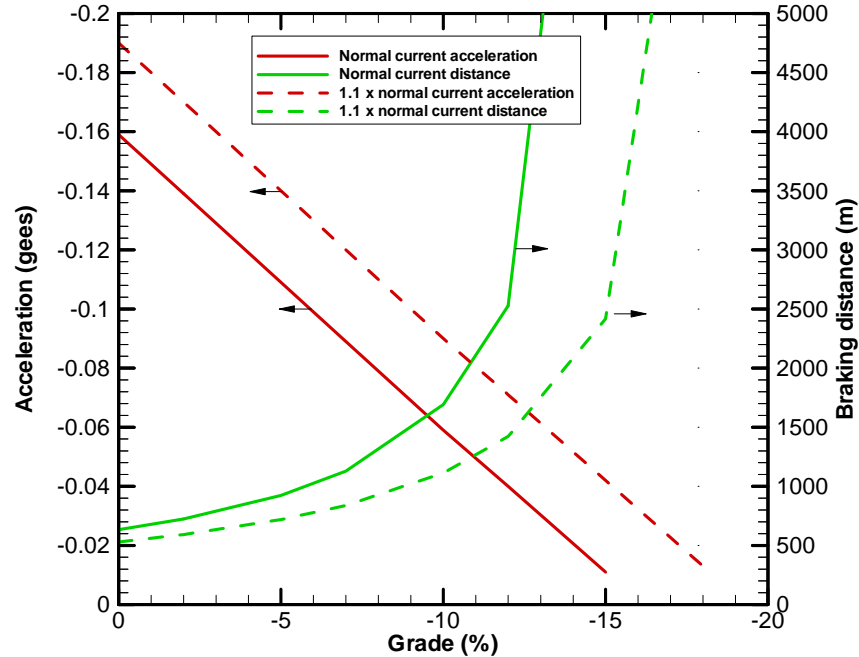
Figure 80: Braking deceleration and distance for 44 tonne COL-200 vehicle with initial speed of 160 kph as a function of grade.

6.5.5. *Development Plan for Improved Motor Design*

During meetings held in early June 2003 in Japan with staff from Chubu HSST Development Corp., Toyo Denki Seizo, and ITOCHU Corp., technical options were discussed to improve the HSST-200 LIM to meet the requirement of the Colorado route. As described in Section 6.3 above, Options 1-7 were considered viable, and these formed the basis of the tradeoffs analysis above.

At that meeting, discussions were held concerning the resources and time required to incorporate the suggested options in a LIM design, and the effort required to produce the first motor for full-scale testing. Although the modifications to improve LIM performance recommended in this study are only a subset of those contemplated at that time, the estimate is believed valid.

This is only a rough estimate based on CHSST and Toyo Denki recent experience with the TKL. This estimate would be modified early in the Basic Design phase and depends upon which options for LIM modification are selected and their impact. The development plan shown in Figure 81 has three design phases: 1) Basic Design performed by CHSST and Toyo Denki focuses first on motor details, then issues related to the motor and its configuration and impact to the vehicle; 2) Detailed Design again involves staff from CHSST and Toyo Denki and addressed details and issues of motor and vehicle; 3) Design for Manufacturing is conducted by Toyo Denki alone and generates the manufacturing process and final drawings of the motor and necessary tooling. In Japan, this production specification and drawings remain the property of the manufacturer, not the customer. This design work is part of the procurement of the motor, and does not start until a contract for fabrication is placed.

Schedule for LIM Development

	Project Year 1				Project Year 2				Project Year 3			
	Q1	Q2	Q3	Q4	Q1	Q2	Q3	Q4	Q1	Q2	Q3	Q4
Basic Design	Motor specific		Motor and Vehicle									
Detailed Design					Motor and Vehicle							
Design for Manufacture							Motor supplier					
First Prototype for Testing												

Figure 81: Rough schedule for development of LIM with improvement options and generate first article for testing.

This estimate may be modified early in the Basic Design depending upon which modification options are selected.

6.6. INVERTER AND PROTECTION CIRCUITS

As discussed above, two configurations of LIMs were considered as loads to the inverter: a 4 series-5 parallel 3-phase delta configuration of the 20 LIMs for the two-car consist, and four groups of 1 series-5 parallel wye (star) configurations where each group would be energized by its own inverter. The goal for each case was to utilize a 3 kV differential between the trolley lines and for the inverters to have sufficient input voltage to achieve 550 V_{rms} output to drive the necessary current through the LIM to achieve the desired thrust. A trolley line voltage difference of 3 kV is desirable to minimize the current that must transfer through the power collector on the vehicles. A 1.5 kV voltage differential would require 4520 A at maximum power per 20 LIMs of a two-car consist compared to 2260 A draw at 3 kV differential. The lower current could be supported by a single trolley rail about twice the overall cross-section dimensions of the existing rail (but solid instead of tube) used at the Nagoya Test Track and result in voltage drop of only 30 V/km or 1% per kilometer.

Collection of the high current from the trolley line must be demonstrated at the maximum speed of 160 kph. The collector for the HSST-Linimo maglev vehicle to be used on the Tobu-Kyuryo Line (TKL) in Nagoya, Japan is shown in Figure 82. It has a maximum current capacity of 600 A with a trolley rail contact height of 13 mm, and has operated up to 110 kph with collector wear on the order of 0.6 mm/1000 km [30]. Extending the capacity to 1130 A/vehicle will require a rail that is 2-3 times wider to handle the current and reduce the wear. Testing of a modified collector designs could be conducted at the Railway Technical Research Institute Test Track at Kokubunji, Tokyo to determine the collector stability and wear characteristics.

---

[30] "Report of Economic Feasibility Study of Levitation Linear Motor Car for Urban Transportation," Japan Transportation Economics Research Center, Aichi Prefecture, March, 1993.
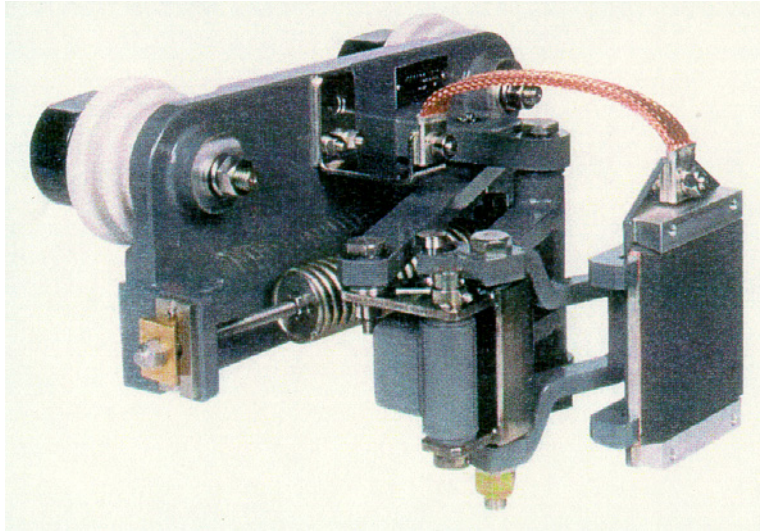
Figure 82: Spring contact pantograph of power collector

Developed by Toyo Denki for the HSST Linimo maglev vehicle for the TKL in Nagoya Japan. Metalized carbon pad is forced against 1.5 kV trolley rail on the guideway to provide power to the vehicle.

Of the two possible series-parallel configurations of the LIMs, the 1 series-5 parallel, wye connection was considered more practical for the following reasons:

1. LIM's from the two vehicles are not connected together. It is desirable to have all the LIMs of one vehicle serviced by the inverters on that vehicle to minimize cabling between vehicles that can be a source of electromagnetic interference (EMI). While conduit and shielding will help mitigate the EMI, they add weight to the vehicles.

2. A wye connection has less complex connections and cablings than a delta connection that also helps minimize cable weight and potential for EMI.

3. While 3 kV-to-ground inverters and protection circuits are available, there are more 1.5 kV systems manufactured worldwide and in use in conventional rail. This provides greater opportunity to locate manufacturers willing to optimize the on-board power condition system for low-weight.

4. No one inverter unit was anticipated to feed all 20 LIMs in the 4 series-5 parallel system, and options such as splitting the loads in parallel to 4 series-3 parallel and 4 series-2 parallel or different configurations with inverters in series was considered. In all those cases, the load of one inverter was distributed across two vehicles and the power levels of the multiple inverters were different.

The proposed configuration for each vehicle is shown in Figure 83 where each group of 5 parallel LIMs in a wye connection is fed by a three-phase, two-level, variable-voltage, variable frequency (VVVF) inverter. Each inverter has its own protection circuits which are connected in series across the +/-1.5 kV trolley rails with the midpoint tied to a third ground rail. This ground rail contact is not a high current contact in normal duty operation, but serves as an electrostatic contact to balance the high voltage across the two inverters and provides a safety ground discharge path for the passenger cabin in the event of a lightning strike.
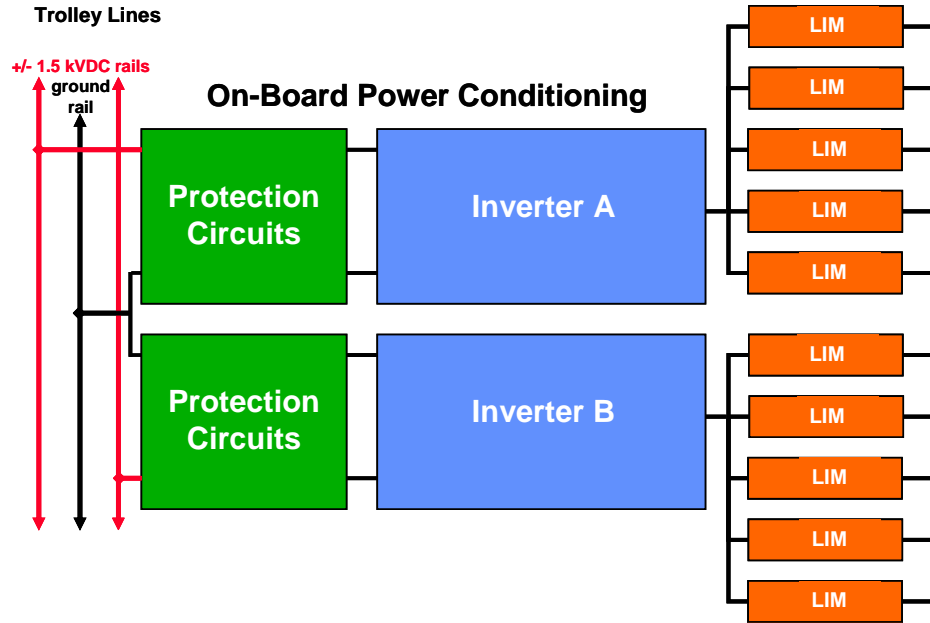
Figure 83: Schematic representation of major components of on-board propulsion system.

The protection circuits typically include low-speed contactors that connect the inverter load to the trolley line, a high-speed circuit breaker to rapidly disconnect the load in the event of a fault, and reactor inductors that block the high frequency switching electrical noise in the inverter from the trolley line. The inverter includes a shunt capacitor that filters the electrical noise and serves as an energy store for transient current demand from the inverter, switches and resistive loads to provide over-voltage protection, particularly during regeneration, and lastly IGBT switches in a three-phase bridge circuit that applies the pulse-width modulated voltage across each phase of the series-parallel LIM configuration. Depending upon the manufacturer, some of the above components may be assigned to the protection circuits or the inverter, but generally, all constant-voltage inverter systems include these items. Based on communication with inverter manufacturers, the power efficiency in the motor direction is in the range of 90 to 95% with most losses attributed to the filter reactor and the switches of the inverter. As such, the inverter components are typically air cooled although heat pipes are commonly used to conduct heat from the switches to the airflow induced from vehicle motion.

The proposed size of the VVVF inverter for the 1 series-5 parallel LIM group is given in Table 6-4 which permits a maximum LIM current of 425 A which is 10% greater than the maximum normal operating current of 386 A at 7000 N thrust/LIM. To achieve the higher current, the output voltage is also increased 10%. The output frequency is the fundamental AC frequency of the output current, and the switching frequency of the multi-pulse width modulation of the output voltage will be several times that frequency.

Table 6-4: Requirements for on-board VVVF inverter and protection circuits for each 1 series-5 parallel group of LIMs.

Parameter	Value
Trolley line input voltage	1500 VDC to ground OR ground to -1500 VDC
Estimated max trolley line current draw	1280 A
Inverter type	2 level or 3 level
Output pulse mode	Multi-pulse or single pulse
Configuration of LIM load to Inverter in each phase	1 series – 5 parallel
Phases, load connection type	3 phases, Star (Y)
Output AC frequency	11 to 120 Hz
Max inverter phase voltage across all series LIMs	629 V rms per phase across 1 LIM at 80 Hz
Max inverter phase current through all parallel LIMs	2125 A rms per phase equally split into 5 LIMs
Power factor of each phase load at max voltage and current	0.44
Maximum output electrical power	1.75 MW
Maximum output apparent power	4.0 MVA
Braking modes	Regenerative and phase reversal

Power from regeneration is returned to the trolley rail, but the local loads of the levitation magnets and vehicle auxiliary power reduce the amount returned to the DC trolley bus system. The returned power reduces the demand from the utility, and excess power is anticipated to maintain the charge on the battery backup systems that will provide emergency propulsion and levitation power in the event of a failure of supply from the utility grid.

6.7. ESTIMATED WEIGHT OF PROPULSION COMPONENTS

Weights of the propulsion components and power conditioning components shown schematically in Figure 83 were estimated based on the values of real and apparent power needed per car.

6.7.1. *LIM Primary Winding and Core*

As discussed in Section 6.5 above, the length of the bogies in the COL-200 vehicle has been increased from 3.4 to 4.3 m, a 26% increase, and the length of the LIM was increased proportionately. The primary winding design has increased poles compared to the HSST-200 LIM, but maintains the same winding pitch and overhang widths. Wire conductors and turns are bundled within a similar preformed coil size, and the two-layer winding fits within a slightly deeper core slot. Considering these modifications, the calculated weights of the LIM's aluminum winding and magnetic-steel core, based on the detailed geometry given in Table 6-2, is estimated at 379 kg.

6.7.2. *Inverters and Protection Circuits*

Using the requirements in Table 6-4 for the inverter with a 5 parallel-LIM load, inquiries were sent to inverter manufacturers whose products are used in maglev, LIM-driven steel-wheel, and conventional rail systems. Responses were received from Hitachi and Toyo Denki in Japan, but unfortunately, not from European suppliers. Hitachi manufactures LIM and rotary induction motor drives and controls for conventional rail transportation that uses 1.5 and 3 kV DC as well as high

voltage AC input. Toyo Denki provides the LIM drive for the HSST maglev system as well as rotary induction and DC traction motors and drives for conventional rail systems.

Data for protection circuits and VVVF inverters from the manufacturers are shown in Table 6-5 where the components are separated as the vendors provided data for high-speed breakers, filter reactors, and inverter cabinets. These data are for existing products that operate with a 1.5 kV DC supply, and do not represent necessarily the entire capability of the manufacturer for future designs. To estimate the mass and volume of these components for the COL-200 vehicle, the inverters were scaled by kVA rating to 8000 kVA/car capacity, and the other components were scaled by kilowatt ratings to 3530 kW/car required capacity.

Table 6-5: Parameters of existing protection circuit and inverter components and projected weight and size of those components for the COL-200 vehicle.

Component	Manufacturer	Length (mm)	Width (mm)	Height (mm)	Weight (kg)	Power (kVA)	Power (kW)	Selected Scaled Components	
								Weight/car (kg)	Volume/car (m³)
VVVF Inverter	Toyo Denki	1600	890	540	368	1487		1980	4.1
	Hitachi	2400	2100	600	900	1750			
High Speed	Toyo Denki	1550	900	540	302		2454		
Breaker	Hitachi	725	400	600	80		894	316	0.7
Filter Choke	Toyo Denki	1240	800	448	341		2454	491	0.6
	Hitachi	1450	850	600	580		894		
								2786	5.5

As seen in the table, a significant effort has been made by Toyo Denki to minimize the mass of the inverters during the development of the Chubu HSST maglev vehicles. The inverter used in the HSST Linimo vehicle described in Table 6-5 is shown in Figure 84. The data for the Hitachi inverter assumes the components are integrated into the vehicle substructure with an optimized cabinet. Further reduction of their components could be expected with a design objective to minimize mass.
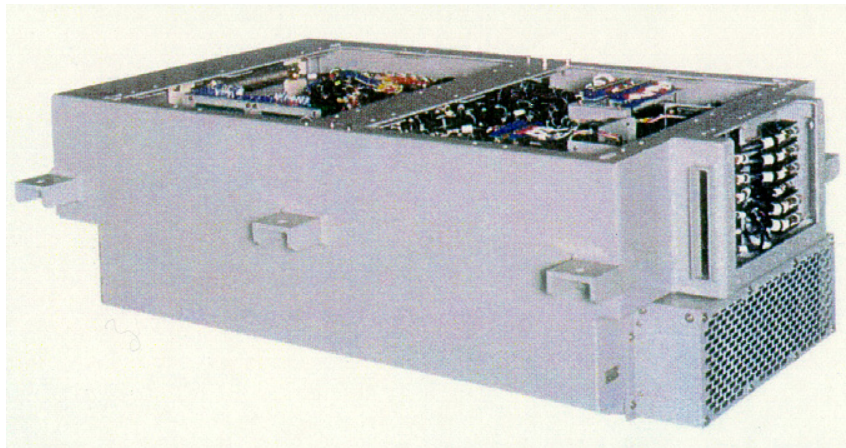

Figure 84: VVVF inverter developed by Toyo Denki for the Chubu HSST Linimo maglev vehicle for the TKL in Nagoya, Japan. Parameters are given in Table 6-5.

Further reduction of weight of inverters for transportation applications is expected due to continued development of higher voltage and higher current IGBTs such as the work being done by Toshiba. Improvements in IGBT technology are expected, especially for devices manufactured for specific applications such as on-board transportation components. In the past 15-20 years, the weight and size of inverters has been reduced about 33%, and additional reductions of 20% could be expected in the next 5 years as the individual switches become capable of higher current capacity and are individually packaged in geometries that minimize the

additional mass/space of cooling and snubber circuits. [31] Collaboration with power-conditioning equipment manufacturers will be necessary to insure low-weight and small-volume objectives are met consistent with the required performance.

6.8. SUMMARY AND CONCLUSIONS

A propulsion trade study has been conducted to identify and evaluate prospective linear motor designs that could meet the system performance requirements of the CMP, and potentially be applicable to other urban maglev transit corridors. This study has focused on the technical characteristics and performance of the linear induction motors used in the Chubu HSST maglev system that had been selected as the project baseline technology.

This work was done in close collaboration with Prof. Eisuke Masada of the Science University of Tokyo, a world expert in linear motors, the power electronics systems that drive them, and maglev systems, and senior staff from Chubu HSST Development Corp. and Toyo Denki Seizo. Their efforts and cooperation have made this analysis possible.

1) The thrust requirements of the 10 LIMs in the 44-tonne, COL-200 vehicle have been defined based upon the requirements for 0.16 g initial acceleration and ability to maintain speed climbing a 7% grade at 160 kph with a 90 kph headwind. The low-speed thrust per LIM is 7000 N and 4000 N at 160 kph.

2) Peak power demand along the route is estimated between 2 – 2.5 MW/vehicle based on an analysis at constant speed of 114 kph. Details have been used in the electrification analysis.

3) HSST-200 LIM has been designed for 200 kph operation on shallow grade, and modifications to the design are necessary to increase the thrust at low-speed and at maximum speed to meet requirements for the COL-200 vehicle. Eleven options were considered and reviewed with CHSST and Toyo Denki staff in Japan with seven modifications considered for further evaluation. The selected options included:
    a) Increasing the maximum voltage per LIM to permit the motor to operate at constant voltage/frequency mode to a higher "breakpoint".

    b) Increase the trolley rail voltage differential to 3000 VDC to permit higher motor.

    c) Change the operating point on the motor's thrust vs. slip frequency characteristic curve toward lower slip frequencies to achieve greater thrust and higher efficiency.

    d) Increase the primary current of the LIM to sufficient values to achieve required thrust.

    e) Use forced air (or liquid) cooling to prevent overheating of the primary.

    f) Decrease the length of the clearance gap between the LIM and the reaction rail.

    g) Utilize solid copper reaction rail in regions of track where higher thrust is needed such as on high-gradient and in station.

4) A LIM performance model was generated from previous work developed at University of Tokyo using Prof. Yamamura's method. Although the code was well benchmarked for the HSST-03 LIM, the impedance model needed additional work to permit analysis of a broad range of LIM parameters. This work demonstrated the importance of using the measured LIM parameters to establish the model and the sensitivity of the improvement options under consideration.

5) The LIM code developed by CHSST based on Prof. Nonaka's spatial harmonic method was reviewed in detail, modified to improve the data input and calculation output, and configured

---

[31] Private communication, J. Kato, Chubu HSST Development Corp., M. Murai, Toyo Denki Seizo, K.K. and Prof. E. Masada, Science Univ. of Tokyo, 2003.

for the generation of performance curves as a function of slip frequency. This modified code was utilized for the assessment of the LIM improvement options. During this work the validity of the assumptions used in the code was reviewed and modified as necessary.

6) The following changes to the HSST-200 LIM have been analyzed and are proposed:

    a) LIM length increased to 2.91 m keeping the same slot width and pitch, but increasing the number of poles from 8 to 10.

    b) To keep a high thrust breakpoint speed, the number of turns per preformed primary winding coil decreased from 5 to 4 while increasing the wire thickness 20% to make use of the available space in the slot.

    c) Wire height increased 10% from 14 to 15.4 mm to achieve the same Ohmic power dissipation per unit volume as obtained in the HSST-200 design.

    d) With changes to LIM geometry, but keeping the same core width, the LIM weight is estimated at 379 kg.

    e) The 10 LIMs per vehicle are separated into two groups of 1 series–5 parallel, in a 3-phase wye (star) configuration, where each group of five is energized by its own inverter. This wye configuration simplifies cabling between LIMs and balances the number of LIMs per inverter.

    f) LIM maximum current increased from 280 A to 386 A to generate 7000 N low-speed thrust.

    g) The difference in voltage between the trolley rails is increased from 1.5 kV to 3 kV DC. One set of 1 series – 5 parallel LIMs is energized by an inverter fed from +1.5 kV and ground trolley rails, and the second set of 1 series – 5 parallel LIMs is energized by an inverter fed from the ground and -1.5 kV trolley rails. This configuration makes use of the more prevalent 1.5 kV inverters used in conventional rail systems.

    h) Increasing the maximum inverter line-to-line voltage has the most direct effect on increasing the speed of the thrust breakpoint and also the thrust at 160 kph to the required 4000 N. For the 1 series-5 parallel LIMs, with a 1.5 kV input voltage, configuring in a wye configuration develops greater maximum voltage per LIM, achieving the required thrust at maximum speed.

    i) Clearance gap decreased from 15 mm to 13 mm to increase thrust, based on recommendation by CHSST and Toyo Denki staff. The 10% increase in attraction force is acceptable within the levitation system.

    j) Changing the reaction rail from aluminum to copper and varying its thickness and/or the slip frequency has a significant impact on the low-speed thrust and attractive force, but does not yield much improvement in thrust at 160 kph compared to the 4 mm aluminum. Given that LIM efficiency changes only by 2 to 3 percent at both the breakpoint speed and at 160 kph compared to the 4 mm thick aluminum, changing to a copper rail does not appear warranted due to the cost.

    k) A value of 100 for relative permeability for the secondary back iron has been used for the final performance calculations. The estimate is conservatively based on common carbon steel data for the anticipated 6700 A/m field intensity. Analysis should be re-assessed when permeability data for the JIS SMA 400AW low-carbon, atmospheric corrosion-resistant steel used in the secondary rail by CHSST (or U.S. equivalent) becomes available.

    l) Calculations with copper primary winding show the Ohmic power/volume and total Ohmic power per phase reduced 40%, but the LIM mass increased 38%. Decreasing the wire cross-section to obtain the same 1.06 W/cm^3 as achieved with the aluminum wire still yields a heavier winding, thus copper is not considered an option for the primary winding.

m) If the slip frequency were kept at 11.5 Hz for speeds from 0 to 120 kph, then increased up to 15 Hz as the speed was increased between 120 and 160 kph, higher thrust could be achieved above the breakpoint speed. The frequency would still be increased with speed after the breakpoint, but the change would be consistent with a constant slip not slip frequency.

n) These modifications have been reviewed by CHSST and Toyo Denki Inc., and their implementation appears feasible. A rough schedule discussed with Chubu HSST and Toyo Denki shows that the first prototype COL-200 LIM for testing could be fabricated in about 2.5 years.

7) The COL-200 LIM generates 6200 to 7000 N of braking force (normal duty) from 160 kph to rest that permits 0.08 g deceleration on a 7% descending slope with a 90 kph tailwind. A vehicle initially at 160 kph on this slope would stop in 1100 m. At maximum emergency braking rate, the vehicle would slow with 0.12 gee's and stop in 840 m.

8) The on-board power conditioning equipment for propulsion consisting of VVVF inverters and protection circuits should be sized for 10% greater current and voltage to accommodate the possibility of higher grade, load, or emergency braking. Alternative sizing may be necessary if the vehicle is intended to operate on higher grades than specified in the requirements.

9) Based on scaling from existing systems, this inverter and protection circuits are estimated to weigh 2.8 tonne and occupy 5.5 m^3 per car. Reduction of weight of the inverter is expected due to continued development of higher voltage and higher current and additional reductions of 20% could be expected in the next 5 years as the individual switches become capable of higher current capacity and are individually packaged in geometries that minimize the additional mass/space of cooling and snubber circuits. Collaboration with power-conditioning equipment manufacturers will be necessary to insure low-weight and small-volume objectives are met consistent with the required performance.

10) Collection of the high current (1130 A/vehicle) from the trolley line must be demonstrated at the maximum speed of 160 kph. Testing of collector designs with larger trolley rails will determine the collector stability and wear characteristics.

6.8.1. *References*

[4] ProCite reference manager, version 5, ISI ResearchSoft, Berkeley, Calif. www.procite.com

[5] Ion Boldea and Syed Nasar, The Induction Machine Handbook, CRC Press, Boca Raton, Florida, 2002.

[6] Ion Boldea and Syed Nasar, Electric Drives, CRC Press, Boca Raton, Florida, 1999.

[7] Ion Boldea and Syed Nasar, Linear Motion Electromagnetic Devices, Francis and Taylor, New York, 2001.

[8] Ion Boldea and Syed Nasar, Linear Motion Electromagnetic Systems, John Wiley and Sons, New York, 1985.

[9] Jacek Gieras, Linear Induction Drives, Clarendon Press, Oxford, 1994.

[10] Jacek Gieras and Z.J. Piech, eds., Linear Synchronous Motors: Transportation and Automation Systems, CRC Press, Boca Raton, Florida, 1999.

[11] E. R. Laithwaite, Induction Machines for Special Purposes, George Newnes Limited, London, 1966.

[12] E. R. Laithwaite, Propulsion Without Wheels, Hart Publishing Co., New York, 1968.

[13] E. R. Laithwaite, A History of Linear Electric Motors, Macmillan., London, 1987.

[14] FTA Urban Maglev Program, CDOT Team report "Task 3, Transit System Performance Requirements," Final Report 1.1, 17oct02.

[15] FTA Urban Maglev Program, CDOT Team report "Task 10, Vehicle Design, Technical Memo 4.1,Vehicle Interior Configuration" 6Jun03.

[16] FTA Urban Maglev Program, CDOT Team Quarterly Review Meeting, Washington, D.C., 9Jul03.

[17] David Munoz, "I-70 GPS Survey," Technical memorandum, October 14, 2002.

[18] FTA Urban Maglev Program, CDOT Team report "Task 14, Integration, Technical Memo 4.0," 22Apr03.

[19] FTA Urban Maglev Program, FTA Assessment Team report "Assessment of CHSST Maglev for U.S. Urban Transportation," July 2002, pp. 6-11.

[20] Private communication, Prof. E. Masada, Science Univ. of Tokyo, 2003.

[21] Sakae Yamamura, Theory of Linear Induction Motors, Second edition, Univ. of Tokyo Press, Tokyo, Japan, 1978.

[22] Keisuke Fujisaki, "A Study on Electromagnetic Suspension Controlled Magnetically Levitated Train," doctoral dissertation, Univ. of Tokyo, December 21, 1985.

[23] S. Nonaka and K. Yoshida, "Analysis of Linear Induction Motors Using a Space Harmonics Technique," Chapter 8 in Transport Without Wheels, E. R. Laithwaite ed., Paul Elek Scientific Books, London, 1977. pp. 187-216.

[24] Y.Higasa, "Comparison of the Method of Calculating LIM Characteristics Based On Spatial Harmonic Theory Against Experimental Data," Chubu HSST Technical Report, 12Nov91.

[25] Y.Takahashi, "Test Apparatus of Linear Induction Motor for Train," Dengakuronn D, vol. 110, 1990-2.

[26] Private communication, Prof. Takafumi Koseki, University of Tokyo, and Prof. Eisuke Masada, Science University of Tokyo, Tokyo, Japan, 5jun03.

[27] Data from Chubu HSST Corporation, Nagoya, Japan.

[28] Trainspotting Bukkes, www.bueker.net/trainspotting/voltage_comparison, 2003.

[29] Review of Propulsion Trade Study LIM modifications and calculations, CHSST and Toyo Denki, 21oct2003.

[30] "Report of Economic Feasibility Study of Levitation Linear Motor Car for Urban Transportation," Japan Transportation Economics Research Center, Aichi Prefecture, March, 1993.

[31] Private communication, J. Kato, Chubu HSST Development Corp., M. Murai, Toyo Denki Seizo, K.K. and Prof. E. Masada, Science Univ. of Tokyo, 2003.

7.0 COMPARISON OF LINEAR SYNCHRONOUS AND INDUCTION MOTORS

7.1. INTRODUCTION

The Propulsion Trade Study was conducted to identify and evaluate prospective linear motor designs that could potentially meet the system performance requirements of the CMP, and be applicable to other urban maglev transit corridors. The analysis focused primarily on the performance of the linear induction motor (LIM) propulsion system of the Chubu HSST (CHSST) that had been selected as the project baseline technology. Potential near-term improvements to that propulsion system have been considered and reported.[32] These modifications have been reviewed by CHSST and Toyo Denki Inc., and their implementation appears feasible. This chapter compares the relative advantages and disadvantages of the linear induction and linear synchronous motor options for urban and suburban maglev transit systems.

For maglev applications, two specific configurations of these linear motors that have been practically tested and applied are considered: the short-stator linear induction motor and the long-stator linear synchronous motor. Conversely, the long-stator linear induction motor utilizes an armature winding in the guideway creating the traveling wave, and a short, reaction rail on the vehicle. This technique has been utilized for drives in factory transportation systems; however, its performance as a public transportation system is inferior to the linear synchronous motor with similar structure. Likewise, the short-stator linear synchronous drive, with an armature winding on the vehicle creating the traveling wave and discrete field windings distributed along the guideway, has a complicated guideway structure that is too difficult to negotiate with the route profile of a transportation system and is economically impractical. The inductor-type linear synchronous motor has also been considered by many researchers, but the increase of vehicle weight and complexity of the rail structure makes this system impractical for commercial systems. The following discussion focuses on the comparison between the short-stator, linear induction motor drive and the long-stator linear synchronous motor drive. In particular, the most mature drives presently being installed and implemented for transportation, the LIM-driven, Chubu HSST and the LSM-driven Transrapid maglev systems, are discussed. Both of these systems use iron-core propulsion motors with relatively small (10-15 mm) propulsion air gaps, and electromagnetic-type (EMS) levitation.

7.2. SHORT-STATOR LINEAR INDUCTION MOTOR DRIVE

7.2.1. *Basic Configuration*

The LIM was developed and is utilized for the Chubu HSST (Maglev) and Linear Metro (Subway supported by the conventional wheels-rail system) for urban transport in Japan. [33,34,35,36] It is also used by Bombardier Transportation in the driverless Advanced Rapid Transit (ART) system to access New York's JFK International Airport. Similar systems are operating in Kuala Lumpur, Malaysia, and on the SkyTrain Millennium Line, in Vancouver, Canada. There also is, or has

---

[32] FTA Urban Maglev Program, CDOT Team report "Task 14, Integration, Propulsion Trade Study, Technical Memo #4," 29oct03.

[33] M. Fujino et al., "High Speed Surface Transport System: Nagoya East Hillside Line and the Operational Testing for 3-Car Vehicle Prototype," Proceedings of the Maglev 2002 Conference, Lausanne, Switzerland, Sept. 2002. Paper PP01102.

[34] M. Fujino, "Total running test operation of the HSST-100 and the project of East Hillside Line in Nagoya," Proceedings of the Maglev 2000 Conference, Rio de Janeiro, Brazil, June 2000, pp. 35.

[35] M. Tanaka, et al., "The results of running tests of HSST-100L vehicle," Proceedings of the Maglev 1998 Conference, Yamanashi, Japan, April 1998, pp. 63.

[36] H. Ohsaki, "Linear Drive Systems for Urban Transportation in Japan," Proceedings of the Maglev 1998 Conference, Yamanashi, Japan, April 1998, pp. 29.

been, limited scale applications with the Birmingham Maglev (United Kingdom), Otis People Mover, H-Bahn Dortmund (Germany), and the Mitsubishi Heavy Industries People Mover (Hiroshima, Japan).

The basic system construction of the short-stator linear induction motor (LIM) drive is shown in Figure 85 to Figure 88. Figure 85 shows the Chubu HSST maglev vehicles that are being installed on the Tobu Kyuryo Line in Nagoya, Japan as part of a 9 km urban transit line. Four propulsion-levitation modules are located on each side of each vehicle that wrap around the guideway levitation-reaction rail. Each vehicle module contains a LIM motor above the aluminum reaction rail and four levitation magnets that pull the vehicle up to the steel section of the guideway rail. Figure 87 shows a side-view cross-section of the LIM with the 3-phase primary winding embedded in the LIM core on the vehicle and the guideway's aluminum sheet and steel that form the secondary circuit of the motor.

Figure 85: HSST Linimo maglev vehicles for the Tobu Kyuryo Line in Nagoya, Japan
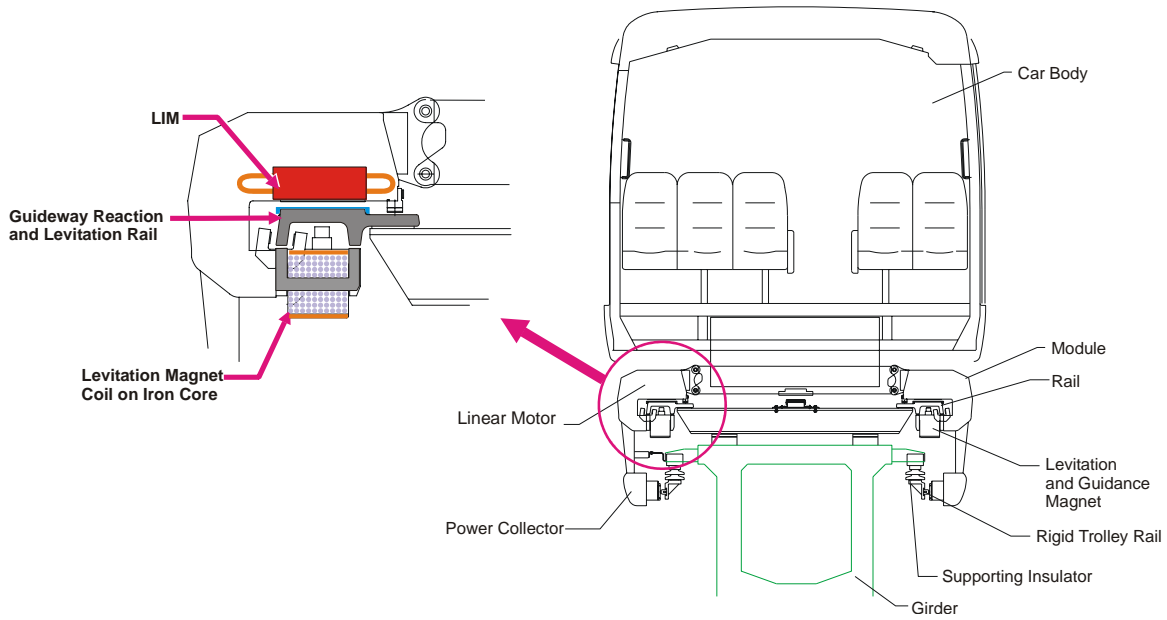
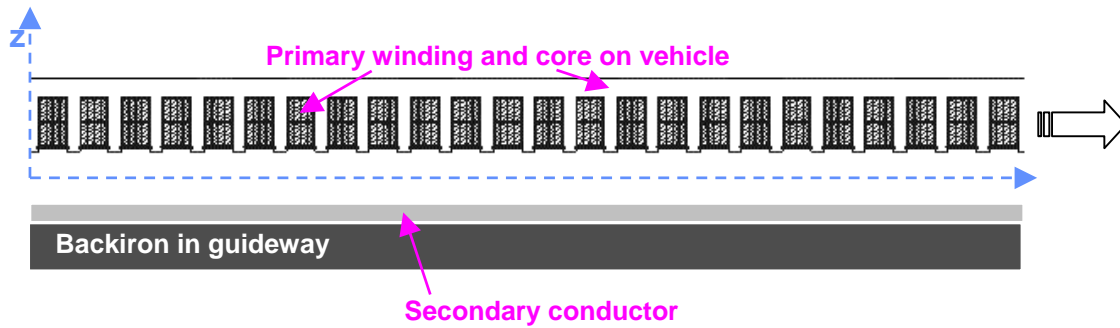**Figure 86: Close-up of propulsion/levitation module for LIM.**

Figure 87: Side-view, cross-section of single-sided LIM components.
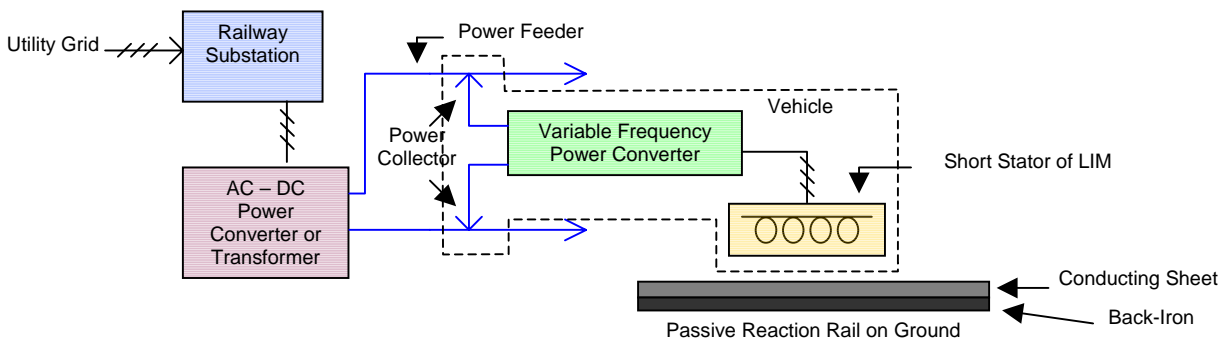

Figure 88: Block diagram of the power circuit for the LIM.

The power feeder shown in Figure 88 is a solid rail carrying DC power (or AC single-phase) such as is currently used in conventional railways. The power collectors are the vehicle's sliding or wheel contacts to the power feeder. Sliding collectors have been operated up to 130 kph at the CHSST Nagoya test track, though testing facilities for higher speed operation exists at the Railway Technical Research Institute (RTRI) Test Track in Kokubunji, Tokyo. Wheeled collectors have been tested up to 200 kph at the RTRI for the DC linear motor car project.

The on-board power converter conditions input DC or AC power from the power feeder to the appropriate variable-voltage, variable-frequency, multi-phase power needed for LIM operation. The converter also contains input and output filters. This equipment is widely used in conventional high-speed urban railways. The linear induction motor as shown is a single-sided structure that generates a non-uniform normal force, side force, and rotational moments on the LIM. Its operation is less efficient compared to conventional rotary induction motors because of the large air gap between the on-board stator and guideway rail resulting in a high leakage flux. This motor has been used in public transportation by the HSST and Linear Metro Subway in Japan. A double-sided LIM with stator windings and cores on both sides of the guideway reaction rail was developed and tested, but the geometry is very difficult to implement with a small clearance gap.

Finally, the passive reaction rail in the guideway consists of an aluminum or copper plate backed by iron. It is structurally very simple and can be integrated with the levitation rail, as is the case with the HSST. The rail's performance and durability has been tested thoroughly for the development of the HSST maglev system and the steel-wheel Linear Metro subway in cooperation with the Japanese Ministry of Transportation.

7.2.2. *Advantages*

A significant advantage of the LIM drive is that the on-board power conditioning system and construction is very similar to that used in conventional urban and high speed electric railway vehicles. This is important from several perspectives. Many of the power conditioning equipment system sections and components are common, and there exists a significant database of practical experience and design with manufacturers and line operators. The basic technology has been well established, and the technical step to move from rotary induction motor drives for steel-wheel vehicles to LIM propulsion is not large. The incentive for this transition to LIM propulsion is the all-weather capability to negotiate tight curves and steep grades, and meet precise stopping requirements with high deceleration that is not possible with power-driven steel-wheels. From the perspective of the public consumer, the transition provides improvement in service and ride quality, and meets their expectations of safety and reliability for transit systems.

The LIM utilizes a very simple reaction rail track, hot-rail power pickup on the vehicle, and passive guideway rails which simplifies the track switches. The reaction rail can be installed discretely along the track, if needed. Vehicles with different design and performance parameters are easily adaptable without changes to the guideway within the guideway load (electrical and mechanical) limits. The guideway can provide small radius horizontal and vertical curves, and a bending switch similar to monorail is applicable. The simple, passive guideway system has been shown to be as safe and reliable as a conventional rail track.

A LIM-driven transit system has a great degree of flexibility to respond to variable or uncertain demand. This includes adjusting the number and size of vehicles on a short-term or long-term basis. In the short term, the ability to add and move vehicles provides rapid response capability for the operator to volatile demand and the recovery from any off-normal shutdown or schedule deviation. In the long-term, if additional power is needed to accommodate an upgrade in the system capacity, the impact to the guideway is almost negligible with the addition of way-side power electrification and conditioning equipment. To meet operational requirements, the block control can be easily adjusted with little, if any, modification to the civil structures.

7.2.3. *Disadvantages*

In general, the energy efficiency of the LIM is lower than the rotary induction motor and the LSM. With the rotary induction motor, the airgap between the stator winding and the rotor is much smaller (a few millimeters) since the gap does not vary, which results in greater efficiency. Air gaps of 10-15 mm are used for LIM drives due to clearance requirements with a varying gap from the vehicle suspension. The on-board LIM primary winding provides all the power that generates the gap field and the induced currents in the reaction rail. As such, with the larger air gap the efficiency is lower than the LSM which uses electro or permanent magnets for the field winding. The weight and size of the on-board power conditioning equipment must also be larger as must the size of the wayside power systems. This increase in weight is what limits the operational speed capability of the LIM-driven system to 200 – 250 kph since the weight penalty makes higher speed operation impractical. However, this is not to say that the efficiency of the LIM is impractical. For the Colorado I-70 route the anticipated average and maximum speeds are 144 and 160 kph, respectively. For this route, higher speeds did not provide significant advantages, but the maximum speed of ~225 kph could be obtained with the COL-200 LIM-driven vehicle. The electrical-to-mechanical efficiency of the LIM at the power pickup hot-rail is 70% at the average speed and 77% at maximum speed.

With the LIM there are also 3-dimensional forces that may influence ride quality. This is due to the coupling between the thrust and the attraction/repulsion force between the primary stator and the reaction rail (commonly referred to as the normal force), and the coupling between these forces and the guiding/decentering lateral force which is transverse to both these forces. Because of eddy currents in the secondary, these forces are not uniform along the LIM in the direction of vehicle motion. These forces do not preclude the utilization of the LIM for propulsion; however, they must be accounted in the design of the guidance and levitation systems. Issues such as harmonics in the normal force and the magnitude of normal and lateral forces at high thrust must be considered as well as the changes in these forces with primary-secondary clearance gap. If the air gap length between the primary and the reaction rail is reduced, the normal force between them becomes larger which can disturb the performance of the levitation system. This being said, it must be noted that LIM-driven systems have been successfully operated at 100 kph and designed for operation at 200 kph mitigating these issues. This coupling of forces also exists for the linear synchronous motor, but forces are uniform along the track due to the laminated structure of the active rail. In designs such as the Transrapid Maglev system, the levitation and thrust forces are applied within the same physical structure and air gap which reduces the mechanical moments applied to the propulsion-levitation bogie module on the vehicle, lessening the requirements of the levitation control system to accommodate the force perturbations.

7.3. LONG-STATOR LINEAR SYNCHRONOUS MOTOR DRIVE

7.3.1. *Basic Configuration*

LSM drives with electromagnets were developed and are utilized for the German Transrapid maglev system for high-speed transportation.[37] This system has been tested in Emsland, Germany since 1984, and is now applied to the 30 km Shanghai Pudong Airport connection to city-center. A very low-speed system for urban applications, the German M-Bahn, was utilized in Berlin for a few years beginning in 1988 as a demonstration track.[38]

The basic system construction of the long-stator linear synchronous motor (LSM) drive is shown in Figure 89 through Figure 91. Figure 89 shows the Transrapid TR08 maglev vehicle that is the type of vehicle being installed in the Shanghai airport-city connector line. As with the LIM-driven

---

[37] Transrapid International, <u>Transrapid Maglev System</u>, Klaus Heinrich and Rolf Kretzchmar, eds., Hestra-Verlag, Darmstadt, 1989.
[38] Innovative Magnetic Transit System M-Bahn, AEG brochure 1989. See Figure 4, page 52.

system, propulsion-levitation modules that wrap around the guideway are located on each side of each vehicle. Each module contains the exciting field magnets of the LSM that also serve as the levitation magnets that pull the vehicle up to the LSM stator magnets packs attached to the guideway. Figure 87 shows a side-view cross-section of the LSM with the 3-phase primary winding embedded in the stator core on the guideway and the vehicle's levitation magnets.

The long stators of the LSM located on the guideway form the active track. The reactive forces of propulsion and vehicle levitation act on the stator cores. The supporting structure is required to have enough strength to handle repeated loading of this force, and the stator coils need to be isolated from ground. Dimensions of the stators are determined by the highest performance requirement of the systems.

In order to reduce operational losses and for stability of the power supply system, the long stator of the LSM is separated into a number of sections controlled by the section switches. The minimum length between two section switches depends on the required acceleration and length of a train. The operating frequency of the section switches becomes high if a large number of trains are operated on the track each day. [37]
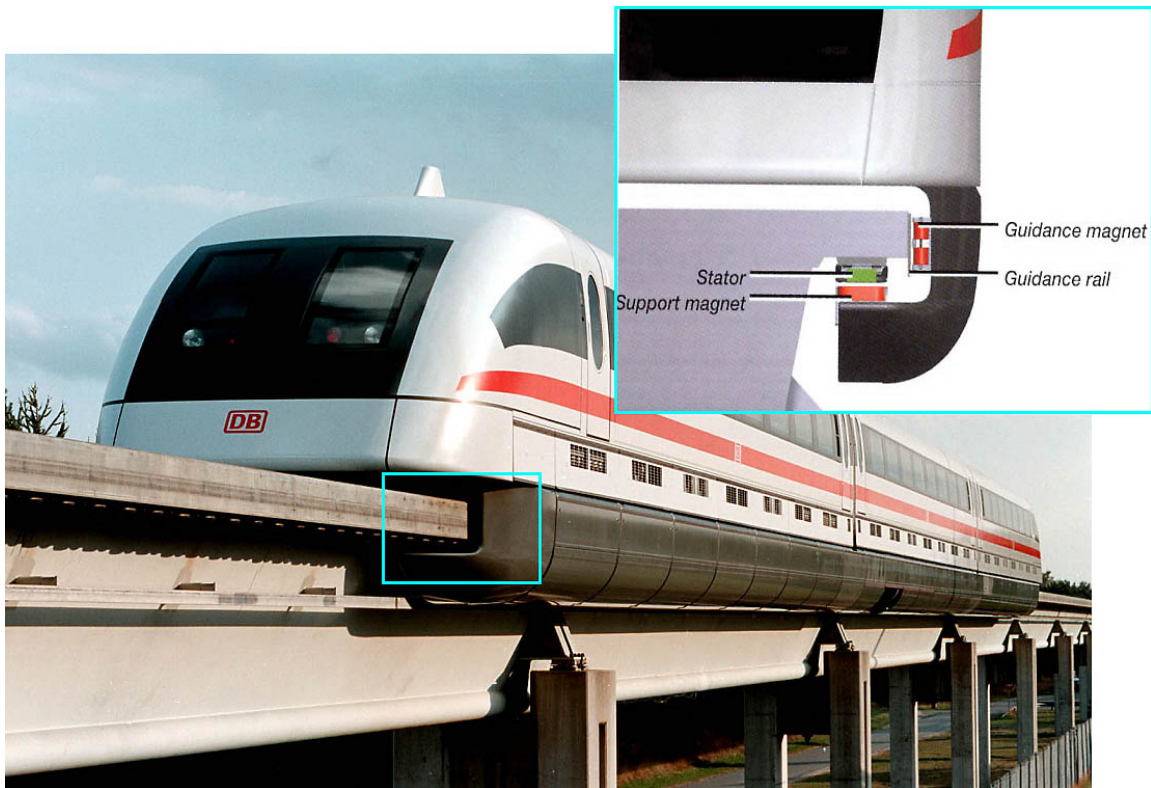

Figure 89: Transrapid TR08 vehicle and close-up of propulsion/levitation module containing on-board exciting magnets for LSM
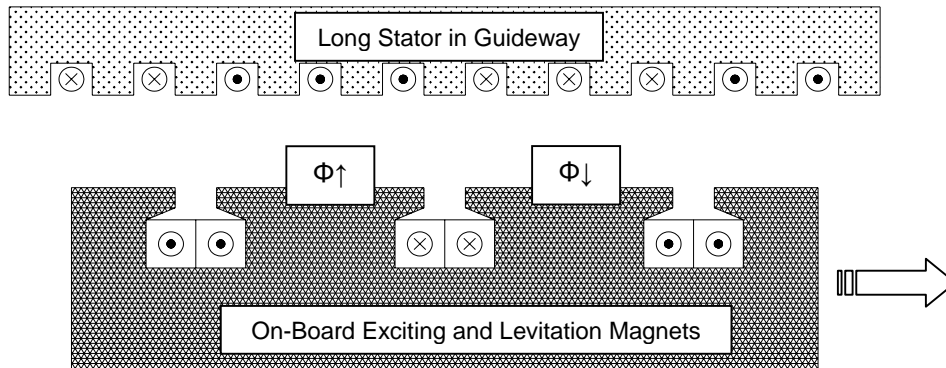
Figure 90: Cross-section of segment of LSM.

Flux, Φ, from the exciting magnet interacts with the traveling magnetic wave from the stator to generate vehicle thrust.

The currents in the stator coils must be synchronized with the train's position and velocity. Proper control of the train can only be accomplished by sending information to the converter stations through the use of sensing equipment and signal transmission systems. Because synchronization is essential to the LSM, the sensing and signal transmission system must have high precision and reliability.

The railway substation shown in Figure 91 is connected to the power grid, so its location may be constrained. In some cases it is advantageous for the system operator to own the transmission line from the grid. The power converter station feeds variable-voltage power to the long stator sections through the transmission lines, and controls both the power's frequency and phase as required by the train's position and velocity. This means that the number of converter stations must equal the maximum number of trains possible on the whole track. An increased number of converter stations will be required near train terminals and intermediate stations. Operational voltage of the converter is limited by the maximum voltage level capability of transmission cables, section switches, and stator windings to prevent arcing and electrical breakdown.
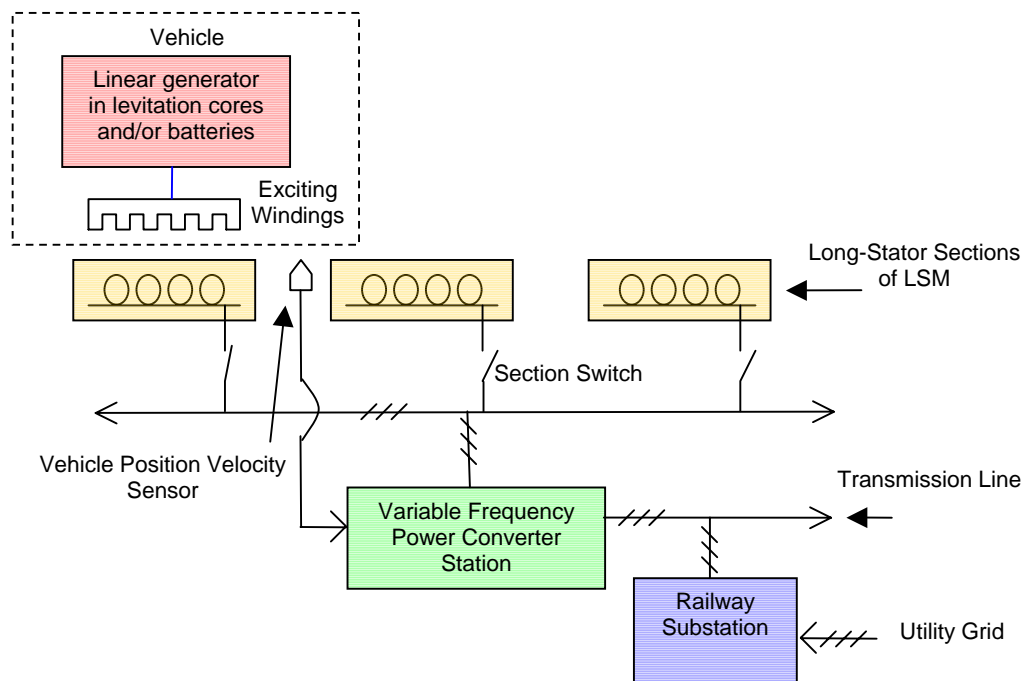
Figure 91: Block diagram of the power circuit for the LSM

7.3.2. *Advantages*

Vehicle drive power is supplied by the long-stator winding attached to the guideway. Because the stator winding and power conditioning equipment is located wayside, the vehicle should be generally lighter. This permits the operation at high-speed (up to 500 kph has been demonstrated) because the vehicle does not bear the weight of the high-power primary propulsion components needed to obtain these speeds, nor does the electric power need to be transferred to the vehicle. The power-rating capability of the motor can be tailored to the requirements of the specific section of route such as regions of high grade or at the station for high acceleration.

The Transrapid and other proposed LSM systems also use the on-board levitation electromagnets (or permanent magnets) as part of the field source for the LSM propulsion. This results in a highly integrated bogie design that reduces vehicle weight and helps reduce the requirements of the levitation control system to mitigate the effects of transverse forces on ride quality. Other systems such as power generation and operation control can be integrated with the drive system.

The placement of main power components on the wayside and reduction in vehicle weight results in high acceleration and deceleration capability. However, the utility of the high acceleration is limited by ride comfort, seat-belt operating conditions, and safety requirements. Within these limits for the FTA urban maglev program, both LIM and LSM have the capability to meet the high-acceleration requirements, and neither has a particular advantage in terms of the superiority of these three factors.

The electrical-to-mechanical conversion efficiency of LSM is high at the terminals of the guideway motor, but the impedance of the active block length of the motor reduces that value. A detailed analysis conducted for the U.S. Department of Transportation National Maglev Initiative modeled

the Transrapid TR07 LSM with a lumped-parameter synchronous motor circuit model.[39] This model was benchmarked with data from the Transrapid TR06-II motor, and the author of that study indicates that the agreement with data was excellent. For the TR07 with an on-board active length of 45 meter with a relatively-short LSM block section length of 300 meters, the efficiency at the terminals of the LSM immediately below the vehicle is 98% at a vehicle speed of 200 kph in maximum-thrust operating mode. The efficiency at the terminals of the LSM block section is 85%, and at the output of the variable-voltage, variable-frequency converter, the efficiency drops to 62% at the same speed and operating condition. The maximum efficiency at the converter output for this LSM, which was designed for higher speed, is 87% at a speed of 480 kph. However, it should be noted that if the block section length of the active LSM is longer, the efficiency is reduced.

7.3.3. *Disadvantages*

One disadvantage of the LSM drive is that it requires data for the exact position of the on-board magnets to ensure that the vehicle is synchronous with the traveling wave generated by the stator winding in the guideway. A very reliable and precise vehicle position and velocity sensing system is essential. This information must be transmitted to the converter station to generate the traveling magnetic field at the appropriate magnitude and frequency.

Compared to the simple reaction rail of the LIM, the active track structure of the LSM is very complicated. It requires continuous installation of stator coils in the guideway and wayside converters to energize each block section of track. This results in many components that must be maintained to assure the safety of the system. The maintenance of proper position of the guideway stator coils is particularly critical so that the proper clearance gap is maintained to the on-board levitation/excitation magnets. Reduction of the normal 1 cm gap can result in significant increase in the vehicle lift force causing the vehicle to "lock-on" to the guideway or impact between the vehicle magnets and the guideway stator. Frequent inspection and maintenance of the guideway coils and stator core is necessary to ensure proper alignment.

There are several operational requirements for the vehicles relative to the guideway. Each block section of the guideway can drive only one vehicle at a time, and that section requires its own converter. The operational density of trains on the route determines the number of converter stations, which implies many converters are necessary for short headway systems. This has particular impact near terminals where the power feeding system becomes complicated and many converters are needed since vehicles are moving slowly, more closely spaced, and switching direction or routes. The vehicle has an LSM motor on both the port and starboard sides, and each of these is powered by independent power supplies at the transitions between stator sections. These supplies must have high reliability for balanced thrust from both sides of the vehicle. The field magnet of LSM is also commonly used for vertical suspension, which means it is operated continuously. This requires a very reliable on-board power supply including batteries. In the event of a malfunction of trackside stators, the riding comfort is significantly deteriorated.

The performance of the transportation system is determined by the configuration of the active guideway, and the system is not adaptable to the change of passenger demand. Vehicles cannot be added easily to accommodate changes outside the original design (although they are easily removed). The LSM must be configured, and the initial investment made to accommodate the highest demand anticipated over the life of the design. For efficient use of capital investment, a very accurate estimate of demand is necessary.

---

[39] "Technical Assessment of Maglev System Concepts, Final Report by the Government Maglev System Assessment Team," James H. Lever, ed., U.S. Army Corps of Engineers Cold Regions Research and Engineering Laboratory report no. 98-12, October 1998, pp 62.

7.3.4. *Alternative LSM Design*

To permit more flexibility of operation and allow short headways for high-capacity operation, a design has been proposed with very short stator sections. With appropriate design, the operation control system (signaling system) can be integrated with the power feeding system. The stator sections of the Locally Commutated Linear Synchronous Motor (LCLSM) are essentially individual coils, each energized by its own wayside inverter.[40] While this reduction in stator length improves the electrical efficiency at the converter to 95% and increases the power factor, it requires an inverter for each coil (or pair) in the guideway. In a previous proposal of this technology in the U.S. National Maglev Initiative, this required 2400 inverters per kilometer of double guideway. The technical assessment of that proposal by the U.S. Government Maglev Assessment Team (USGMAT) concluded that while the LCLSM offered high efficiency and possibility for very short vehicle headways and operational flexibility, the guideway stator investment cost was "critically dependent upon the high-volume cost reduction (factor of 10)" for the IGBT switch based inverters.

Another important issue with the concept is the potential reliability of the system with such a large number of inverters. The USGMAT report makes reference to the fact that with individually-controlled coils, the system could operate in a degraded mode even if a few coils or inverters fail. However, this capability will be highly dependent upon the nature of the failure. The resulting ride quality and operational safety may be significantly affected, and the ability to operate in degraded mode in not at all obvious, particularly in light of the team's assessment that the synthesis of the stator's traveling wave from individually-energized coils was a demanding technical requirement and unproven at that time. Sub-scale testing of this concept has been done that shows thrust can be delivered even with some faulted coils, but it is not clear that a full-scale system with such faults would be necessarily operational, or that any level of operation other than vehicle recovery is desirable.

A concept of this type of linear motor for the maglev railway was proposed by Dr. Matsui of RTRI Japan in late 1960's.[41] It was named as "Linear DC Motor", because its principle of operation was quite similar with the brushless DC motor. The idea and its characteristics have been reported by Dr. Matsui and his colleague, Mr. Umemori. [42] The primary coils and the H-bridge switches are located along the track. The on-board electromagnet acts as the field magnet of the motor. The on-board magnets also give the lift force to the vehicle, though high current must be fed to the vehicle to have enough levitation performance.

A feasibility study of this type of maglev system was also carried out by a technical committee of the Railway Electrification Association of Japan with the support of former Japan National Railways, and the author (Masada) was a member of that committee. The committee's assessment of the system identified two problems: 1) large and heavy on-board magnets are needed for levitation, and 2) H-bridges with power electronic devices for commutation between ground windings are too expensive and complicated for reliable operation. RTRI has changed the concept of system to solve the first problem with rubber-tire wheels and studied its feasibility for suburban transport in Yokohama as Automated Linear-motor Pneumatic-tire System (ALPS). [43] A report written by Mr. Miki of RTRI shows that the construction costs for the system are about 20% less than a conventional system because of smaller curvature and higher gradient

---

[40] Ibid., pp 11, 80.

[41] K. Matsui et Al., "D.C. Linear Motor Controlled by Thyristors and the Testing Equipment for its High Speed Characteristics", p.149-154, Linear Electric Machines, IEE Conference Publication No.120, London, 21-23 October 1974.

[42] T. Umemori, et al., "Development of DC Linear Motor – Fundamental construction and feasibility," Paper F78 757-7, and "Development of DC Linear Motor (II) – Research for a ground coil and a field magnet," Paper F78 756-9, both presented at the IEEE Power Engineering Society Summer Meeting, Los Angeles, California, July 16-21, 1978.

[43] A. Miki, "ALPS and its future prospect", Proc. Railway Technology Research Institute Seminar, p.86-96, Tokyo, Nov. 1987.

track allowed to the linear motor drive. However, uncertainty of the reliable operation of rubber tires in high speed and of the basis of investment costs, the project was dropped, and RTRI has stopped further study.

Dr. Matsui has shifted his interests from the original concept to the Belt type Transit System by Magnet (BTM) people mover to solve the second problem. A rotating magnetic belt equipped along the track adheres on board magnets and propels the vehicle in the original system, analogous to an LSM. It was utilized as a transport system of an International fair 1990 in Osaka. Because it was noisy and expensive, the design was modified to equip the moving belt with permanent magnets arrays on board. The belt adheres to the ferromagnetic rail of the track and propels the vehicle. A small scale practical application has been installed and operated since 2003 as a incline-type people mover, which has a mean gradient of 30° at Katsura-dai near Otsuki about 90 km west of the city center of Tokyo, Japan. [44]. While this example is neither a conventional LSM nor LIM, the simplicity and low-cost of the on-board driven propulsion for this low speed system is evident.

Based on the design reviews and experience with this type of system, it is concluded that the locally commutated linear synchronous motor has theoretically interesting characteristics for a maglev or a railway transport, but its realization as a practical system is difficult due to costs and reliability of a large number of switches.

7.4. COMPARISON BETWEEN MOTOR DRIVES

7.4.1. *Flexibility to Variable and Uncertain Demand*

As discussed above, a LIM-driven transit system has a great degree of flexibility to respond to variable or uncertain demand by adjusting the number and size of vehicles on a short-term or long-term basis. The ability to add and move vehicles provides the operator rapid response capability to volatile demand and the recovery from any off-normal shutdown or schedule deviation. If additional power is needed to accommodate an upgrade in the system capacity, the impact to the guideway is almost negligible requiring only the addition of way-side power electrification and conditioning equipment. To meet operational requirements, the train control can also be easily adjusted with little, if any, modification to the civil structures.

The LSM lacks flexibility to change system performance. Replacement of ground facilities is necessary to change system capacity or its operational mode, which is quite similar to building a new system. Its active track and power supply installation must be designed and installed for the highest demand and capacity of the system contemplated during the design phase. This may significantly shorten the useful life of the system or greatly increase the life-cycle costs if actual demand does not follow planned usage.

Line operators may experience off-normal schedule delays, interruptions, or shutdowns due to causes beyond their control or equipment failure. Rapid recovery of scheduled operation is critical to maintaining ridership. The ability of the LIM drive to move and stage vehicles on the guideway with moving block control provides a great amount of flexibility to rapidly restore service. This includes tailoring vehicle configurations for short-term, high-capacity operation to immediately accommodate the high-demand resulting from any unscheduled stoppage or deviation from normal scheduled service. The LSM requires a single vehicle per section of track, and cannot accommodate a surge in service throughput, unless the system was highly underutilized previously. The required movement of a single vehicle on a fixed guideway section greatly limits the flexibility to stage vehicles to respond to off-normal demand profiles or incidents.

---

[44] "Belt type Transit System by Magnet", Leaflet of Nihon Densetsu Kogyo, 2000.

In the event of a malfunction of the propulsion motor, the speed of recovery of service is very important. In the case of LIM propulsion, the vehicle is simply moved and replaced. This can be done with the aid of another transit vehicle or special service vehicle. If the vehicle is LSM powered, it is much more likely that the track may need time-intensive repair or replacement of stator winding sections. During that repair and re-qualification testing, the entire track is out of service. Service vehicles for such incidents may need to be independently powered, and may be unable to utilize the guideway structure effectively.

7.4.2. *Reliability of Operation*

Operational reliability of the LSM strongly depends on the detection and signal transmission system for vehicle position and velocity to ensure that the magnetic wave generated in the stator winding is synchronous with the movement of the excitation magnets on the vehicle. Doubly-redundant systems are required. Reliability of the LIM in a high-vehicle-density operation of a transportation system is based on existing conventional-rail technologies, and has been well established, for example in the Linear Metro system in Tokyo, Japan.

Although many future transit systems are contemplating driverless operation, for systems where drivers are determined to be necessary, the human factors have been well established for the LIM drives. The operators of conventional railways can easily adapt to the new LIM system using much of their previous experience.

The reliability of the electrical and mechanical components of the linear drive must be evaluated, and it is very important to obtain duration-test data from the designed track to fully qualify the reliability of the drive. This information is compared to corresponding data from previous installations or test tracks to determine the effects of design, fabrication, or installation process modifications. The larger the database of previous applications and lifetime testing of a technology, the higher the confidence will be in a planned system's reliability. The application of LIM drives in steel-wheel transit systems and the historic usage of similar power conditioning equipment in conventional, rotary drive rails systems provides a significant experience base for confident projection of LIM designs to future maglev applications. Although LSM has been significantly evaluated at test tracks, the reliability of active tracks and section switches must be established with duration tests under revenue service conditions. Collection of this data is still in progress, and will not be completed for a few years.

7.4.3. *Capital Cost*

The capital cost for a maglev system is dominated by the cost of the civil structures, including the guideway; the size of the guideway depends on the loadings, including the weight of the vehicles. To obtain an accurate cost comparison between the LIM and LSM propulsion methods, a detailed analysis must be done for a given route and ridership requirements. However, there are features of each drive system than can be identified which have significantly different cost elements.

The weight of the vehicle using the LSM drive is expected to be lighter than one using the LIM since there is little on-board power conditioning equipment. This would, in principle, reduce the cost of the guideway. However, from the design experience for the CMP, the live load is a small part compared to the dead load weight of the structure itself, and the weight of the car does not strongly influence the cost of the guideway. It is also interesting to note that the 24.3 meter long, LIM-driven COL-200 vehicle that carries 103 passengers weighs 44 tonne fully loaded, while the 24.8 meter long, LSM-driven Transrapid vehicle that carries 126 passengers weighs approximately 60 tonnes fully loaded.[45] While the Transrapid vehicle can achieve higher speed, its weight would not decrease if the vehicle were limited to the 200 kph design speed of the COL-200.

---

[45] "High-Tech for Flying on the Ground," Transrapid International technical brochure, 2002.

The reaction rail structure in the guideway of a LIM-driven vehicle is very simple with a conducting sheet anchored to steel that serves as back-iron for the motor. The active guideway of the LSM drive includes laminated stator cores, stator coils, section switches, feeder cables, and signaling system for synchronization of operation that is much more expensive. The stator coils and core components must be very rugged to withstand the repeated cycling of mechanical forces without degradation of insulation, operate for years in all-weather conditions, and be low cost.

As the complexity of the reaction rail and power distribution of a LIM-driven system is significantly less than that for an LSM system, the time required for construction and operational testing is also considerably shorter. This results in lower overall capital investments costs.

The number of power converters per unit length of track may be similar assuming the same number and type of vehicles on that given length of track. The LIM drive requires only a wayside rectification system to supply the constant DC voltage to the vehicle on a single or double hot rail from the wayside distributed utility electric power. However, each vehicle has a variable-voltage, variable frequency inverter on board to drive the LIM. The power to each of the LSM guideway stators is also conditioned through rectification to DC and then reformed to 3-phase AC at variable voltage and frequency; one inverter is needed per stator section assuming each section powers a separate vehicle. However, even if the LSM track is not utilized at full capacity, all the inverters and distribution network are required in the initial capital investment and all are operated as vehicles use each stator section.

While the LIM drive may have lower energy efficiency, power factor, and feeder voltage, this does not significantly increase the investment cost compared to the LSM. This is because the LSM has a more complicated converter station, lower voltage coils, and 3-phase feeder to stators.

Because of the complexity of the LSM active guideway structure and the synchronous operation of a LSM train, the system structure near end terminals requires more physical space than LIM-driven systems which further increases investment cost. The mechanical switch from track to track is larger, and it takes more physical space to transfer LSM vehicles from one track to another. As every LSM track section requires a converter, transfers of many vehicles with short headways at slow speed requires more power converters in these areas, all installed at the time of initial operation.

In the comparison of capital cost between maglev systems based on LIM and LSM, it is very clear that the capital cost of the guideway for the system with LSM is very substantially higher than that for the LIM. Conversely, the capital cost of vehicles for the LIM-driven system is higher than for one driven with an LSM. While the total capital costs of either the LIM or LSM may be greater than that for a conventional railway system, the increase of the LIM-driven system cost above the conventional system cost is certainly less than the cost increase for an LSM-driven system.

Projected capital costs for single and double-track applications of the Transrapid LSM system can be found in the literature and are shown in Table 7.4-1. [46, 47, 48, 49] Perhaps the most important entry is the 30 km Shanghai airport to city center connection that has been recently constructed and is in commercial service, compared to the estimated costs from the other projects' plans. Although the cost data has not been corrected for inflation, the values originate mostly from two reports that are quite recent and use similar methodology. Most cost data from the references are given in German Marks (DM) or Euros (€), and the conversion to U.S. dollars is cited in the

---

[46] P. Holmer, "Faster Than a Speeding Bullet Train," *IEEE Spectrum*, Aug. 2003, pp. 30-34.

[47] "Concept for the financing and private sector operation of the superspeed maglev system Berlin-Hamburg," Magnetschnellbahn Berlin-Hamburg GmbH report, January, 1994.

[48] "Magnetschnellbahn Streckenauswahl Vorstudie," Die Bahn report, Berlin, October 15, 2000.

[49] H.G. Lindlar, "Machbarkeitsstudie fuer Metrorapid Rein-Ruhr und Transrapid Muenchen," ETR (Eisenbahntechnische Rundschau, Darmstadt: Hestra), vol. 51, no. 5, pp 285-295, 2002.

table footnote. Variation in the cost per unit track length is expected due to the different operational, geographic, environmental, and ridership requirements of the individual routes. However, the table shows the cost per unit track length decreases with distance as expected.

Urban and suburban type maglev costs may be closest to the estimates for the Metrorapid system that has 6 stations total and 16 km average distance between stations. This affects the cost of the system and reduces the average speed significantly. A plot of the data as a function of average speed is shown in Figure 92 where a trendline has been added for the LSM data (excluding the value for the Berlin Airport Connection that is much greater than the other data due to tunneling and number of stops). While there is scatter in the data, there is a definite trend for decreasing cost per unit track length as average speed increases. A data point for the FTA Urban Maglev CDOT Project (256 km, 114 kph average speed, double track, 36.7 M$/mile including contingency) has been added for comparison that shows the significantly lower cost for this LIM-driven technology.[50]

Table 7.4-1. Comparison of Investment Costs Between Various Transrapid Applications

System	Distance km	Avg Velocity kph	Track Type	Investment Costs per Unit Guideway Length				Reference	
				MDM/km	M €/km	M$/km*	M$/mile*	Number	Date
Berlin Airport Connection	25	94	double	189		121	194	17	2000
Shanghai Airport Connection	30	222	single			43	69	15	2003
Munich Airport Connection	37	220	double	78.3		50	81	17	2000
					42.2	53	85	18	2002
Metrorapid Dusseldorf	78	120	double	93		59	96	17	2000
					39.7	50	80	18	2002
Frankfurt-Hahn Airport	116	166	single/double	54		35	56	17	2000
Berlin-Hamburg	284	233	double	31.4		20	32	16	1994
Gronigen-Hamburg	293	245	double	35.9		23	37	17	2000

* Cost Conversion of DM to Euro using 31December 1998 irrevocably fixed conversion rate of 1.95583 DM/Euro adopted by European Monetary Union Member States.
   Conversion of Euro to US Dollar at current rate of 0.8 €/USD

---

[50] FTA Urban Maglev Program, CDOT Team report "Final Report Interim," pp. 20, 7Jan04.
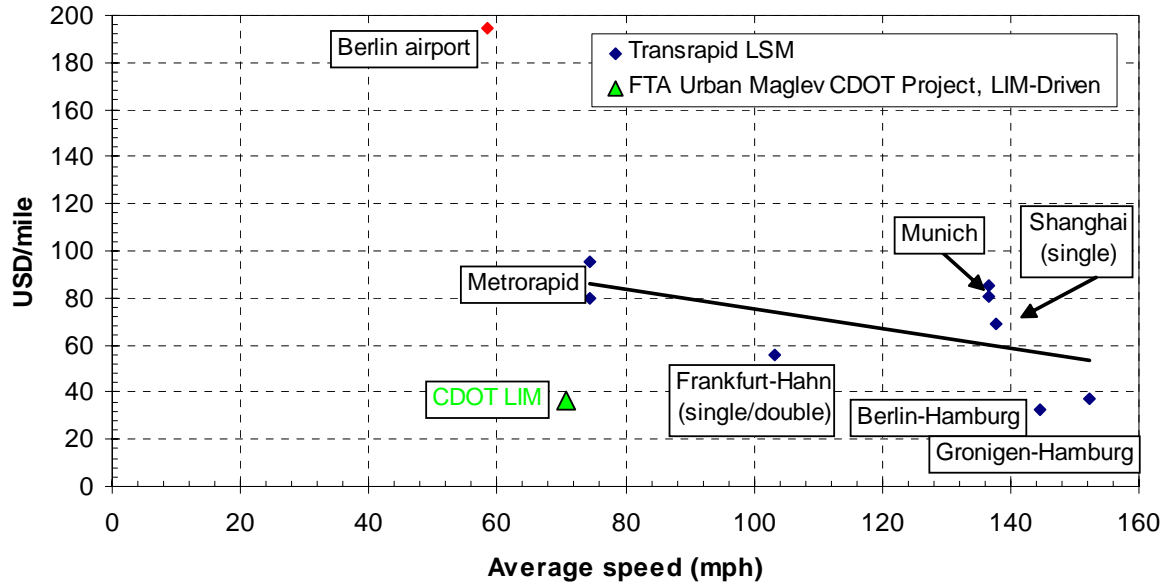
Figure 92: Comparison of investment costs between LSM-driven Transrapid applications.

Guideways are double tracks unless noted. Linear fit is to Transrapid data only excluding the Berlin Airport Connection. Cost estimate for the LIM-driven CDOT system was performed in the FTA Urban Maglev Program.

7.4.4. *Operational Cost*

The operational cost for a maglev system has major contributions including energy and manpower. Again, an accurate cost comparison between the LIM and LSM propulsion methods requires a detailed analysis for a given route and ridership requirements. However, there are features of each drive system than can be identified which can significantly affect these cost elements.

In general, the higher energy efficiency of LSM drives will reduce the energy cost compared to LIM systems. However, this very much depends on the design of motor and power supply system. If the section length of the LSM stator becomes long, the efficiency is reduced. For comparison of the two drive types, the efficiency and power factor of the TR07 LSM discussed above and the LIM motor that has been proposed for the COL-200 vehicle are shown in Figure 93. The values for the LIM are taken at the input terminals and the values for the LSM at the input to the block section. [32, 39 (see pg.67)] The figure shows that the efficiency (ratio of mechanical power to input real power) of the two drives is very similar, but the power factor (ratio of real power to apparent power) is larger for the LSM. The load seen by the utility is the real power, and hence, for this case, the energy usage is the same assuming the same thrust vs. speed profiles along the route. The consequence of the lower power factor for the LIM is the penalty of increased weight of the on-board power conditioning equipment to deliver the higher apparent power.
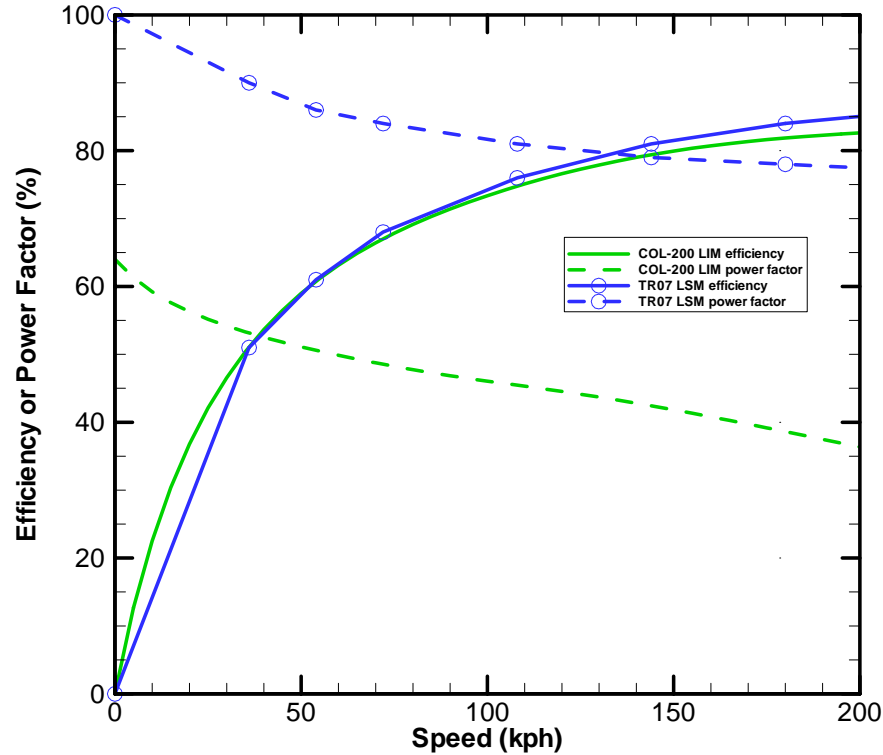
Figure 93: Efficiency and power factor at the terminals of the LIM for the COL-200 vehicle [32], and the input to a 300 meter block section of the TR07 LSM. [39].

Since most future maglev systems are expected to utilize driverless operation, manpower for drivers is not considered here. However, a more significant manpower staff is associated with the maintenance of the vehicle and guideway system. Vehicle maintenance between the two technologies is expected to be similar with the exception of the periodic maintenance of the on-board LIM stator and power conditioning equipment. The incremental effort for that inspection of a few parts is further minimized by the incorporation of a few sensors that provide state-of-health indications to monitor systems. To ensure the safety of operation, the guideway must also be inspected, and the manpower required for that effort is directly related to the complexity of the guideway system. The inspection and maintenance costs of LIM systems are estimated to be significantly lower than for LSM-driven systems due to the lower complexity and the significant degree of experience with LIM reaction structures in revenue service. It is highly probable that the LIM reaction structure inspection can be conducted with automated equipment. Development of the experience with the LSM is especially required in the early stage of operation. Because the LSM is a new type of system scheduled for revenue service, its operational cost estimate will have a greater uncertainty. It is not presently clear that inspection of the LSM stators in the guideway can be fully automated due to the complexity of the LSM stator winding and laminated core. If such automation is possible, the inspection equipment would necessarily be much more complicated than that needed for a LIM reaction rail.

7.5. CONCLUSION

Each of the LIM and LSM type drives has their advantages and disadvantages for maglev propulsion. Although the guideway is more costly for the LSM, it is the only appropriate choice for high-speed operation (>>200 kph) as the weight penalty of the on-board power conditioning equipment for the LIM alternative becomes prohibitive at high speed, and the ability to transfer the high electrical power to the vehicle for LIM propulsion becomes impractical in this speed

regime. At low speeds (≤100 kph) the LIM drive has already demonstrated the capability to provide economical, all-weather propulsion in maglev and steel-wheel transit systems. For speeds on the order of 200 kph, with high passenger demand and short headways, the issue is which technology is most cost effective considering the life-cycle of the installed design.

Calculations and designs for the CMP have shown that the modified design of the tested and proven Chubu HSST LIMs can achieve speeds approaching 200 kph and operate on high grades. Speeds of 230 kph can be reached on level grade (with 90 kph headwind) with this design, and with additional, minor improvements, 250 kph is feasible. The LIM technology is very similar to, and directly benefits from, the experience in the rotary-motor powered, steel-wheel, conventional rail industry. The simple structure of the LIM's reaction rail in the guideway and adaptive moving-block control provides a high degree of flexibility for the line operator to adjust the performance of the transit system in response to short-term ridership fluctuations, rapid recovery to scheduled service from off-normal events, and long-term growth in passenger demand with minimal modifications to civil structures. The simple construction of the propulsion track will result in a less costly guideway investment, lower cost maintenance, and higher reliability. While the electrical efficiency and power factor are, in general, lower for the LIM compared to the LSM, the efficiency of the COL-200 LIM design is comparable to the LSM-driven Transrapid TR07.

From the various aspects of the technologies discussed above, the LIM-drive is preferable for Colorado Project route. The base technologies for the propulsion and levitation have been well established and proven in testing as a transportation system. This LIM-drive is a lower cost alternative with flexibility to changes in demand to maximize the utility of the capital investment.

7.5.1. *References*

[32] FTA Urban Maglev Program, CDOT Team report "Task 14, Integration, Propulsion Trade Study, Technical Memo #4," 29oct03.

[33] M. Fujino et al., "High Speed Surface Transport System: Nagoya East Hillside Line and the Operational Testing for 3-Car Vehicle Prototype," Proceedings of the Maglev 2002 Conference, Lausanne, Switzerland, Sept. 2002. Paper PP01102.

[34] M. Fujino, "Total running test operation of the HSST-100 and the project of East Hillside Line in Nagoya," Proceedings of the Maglev 2000 Conference, Rio de Janeiro, Brazil, June 2000, pp. 35.

[35] M. Tanaka, et al., "The results of running tests of HSST-100L vehicle," Proceedings of the Maglev 1998 Conference, Yamanashi, Japan, April 1998, pp. 63.

[36] H. Ohsaki, "Linear Drive Systems for Urban Transportation in Japan," Proceedings of the Maglev 1998 Conference, Yamanashi, Japan, April 1998, pp. 29.

[37] Transrapid International, Transrapid Maglev System, Klaus Heinrich and Rolf Kretzchmar, eds., Hestra-Verlag, Darmstadt, 1989.

[38] Innovative Magnetic Transit System M-Bahn, AEG brochure 1989.

[39] "Technical Assessment of Maglev System Concepts, Final Report by the Government Maglev System Assessment Team," James H. Lever, ed., U.S. Army Corps of Engineers Cold Regions Research and Engineering Laboratory report no. 98-12, October 1998, pp 62.

[40] Ibid., pp 11, 80.

[41] K. Matsui et Al., "D.C. Linear Motor Controlled by Thyristors and the Testing Equipment for its High Speed Characteristics", p.149-154, Linear Electric Machines, IEE Conference Publication No.120, London, 21-23 October 1974.

[42] T. Umemori, et al., "Development of DC Linear Motor – Fundamental construction and feasibility," Paper F78 757-7, and "Development of DC Linear Motor (II) – Research for a ground coil and a field magnet," Paper F78 756-9, both presented at the IEEE Power Engineering Society Summer Meeting, Los Angeles, California, July 16-21, 1978.

[43] A. Miki, "ALPS and its future prospect", Proc. Railway Technology Research Institute Seminar, p.86-96, Tokyo, Nov. 1987.

[44] "Belt type Transit System by Magnet", Leaflet of Nihon Densetsu Kogyo, 2000.

[45] "High-Tech for Flying on the Ground," Transrapid International technical brochure, 2002.

[46] P. Holmer, "Faster Than a Speeding Bullet Train," IEEE Spectrum, Aug. 2003, pp. 30-34.

[47] "Concept for the financing and private sector operation of the superspeed maglev system Berlin-Hamburg," Magnetschnellbahn Berlin-Hamburg GmbH report, January, 1994.

[48] "Magnetschnellbahn Streckenauswahl Vorstudie," Die Bahn report, Berlin, October 15, 2000.

[49] H.G. Lindlar, "Machbarkeitsstudie fuer Metrorapid Rein-Ruhr und Transrapid Muenchen," ETR (Eisenbahntechnische Rundschau, Darmstadt: Hestra), vol. 51, no. 5, pp 285-295, 2002.

[50] FTA Urban Maglev Program, CDOT Team report "Final Report Interim," pp. 20, 7Jan04.

8.0 *CMP WINTERIZATION REQUIREMENTS*

This section provides additional detailed winterization data and vehicle requirements for maglev operations in the Colorado I-70 mountain corridor during winter storm events.

This chapter is divided into three main sections:

1. HSST Transit Operations Experience
2. HSST Winterization Experience and Recommendations
3. Detailed discussion of winterization requirements for Colorado car.

8.1. HSST TRANSIT OPERATIONS EXPERIENCE

HSST has extensive experience with their maglev transit system including operation in moderate winter climates. The operational experience in a moderate winter climate provides the data and basis for the winterization requirements for the winter operational conditions that will be confronted in the Colorado Rocky Mountains.

Development of the High Speed Surface Transport (HSST) began in the early 1970s, under the auspices and direction of Japan Airlines in order to introduce a new form of transport (fast, efficient and environmentally friendly) to connect airports with city activity centers. Japan Airlines' objective was to develop a system that could be used in lower speed applications such as in urban areas where tight turns are necessary as well as having higher speed capability in more open areas. The development process has had the same basic principles from the early development process to the current deployment in Nagoya, Japan. The transit vehicles were designed using electro-magnetic suspension (EMS) generating attractive magnetic forces with a U-shaped magnet wrapped around an iron rail creating levitation forces. Linear induction motors provide the propulsion. With the Nagoya, Japan TKL deployment additional aspects of operating in moderate winter climates have been taken into consideration in the overall vehicle development process. The following describes the development process for the HSST vehicle.

    a.   **Developmental Process**
        1970-1978
        Japan Airlines constructed a 1.3 km (0.8 mile) track and carried out a series of operational experiments with two test vehicles, designated HSST-01 and -02. Following was an operational testing program where prototypes were successfully tested at speeds of up to 308 km/hr (193 mph). Over the next several years, Japan Airlines (HSST) concentrated their efforts on developing a commercial version of the vehicle.

    b.   **Operations**
        The development of the HSST 100-S and 100-L vehicles has gone through an extensive series of passenger-carrying deployments to allow for the proper assessment by the Japan Ministry of Transport prior to issuing a railway business license for commercial operations. In combination, HSST vehicles have carried passengers for over 42 months transporting over 3 million passengers. FTA survey teams have visited the Nagoya, Japan TKL deployment working in conjunction with the FTA Urban Maglev Development Program and declared the CHSST technically capable to be deployed in the United States.

        March, 1985   Tsukuba Science Exposition, HSST-03
                -     track length of 350 meters (0.22 miles)
                -     vehicle - 50 passengers
                -     610,000 regular passengers transported

May-Oct. 1985   Vancouver Transport Exposition, HSST-03
- track length of 450 meters (0.3 miles)
- vehicle - 50 passengers
- 470,000 regular passengers transported
- distance traveled 7770km (4828 miles)

1986-1989   Aoi Exposition, Okazaki, Japan, HSST-03
- track length of 175 meters (0.11 miles)

Spring 1988   Saitama Exposition, HSST-04
- track length of 327 meters (0.2 miles)

Mar.-Oct.1989   Yokohama Exposition, HSST-05
- track length of 515 meters (0.32 miles)
- 1.2 million regular passengers transported
- distance traveled 29,000 km (18,000 miles)
- Japan Ministry of Transport issued a railway business license for commercial operations

c.   Additional Development/Deployment

1991   CHSST Corporation formed by Aichi Prefecture, Nagoya Railroad and HSST Corporation to produce commercial vehicles for deployment.

1991   CHSST constructed 1.6 km (1 mile) track in Nagoya for full-scale commercial operation of HSST's 100-S (short wheel base) and 100-L (long wheel base).

April 1993   Japan Ministry of Transport (MOT) issues acceptance of the technology confirming no technical deficiencies and enacted laws for public transport use for operational speeds in the Nagoya application up to 100 km/hr (62 mph).

d.   Nagoya Deployment

1999   HSST deployment begins in Aichi Prefecture, Nagoya for a feeder line 9 km (5.6 miles) long with nine stations connecting a terminal of the Nagoya City subway in the eastern section of downtown Nagoya to one of the Aichi Circle Line station. The route includes areas of tight horizontal and vertical curvature, a tunnel section and sections with steep grades (up to 6%). The climate in Nagoya has some moderate winter conditions with light snow and sleet occurring infrequently. The HSST system design was reviewed with winter conditions to determine design adjustments necessary for operations.

2002   Civil works (guideway, tunnel section, stations, maintenance facility and control center) underway with over 50% completed by May 2003 and total completion by the summer of 2004.

First completed train-set of 3 vehicles delivered to Nagoya track for operational running.

First train-set to be returned for final operational completion in June 2003. Remaining 21 vehicles to be manufactured and

delivered to Nagoya track for pre-operational performance running.

Train-set to be deployed on open sections of guideway for pre-operational performance running.

8.2. HSST WINTERIZATION EXPERIENCE AND RECOMMENDATIONS

CHSST engineers have assessed the Nagoya TKL deployment from the perspective of winter operations conditions and determined the following courses of action to be taken on various subsystems of the HSST system to assure operations during winter conditions.

8.2.1. *Guideway*

Guideway impacts from winter operating conditions result in:

a. Disruption of normal vehicle operation due to snow accumulation on reaction plate and skid surface; and,
b. Icing of brake surface, where mechanical brakes are applied, reducing the performance of the brake.

Mitigation efforts include:

a. Application of special coating that assists in clearing snow on the reaction plate and skid surface;
b. Use snow/ice plow that can remove or scrape snow/ice/frost from rail surface to prevent accumulation during normal train operation;
c. Operate trains during all hours including night time in winter storm conditions;
d. The specific places where extreme weather conditions are historically observed should be sheltered. The extreme weather conditions include heavy snowfall accumulations, major snow drifting, strong wind gusts or avalanche paths.
e. Apply rail heating at braking surface as needed. Rail heating is assessed in detail in Section 8.3 and Appendix 5 to provide the economics and alternatives to heating.
f. Use a gas turbine engine driven maintenance servicing car that can produce compressed air to blow snow/frost away and dry braking rail surface. This type of car is useful since heavy maintenance work can be done safely without trolley electric power.

8.2.2. *Guideway Equipment*

Specific guideway equipment will also be impacted by winter conditions including:

a. Power rails may accumulate snow or ice damaging the power collectors and disrupting normal power collection.
b. The signal line may accumulate snow or ice that will interfere with the vehicle antenna disrupting normal functions.

Mitigation efforts include:

8.2.2.1. Power Rails

Moving the contact surface of the power rail and the collector shoes under the surface of the power rail and installing power rail covers on the rail to prevent snow accumulation on the power rail itself. (See typical cross section of guideway/power rail in Figure 94.)
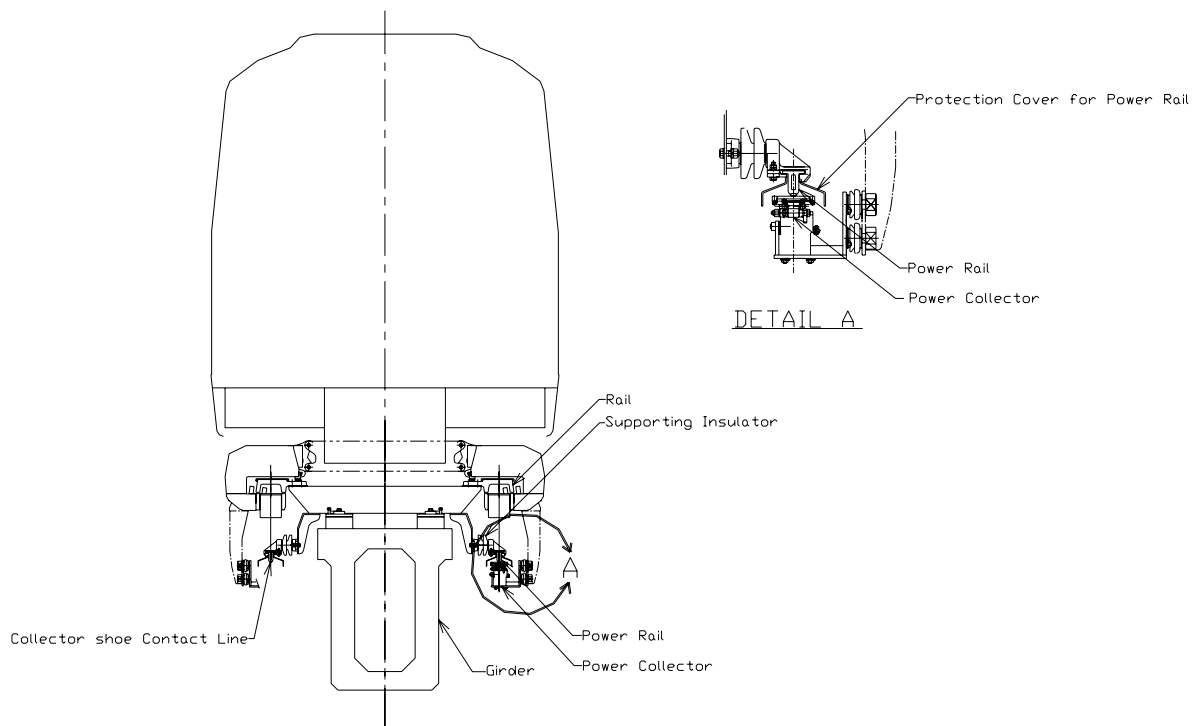
Figure 94: Power Rail Construction

8.2.2.2. Signal Line

For the current speed detection equipment, change the signaling line location from the upper to side surface of girder and install it vertically. Adopt vehicle speed detection equipment that can eliminate belt-wise line on girder beam. Radio wave (Doppler effect) type speed detection equipment is a candidate.

8.2.2.3. Switch

The switch mechanism and locations for switches are critical to maintaining headways and safe operations.

Switch issues include:

a.   Snowfall/ice on guide rail interferes with the switch girder wheel disrupting the girder wheel causing malfunctioning switches. Mitigation efforts include:

1.   Using snow plows at switch locations to remove snow
2.   Providing heating equipment along the guide rail
3.   Shelter the entire switch and immediate surrounding area
4.   In case of power collection from under the surface of the power rail, the trolley line may need a special device such as a flapping mechanism connecting the trolley line at switching.

b.   In-operation or malfunctions of electric/electronic equipment or parts due to cold weather and/or snow and ice buildup (such as limit switches and wayside control boxes). Mitigation efforts include:

> 1. Use parts or standardize specifications using cold weatherproofing and covering.
> 2. Add heating elements.

8.2.3. *Vehicle*

Japanese transit vehicle manufacturers have experience manufacturing transit vehicles for transit properties where winter operations are prevalent, including Chicago's Metra system and systems in New York State.

In the HSST vehicle there are numerous under-floor equipment arrangements that may be impacted by winter operations. A number of these items are discussed below with potential mitigation techniques cited.

8.2.3.1. Power Collector

This includes the power collector where snow and/or ice accumulation on the power collection rail may damage the vehicle power collectors disrupting normal power collection. A potential mitigation to this situation is the installation of additional power collector-like devices that function as snow/ice scrapers to protect the power collector. Additionally the material of the contact shoe should be weatherproof such as a ceramic material.

8.2.3.2. Doors

Vehicle doors historically are impacted by cold temperatures, snow and ice buildup causing the door to become inoperative or to malfunction causing a delay in operations. Door problems can be handled through proper heating at the doorsills and around the door operations mechanisms. An additional solution for the door operator mechanisms is to use an electric motor that has a larger initial torque than the conventional air driven mechanisms.

8.2.3.3. Bogie

Snow accumulation around module bogies disturbs and alters the smooth and correctly aligned vehicle movement. A number of mitigation measures can be taken including:

1. Application of an ice-proof coating on the bogie structure surface to prevent ice/snow accumulation.
2. If needed, install heating devices.
3. Use snowplows at the leading and rear end module to clear snow from the rail surface.
4. Install shrouds or boots preventing snow/ice intrusion at or around components such as ball bearings of the movable link and linear bearing to guarantee smooth movement.

8.2.3.4. Brake

Brake caliper surface icing will prohibit the correct performance of the brakes. This situation can be corrected by providing a heating device at the brake caliper. Additionally, an ice-proof coating can be applied to the surfaces eliminating ice buildup.

Snow accumulation around the brake body can also prohibit smooth brake operation. This situation can be corrected by covering the brake body.

8.2.3.5. Electric/Electronics Equipment Box

A potential issue is that equipment becomes inoperative due to snow/water intrusion into equipment boxes. This can be corrected by providing equipment boxes or compartments that are watertight either by using boxes with double packing (sealing) or providing special latch mechanisms. Additionally, sufficient backpressure can be provided through air ducts to prevent water and snow intrusion.

In addition to snow and water intrusion, electric and electronic equipment can become inoperative due to low temperatures. Electronic parts, especially the CPU, are not usually guaranteed below zero degrees Celsius. This situation can be corrected by heating the equipment boxes electrically or through warm air directed through air ducts.

8.2.3.6. Electric Coupler

The electric coupler between vehicles can be impacted through snow, water or ice accumulation causing poor electric conduction on the connector pins. This situation can be corrected by heating the coupler assembly.

8.2.3.7. Pneumatic System Parts

There are a number of values, rubber rings and other rubber parts, and water separators that may become inoperative or deteriorate due to cold temperatures and icing. For values a simple solution is the installation of jacket type heaters. For the water separators, installation of heater equipment will resolve this issue, while for rubber parts that may deteriorate, the use of cold-resistant rubber parts is appropriate.

8.2.3.8. Hydraulic System

Cold temperatures can cause hydraulic system deterioration due to a change of viscosity. The hydraulic system can also be impacted through deterioration of rubber parts through cold temperatures. Change in fluid viscosity can be dealt with by using fluids adequate for cold temperature operations. For rubber parts deterioration, the use of cold-resistant rubber parts will correct this situation.

8.2.3.9. Leveling Equipment Value

The leveling value can become inoperative due to cold temperatures or ingestion of snow, water or ice. This can be corrected by installing jacket type heaters to heat the valve or by placing the entire valve into a box.

8.2.3.10. Air Conditioning/Heating and Ventilation

Air conditioning and heating systems can become less efficient in winter conditions due to low temperatures and snow/ice ingestion into the air intake. This situation can be mitigated by installing larger capacity equipment for increased air movement. Also snow intrusion can be eliminated by placing a louver-shaped covering at the air intake or installing a centrifuge.

8.2.3.11. Windows

Transit vehicle windows in the passenger compartment as well as at the front and back of the train-set can deteriorate due to low temperatures and can fog from temperature differences between the inside and outside of the vehicle. Windows can be double pane, tempered or be manufactured with polycarbonate material. In addition window heaters can be used as defoggers or anti-icing systems can be installed.

8.2.3.12. Horn

The vehicle horn can be impacted by icing on vibrating parts or by snow intrusion into the horn assembly. These situations can be corrected by adding a heater for icing and a mesh guard to prevent snow intrusion into the horn assembly.

8.2.3.13. Lubricants and Grease

Lubricants and grease can deteriorate in performance due to an increase in viscosity. These situations can be corrected by using lubricants and greases that are specifically manufactured for

cold weather climates.

8.3. COLORADO WINTER CLIMATE AND SYSTEM WINTERIZATION APPROACH

The following sections discuss the winter conditions in which the CMP will operate. Additionally, specific approaches for winterization mitigation actions for specific elements of the system are presented.

8.3.1. *Corridor Characteristics*

The characteristics of the CMP corridor in terms of weather conditions and related aspects are presented below.

8.3.1.1. Elevation

The Colorado I-70 mountain corridor is a demanding environment due to the extreme changes in elevation along the 266 km (165 mile) right-of-way beginning at DIA [elevation 1615 m (5300 ft.)] and ending at Eagle County Airport [near Gypsum, CO, elevation 1844 m (6050 ft.)]. The route climbs and descends two mountain passes with elevations between 3251 m (10666 ft.) and 3401 m (11158 ft.). Extreme alpine weather conditions, rockfalls and avalanche potential contribute to the design challenges.

8.3.1.2. Temperature

Daily wintertime temperatures can vary along the route by as much as 30°C (54°F). The most extreme seasonal temperatures of –47°C (winter) to 38°C (summer) have been measured at Eagle County Airport. This represents a potential annual 85°C (153°F) temperature differential.

8.3.1.3. Snowfall

Snow can fall at rates exceeding 75 mm/hr (3 in/hr) with daily accumulations of over 0.75 m (30 in). On the mountain passes, a snowfall rate of 125 mm/hr (5 in/hr) has been observed to occur about every five years (Atkins, 2003). A snowfall rate of 0.3 m/hr (13 in./hr.) was recorded on Berthoud Pass in 1933 (Judson, 1965). See Figure 95 and Figure 96 for early winter conditions.

(elev. 3356 m, 11,012 ft). Photo taken 11/7/02.

Figure 95: Eastbound I-70 at East Portal Eisenhower Memorial Tunnel

(elev. 3251 m, 10,666 ft). Photo taken 11/7/02.

Figure 96: Eastbound I-70 at Vail Pass

8.3.1.4. Wind

Maximum wintertime wind gusts of 50 m/s have been measured at Georgetown Lake within the past three years. Mean daily peak wind speeds are shown in Figure 97.
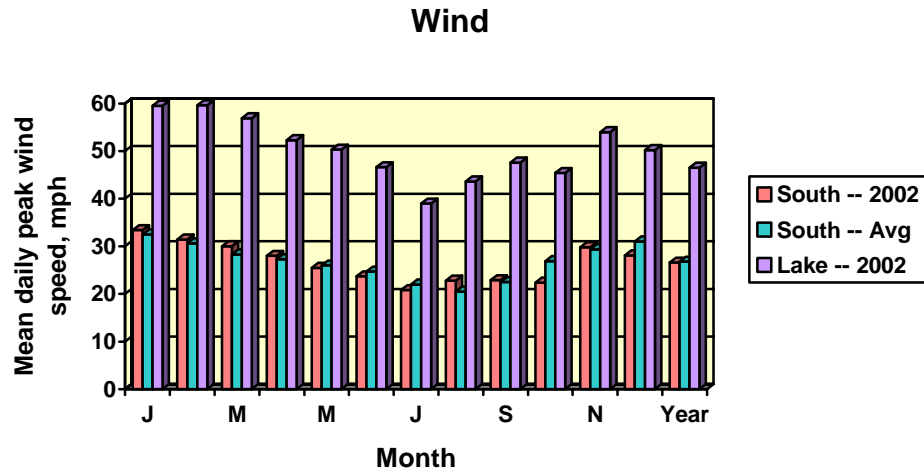
Wind

Figure 97: Year-long wind data for Georgetown.

(Notice that the wind peaks generally occur in the winter and spring months. "South" readings were acquired from a weather station located in Georgetown on top of a residential building.)

Wind data from several ski areas located near the I-70 mountain corridor has been collected over the past year. However, the wind conditions in Georgetown (and particularly those associated with the Georgetown Lake) are a factor of 2 more severe than that at any of the other locations considered. A potential reason for this phenomenon is explained by considering the photograph provided in Figure 98.

One reason for the severe winds in the Georgetown Lake area can be attributed to the relatively narrow canyons along I-70 and the venturi effect. It is well known that a fluid in subsonic flow accelerates as it approaches the throat of a nozzle or venturi. The narrow canyons provide the "throat" for flow acceleration. In addition, Georgetown is located at the confluence of two major airflow streams.   One canyon seen on the upper left of the photograph descends from the Guanella Pass area. This pass connects the immense high altitude valley area called South Park (to the southwest of Georgetown) with the Clear Creek canyon (to the west and east of Georgetown), along which I-70 passes. Clear Creek canyon comes down from the upper right in the photograph. You can see I-70 turning right as it follows this canyon. Occasionally, cold wind falls and is pushed down both of these canyons into Georgetown, developing a mixing layer. The resulting large-scale turbulent flow can have a buffeting effect on over-the-road trucks as is evident from the occasional truck that is overturned in this area. In February 1884, the Georgetown Courier reported that the engine, tender and three passengers cars of a narrow gauge train were overturned by the wind at the same approximate location of today's Georgetown Lake (Georgetown Courier, 1884).

Figure 98: Photograph of I-70 looking westbound at Georgetown Lake

8.3.1.5. Corrosion

Because of its proximity to I-70, it is anticipated that there may also be impacts on the maglev guideway components due to wintertime deicing salts currently added by CDOT to maintain tire traction to I-70. Similar concerns as to that mentioned above, regarding deicing salts, have been directed to CDOT officials by the electrical utilities maintenance personnel (Griffin, 2003). The utilities have stated that there are accelerated failures of electrical components due to salt enhanced corrosion at locations near I-70. Generally, CDOT uses an aqueous solution of 30% magnesium chloride ($MgCl_2$) and a zinc (Zn) based corrosion inhibitor. They also use a product called M1000 and M2000. This material also consists of 30% $MgCl_2$ and water but also includes other proprietary constituents that inhibit corrosion and lower the solution eutectic temperature.

8.3.2. *Maglev System Winterization*

Several failure mechanisms or modes have been identified as a result of the climate and environmental conditions specific to the Colorado I-70 urban and mountain corridor. These mechanisms are listed below and discussed in detail in the Appendix.

1. Avalanche
2. Frost Formation
3. Freeze/Thaw cycles
4. Differential Thermal Expansion
5. Snow and Ice Buildup
6. Corrosion
7. Fatigue

After a clear understanding of the failure modes was obtained, critical system components were analyzed for potential failure. The Failure Modes and Effects Analysis technique is used to focus on those components and subsystems that, were they to fail, have the greatest potential impact.

Potential solutions are then proposed and a cost associated with the solution is estimated for each critical component and subsystem. Conclusions and recommendation then were formulated to summarize the winterization effort.

8.3.3. *Failure Modes and Effects Analysis - Impacts of Ice, Snow and Dirt*

Failure Modes and Effects Analysis (FMEA) is a systematic tool to aid in making appropriate design decisions based on the anticipation of severity, likelihood of occurrence and capability of detection of a failure. Usually, the technique is used in conjunction with testing so that statistical models can be developed that lead to accurate selection of coefficients for the likelihood of occurrence. However, in this analysis, as we have no test program in place, we are limited to best estimates and projections based on sound engineering judgment. More details of this analysis technique can be found at the following website.
 http://www.fmeca.com/ffmethod/history.htm

The details of the FMEA analysis for the following system components can be found in Appendices 1-4. The results of the analysis are provided below in Table 8.3-1.

 The Guideway systems are subdivided into the following:

1. Vehicle / Guideway Interface
2. High Speed Switches
3. Circuit Breakers
4. Power Collection Mechanisms
5. Snow Removal and Maintenance Cleaning Equipment
6. Auxiliary Heating Systems
7. Impacts of Wind.

The Vehicle systems are divided into the following subsystems:

1. Mechanical Latches (vehicle doors and other openings)
2. Motors and actuators (vehicle doors and other openings)
3. Vehicle Braking Systems
4. Vehicle Bogie compartment winter design requirements.

In addition, considerations are given to the stations, station access and parking according to the following:

1. Environmental Design Considerations
2. Snow and Ice Removal
3. Auxiliary heating requirements.

Table 8.3-1 Results of the FMEA Analysis. (The top five RPNs are highlighted in bold)

Subsystem	Severity	Likelihood of Occurrence	Capability of Detection	Risk Priority Number (RPN)
Guidway/Transit System Concerns				
Guideway/Vehicle Interface <50 mm snow depth	7	5	3	**105**
Guideway/Vehicle Interface >50 mm snow depth	8	5	3	**120**
High Speed Switches	9	5	2	**90**
Circuit Breakers	9	4	2	72
Power Collection - LIM	8	5	2	**80**
Power Collection - LSM	6 or 7	4	2	48 or 56
Snow Removal and Maintenance Cleaning Equipment	9	4	2	72
Auxiliary Heater Systems	6 or 9	4	2	48 or 72
Impacts of Wind (transit system concern)	9	4	2	72
Vehicle Concerns				
Mechanical Latches	4 or 9	3	2	24 or 54
Motors and Actuators	9	3	2	54
Vehicle Braking Systems	9	3	2	54
Vehicle Bogie compartment winter design requirements	10	4	5	**200**
Station Concerns				
Environmental Design Considerations	5	3	2	30
Snow and Ice Removal	6	4	2	48
Auxiliary Heating Requirements	2	4	2	16

8.3.4. *Potential Vehicle Subsystem Solutions from Impacts on the Guideway*

8.3.4.1. **Vehicle-Guideway Interface**

The HSST vehicle/guideway interface is illustrated in the schematic shown in Figure 99.

The HSST system incorporates a 14-15 mm gap between the aluminum reaction rail and the bottom surface of the linear induction motor (LIM). This gap is actively maintained by using a proximity sensor located on the bottom side of the rail. Current flowing through the wire wrapped around the levitation magnet is varied thus controlling the strength of the magnetic field attracted to the lower tines of the steel structural rail. A caliper brake located around the outer tine on the bottom portion of the steel rail provides the secondary braking system. Electrical power is collected on one side of the vehicle via the vehicle power collector in sliding contact with the third rail.
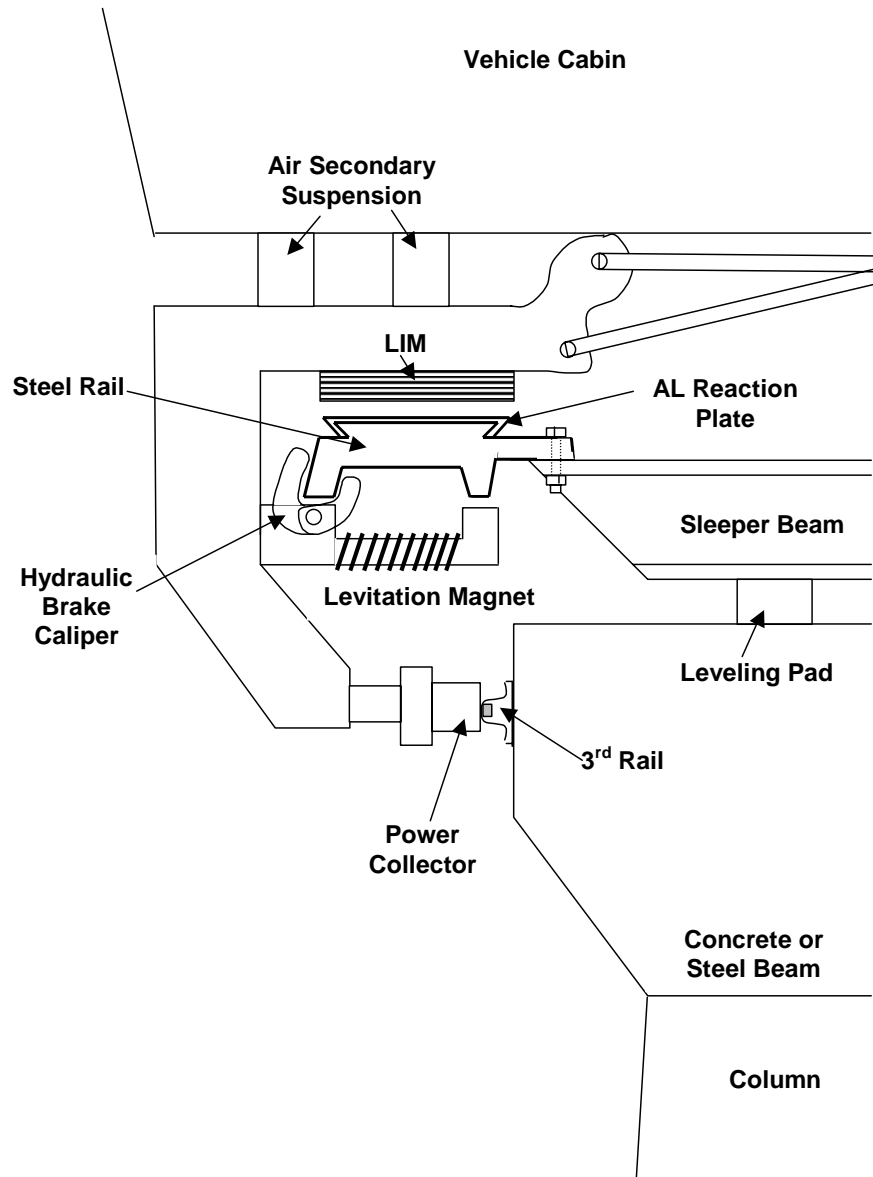
Figure 99: Schematic of the vehicle/guideway interface on the HSST 100-L

In addition, cross sections of the steel structural rail with aluminum reaction plate and third rail are shown in Figure 100 and Figure 101, respectively. The U.S. quarter was included in each photograph to provide a concept of scale to the components illustrated schematically in Figure 100.

Urban Maglev Transit Technology Program

Figure 100: Cross section of the HSST structural steel and aluminum reaction rails. A U.S. quarter is laying on top of the rail for scale purposes.
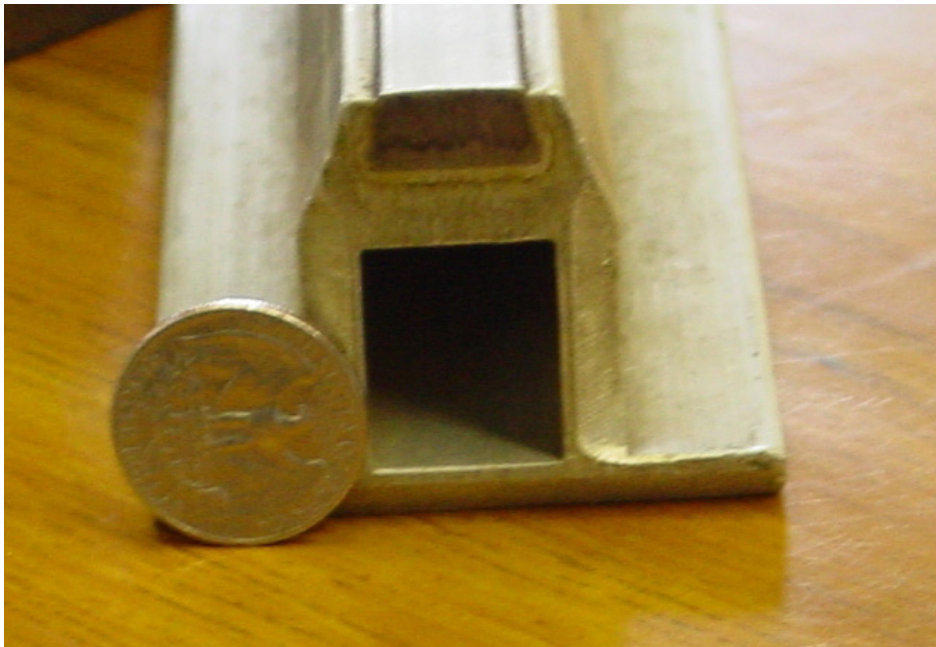
Figure 101: Cross section of the HSST electrified third rail. A U.S. quarter dollar coin is positioned next to the rail for scale purposes.

As can be seen in Figure 99, the HSST vehicle electromagnetic suspension (EMS) and propulsion (LIM) systems wrap around the structural and reaction rail. Therefore, these subsystems will be considered here. Of course the braking systems are also an integral part of this vehicle/guideway interface, although those will be discussed later in section 8.3.4.3. The goal of addressing the winterization issues associated with the vehicle/guideway interface is to significantly improve the system reliability in the severe winter conditions that can exist within the Colorado climate.

178   *Colorado Maglev Project*
Part 3: Comprehensive
Technical Memorandum

The vehicle/guideway interface can be divided into components that remain on the vehicle and those associated with the guideway. Guideway subsystems will be considered first.

Many potential solutions to winterization problems associated with these subsystems have been previously identified by LaMarca and King (1980). The findings are summarized below.

Much of the impact due to winter climate can be eliminated with a guideway design that allows for adequate drainage. This will minimize the impact of the freeze thaw cycle failure mechanism. Therefore, it is important to severely limit the number of horizontal surfaces that can collect and retain snow and ice.

Careful thermal design of active electrical heating elements for critical subsystems can yield large payoffs in system efficiency (see thermal analysis Appendix 5). It is best to incorporate these designs into the guideway at the outset so that they are an integral part of the design.

Weather information discussed previously was used in conjunction with knowledge of the existing HSST 100-L and Colorado vehicle to design an electrical heating system. The structural/reaction and third rails can be most easily heated electrically as shown in Figure 102.
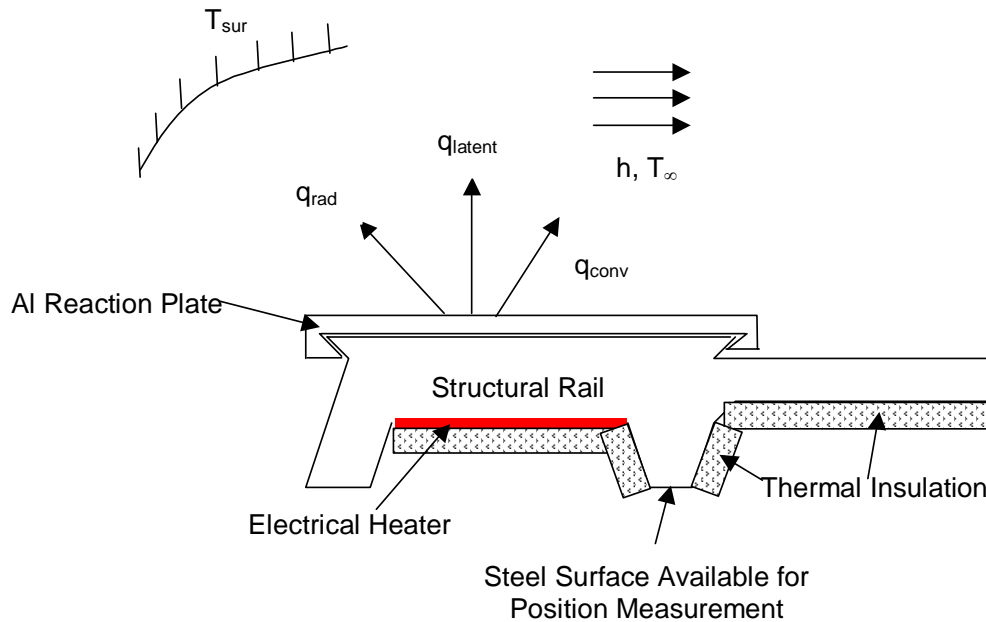
Figure 102: Schematic of the electrical heater design solution with heat balance terms shown.
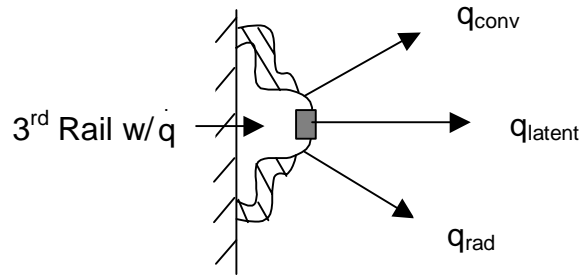
Figure 103: Schematic of the third rail with thermal insulation covering approximately 70% of the surface area potentially exposed to the surroundings.

Thermal analysis yielded the following electrical power heating requirements for insulated structural/reaction and third rail components for two separate tracks (two directions) of 16 km (10 mile) lengths (see Figure 104).
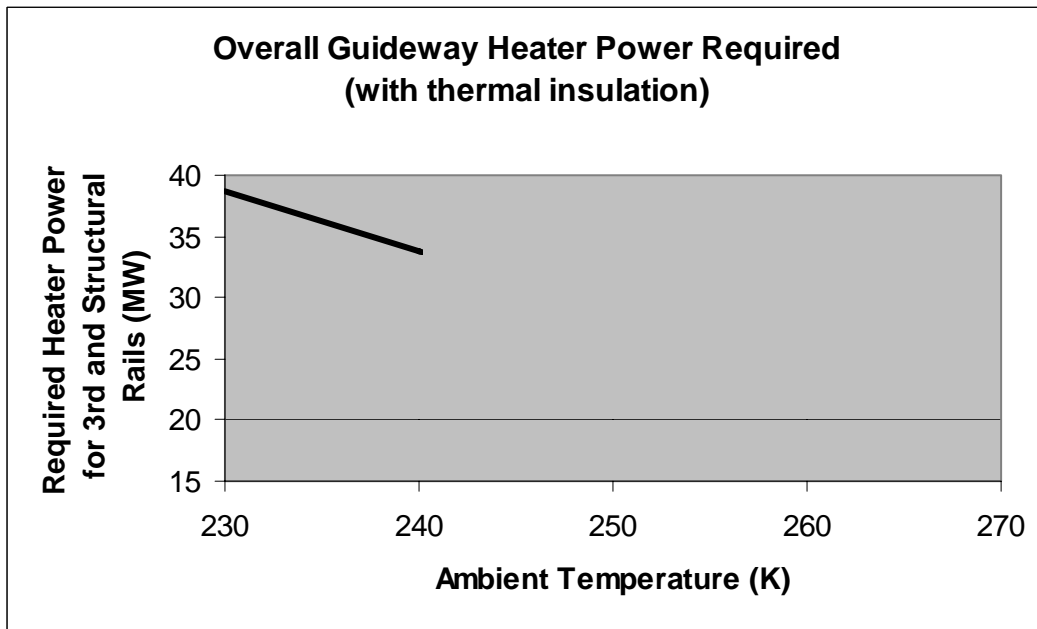

Figure 104: Heater power required of all structural/reaction and third rails, two directions, 16 km of track, *with* **thermal insulation.**

A costs analysis was performed for the rail heaters, the results of which are provided in Table 8.3-2. Heater and thermal insulation costs were acquired from Watlow Polymer Technologies Corporation. Engineers at Watlow have suggested the use of a polymer encapsulated heating element that is 0.14 m wide by 4.9 m long, the power flux is 3100 W/m^2.

Table 8.3-2 Analysis of heater cost for the guideway of the Colorado Project

Length of track section (km)	282
3rd rail Effective Diameter (m)	0.14
Structural rail width (m)	0.14
Heater Cost per m^2	$465.00
Width of insulation for structural rail (m)	0.36
Width of insulation for third rail (m)	0.18
Cost of insulation (1/2 inch PVC foam closed cell) ($/m^2)	$26.91
Cost of heater for third rail	$73,180,800.00
Cost of heater for structural rail	$73,180,800.00
Cost of insulation for third rail	$11,049,500.00
Cost of insulation for structural rail	$5,333,286.43
Total Cost of heaters for the rails	**$162,744,386.43**
Cost per mile	**$929,967.92**
Number of laborers	2
Labor costs per hour	$30
Linear heater installation progress per hour (m) - (ft)	19.5
Total man hours of labor	57750.0
Total installation labor costs	**$1,732,500.0**
Cost of Connectors	$2.00
Number of connectors	924032
Cost of connectors	**$1,848,064.00**
Total Cost of winterizing the rails	**$166,324,950.43**
Cost per mile	**$950,428.29**

8.3.4.2. **High speed switches**

Four different switches have been previously analyzed as part of Task 12. They are named in the columns shown in Table 8.3-3 below. All four of the switches could be actuated with hydraulic cylinders. After discussing the use of hydraulic cylinders with a manufacturer's representative (Bush, 2003) and the associated concerns for winter use, Mr. Bush suggested the following.

1. Cold weather seals
2. Stainless steel rod
3. 5606 hydraulic fluid (also used in military aircraft).

In general, hydraulic systems have been designed for harsh weather operation and there has been a great deal of previous experience with these systems. If they are properly maintained, then it is believed that the system reliability is high.

Table 8.3-3 Material cost estimate for winterizing the switches discussed in an earlier Task 12 report.

	Bending Beam	Pivoting High Speed	Moving Table	Docking
Heater Areas (m^2)	1.30	2.47	162.19	119.44
Heater Power Requirements (W)	4019	7665	502794	370275
Heater Cost ($)	$1,205	$1,150	$75,419	$55,540
Insulation Cost ($)	$69	$67	$4,364	$3,215
Total Material Cost	$1,275	$1,216	$79,785	$58,755

Regardless of the actuator used, the bending beam and pivoting high-speed switch would be guided by a steel wheel riding on a steel rail. The wheel and rail assembly would rest on columns raised over 2 m above the ground level. To minimize the impact of snow and ice on this switch guidance system, it is proposed that heaters be used to warm the rail when there is substantial snowfall. The heaters should also be insulated to direct the heat where it is need and therefore, minimize the energy consumption. This is shown schematically in Figure 105 below.
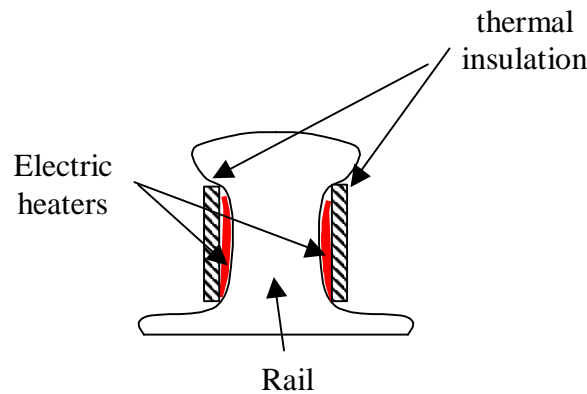
Figure 105: Heater configuration for the switch guidance rails on pivoting and bending beam switches.

Moving table and docking switches would likely be raised with air bearings prior to actuation. It will be important to keep the surface below which the air bearings are acting free of snow and ice. Estimates of the heater area necessary to prevent snow and ice from accumulating on these horizontal surfaces and their associated costs are provided in Table 8.3-3.

In the analysis of switches performed as part of Task 12, it was stated that the pivoting switch can be actuated by a series of three electric motors. With regard to winterization, it is important that these motors be located above the ground and beneath the switch guideway. They should be housed within a vented enclosure. There may be a need to periodically electrically heat the vents to prevent the buildup of snow and ice that would tend to clog the vent.

8.3.4.3. Vehicle braking systems

Primary braking system on the HSST system is electromagnetic through pole reversal on the linear induction motors (LIM). Secondary brakes are hydraulically actuated brake calipers that clinch the outer tine of the steel structural rail (see Figure 99). The tertiary braking system is to de-energize the electromagnetic levitation allowing the vehicle to rest on brake shoes mounted between the LIMs. These shoes will contact and thus form a friction surface with the aluminum reaction rail.

Winterization for all three of these braking systems involves keeping the structural rails, LIMs and brake calipers free of snow and ice. The structural rails will likely include an electrical heating system as previously discussed. However, improved rail drainage may result from incorporating an incline to the rail design as shown in Figure 106. The incline is shown as directed toward the centerline of the track. However, it could also be inclined away from the track centerline.
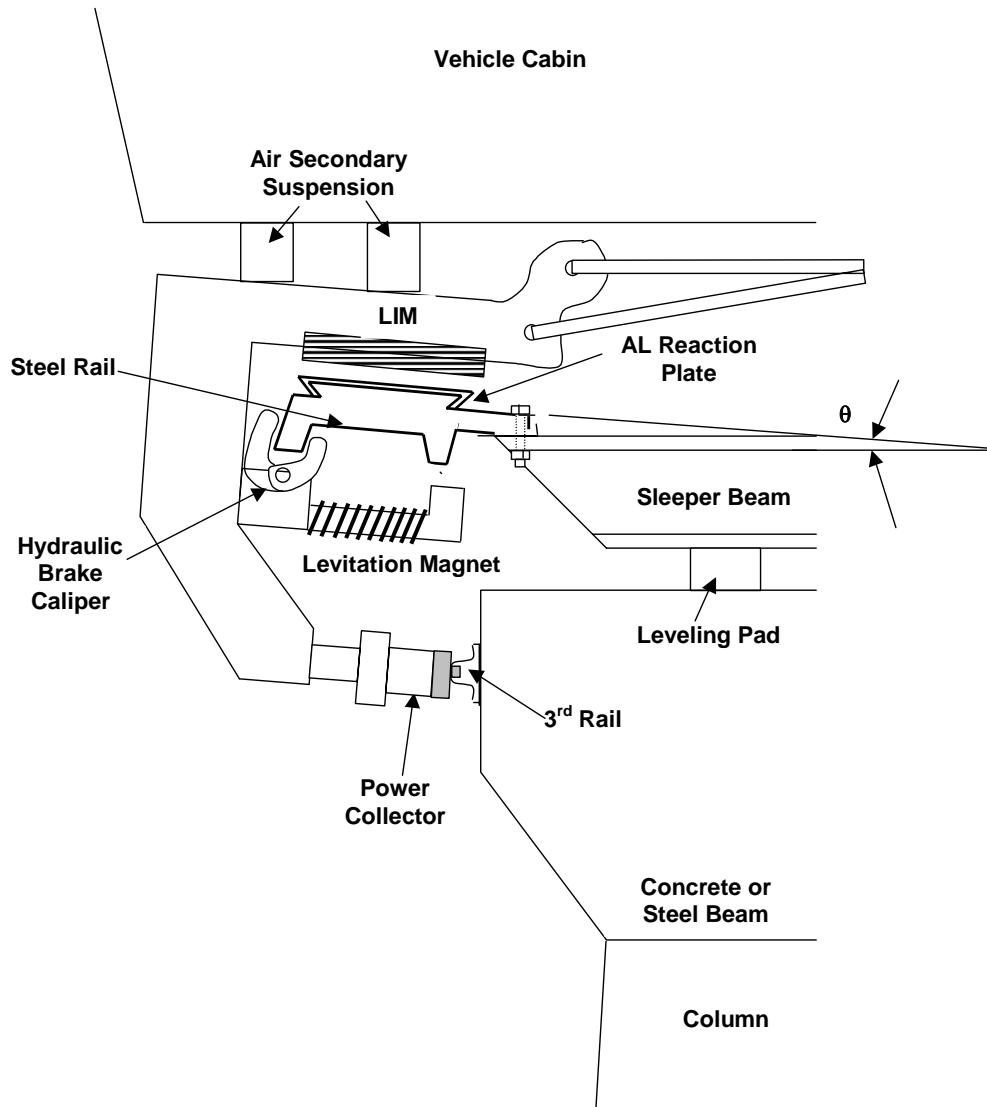

Figure 106: Winterized structural rail design to promote drainage from the reaction rail surface.

Because of Joule heating of the aluminum windings within the LIM, substantial heat dissipation is expected to provide the necessary energy to melt snow and ice. The actual heat dissipation could not be determined because the actual length and cross sectional wire dimensions of the aluminum are unknown.

Should the quantity of heat dissipation be insufficient, high resistance heating wire could be wound throughout the LIM during motor construction and be periodically energized to augment the removal of snow and ice.

Hydraulic brake calipers can also be periodically heated electrically to remove snow and ice. The decision to energize any of the previously mentioned auxiliary electrical heating system could be made based on operator judgment or in response to optical reflection measurements.

8.3.5. *References*

Adkins, Dale, Colorado Avalanche Information Center (CAIC), Personal Communication, 2003.

Barlo, T and Zdunek, A, IIT Research Institute, Chicago, IL "Electrolytic Corrosion in DC Powered Transit Systems," 8 Reports Prepared for the National Cooperative Transit Research and Development Program (NCTRP) Project 48-1, TRB, National Research Council, Washington DC, 1985-1987. http://www.iti.northwestern.edu/research/a_projects/stray2.html

Bush, Joe, Personal Communication, Zemarc Corp., March, 2003.

Dyer, J. M., J. L. Hoke, B. D. Storey, A. M. Jacobi, and J. G. Georgiadis, "An Experimental Investigation of the Effect of Hydrophobicity on the Rate of Frost Growth in Laminar Channel Flows," ASHRAE Transactions, 106:1, 143-151, 2000.

Georgetown Courier, "Wind Topples Colorado Central Passenger Train", February 28, 1884.

Griffin, Rich., Colorado Department of Transportation (CDOT), Personal Communication, 2003.

Hewitt, M.A., Downtown People Movers (DPM) Winterization Test Demonstration, Final Report, USDOT Transportation Systems Center, OTIS-TTD-WINT-109, Otis Elevator, Denver, CO, May, 1980.

Judson, A., "The Weather and Climate of a High Mountain Pass in the Colorado Rockies", US Forest Service Research Paper RM-16, Rocky Mountain Forest and Range Experiment Station, US Department of Agriculture, 1965.

Kato, Junro, Chubu HSST, Personal Communication, 2003.

Kovacs, G. T. A., "Micromachined Transducers Sourcebook," McGraw-Hill, Inc., New York, NY, 1998.

LaMarca, J and King, C., "Rail Transit Winterization Technology and System Operation Study", USDOT Report, UMTA-MA-06-0025-80-9, Sept. 1980.

Websites referenced
Circuit Breakers
http://www.metatechcorp.com/aps/cold_weather_operating_problems_.htm

Instrumentation for Civil Infrastructure
http://www.calit2.net/eci/synopsis.html
http://www.spa.com/civil.pdf
http://mail.mems-exchange.org/pipermail/mems-talk/2001-November/005609.html

Deicers used in highway applications
http://www.anti-icers.com/m1000_environmental_properties.htm
http://www.anti-icers.com/m1000_performance_properties.htm

Failure Modes and Effects Analysis
http://www.fmeca.com/ffmethod/history.htm

APPENDIX 1: FAILURE MODES

Avalanche

The Colorado Department of Transportation (CDOT) has commissioned the development of the Colorado Avalanche Information Center (CAIC). CAIC is a division within the Colorado Geologic Survey and manages the avalanche prediction program for CDOT. The Avalanche Atlas is available on CDROM and represents a well-documented reference containing the locations and mapped extent of major and periodic avalanches throughout the state. Many avalanche areas are located along the I-70 mountain corridor.

Avalanches are powerful gravity flows of snow and ice that can seriously impact an elevated guideway and or maglev vehicle. The head of the avalanche will entrain air into the flow, thus effectively lubricating the slide allowing it to continue further than a casual observer might imagine possible. However, because of the measurement and data archiving efforts of CAIC, the avalanche locations are known and where possible can be avoided. CDOT also has an active avalanche control team that utilizes artillery to control avalanches along all avalanche-prone state highways. The artillery is used to activate avalanches before dangerous quantities of snow and ice have accumulated thereby limiting the extent of any slide. A photograph of an avalanche chute adjacent to I-70 just east of the Eisenhower tunnel is shown in Figure A.1.1.

Figure A.1.1: Avalanche chute that can potentially affect traffic along the I70 corridor east of the Eisenhower tunnel.

In particularly difficult areas, avalanche sheds can be constructed to allow the avalanche to pass over the top of track thus preventing harmful impact to the guideway or a passing vehicle. An

example of an avalanche shed is shown in Figure A.1.2. It is likely that the track elevation would have to drop to near ground level in these locations to minimize the cost associated with the avalanche shed construction.

Figure A.1.2: Avalanche shed located in the Swiss Alps.

Frost formation

Frost forms on solid bodies at nucleation sites. For instance, certain types of bacteria have been found to provide nucleation sites on the leaves and flowers of fruit trees. Growers have used this knowledge to displace these bacteria with others that do not exhibit this characteristic. Thus, they are able to prolong the formation of frost that would otherwise damage the fruit at a particularly fragile time in its development. Similar phenomenon likely will occur on other solid matter. A nucleation site is provided by a nick or scratch in the material. As the temperatures of these materials fall below the frost point for the air, water vapor will sublimate onto the nucleation sites. Frost will continue to accumulate as long as there is sufficient moisture in the air and the temperature of the materials remain below the frost point. Ongoing research at the University of Illinois is aimed at understanding frost formation mechanisms with hopes of identifying materials and coatings that prolong the formation of frost (Dyer et al., 2000). Although the major application of this research is related to alleviating frost buildup on refrigerator and heat pump evaporators, this work could also be useful in the effort to prolong frost buildup on critical components of the maglev transportation system.

Freeze/Thaw Cycles

The thermal expansion is a thermodynamic property of a material and is mathematically defined as follows

$$\alpha = -(M\rho/MT)/\rho$$

Where α is the volumetric thermal expansion coefficient ρ is the material density and T is the material temperature. Because the thermal expansion coefficient of water is negative from the point of minimum density (4^0C), through the fusion temperature and below, freeze thaw cycles will

likely cause crack formation and propagation within porous materials containing water. If the porous material is saturated with water in its pores, when the water freezes and consequently expands, it will likely have nowhere to move. The resulting stress grows large enough to locally yield and crack the material. Over time the cycle of freezing and thawing processes continues until there are sufficient micro cracks to form larger cracks that compromise the structural integrity of the beam or column. These cracks also form paths for surface tension driven (or capillary) flows of water and minerals that can contribute to crack enlargement and corrosion of metallic reinforcement and thus further accelerates the failure mechanism. Although one would normally consider reinforced concrete to be the major material in question, any porous material that can absorb water is susceptible to similar damage.

Differential Thermal Expansion
In systems composed of composite materials, failure due to fatigue in thermal cycling is a possibility. The example provided above in the discussion of freeze thaw cycles is actually a failure due to the differential thermal expansion between porous concrete and the water contained within it. In general, water has a thermal expansion coefficient that is many times larger than that of concrete. It is due to this difference (of the thermal expansion coefficients) in combination (product with) the temperature difference from the reference condition (temperature at the time of the composite formation or manufacture) that results in the thermal stress. Ideally, the thermal design engineer will select materials with the same thermal expansion coefficients to avoid the resulting internal stresses. However, this may be impossible when other (structural or electromagnetic) properties are also considered essential to the design. In these situations, one can potentially use adhesives that accommodate shear over a broad temperature range to alleviate these problems or consider alternative means for fastening the dissimilar materials.

There are two examples from the HSST maglev system that warrant further investigation. The first is the structural and reaction rail composite and the second is the electrified third rail utilized in the HSST system. Photographs of these rail sections are shown in Figure A.1.3 and Figure A.1.4, respectively. The HSST structural steel and reaction rails are adhesively bonded. The HSST electrified third rail is composed of an aluminum extrusion with a stainless steel bar inlaid and crimped into it. The plot shown in Figure A.1.5 represents the thermal expansion of steel, aluminum and copper over the extreme temperature range measured at Eagle County Airport. A rail length of 23.8 m (78 ft.) was used in the calculation because this represents the maximum length of product that can be reasonably carried on a truck over the highway.

The following equation was used to estimate the differential thermal expansion that is illustrated in Figure A.1.5 and Table A.1.1 includes the thermal expansion coefficients used in the calculations.

$$L_2 - L_1 = \alpha(T_2 - T_1)$$

L_2 and L_1 are the final and reference lengths, and T_2 and T_1 are the final and reference temperatures, respectively. α is the thermal expansion coefficient. The L_2 length is calculated for each material and the difference between the L_2 for aluminum and that of steel are calculated. The same is done for copper and steel. The results are plotted on the ordinate of Figure A.1.5.

Table A.1 Thermal Expansion Coefficients (Baumeister, 1977)

Material	α (C^{-1})
Aluminum	2.40E-05
Copper	1.70E-05
Steel	1.30E-05

Figure A.1.3: Cross section of the HSST structural steel and aluminum reaction rails. A U.S. quarter dollar coin is positioned on top of the rail for scale purposes.
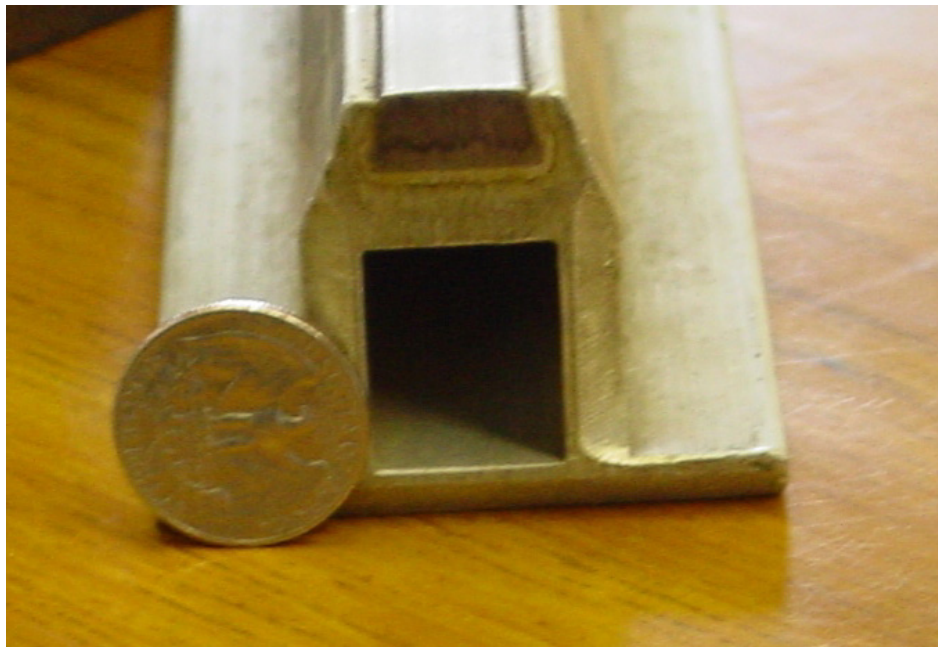

Figure A.1.4: Cross section of the HSST electrified third rail. A U.S. quarter dollar coin is positioned next to the rail for scale purposes.
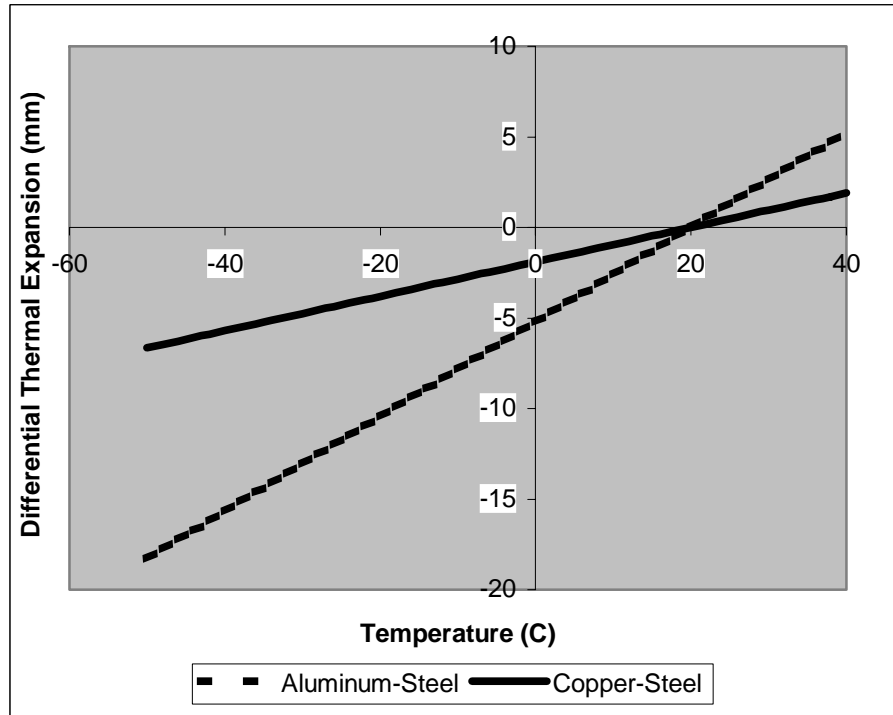
Figure A.1.5: Differential thermal expansion between aluminum and steel and copper and steel over the extreme temperatures previously measured within the I-70 mountain corridor.

As shown in Figure A.1.5, with a reference temperature of 20°C, differential thermal expansion approaches 18 mm in the aluminum-steel system as the temperature approaches –50°C. Depending on the type of adhesive used, the resulting thermal stress induced shear could cause a failure in the adhesive bond, especially over a number of thermal cycles.

This problem could be alleviated in two possible ways. The first approach may be to use copper instead of aluminum for the reaction rail. This may also result in higher linear induction motor efficiencies because the electrical conductance of copper is approximately twice that of aluminum. However, this would also dramatically increase the system cost since aluminum is much cheaper per unit weight and is much less dense than copper. The other possibility is to consider using explosive welding technology to fasten the aluminum reaction plate to the steel. This has already been done commercially with good success. Figure A.1.6 illustrates the type of interface that can be achieved with an explosive weld technology. Further testing would be necessary to determine the impact of cold climate but this interface would likely support substantial shear from differential thermal expansion. Note the wavelike pattern at the interface. This is much like the wave breaking Kelvin-Helmholtz instability observed between two shearing fluids. If the weld is done properly, these interlocking breaking waves form a significant mechanical bond between two dissimilar materials that could not otherwise be welded.
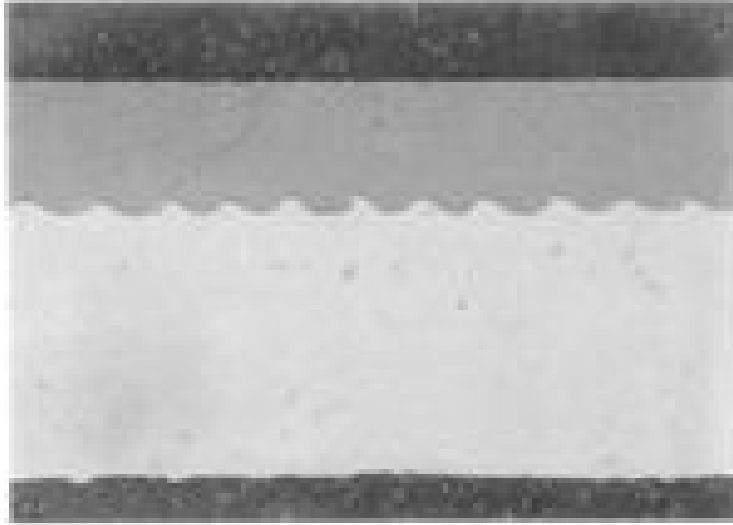
Figure A.1.6: Photograph of an explosive weld interface between aluminum and steel.

Explosive welding was used to fasten the copper reaction rail to a steel substrate on the Tokyo OEDO line, a linear induction powered subway shown in the photograph below.

Figure A.1.7: Tokyo's newest subway, the OEDO line has a linear induction propulsion system. The copper reaction rail (located between the two guidance rails) is explosively welded to a steel substrate.

Snow and Ice Buildup

Snow and ice have a tendency to buildup on solid objects during the winter months, especially when there is insufficient drainage incorporated into the transit system design at the outset. During the day, it is common for the temperature to rise above freezing, allowing accumulated ice and snow to melt. If there is not sufficient drainage, then the liquid water pools and refreezes at night when the air temperature drops below freezing or thermal radiation to the clear black sky cools the water to below freezing temperatures, even when the air temperature is well above freezing.

Because of the tight tolerances associated with maglev systems, the prospect associated with the buildup of snow and ice is a significant concern. The schematic shown in Figure A.1.8 illustrates the vehicle/guideway interface.
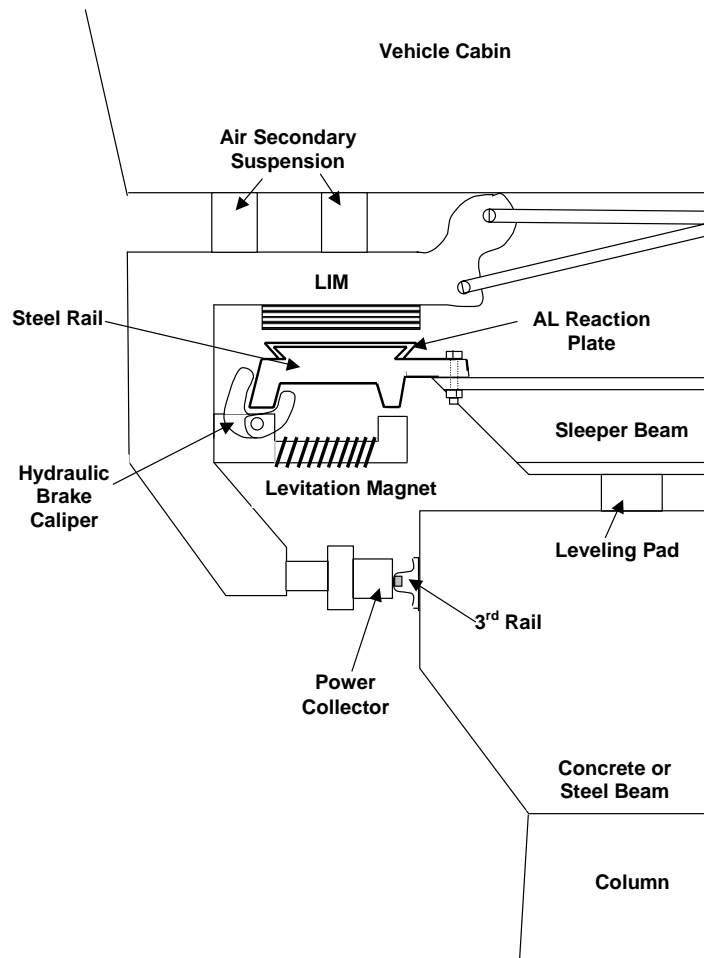

Figure A.1.8: Schematic of the vehicle/guideway interface on the HSST low-speed maglev system.

A report entitled, "Rail Transit Winterization Technology and Systems Operation Study" (LaMarca and King, 1980) was reviewed for the present study. LaMarca and King interview several rail transit lines following the extreme winters of 1978 and 1979. During these years, there were record quantities of snow and cold temperatures along the Eastern Seaboard and Midwestern states. The transit organizations also experienced a record number of component and system failures and learned by their experiences. According to that study, the major failure mode for the transit systems operating electric powered rail vehicles was due to the impact of snow and ice buildup or freeze/thaw processes on system components.

The dielectric constant is used to describe the rate at which current flows through a material (current rate is ~inversely proportional to the square root of the dielectric constant). Because the dielectric constant for air (κ~1 at sea level) is so different from that of water (κ~90), any water (especially in liquid or solid phase) that substantially displaces dry air within electromagnetic systems (vehicle propulsion and levitation, track or door actuators, etc.) will at least cause

performance problems but may also cause arcing and eventual component failure. This problem is exacerbated at high altitude because there are already fewer air molecules (which electrically "insulate") in the thin air than at sea level. Therefore, even in dry conditions, there is a higher propensity for arcing, between surfaces of large electrical potential difference, than at sea level. For this reason, conventional electric motors must be designed specifically for high altitude applications and measures should be taken to avoid the induction of snow and ice into these electric motors.

Additional problems associated with snow and ice buildup have been attributed to aging and wear of the varnish applied to the motor coils, allowing water to short the coils causing motor failure. A picture of the linear induction motor taken while touring the Toyo Denki manufacturing plant in Yokohama is shown below in Figure A.1.9. The motor coils have just been removed from a varnish-curing oven. A vacuum chamber is also used (prior to curing) to allow maximum penetration of the varnish into the all parts of the motor coil. This process will be a necessary maintenance requirement every several years (schedule to be determined) as the varnish ages and cracks with cyclic loading and age. It should be noted that a layer of black paint is also applied to the motor coils after the varnish has cured.

Figure A.1.9: Linear induction motor coils after being removed from the oven used for varnish curing at the Toyo Denki manufacturing plant in Yokohama.

Corrosion

An interesting article was found that originated with Northwestern University's Infrastructure Technology Institute (ITI). http://www.iti.northwestern.edu/research/a_projects/stray2.html

The authors carefully layout the potential corrosion mechanisms for existing DC electric-powered rail transit systems. Based on the literature and interviews with several operational transit organizations, they cite pitting and general corrosion as the two most common forms of corrosion that attack primarily metals used in transit systems. Electrochemical or galvanometric corrosion, requiring an anode, cathode, electrolyte and electrical (metallic) conduction path, has been identified as a significant corrosion mechanism because of the potential for high rates of metal removal. The anode, cathode and conduction path can be provided by a single metallic component or structural reinforcement on the transportation system. The available electrolyte is

water from precipitation (in any form). Since numerous metal ions (forms of pollution) now circle the globe through our atmosphere and because of the proximity of the planned transit system to the I-70 right-of-way, road salts (specifically $MgCl_2$), used as deicers, will add to the chemical activity of the available water, allowing more aggressive corrosive attack, than that of deionized water.

Also problematic are stray currents or current that deviates from the transit system current flow design paths, likely through ground paths. According to the study cited above, this stray current mechanism can many times cause more damage to other (seemingly unrelated) proximal infrastructure (metallic gas pipelines, metallic water lines and other conductive utility conduit) than to components associated directly with the transit system.

Fatigue

Corrosion and cracking due to differential thermal expansion cycling or more importantly, cyclic loading from the normal system operations and wind loads can lead to enhanced problems with component or system fatigue failure. Nucleation for a fatigue crack may be an existing microscopic defect or macroscopic scratch or indentation. Electrolytic corrosion can result in additional material removal. Cyclic loading, with peak-to-peak amplitudes well below the material ultimate or yield strength causes existing defects or micro-cracks to propagate. Careful numerical vibration analysis of the vehicle structural components will be necessary to fully understand the extent of potential fatigue damage. This effort can also provide the maintenance staff with appropriate time intervals for inspection of critical structural elements. Typical cyclic loading due to the levitation forces of a moving vehicle are shown in Figure A.1.10. This curve corresponds to a two-vehicle train.
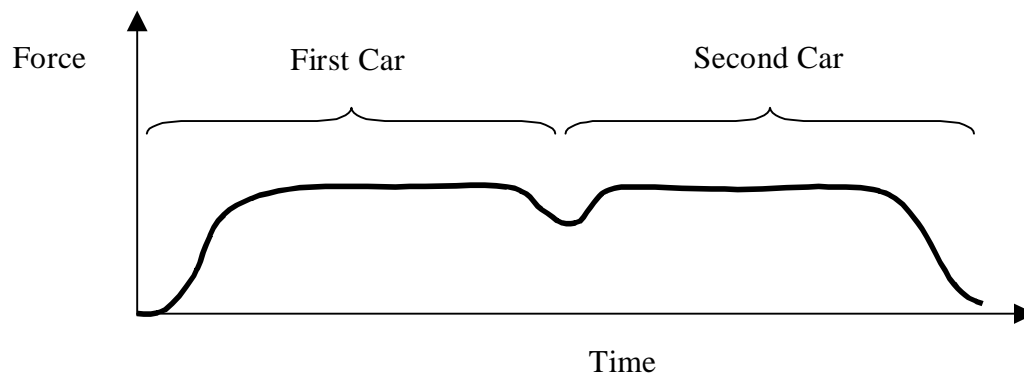

Figure A.1.10: Typical cyclic loading associated with the levitation magnets of a two-car HSST train (from tests performed in 1989). (Kato, 2003)

With recent advances in microelectronic sensors, it is possible to incorporate displacement sensors within the guideway and vehicle structure during the capital construction activities to later monitor the development and propagation of cracks or the local stress within the operational structures. http://www.me.gatech.edu/Diagnostics/B1.PDF

APPENDIX 2: SEVERITY OF THE FAILURE MODES

A website containing a Table summarizing the severity levels for a design can be found through the following URL. http://www.fmeca.com/ffmethod/tables/dfmea.htm

Guideway Systems

Vehicle/Guideway Interface

The severity of the winter climate induced failure modes on the vehicle/guideway interface will depend on the levitation technology selected for the Colorado Project. The HSST system utilizes an Electromagnetic Suspension (EMS) system, thus requiring a feedback control for the gap between the linear induction motor (LIM) coil, located on the vehicle, and the reaction rail (see Figure A.1.8). On the HSST system, the gap should be maintained at 14-15 mm to assure proper motor function. However, 15 mm of snow can fall within a several minutes in Colorado. Therefore, the impact of snow and ice on magnetic levitation should be considered.

Water is a diamagnetic material that has a slightly smaller (magnetic) permeability than that of a vacuum. The permeability is the ratio of the magnetic flux density to the magnetic field strength. Materials with smaller permeability will spread the lines of magnetic flux, resulting in a slightly reduced magnetic force. A reduced force will mean a smaller gap between the vehicle and guideway, for a given current flow through the levitation magnet. The severity rating for a few inches of snow on the guideway is estimated to be a rating of 7, high effect, product is operable, but at a reduced level of performance. However, if additional snow and ice accumulates then the severity would move upward. The next step is an 8 rating indicating that the product is inoperable with loss of primary function.

Similar concerns would confront the propulsion system because this subsystem also depends on the propagation of magnetic flux between the active coils and passive reaction coil or plate. However, there will also be a significant amount of heat dissipated by the propulsion, which will tend to melt the snow and prevent snow and ice build up.

Effective water drainage, to prevent the freeze/thaw failure mechanism, will be a critical consideration in the design of the guideway and propulsion motor components.

High Speed Switches
At this juncture, the baseline switches are either a bent beam, a lateral translating table or a docking switch. In any case, reliable actuator and latching operations are absolutely necessary for the safe transition to or from the main guideway and the station. Both the actuators and the latches can and should be placed into positions sheltered from the weather by the guideway and appropriate enclosures so that moisture does not contribute to actuator failure. In addition, these components should be designed to allow adequate drainage to avoid failure due to freeze/thaw cycles. Either of these devices are fully functional or not. Because the importance of the properly functioning switch and the deleterious impact of an improperly functioning switch, the design of the switch has a severity rating of a 9; failure affects the safe product operation or involves noncompliance with government regulation with warning. The switches will require redundant and fail safe sensors to indicate the health and position of the switches.

Circuit Breakers
These devices will be used to control the flow of electrical energy to propulsion and on-board control, lighting and passenger comfort systems. Failure of the circuit breaker could result in a power outage or the inability to impose a power outage in the event of a fire or other emergency

situation. Evidence of previous circuit breaker failures due to the impact of extremely cold temperatures was found.
http://www.metatechcorp.com/aps/cold_weather_operating_problems_.htm

However, the circuit breakers will also be instrumented so that their position (open or closed) may be ascertained. Therefore, the severity rating for this device is 9. Failure affects the safe product operation or involves noncompliance with government regulation with warning.

Power Collection Mechanisms
There are two applicable means of getting power to the vehicle. The first is by a brush on a third rail or a pantograph on a caternary. These techniques are similar because they each require a sliding contact. The second is by way of electromagnetic induction, a non-contact alternative. The quantity of power transmitted by either of these techniques depends on the vehicle size and the type of propulsion system selected. In the case of a linear induction motor propulsion system, the vehicle contains the active motor components and thus will require substantial power to pass through the collection mechanism. With a linear synchronous motor drive, the guideway is active, thus only power for the on board control, lighting and passenger comfort systems is required to pass through the collection system. The failure modes and severity for each will be considered here. The severity will remain the same regardless of means used to transmit the electrical energy to the vehicle.

More reporting is available for sliding contact because these techniques have been used for nearly 100 years. Two recent studies that discuss winterization issues are cited here. LaMarca and King (1980) summarized the experiences of several eastern and Middle Western transit organizations as they worked to maintain electrically powered rail service during the exceptionally difficult winters of 1978 and 1979. Hewitt (1980) reported on testing results from a winterization study on a compressed air levitated, linear induction powered people mover vehicle. All of the vehicles discussed in both studies relied on sliding contact for power collection to the vehicle.

If the vehicle is powered by linear induction motor, it cannot move under its own power. Therefore, the severity of a loss in the power collection subsystem is very high, 8; product is inoperable with primary loss of function. If the vehicle has a linear synchronous motor propulsion system, then a loss of functionality on the vehicle power collection system will result only in the loss of power for lighting, comfort systems and on-board controls. With adequate central control capabilities, the severity effect is moderate, 6; product is operable but comfort and convenience items are inoperable. It is also possible that the system may be operable but at a reduced level of performance or a severity rating of 7.

Snow Removal and Maintenance Cleaning Equipment
In both of the transit winterization studies cited in the previous section, snow removal was imperative for safe product operation. Specialized vehicles or transit vehicle modifications were required to provide the necessary equipment for adequate snow/ice removal. In addition, any transit system will rely heavily on accurate weather forecasting so that adequate preparations can be made. Therefore, the severity rating for effective snow removal and maintenance cleaning equipment is hazardous with warning, 9; failure affects safe operation or involves noncompliance with government regulation, with warning.

Auxiliary Heating Systems
Auxiliary heating systems are used to keep critical components of the guideway clear of ice and snow to maintain optimum transit system performance. Examples of these critical components include the third rail (in slider contact power collection systems), communications links, emergency braking surfaces, vehicle electrical ground contacts, etc. Depending on which critical component heater fails, the severity will vary from a moderate, 6, product is operable, but comfort and convenience items are inoperable to at least a hazardous with warning, 9, failure affects safe operation or involves noncompliance with government regulation, with warning. The severity 6

corresponds to loss in communications, whereas the severity 9 occurs for a loss of primary power collection capabilities, emergency braking capability or vehicle electrical ground contacts. Severity will be a 10 without any type of warning that this failure(s) had occurred. Therefore, it is imperative that these auxiliary heating systems have multiple sensors to indicate the condition of heater system health.

Impacts of Wind (transit system concern)

Little is known about the impacts of wind on the envisioned transit system. However, the system as planned is for an elevated guideway; therefore, because of the nature of the earth's boundary layer, the guideway and vehicles would be exposed to higher velocity winds than their counterparts on the ground. Additionally, because of drifting snow induced by the wind, ground-based rescue vehicles may have difficulty responding to a stranded transit vehicle where help is required. This impact will be categorized as a transit system concern. Kato (2003), senior engineer at HSST, has recommended the following actions with regard to wind.

Table A.2.1. Impact of wind speed on existing HSST system.

Wind Speed (m/s)	System Impact
20	System speed is degraded
25	System operation ceases
50	System survives

Because it is assumed that adequate weather forecasting is available, the severity rating is 9; failure affects safe operation or involves noncompliance with government regulation, with warning.

Vehicle Systems

Mechanical Latches (vehicle doors and other openings)

Mechanical latches for doors will likely be interlocked to the drive system such that if the control system senses an open door, the vehicle will not operate. Depending on the importance of other subsystems that have access openings, the severity of a latch failure will be at least a very low, 4, fit and finish or squeak and rattle item does not conform, most customers notice defect but can be as high as a 9, failure affects safe operation or involves noncompliance with government regulation, with warning.

Motors and actuators (vehicle doors and other openings)

A door or opening that has an actuator or motor drive attached to it will be critical for the safe operation of the vehicle. Therefore, the severity is hazardous with warning, 9; failure affects safe operation or involves noncompliance with government regulation, with warning.

Vehicle Braking Systems

The primary braking system will likely be electromagnetic. These systems are not dependent on friction but are dependent on the availability of external power. Emergency braking systems will likely be friction dependent. The severity of a failure in any of the braking systems will be at least a 9; failure affects safe operation or involves noncompliance with government regulation, with warning.

Vehicle Bogie compartment winter design requirements

Examples of these components include a shroud around the base of the vehicle chassis that will prevent the accumulation of snow and ice onto critical systems located below the passenger

compartment.   Significant applicable experience was gained in the Denver winterization study (Hewitt, 1980) that will be valuable to the design of the vehicle for the Colorado advanced transit system. The impact of a failure of critical subsystems located in this area is serious. Therefore, the severity is 10; failure affects safe operation or involves noncompliance with government regulation, without warning.

Stations

Environmental Design Considerations
These are station design considerations such as building orientation and window placement to incorporate the sun into passive heating and natural lighting or to accommodate a mountain view. In addition, this would include the placement of walls or roof coverings to protect the waiting passengers from wind and snow. Failure of these components results in a low effect with regard to severity. Therefore, a rank of 5 (product is operable, but comfort or convenience operate at a reduced level of performance) is appropriate.

Snow and Ice Removal
Conventional snow plows, snow blowers and deicers would likely be utilized for this activity. Failure of these units would not affect the operability of the transport system but would make it uncomfortable for passengers having to trudge through deep snow to get to the vehicle. Therefore, a moderate severity rank of 6 is selected; product is operable but comfort and convenience item(s) are inoperable.

Auxiliary heating requirements
These include radiant heaters in wind brake cubicles on the loading zone and perhaps embedded resistance heaters in the outdoor heavily utilized walkways. Again, the severity is moderate 6; product is operable but comfort and convenience item(s) is inoperable.

APPENDIX 3: LIKELIHOOD OF OCCURRENCE OF THESE FAILURE MODES

As previously mentioned, the likelihood of occurrence is usually based on statistical information built upon high levels of experience with a particular design. Since the proposed system has been built as the 100-L model, though the 200 Colorado vehicle has not been built, we must rely on the experience reported in previous studies of systems that have some similarity to that proposed for Colorado project. In addition, climactic conditions from the Colorado plateau in Denver to the alpine passes are more extreme than those previously reported in the literature. Therefore, the likelihood of occurrence estimates are best educated guesses based on sound engineering judgment. These are summarized in Table 8.3-1.

A website containing a Table summarizing the likelihood of occurrence levels for a design can be found through the following URL. http://www.fmeca.com/ffmethod/tables/dfmea1.htm

APPENDIX 4: CAPABILITY OF DETECTION OF THESE FAILURE MODES

Recent advances in microelectronics and sensor technology can be used to inexpensively monitor the health and enhance the security of the transit system. It is assumed that sensors and data acquisition systems are inexpensive enough to provide substantial redundancy in measurement. Therefore, the ratings for Capability of Detection are generally between 2 (Very high chance that a design control will detect the cause of a failure or a subsequent failure mode) and 3 (High chance that a design control will detect the cause of a failure or a subsequent failure mode). However, because of the problems discussed in Hewitt (1980) associated with a vehicle bogie skirt and the relative difficulty of instrumenting this skirt, the "Vehicle Bogie compartment winter design requirements" category was given a 5, (Moderate chance that a design control will detect the cause of a failure or a subsequent failure mode).

A website containing a Table summarizing the likelihood of occurrence levels for a design can be found through the following URL. http://www.fmeca.com/ffmethod/tables/dfmea2.htm

APPENDIX 5: THERMAL ANALYSIS OF THE AUXILIARY HEATER REQUIREMENTS FOR THE VEHICLE/GUIDEWAY INTERFACE

Analysis of Structural and Reaction Rail Heating due to Motor Inefficiency

The first step in determining the auxiliary heater size, is to estimate the amount of heat that is dissipated within the reaction plate/structural steel rail as a result of inefficiencies within the linear induction motor (LIM). Inefficiencies are normally attributed to "end effects" in a LIM. However, there are limited paths for the unuseful energy to be dissipated. Either the energy is lost as heat dissipation from the motor coils due to Joule heating or it is lost as heat dissipated due to the Joule heating caused by eddy currents within the aluminum reaction and steel structural rail.

To estimate this rail heating effect, the problem is divided into two parts. The first part involves the calculation of the temperature that the rail achieves as the vehicle passes over it and the second part includes the calculation of the rail temperature drop expected due to heat transfer with the surroundings.

The volume of rail material into which the eddy currents are dissipated is estimated by scaling the photographs shown in Figure A.1.3 and Figure A.1.4. The material properties used are provided in Table A.5.1. Composite Al/Steel properties are the mass weighted averages for the composite.

Table A.5.1 Thermophysical properties of rail materials.

Property	Al	Cu	Steel	Composite Al/Steel
Density (kg/m^3)	2770	8933	7854	7070
Specific Heat (J/kg K)	831	385	434	446
Thermal Conductivity (W/m K)	177	400	62	--

This problem was simplified by considering the rail as passing through an induction furnace at a speed V, while an internal volumetric heat generation was input to the rail. For simplicity, the volumetric heat generation is assumed to be uniformly distributed throughout the steel aluminum rail composite. No heat losses to the surroundings are considered during this stage. An energy balance was performed about a differential element as shown in Figure A.5.1
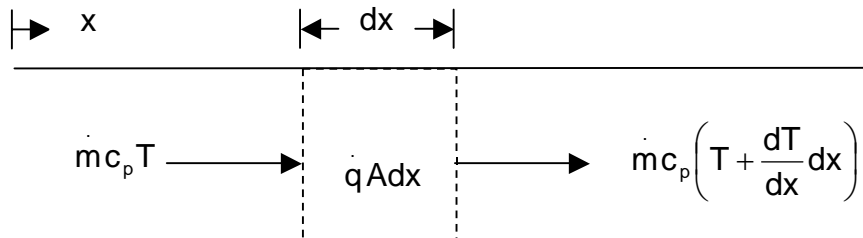

$$\dot{m}c_pT \longrightarrow \dot{q}Adx \longrightarrow \dot{m}c_p\left(T + \frac{dT}{dx}dx\right)$$

Figure A.5.1: Energy balance about a differential control volume within the structural and reaction rail.

where $\dot{m} = \rho VA$, ρ is the material density, V is the vehicle velocity, and A is the cross sectional area of the rail, c_p is the rail specific heat, T is the rail temperature as a function of rail length, x,

and $\dot{q}$ is the volumetric heat generation rate. The energy balance results in the following first order differential equation.

$$\frac{dT}{dx} = \frac{\dot{q}A}{\dot{m}c_p} \quad \text{eqn. A.5.1}$$

Solution to the equation A.5.1 is provided below and plotted in Figure A.5.2.

$$T(x) - T_i = \frac{\dot{q}A}{\dot{m}c_p} x \quad \text{eqn. A.5.2}$$

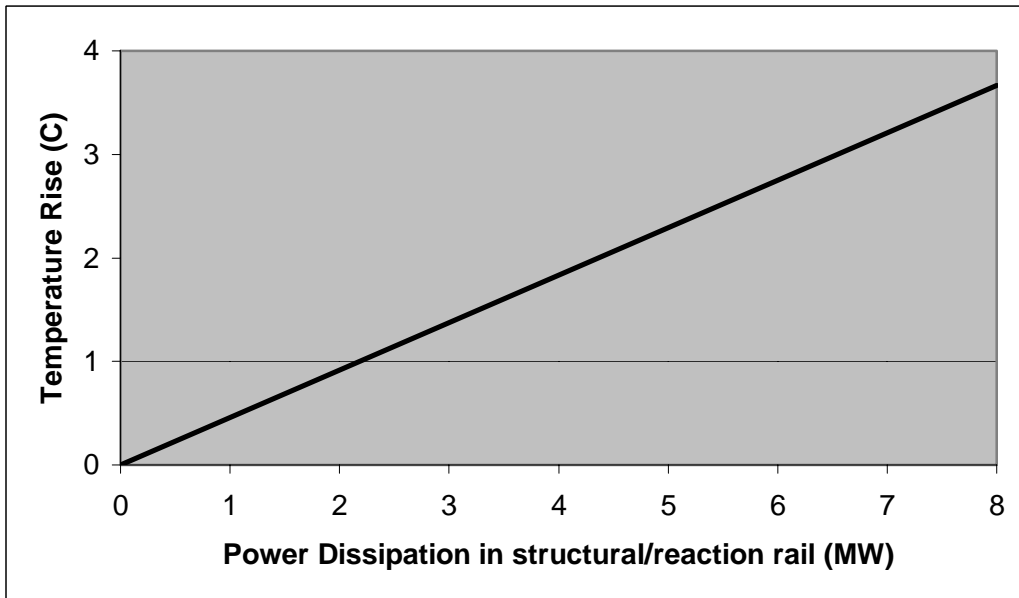The length of the four-car train is assumed to be 92 m (four cars total in two, two-car sets); the train velocity is 160 kph.

Figure A.5.2: Estimate of temperature rise in the rail as a vehicle passes over it as a function of unuseful energy imparted due to motor inefficiencies.

Power dissipation will depend on the power input to the vehicle. A typical LIM efficiency is assumed to be 60%. Therefore, we can assume that approximately 40% of the input propulsion energy is available to heat the reaction and support rail.

The question now becomes, at what distance from the moving train will the rails be cooled to their initial temperature? This can be accomplished with a similar model to that used before, except now we consider the rail after it leaves our imaginary induction furnace and predict the axial temperature distribution. Figure A.5.3 will help illustrate the concept.
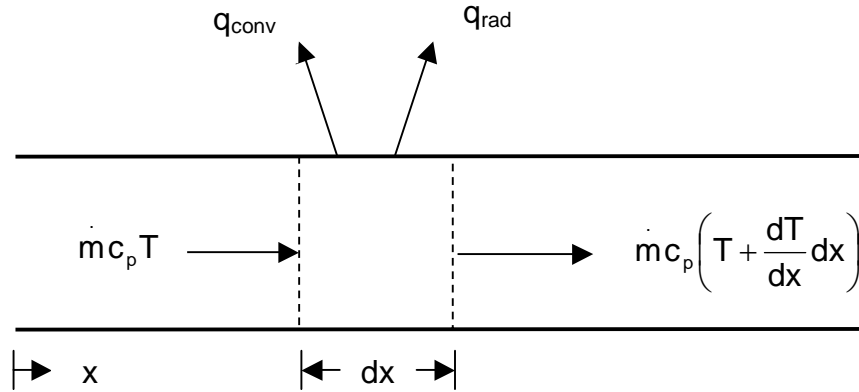
Figure A.5.3: Energy balance about a differential control volume within the structural and reaction rail with heat losses to the surroundings.

The additional heat loss terms shown in the figure are given by

$$q_{conv} = hPdx(T(x) - T_\infty) \qquad \text{eqn. A.5.3}$$

$$q_{rad} = \sigma\varepsilon Ldx(T(x)^4 - T_{sur}^4) \qquad \text{eqn. A.5.4}$$

where h is the convective coefficient, P is the perimeter of the rail cross section, T_∞ is the ambient air temperature, σ is the Stefan-Boltzmann constant, ε is the surface emissivity, L is the width of the rail exposed to the sky and T_{sur} is the temperature of the sky taken to be absolute zero (clear night sky). The energy balance results in the following first order nonlinear differential equation.

$$\frac{dT}{dx} + \frac{hP}{\dot{m}c_p}(T(x) - T_\infty) + \sigma\varepsilon L(T(x)^4 - T_{sur}^4) = 0 \qquad \text{eqn. A.5.5}$$

Equation A.5.5 was solved using a fourth order Runga-Kutta numerical integration technique and the results are shown in Figure A.5.4.

The convective coefficient is calculated as though the wind were moving laterally across the top of the rail (considered a flat plate) at 25 m/s. The lower portion of the steel structural rail is treated as two planar fins and an overall heat transfer coefficient is used to represent that loss. Radiation heat transfer is assumed to be significant only from the top of the rail. The emissivity is assumed to be that of oxidized aluminum.

As is shown in Figure A.5.4, assuming that the rail has achieved a 3°C temperature increase above equilibrium, the train has traveled approximately 1.5 km before the rail has cooled back down to the equilibrium temperature. This corresponds to a time of approximately 34 seconds or half a minute. If the ambient temperature is around the freezing mark and trains are running on 3.8 minute headways, then this amount of heating is insufficient to keep the rail between trains above freezing. Therefore, conditions will likely exist in which auxiliary electric heating of the steel structural and reaction rails are necessary.
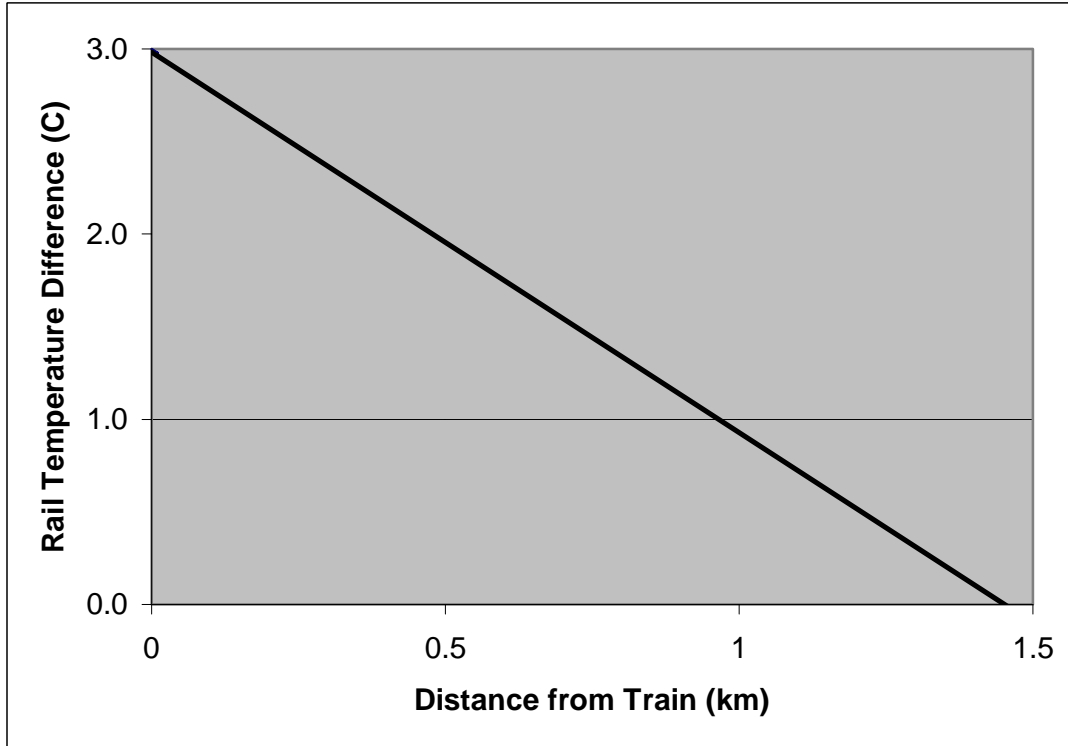
Figure A.5.4: Estimate of temperature fall in the rail as a vehicle leaves that portion of the track. Heat losses due to convection and radiation to black sky.

Analysis of Heater Sizing for Structural and Reaction Rail

Similar thermal analysis was done to size the electrical heaters required to melt the snow and ice from the steel structural and aluminum reaction rails. There is only a need for the heaters to be energized if there is precipitation and the ambient temperature is near or below the freezing point. Therefore, an integral part of the system to remove snow and ice will be weather stations distributed at various locations along the corridor. A moisture sensor integrated with a temperature sensor would be used to determine if the track heaters should be energized.

The schematic shown in Figure A.5.5 below illustrates the components used in the model to predict the heater power requirements. The outer tine cannot be insulated because the vehicle brake caliper must contact this to allow the secondary braking. The inner tine can be insulated but the tip is left open so that a proximity measurement can be made to allow vehicle levitation gap distance control. The top surface of the reaction rail cannot be insulated because the linear induction motor moves just 15 mm above it. In addition, it is not recommended that the top portion of the steel rail not be insulated because the upper surface should be clear of snow. The upper surfaces are also exposed to intense ultraviolet solar radiation at high altitudes; therefore, most polymer based insulating materials would disintegrate very quickly unless it were coated with an expensive ultraviolet inhibitor.
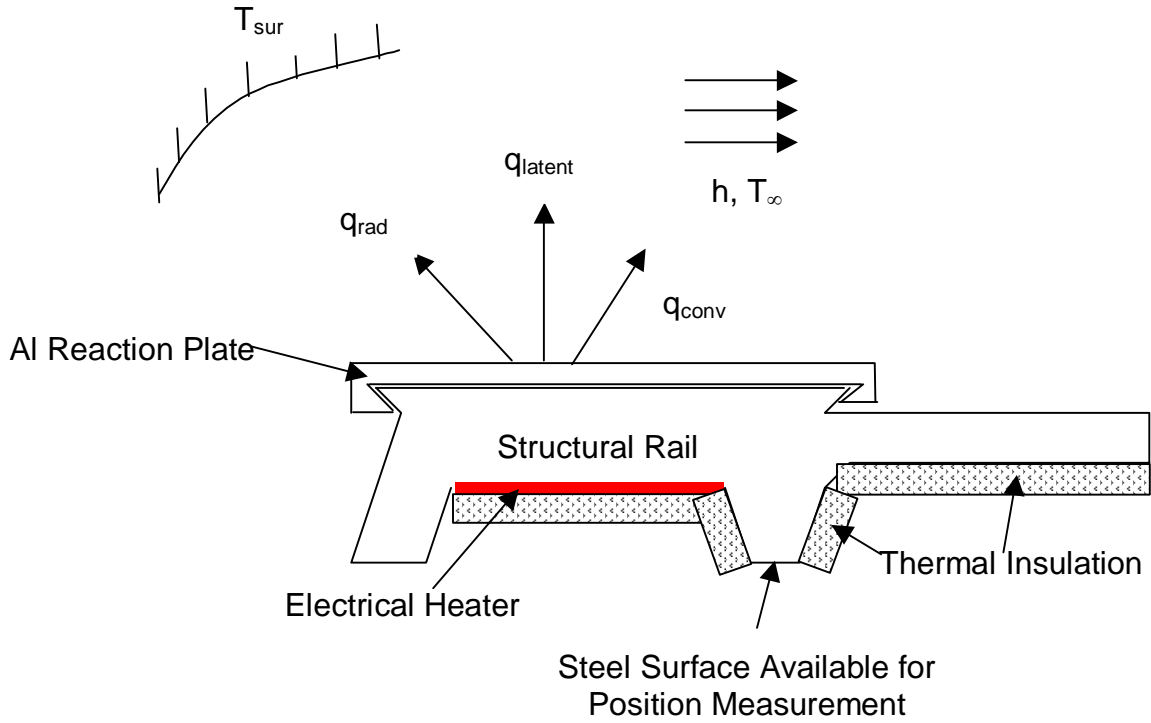
Figure A.5.5: Schematic of the electrical heater design solution with heat balance terms shown.

Equations A.5.3 and A.5.4 would be used again to account for the heat losses due to convection and radiation with the exception that each equation was divided by dx, resulting in a heat transfer per unit rail length. However, there is an additional term included here that involves the latent heat of fusion. It is written as follows

$$q'_{latent} = \dot{m} h_{if} \qquad \text{eqn. A.5.6}$$

where q'_{latent} is the heat transfer per unit length of rail required to melt snow, $\dot{m} = D L \rho_{snow}$ and L is the upper rail surface width exposed to the snow. Snow properties used in the calculation are provided in Table A.5.2 below.

Table A.5.2 Input variables used in heater sizing calculations.

Input Variable	Value of Input Variable
Ambient Temperature (K)	230 – 270
Surroundings Temperature (K)	230 – 270
Wind Speed (m/s)	25
Frost Formation Rate on Third Rail (mm/hr)	1
Frost density (kg/m^3)	920
Snowfall Rate (mm/hr)	76.2
Snow Density (kg/m^3)	100
Heat of Fusion for Water (J/kg)	333,430
Aluminum Properties	
Electrical Resistivity (Ω-m)	2.7 x 10^{-8}
Emissivity	0.8
Stainless Steel Properties	
Electrical Resistivity (Ω-m)	7.2 x 10^{-7}
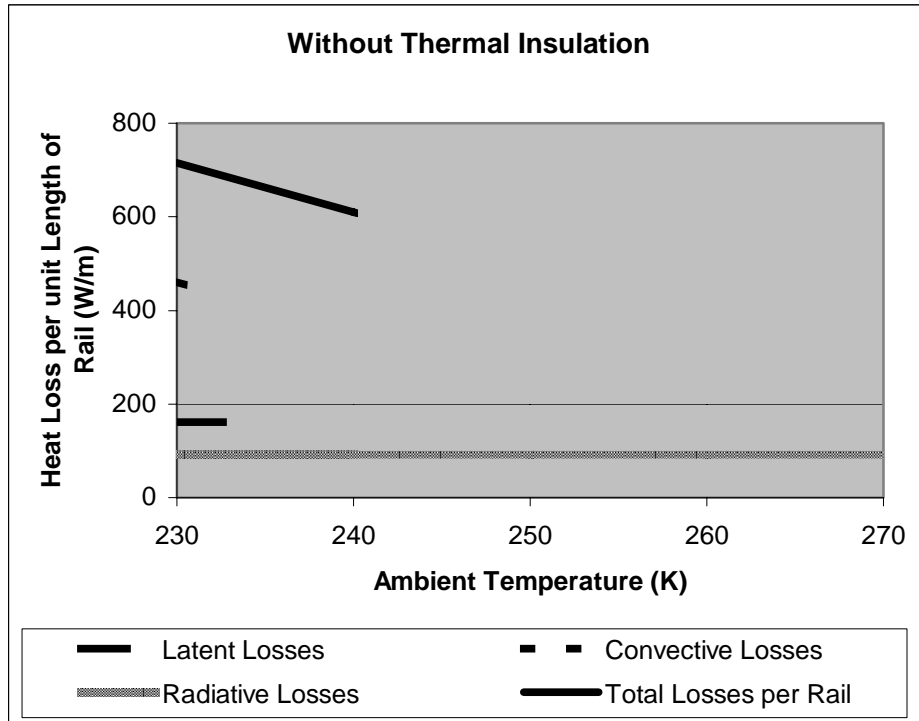
Figure A.5.6: Results of the structural rail heater sizing thermal analysis *without* **thermal insulation attached below the rail as shown in Figure A.5.5.**

Heat loss per meter of rail ***without*** thermal insulation added (as shown in Figure A.5.5) is provided in Figure A.5.6 for various ambient temperatures. The design point is to maintain the rail at a temperature of 274 K or 1°C. At ambient temperatures below 260 K (-13°C) convective

losses begin to dominate (recall that the wind speed for this analysis is assumed to be 25 m/s, a high wind).

Figure A.5.7 shows the results of the heat loss with the thermal insulation (shown in Figure A.5.5) in place. With the addition of thermal insulation and only on the bottom of the structural rail (as shown), the maximum power required drops from 715 W/m to 435 W/m.
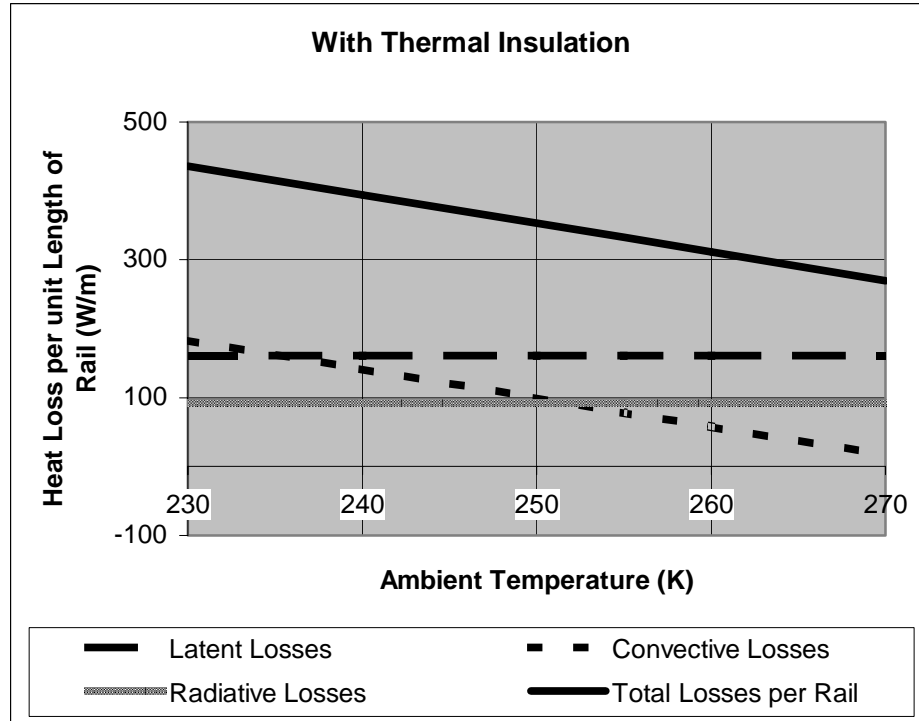

Figure A.5.7: Results of the structural rail heater sizing thermal analysis **with** thermal insulation attached below the rail as shown in Figure A.5.5.

Analysis of Heater Sizing for the Electrified Third Rail

The third rail has been previously identified as an area of concern with regard to winterization issues (LaMarca and King, 1980). Therefore, it was selected for auxiliary heater sizing. A photograph of the third rail cross section used at the Chubu HSST test track is shown in Figures A.1.3 and A.1.4. Since the U.S. quarter was in the picture, the cross sectional area of both the aluminum and stainless steel could be ascertained. The cross sectional area of the aluminum is found to be 9.24 x 10^{-4} m^2 while that of the stainless steel inlay is 1.15 x 10^{-4} m^2. As was done with the structural and reaction rail assembly, estimates were made of the anticipated Joule heating of the third rail by virtue of the fact that current is flowing through it on its way to power the vehicle and then return back to the power substation. Figure A.5.8 illustrates the way in which electrical power moves from the substation (see the red arrows) to the vehicle via the third rail, through the vehicle inverters and LIMs then back along the third rail on the opposite side of the support beam and back to the substation. As the vehicle moves further from the substation, the length of rail that can dissipate heat is 2L.
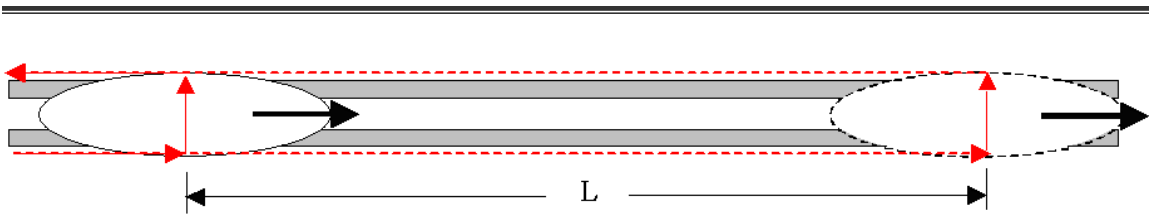
Figure A.5.8: Schematic of current flow from the substation to the vehicle as it moves down the track.

The thermal analysis follows the steady-state energy balance about the third rail. Figure A.5.9 illustrates the energy balance.
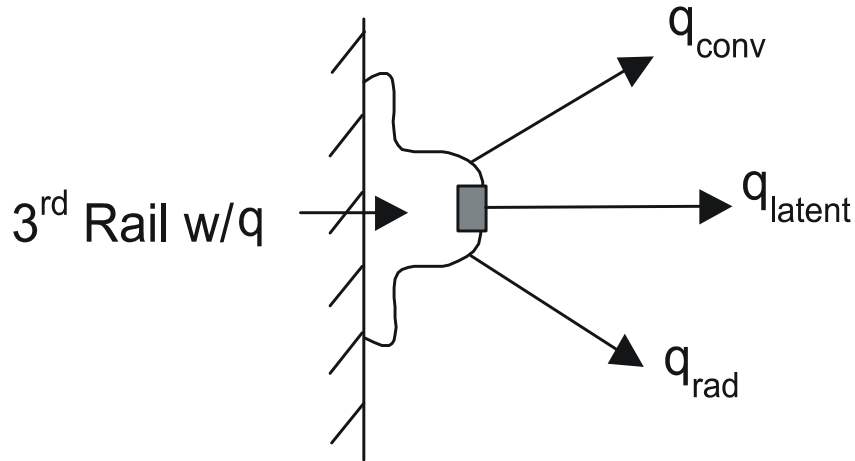

Figure A.5.9: Energy balance on third rail.

The $\dot{q}$ in the Figure above refers to the internal volumetric heat generation induced by Joule heating. Therefore

$$\dot{q} = \frac{I^2 \rho}{A_c^2} \qquad \text{eqn. A.5.7}$$

where I is the current flowing through the third rail, ρ is the rail electrical resistivity and A_c is the rail cross sectional area. The energy balance becomes (on a per unit rail length basis)

$$\dot{q}A_c = hP(T - T_\infty) + \sigma\varepsilon P\left(T^4 - T_{sur}^4\right) + h_{if}\, \dot{m}_{frost} \qquad \text{eqn. A.5.7}$$

The P refers to the perimeter of the third rail exposed to the convective and radiative environments and is the mass rate of frost formation on the third rail per unit length. The steady state temperature can be determined by solving Equation A.5.7. This is done using the Newton-Raphson root finding technique. The results indicate a 63°C higher temperature within the third rail than ambient. This corresponds to a vehicle power demand of 10 MW. However, after investigating the power lost by Joule heating of the third rail, it is found that the losses in the third rail alone are of the same order as the demand ~10 MW. Clearly, this is unacceptable for an energy efficient transit system. Therefore, the cross sectional area of the third rail must be increased. This is illustrated in Figure A.5.10. The power dissipated within the third rail as a function of the third rail cross sectional area is shown for both 10MW and 5MW vehicle power

demand. Also included on the figure is a vertical dashed line corresponding to the cross sectional area associated with the existing HSST third rail. It should be noted here that the Colorado team is considering larger vehicles for the I-70 corridor than currently exist at HSST. In addition, the team is taking the first steps to redesign the vehicle propulsion systems to provide for higher vehicle velocities, even within areas of steep grade. All of these changes contribute to higher power demand. 10 MW appears to be the first reasonable estimate of the maximum power demand for a four-car train.
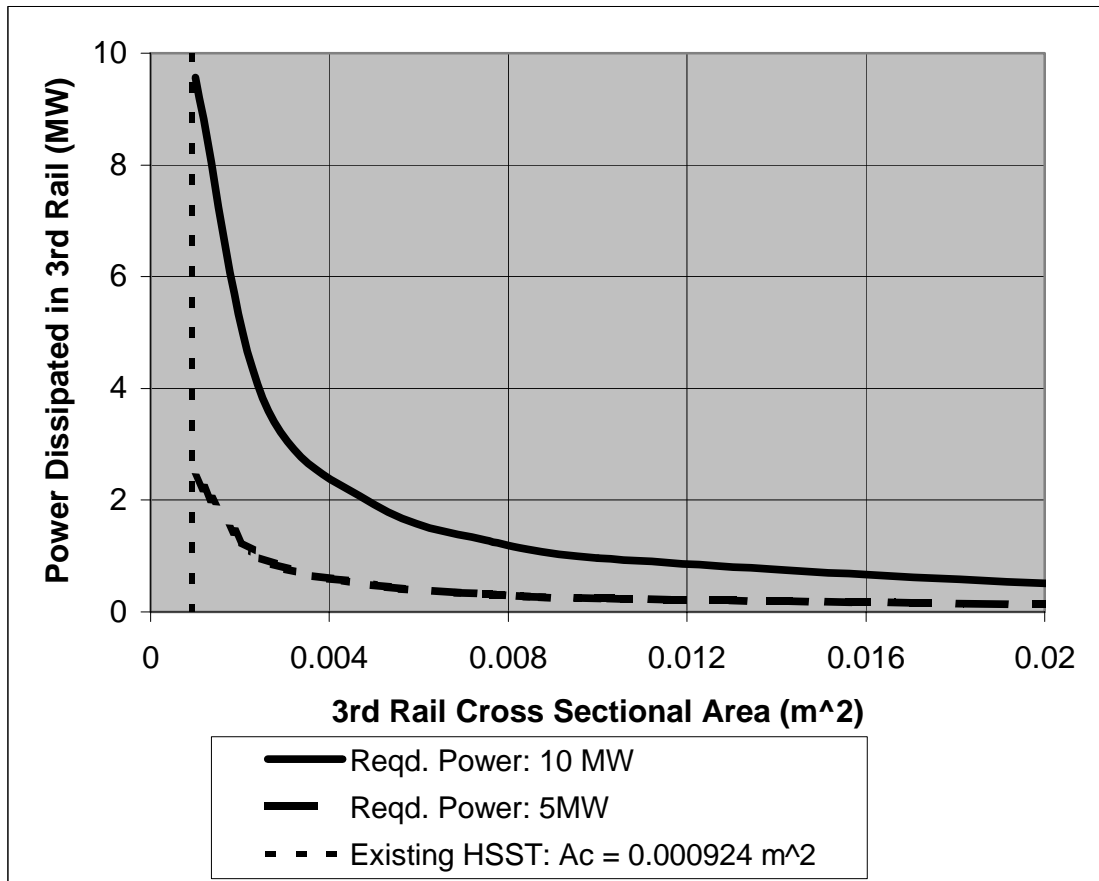
Figure A.5.10: Power dissipated within versus cross sectional area of the third rail.

An acceptable power loss in the third rail is arbitrarily selected at 10% of the total power demand. As is shown on Figure A.5.10, the 1 MW level of Joule heating loss can be achieved when the third rail cross sectional area is approximately 0.01 m^2, over an order of magnitude larger than the existing third rail. This cross sectional area includes the parallel resistance associated with the stainless steel inlaid bar. This bar is important for favorable power collector system wear characteristics. With the increased third rail cross sectional area and reduced thermal power dissipation in the rail, only a 2°C temperature rise above ambient is expected within the third rail. This is clearly insufficient to keep ice from forming on the third rail when the ambient temperature drops below –2°C. Therefore, auxiliary heaters will be necessary to keep the system running with high reliability when the temperature drops below –2°C.

Again taking the design set point of maintaining the third rail at a temperature slightly above ambient (274K or 1°C), the amount of heat that must be added to the third rail was calculated using the energy balance relationship described by eqn. A.5.7. Input conditions used to solve for the required heat input are provided in Table A.5.2.

The results are plotted in Figure A.5.11 as a function of ambient temperature. Overall Power refers to the heater power required for a 16 km (10 mile) run of track (currently the average distance considered between power substations).

This estimate does not include the power dissipated in the third rail due to Joule heating. At 10 MW of power drawn, this would drop the heater power required from 565 W/m to 505 W/m. However, the analysis performed also does not include conductive losses through the concrete beam. To minimize this heat flow, a plastic gasket will be sandwiched between the electrical resistance heater and concrete beam to add additional thermal resistance.
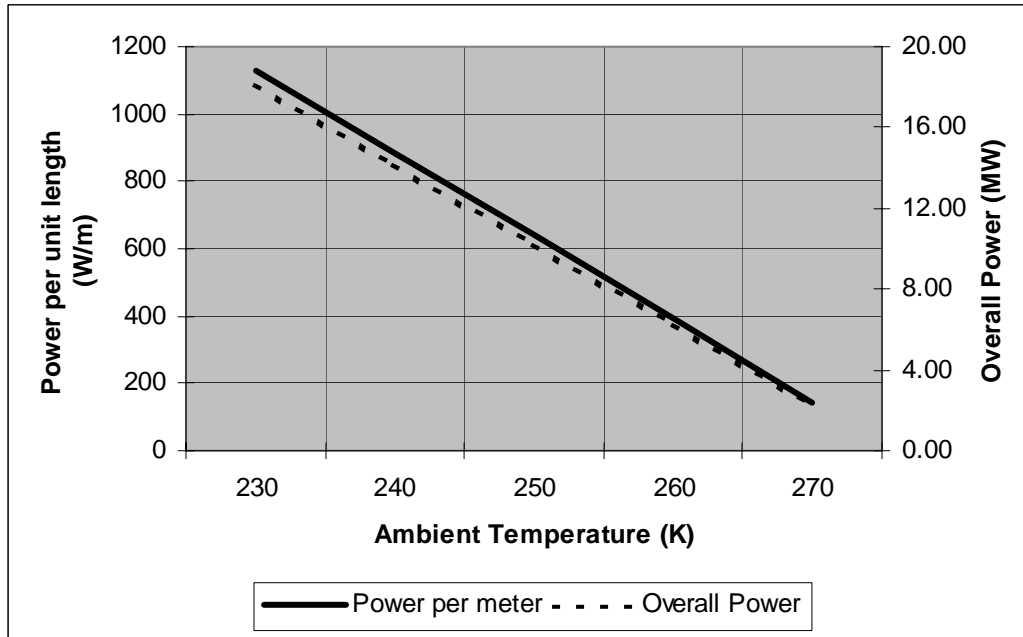

Figure A.5.11: Heater power per meter required to maintain the third rail above 274 K as a function of ambient temperature. Overall heater power refers to the 3rd rail heater power required for a 16 km (10 mile) section of track, two rails, one source and one return.

These power requirements are quite high and when combined with the requirement for heating the structural and reaction rail, the auxiliary heater power requirements exceed those of vehicle propulsion. Wind speed and ambient temperature has a significant impact on auxiliary heater power required. Therefore, decisions regarding the conditions for which normal or reduced system operation characteristics will depend partly on rate of frost formation, wind speed and ambient temperature.

To reduce the quantity of heater power required by the third rail, thermal insulation could be added as shown in Figure A.5.12 below. Consider the case in which 70% of the potentially exposed area is now covered with thermal insulation.
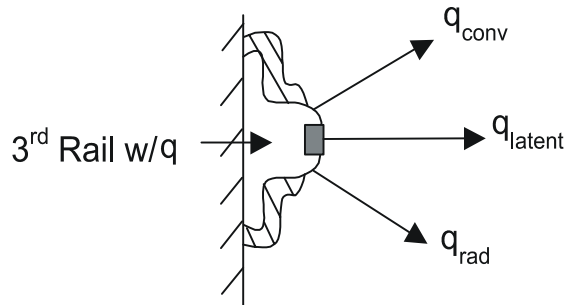
Figure A.5.12: Schematic of the third rail with thermal insulation covering approximately 70% of the surface area potentially exposed to the surroundings
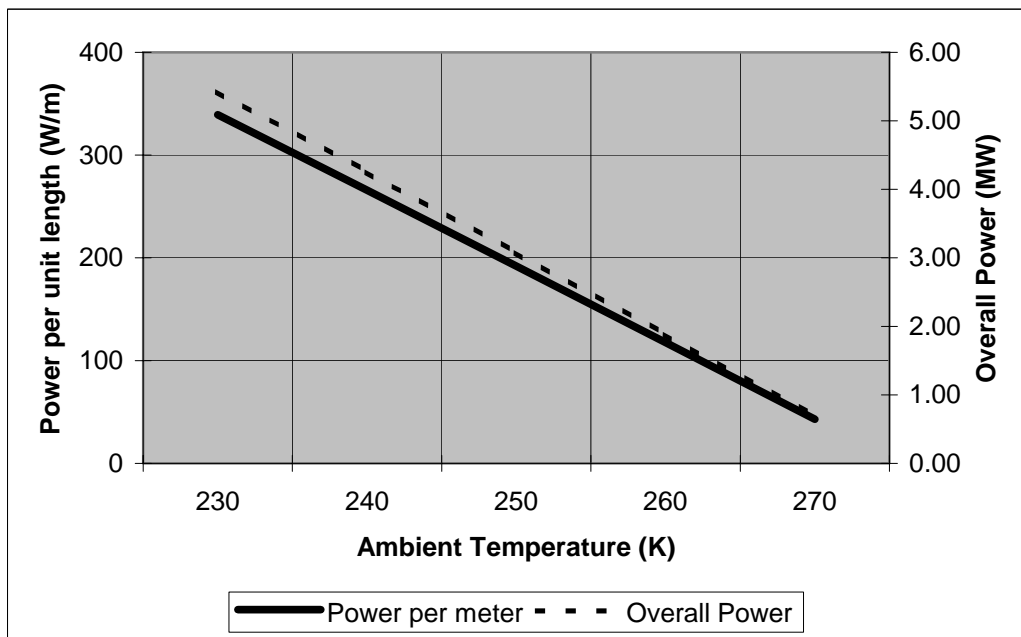

Figure A.5.13: Power per m required for the third rail with thermal insulation over 70% of the potentially exposed area.

Even a modest quantity of thermal insulation nearly halves the amount of heat energy needed to prevent the formation of ice. The overall electrical power required for a 16 km length of track (two directions) is plotted in Figure A.5.14 and Figure A.5.15 both without and with thermal insulation, respectively.
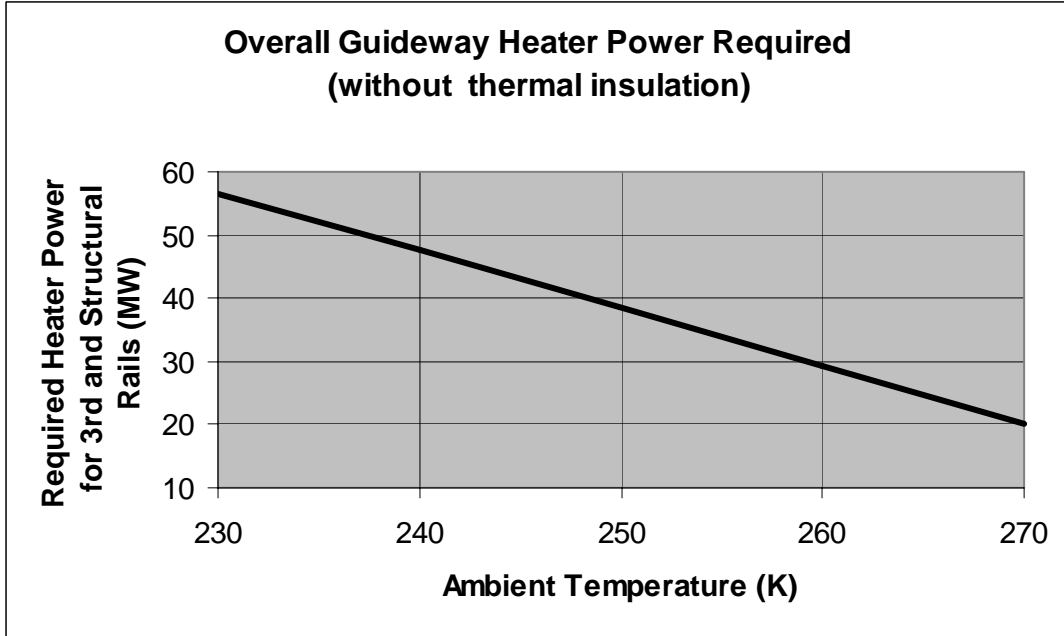
Overall Guideway Heater Power Required
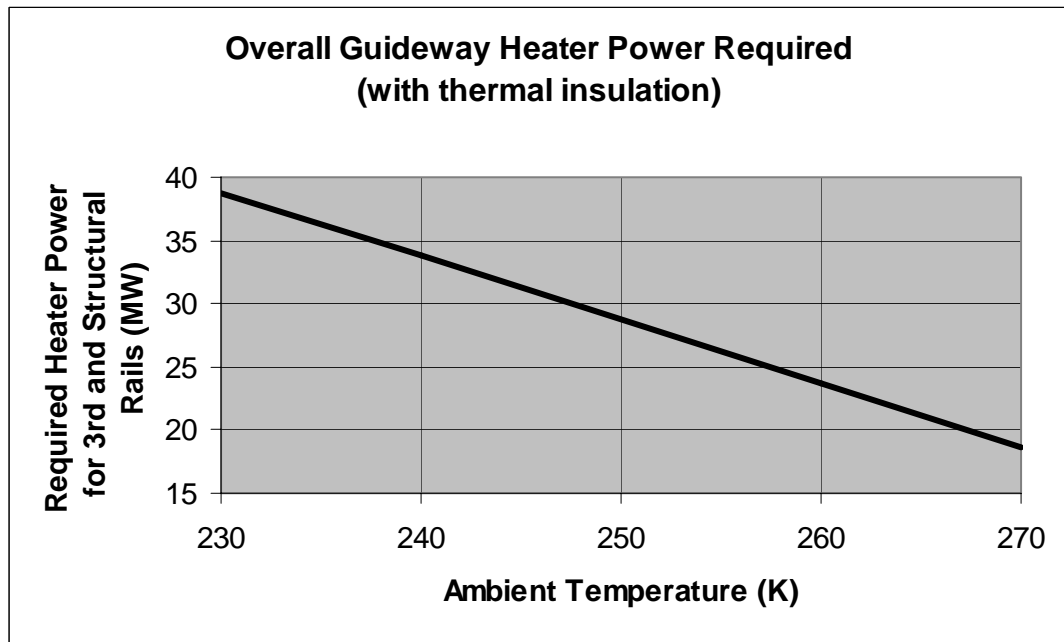## (without thermal insulation)

Figure A.5.14: Heater power required of all structural/reaction and third rails, two directions, 16 km of track, without thermal insulation.

Overall Guideway Heater Power Required
(with thermal insulation)

Figure A.5.15: Heater power required of all structural/reaction and third rails, two directions, 16 km of track, *with* thermal insulation.